IJOCTA
An International Journal of Optimization and Control: Theories & Applications
2010

ISSN:2146-0957
eISSN:2146-5703

Volume:13 Number:2
July 2023

An International Journal of Optimization and Control:

Theories & Applications

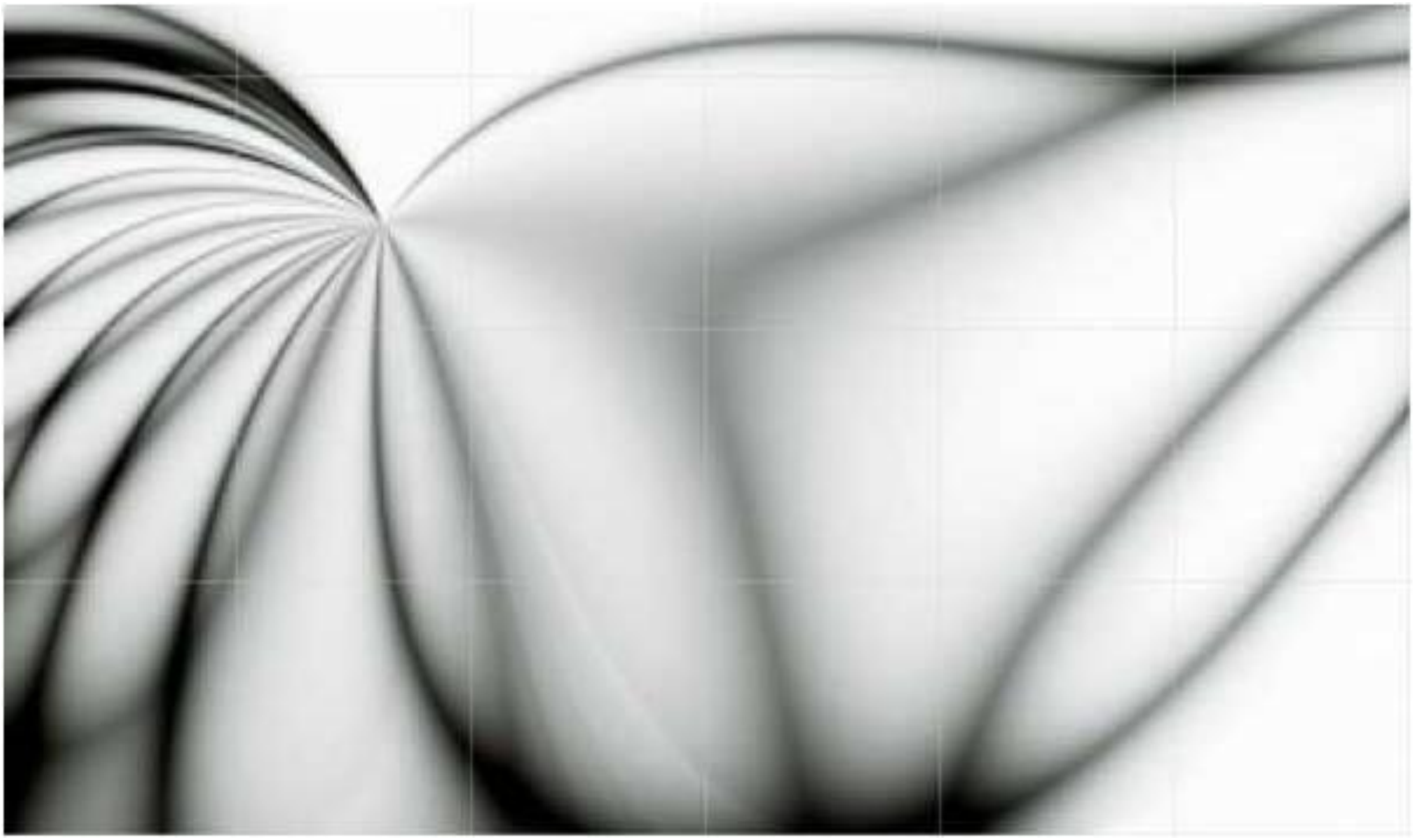

www.ijocta.org

IJOCTA

http://www.ijocta.org
editor@ijocta.org

An International Journal of Optimization and Control:
Theories & Applications

Volume: 13, Number: 2
July 2023

Publisher & Owner *(Yayımcı & Sahibi)*:

Prof. Dr. Ramazan YAMAN
Atlas Vadi Campus, Anadolu St.
No. 40, Kagithane, Istanbul, Turkey
Atlas Vadi Kampüsü, Anadolu Cad. No. 40, Kağıthane, İstanbul, Türkiye

ISSN: 2146-0957
eISSN: 2146-5703

Press *(Basımevi)*:

İdeal Kültür, Topkapı Mahallesi, Kahalbaşı Sokak, No: 31/1, 34093, Fatih, İstanbul, Türkiye
Ideal Kultur, Topkapi District, Kahalbasi Street, No: 31/1, 34093, Fatih, Istanbul, Turkey

Date Printed *(Basım Tarihi)*:

July 2023
Temmuz 2023

Responsible Director (Sorumlu Müdür):

Prof. Dr. Ramazan YAMAN

IJOCTA is an international, bi-annual, and peer-reviewed journal indexed/ abstracted by *(IJOCTA, yılda iki kez yayımlanan ve aşağıdaki indekslerce taranan/dizinlenen uluslararası hakemli bir dergidir)*:

- Emerging Sources Citation Index (ESCI)
- Scopus - Applied Mathematics
- Scopus - Control and Optimization
- Zentralblatt MATH
- ProQuest - Electronics & Communications Abstracts
- Proquest - Computer & Information Systems Abstracts
- Proquest - Mechanical & Transportation Eng. Abstracts
- EBSCOHost
- MathSciNet
- TR Dizin - Ulakbim (Science Database)
- Directory of Open Access Journals (DOAJ)

An International Journal of Optimization and Control: Theories & Applications

Volume: 13 Number: 2
July 2023

CONTENTS

RESEARCH ARTICLES

An International Journal of Optimization and Control: Theories & Applications
ISSN:2146-0957 eISSN:2146-5703
Vol.13, No.2, pp.139-150 (2023)
http://doi.org/10.11121/ijocta.2023.1247

RESEARCH ARTICLE

Adaptive MIMO fuzzy PID controller based on peak observer

Kemal Uçak,* Beyza Nur Arslantürk

Department of Electrical and Electronics Engineering, Muğla Sıtkı Koçman University, Turkey
ucak@mu.edu.tr, beyzanurarslanturk@posta.mu.edu.tr

ARTICLE INFO

Article History:
Received 27 March 2022
Accepted 8 February 2023
Available 9 July 2023

Keywords:
Adaptive control
Fuzzy PID controller
MIMO fuzzy PID controller
Peak observer
Peak observer based optimization

AMS Classification 2010:
93B52; 93C35; 93C40; 93C42

ABSTRACT

In this paper, a novel peak observer based adaptive multi-input multi-output (MIMO) fuzzy proportional-integral-derivative (PID) controller has been introduced for MIMO time delay systems. The adaptation mechanism proposed by Qiao and Mizumoto [1] for single-input single-output (SISO) systems has been enhanced for MIMO system adaptive control. The tracking, stabilization and disturbance rejection performances of the proposed adaptation mechanism have been evaluated for MIMO systems by comparing with non-adaptive fuzzy PID and classical PID controllers. The obtained results indicate that the introduced adjustment mechanism for MIMO fuzzy PID controller can be successfully deployed for MIMO time delay systems.

1. Introduction

Fuzzy controller (FC) has a more effective control performance compared to standard controller structures with fixed parameters since FC inherently has naturally changing dynamics due to its structure. The FC exhibits a time-varying PD controller behavior when examined under certain conditions as given in [1]. Considering that the system dynamics are uncertain and may change over time in controller structures, controller performances can be improved by integrating adaptive structures into classical control structures. For this reason, fuzzy PID structures that combine the nonlinear inference competence of fuzzy mechanisms(FM) with the robustness of classical PID structures are very often opted. By combining FM with adaptive control structures, the control performance of fuzzy PID architectures can be enhanced and empowered against uncertainty in control systems.

In technical literature, there are various parameter adjustment mechanisms for fuzzy controllers. Peak observer based adaptation method introduced in [1] can be considered as the simplest of these adaptation structures. Qiao and Mizumoto have proposed to tune the controller parameters by taking into account the overshoot value of the controlled systems. In [1], one of the scaling coefficients for controller input and output has been considered to enhance the closed-loop system performance. Chou and Lu introduced a real time implantable self-tuning fuzzy controller based on adjustment of scaling factors [2]. The update values of the controller parameters (ΔK) are calculated over the look-up tables created depending on the tracking error and the derivative of the error [2]. Adaptation schemes are to adjust the scaling factors according to individual adjustment rules and look-up tables [2]. Adjustments of scaling factors are converted into numerical adjustment tables by applying appropriate membership functions, with only matrix maps [2]. Jung et al. [3] deployed a real-time self-tuning mechanism based on variable reference tuning index to control the steam generator of a nuclear power plant for overshoot and non-overshoot cases. Maeda

*Corresponding Author

and Murakami [4] proposed to tune scaling coefficients and rule base to improve fuzzy controller performance by considering the reaching time of the system output, overshoot and amplitude of oscillations in system response. Mudi and Pal [5] introduced a robust gain tuning mechanism based on an additional fuzzy architecture to adjust output scaling coefficients of Fuzzy PI and PD controllers. The rule base required for the output scaling coefficients is defined depending on the derivative of the tracking error and the tracking error [5]. Zheng [6] proposed to update cores, supports, boundaries and the universe of discourse of the fuzzy variables to enhance controller performance. Chung et al. [7] utilized a fuzzy tuner to adapt the input-output scaling coefficients of a fuzzy PI controller to improve rise time, overshoot and steady state error of the controlled system. Chao and Teng [8] introduced two stage mechanism which is composed of a direct adaptation and a gradient descent based indirect adaptation mechanism to tune scaling coefficients of a PD type fuzzy controller for linear and nonlinear dynamical systems. Woo et al proposed an adaptation mechanism in which the controller parameters are adapted throughout the entire transient state [9]. Hu et al. obtained a PID mechanism with non-linear behavior by introducing a nonlinearity to the tracking error signal through a fuzzy mechanism [10]. The parameters of the fuzzy mechanism are seeked via genetic algorithms (GA) [10]. Ketata et al. have presented various look-up table-based fuzzy controller architectures constituted over tracking error and derivative of tracking error [11]. Kim and Chung introduced a fuzzy PID controller which is composed of fuzzy "PD" and linear "I" parts [12]. Kien et al. proposed a fuzzy inverse controller structure that tries to perform the inverse of the dynamics of the system [13]. Jaya algorithm is deployed for parameter adaptation [13]. In order to ensure stability, a sliding mode control surface is utilized [13]. Cherrat et al. proposed a fuzzy-based self-tuning mechanism to estimate the PID controller [14]. Gil et al. introduced a fuzzy adaptation mechanism in which the fuzzy PID controller parameters are adapted offline via the non-linear model and online via the local linear model [15]. Yordanova et al. [16] introduced a novel model free supervisor based adaptive fuzzy controller for nonlinear dynamical systems. Pinto et al. developed a fuzzy adaptation mechanism for SISO and MIMO systems, which estimates the gains of the PID controller [17]. Yeşil et al. presented a review paper that aims to examine various studies on fuzzy PID controllers in the literature and to classify these fuzzy controllers into categories [18]. In the related review paper, fuzzy controller architectures were categorized under three main headings: Direct action (DA) type fuzzy PID controllers, fuzzy gain scheduling (FGS) type fuzzy PID controllers and mixed type fuzzy PID controllers [18]. Kumaar et al unveiled a deep survey of classical and fuzzy PID controllers [19]. The paper [19] presents the historical development of fuzzy logic-based structures. Guzelkaya et al. [20] utilized a relative rate observer to tune the input scaling factor corresponding to the derivative coefficient and the output scaling factor corresponding to the integral coefficient of the PID type FLC. Peak observer based adaptation mechanisms have been utilized in various studies [21, 22], but only two scaling coefficients have been adapted in all these structures, as proposed in [1].

In this paper, the adjustment mechanism proposed by Qiao and Mizumoto [1] has been enhanced for all scaling coefficients of the fuzzy PID controller. Thus, all scaling coefficients of the controller can be tuned by considering the overshoot value observed via peak observer. In addition to this, the adaptation mechanism proposed for SISO systems has been improved for MIMO systems. Therefore, the introduced MIMO fuzzy PID has 16 parameters to be optimized. The introduced adaptation mechanism has been examined on a MIMO time-delay system. The tracking and stabilization performance of the introduced controller has been evaluated.

This paper is organized as follows: The basics of the adaptive fuzzy PID based on peak observer [1] has been overviewed in Section 2. In section 3, the introduced adjustment mechanism for MIMO systems has been presented. The performance evaluation of the introduced method has been examined on a MIMO time delay system in Section 4. The paper ends with a brief conclusion part in Section 5.

2. Adaptive fuzzy PID controller

2.1. An overview of fuzzy PID controller

The structure of the incremental PID Type Fuzzy controller is illustrated in Figure 1 where K and K_d are input scaling coefficients, and α and β are output scaling coefficients of PD and PI part of the PID controller, respectively. The mathematical expression of the produced control law is derived as follows [1, 23–25]:

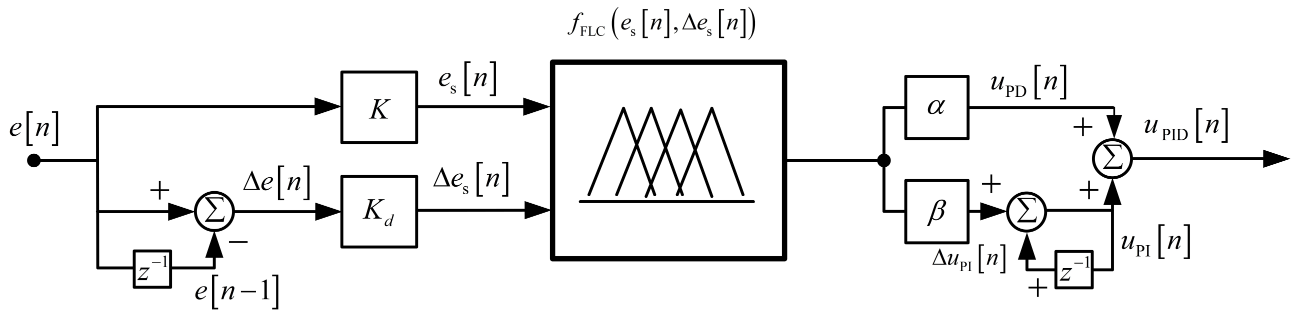

Figure 1. Fuzzy PID controller [1, 23–26].

$$u_{PID}[n] = \overbrace{\alpha f_{FLC}(e_s[n], \Delta e_s[n])}^{u_{PD}[n]} + \underbrace{\beta f_{FLC}(e_s[n], \Delta e_s[n]) + u_{PI}[n-1]}_{u_{PI[n]}} \tag{1}$$

where $e_s[n]$ and $\Delta e_s[n]$ are scaled error and derivative of error. Triangular type input membership functions with cores $\{-1, -0.4, 0, 0.4, 1\}$ [1] depicted in Figure 2 are deployed. For given inputs of $e_s[n]$ and $\Delta e_s[n]$, four(4) rules illustrated in Figure 2 are fired at each sampling time. Thus, the output of the FLC can be obtained as follows using product-sum inference method and center of gravity method for defuzzification [1, 23–25]:

$$\begin{aligned} f_{\mathrm{FLC}}(e_s[n], \Delta e_s[n]) &= \overbrace{A_i(e_s[n]) B_j(\Delta e_s[n])}^{w_{i\ j}} u_{i\ j} \\ &+ \overbrace{A_{i+1}(e_s[n]) B_j(\Delta e_s[n])}^{w_{i+1\ j}} u_{i+1\ j} \\ &+ \underbrace{A_i(e_s[n]) B_{j+1}(\Delta e_s[n])}_{w_{i\ j+1}} u_{i\ j+1} \\ &+ \underbrace{A_{i+1}(e_s[n]) B_{j+1}(\Delta e_s[n])}_{w_{i+1\ j+1}} u_{i+1\ j+1} \end{aligned} \tag{2}$$

where w_{ij}'s stand for the firing strength of fired rule, and membership values are given as follows [1, 23–25]:

$$\begin{aligned} A_i(e_s[n]) &= \frac{e_{i+1} - e_s[n]}{e_{i+1} - e_i} \\ A_{i+1}(e_s[n]) &= \frac{e_s[n] - e_i}{e_{i+1} - e_i} \\ B_j(\Delta e_s[n]) &= \frac{\dot{e}_{j+1} - \Delta e_s[n]}{\dot{e}_{j+1} - \dot{e}_j} \\ B_{j+1}(\Delta e_s[n]) &= \frac{\Delta e_s[n] - \dot{e}_j}{\dot{e}_{j+1} - \dot{e}_j} \end{aligned} \tag{3}$$

The fuzzy control rule base utilized to constitute the FLC controller introduced in [1] is given in Table 1 for corresponding membership functions.

Table 1. Fuzzy control rule base [1, 25, 27].

MFs	$\dot{e}_{-2}$	$\dot{e}_{-1}$	$\dot{e}_0$	$\dot{e}_1$	$\dot{e}_2$
e_{-2}	-1.0	-0.7	-0.5	-0.3	0.0
e_{-1}	-0.7	-0.4	-0.2	0	0.3
e_0	-0.5	-0.2	0.0	0.2	0.5
e_1	-0.3	0.0	0.2	0.4	0.7
e_2	0.0	0.3	0.5	0.7	1.0

Linearization can be conducted in the neighborhood of the fired rules as detailed in [1] in order to analyze the dynamic behavior of the fuzzy PID controller by comparing with standard PID. Thus, the produced fuzzy control law can be rewritten as [1, 25]:

$$\begin{aligned} u &= A + Pe_s[n] + D\Delta e_s[n] \\ A &= u_{ij} - Pe_i - D\dot{e}_j \\ P &= \frac{u_{i+1\ j} - u_{ij}}{e_{i+1} - e_i} \\ D &= \frac{u_{i\ j+1} - u_{ij}}{\dot{e}_{j+1} - \dot{e}_j} \end{aligned} \tag{4}$$

Using α and β parameters, the equivalent standard PID components can be derived as follows: "$\alpha KP + \beta K_d D$" represents the proportional term, "βKP" stands for the integral term and "$\alpha K_d D$" can be interpreted as the derivative term [1, 25].

2.2. Peak observer based adaptation mechanism

The adjustment mechanism based on peak observer [1, 18, 20, 21] is shown in Figure 3. Qiao and Mizumoto [1] aimed to decrease the integral coefficient while increasing the derivative parameter to increase the resistance against the overshoot and oscillation of the system by keeping the proportional term constant.

Therefore, Qiao and Mizumoto [1] proposed to update K_d and β parameters by observing the

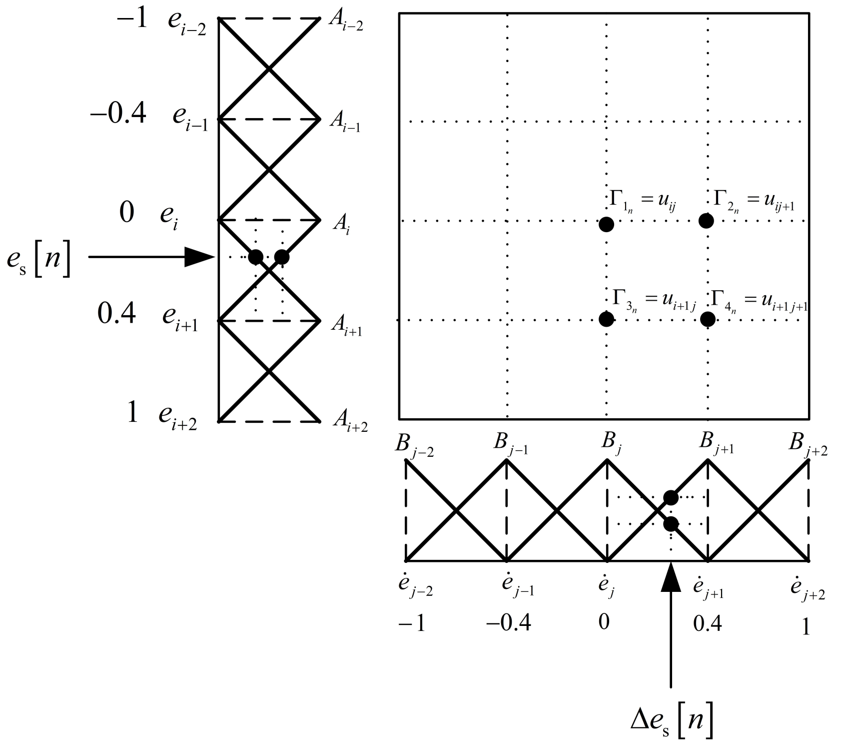

Figure 2. Input membership functions and fuzzy rule base [1, 23–25].

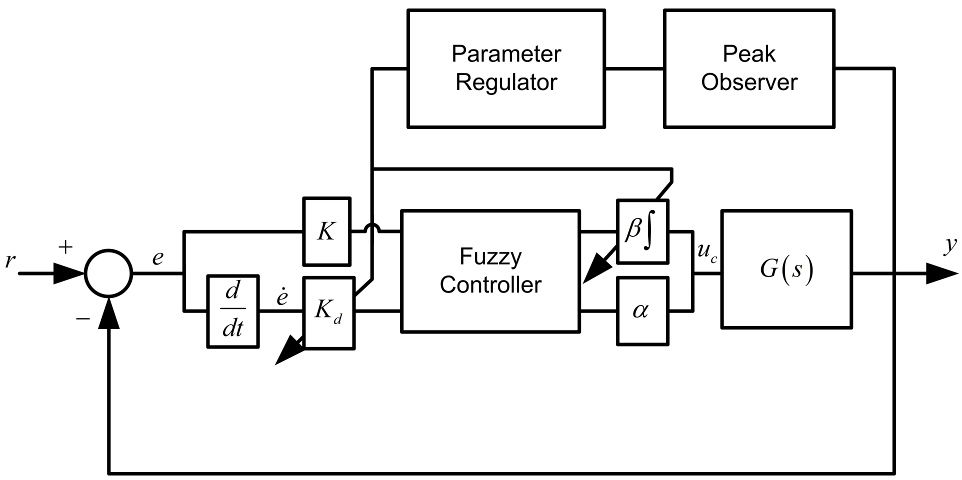

Figure 3. Peak observer based adaptation mechanism [1, 18, 20, 21].

absolute error value ($\delta_k = |e_k|$) at peak times as follows:

$$K_d = \frac{K_{d0}}{\delta_k},\ \beta = \beta_0 \delta_k \tag{5}$$

where $t_k,\ k \in \{1, 2, 3, \cdots\}$ are the peak times.

3. Adaptive MIMO fuzzy PID controller

In this study, firstly, it is aimed to adapt all parameters of a fuzzy PID controller, inspired by the peak observer approach of Qiao and Mizumoto in [1]. In addition, it is intended to extend the enhanced mechanism to MIMO fuzzy PID controllers. The proposed adaptation mechanism for a MIMO system is shown in Figure 4 where m stands for the mth system input and k denotes the kth controlled output of the MIMO system. The input-output scaling coefficients of the MIMO Fuzzy PID controller are adapted as follows:

$$\begin{bmatrix} K_{mk_{new}} \\ K_{d_{mk_{new}}} \\ \alpha_{mk_{new}} \\ \beta_{mk_{new}} \end{bmatrix} = \begin{bmatrix} K_{mk}\delta_m \\ \frac{K_{d_{mk}}}{\delta_m} \\ \frac{\alpha_{mk}}{\delta_m} \\ \beta_{mk}\delta_m \end{bmatrix} \tag{6}$$

where δ_m indicates the corresponding peak observer value [1, 25]. Thus, the derivative coefficient is increased while the integrator is decreased by keeping the proportional term fixed [25]. The internal structure of MIMO fuzzy PID controller

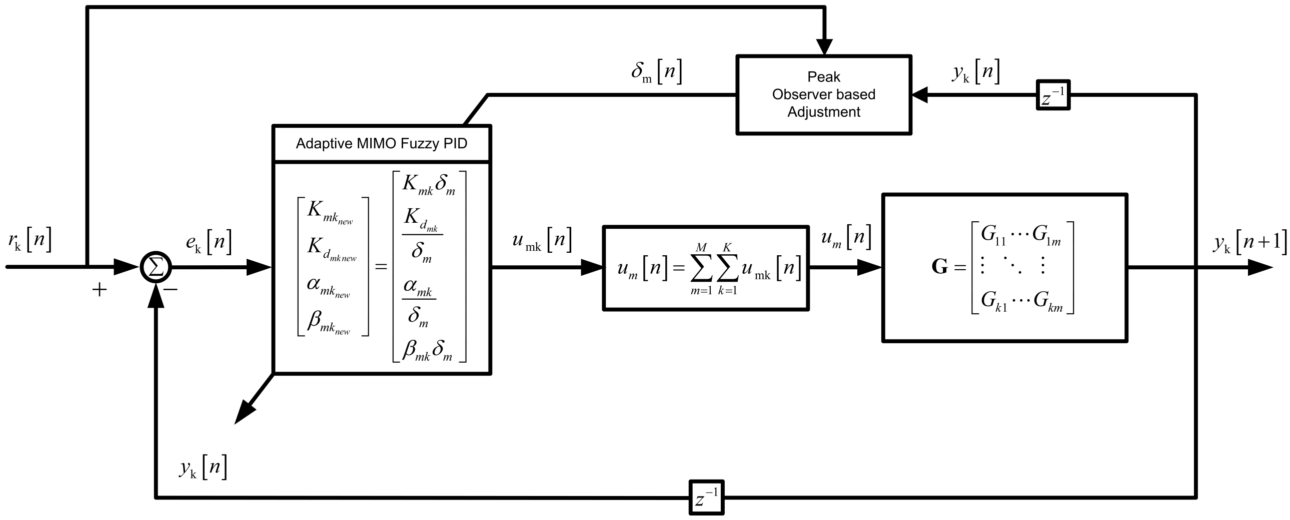

Figure 4. Adaptive MIMO fuzzy PID controller based on peak observer [1, 25].

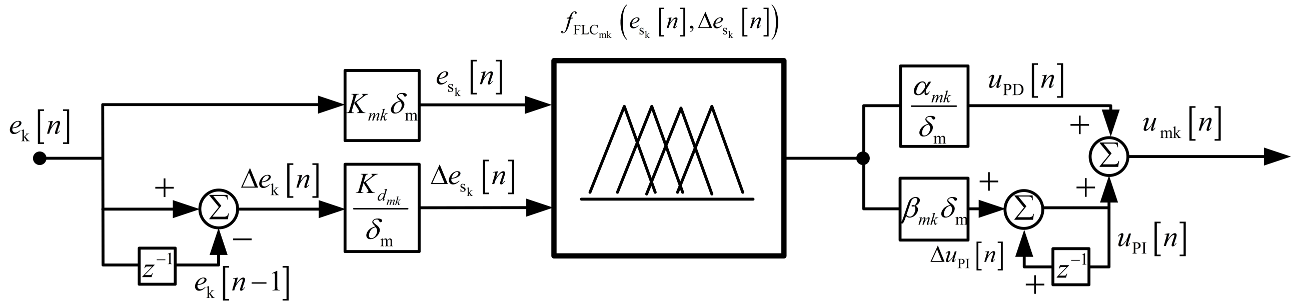

Figure 5. Inner structure of adaptive MIMO fuzzy PID controller [25].

representing the main and coupling controllers is given in Figure 5. Triangular type membership functions given in Figure 2 are used as input membership functions, and the fuzzy rule base in Table 1 is deployed to construct the fuzzy rules. As the inference mechanism and the defuzzification method, product operation and center of gravity method are used respectively.

In the case that δ term is interfused to the standard PID terms, the proportional term is fixed and acquired as $\alpha KP + \beta K_d D$, the integral term is derived as $\beta_0 K_0 \delta^2 P$, and the derivative term is given as $\frac{\alpha K_d D}{\delta^2}$ [25].

4. Simulation results

The tracking and stabilization performances of the introduced adaptation mechanism have been evaluated using the following two input two output(TITO) time delay system.

$$\begin{bmatrix} y_1(s) \\ y_2(s) \end{bmatrix} = \begin{bmatrix} \frac{6}{(s+1)(s+2)(s+3)} & \frac{1}{(s+15)} e^{-0.25\ s} \\ \frac{1}{(s+14)} e^{-0.275\ s} & \frac{6}{(s+1)(s+2)(s+3)} \end{bmatrix} \begin{bmatrix} u_1(s) \\ u_2(s) \end{bmatrix} \tag{7}$$

As given in (7), the coupling dynamics of the system have time delay dynamics. Considering the pade approximation, the time delay can be defined by an infinite number of zero-pole pairs. For this reason, there is a serious interaction between system dynamics. This interaction directly affects the controller performance.

4.1. Tracking performance

The tracking performance of the adaptation mechanism is examined for staircase input signals. The initial values of the fuzzy PIDs are given in Table 2. The performance of the non-adaptive and adaptive MIMO fuzzy PID controller and control signals are depictured in Figure 6 where black trajectory refers to non-adaptive mechanism and blue trajectory belongs to peak observed based adaptation mechanism.

Table 2. Initial controller parameters for tracking case.

Parameters	FLC_{11}	FLC_{12}	FLC_{21}	FLC_{22}
K_{mk}	0.25	0.125	0.125	0.25
$K_{d_{mk}}$	0.25	0.125	0.125	0.25
α_{mk}	0.25	0.125	0.125	0.25
β_{mk}	0.75	0.125	0.125	0.75

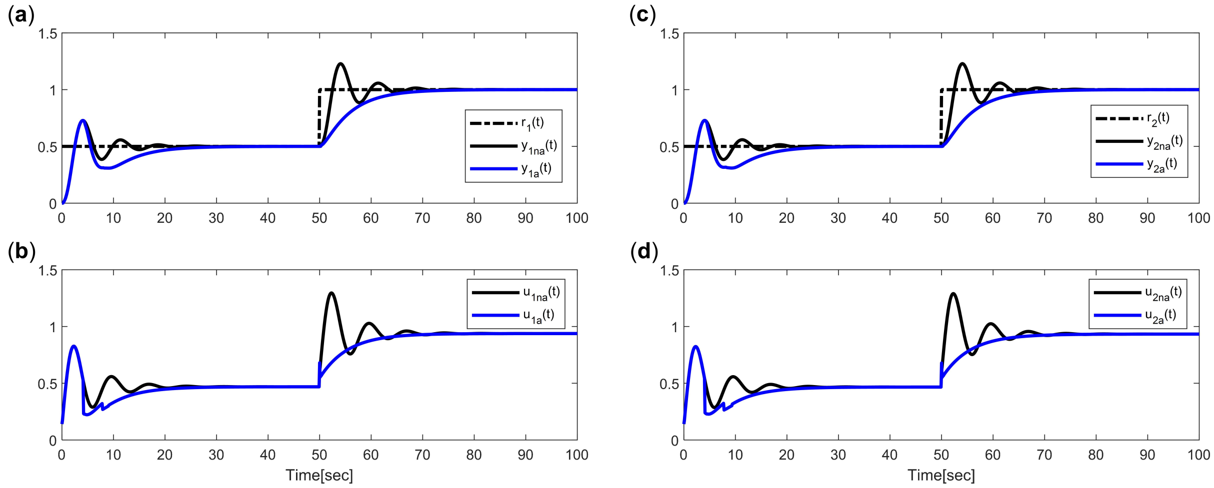

Figure 6. System outputs(**a**,**c**), control signals(**b**,**d**) for non-adaptive and adaptive MIMO fuzzy PID (Tracking Case).

As can be clearly seen from Figure 6(**a**,**c**), oscillations observed in non-adaptive fuzzy controller are suppressed successfully in case the peak observer-based adaptation mechanism is active. The adaptation mechanism is activated with the first peak and improves the control performance. In order to numerically evaluate the performances of the controllers, the behaviors between 50 and 100 sec are observed by taking into account the overshoots(OS %), settling times(t_s) and steady state errors(e_{ss}). While the non-adaptive system has 22.87 % overshoot(OS) and 18.5 sec settling time, peak observer based adaptive system has no overshoot and 15.5 sec settling time. Both controllers has no steady-state errors. These numerical values are tabulated in Table 3.

Table 3. Comparion of non-adaptive fuzzy PID and peak observer based fuzzy PID with respect to overshoot, settling time and steady state error.

Controller Type	OS %	t_s	e_{ss}
Non-adaptive FLC	22.87	18.5	0
Peak Observer FLC	0	15.5	0

The evaluations of the main fuzzy PID controller parameters are shown in Figure 7. The alternation of the coupling fuzzy PID controllers are depictured in Figure 8. By dynamically adapting the controller parameters, a closed-loop system response with less oscillations or even without overshoot can be achieved.

Table 4. Initial controller parameters for stabilization case.

Parameters	FLC_{11}	FLC_{12}	FLC_{21}	FLC_{22}
K_{mk}	0.485	0.2	0.1	0.5
$K_{d_{mk}}$	0.5	0.25	0.2	0.475
α_{mk}	7.5	0.25	0.5	7
β_{mk}	2	0.1	0.2	2

4.2. Stabilization performance

In order to examine the effectiveness of the proposed adjustment mechanism, the controller performance has been evaluated for the stabilization problem. For this purpose, the case that the non-adaptive MIMO fuzzy PID controller cannot control is considered. The initial values of the controller parameters are given in Table 4. As can be seen from Figure 9, non-adaptive MIMO fuzzy PID controller can not control the system dynamics. In case the peak observer based mechanism is activated, the system dynamics can be successfully forced to track the desired reference signals as illustrated in Figure 10. The evaluation of input-output scaling coefficients are given in Figures 11-12.

As given in Figures 11-12, since α and K_d parameter values increase, the derivative laws can increase the resistance against the overshoot and oscillation of the system [1]. Similarly, K and β parameter values decrease, thus decreasing the equivalent integral terms. The fact that the controller parameters are not updated until the next peak value can be considered as one of the most important disadvantages of this structure. However, this structure is open to development.

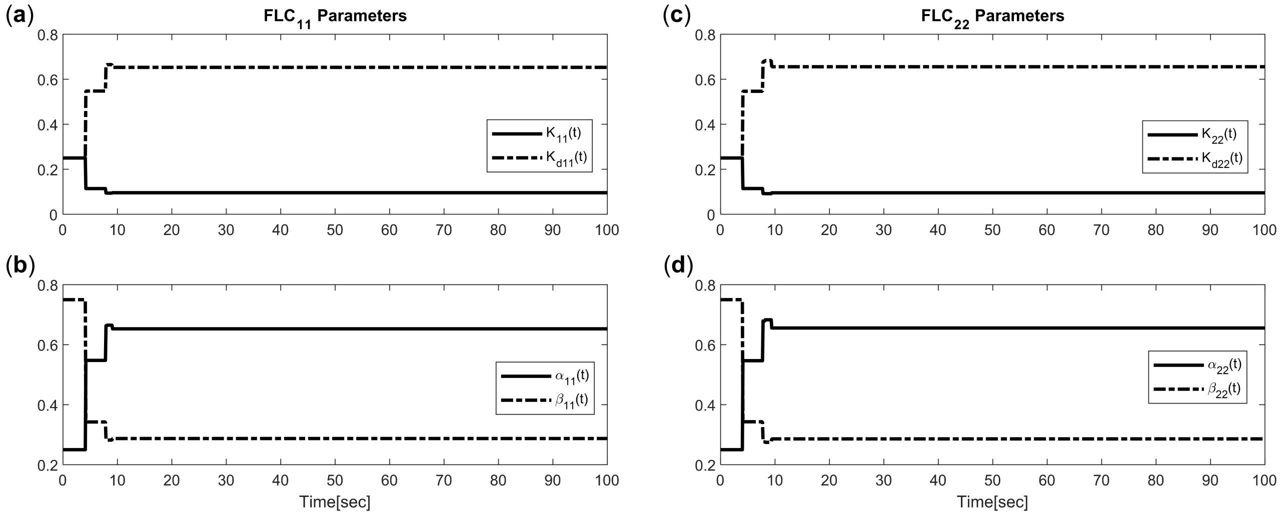

Figure 7. Input scaling coefficients (**a**,**c**), and output scaling coefficients (**b**,**d**) for FLC_{11} and FLC_{22} (Tracking Case) .

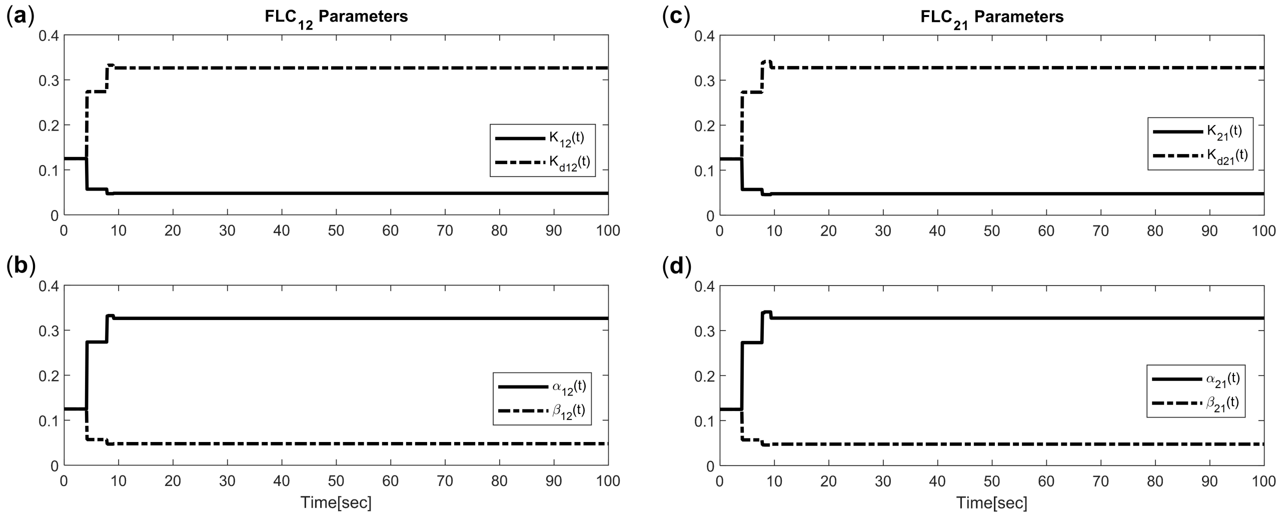

Figure 8. Input scaling coefficients (**a**,**c**), and output scaling coefficients (**b**,**d**) for FLC_{12} and FLC_{21} (Tracking Case) .

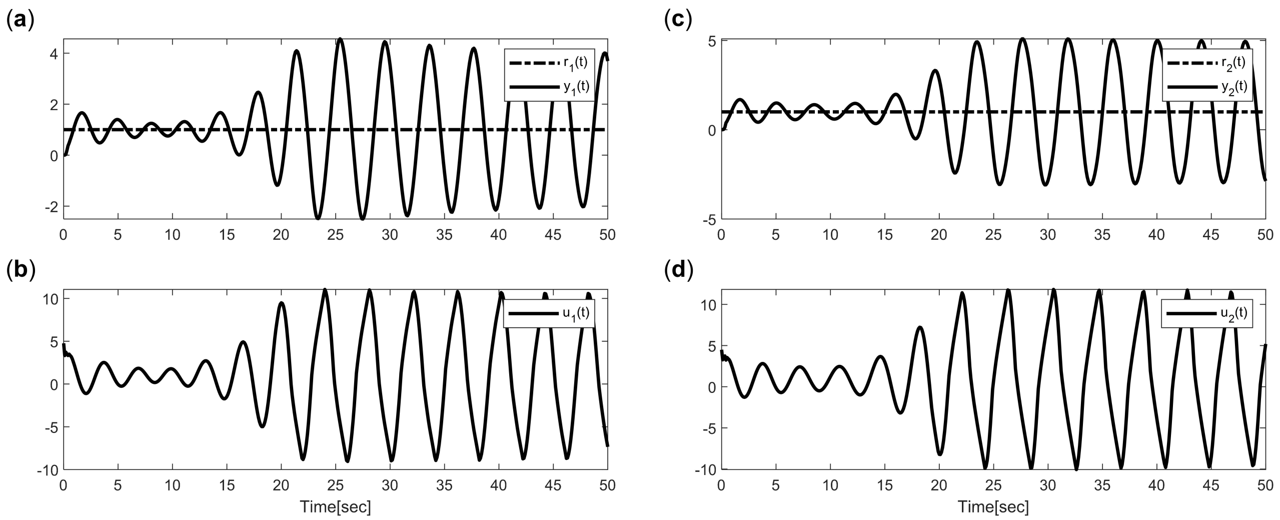

Figure 9. Syste outputs (**a**,**c**), control signals for non-adaptive MIMO fuzzy PID (Stabilization Case).

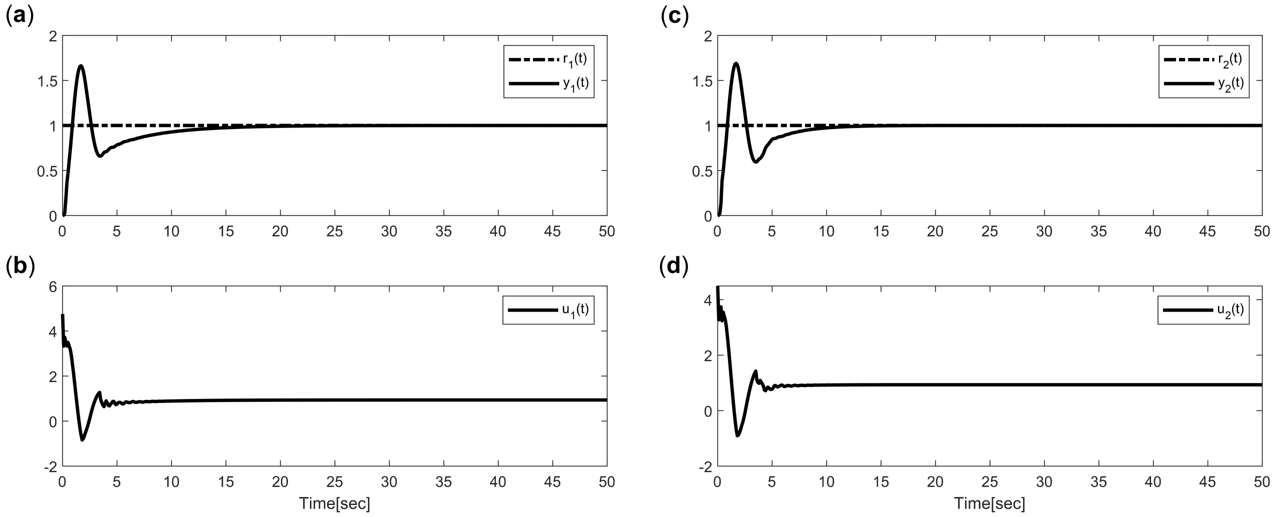

Figure 10. System outputs (**a**,**c**), control signals (**b**,**d**) for adaptive MIMO fuzzy PID (Stabilization Case).

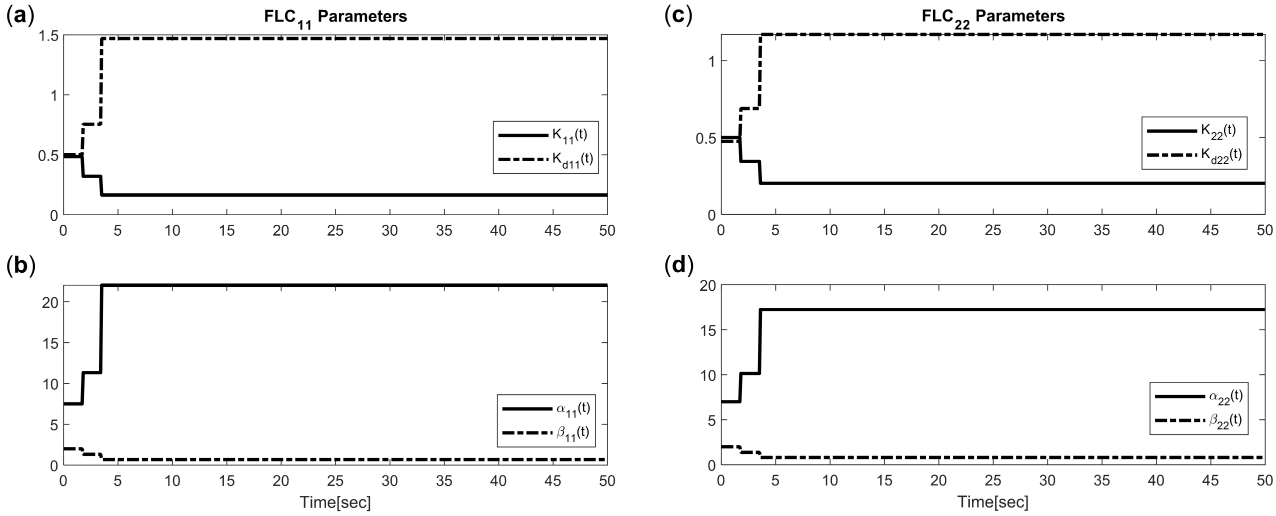

Figure 11. Input scaling coefficients (**a**,**c**), and output scaling coefficients (**b**,**d**) for FLC_{11} and FLC_{22} (Stabilization Case) .

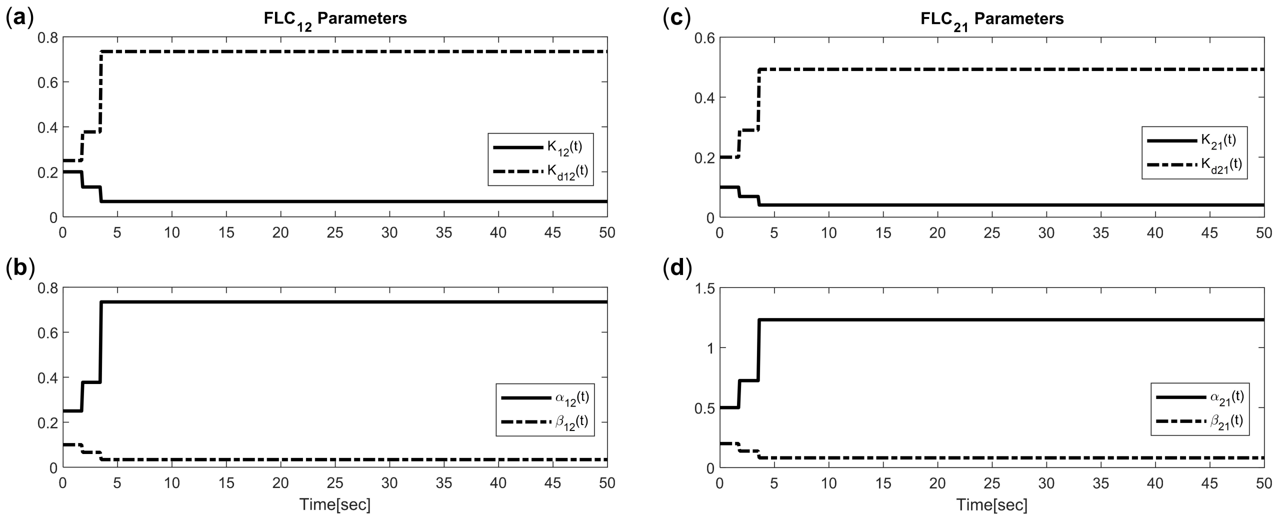

Figure 12. Input scaling coefficients (**a**,**c**), and output scaling coefficients (**b**,**d**) for FLC_{12} and FLC_{21} (Stabilization Case) .

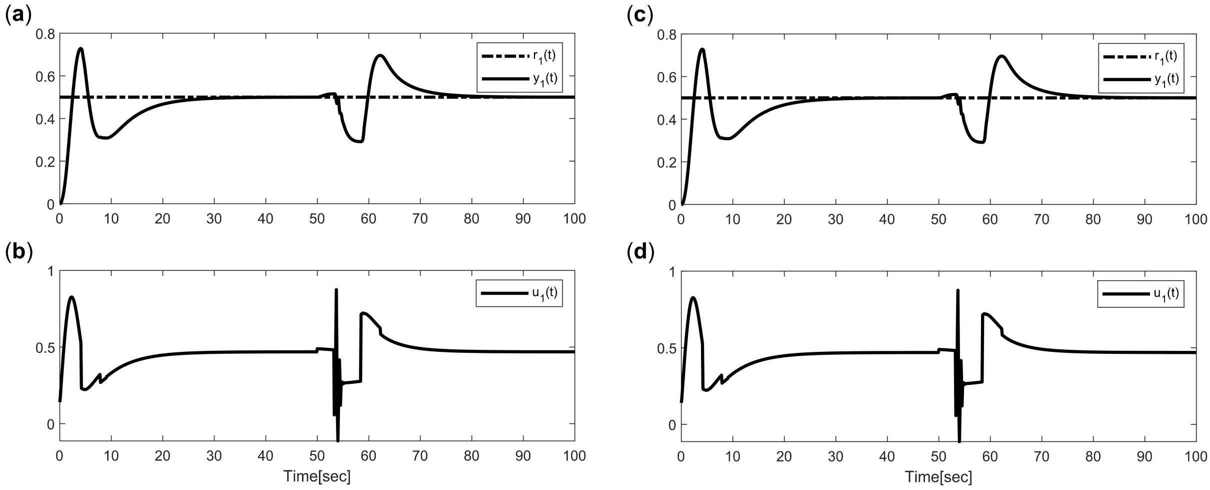

Figure 13. System outputs (**a**,**c**), control signals (**b**,**d**) for adaptive MIMO fuzzy PID (Disturbance Rejection Case)

.

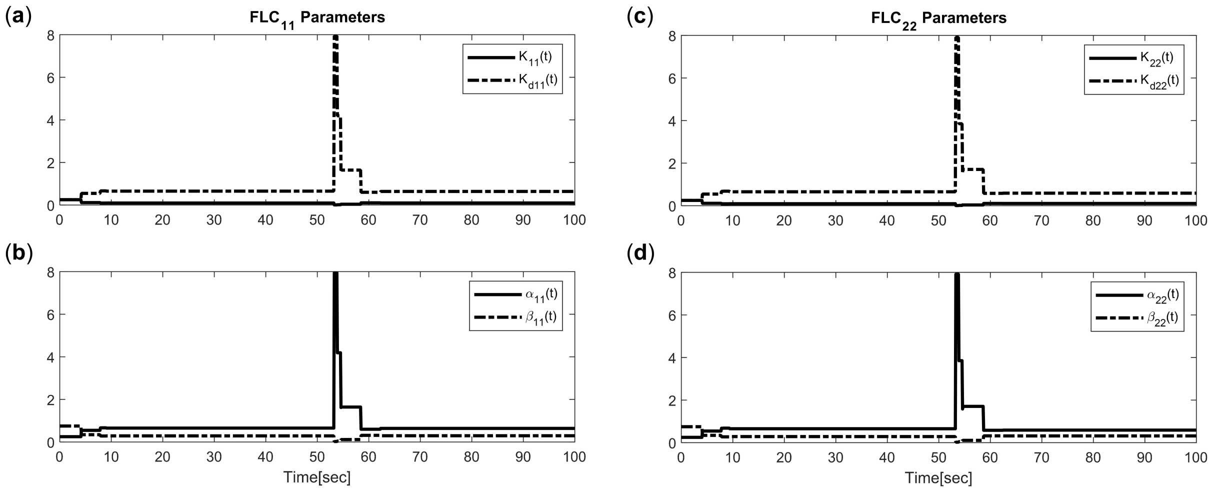

Figure 14. Input scaling coefficients (**a**,**c**), and output scaling coefficients (**b**,**d**) for FLC$_{11}$ and FLC$_{22}$ (Disturbance Rejection Case)

.

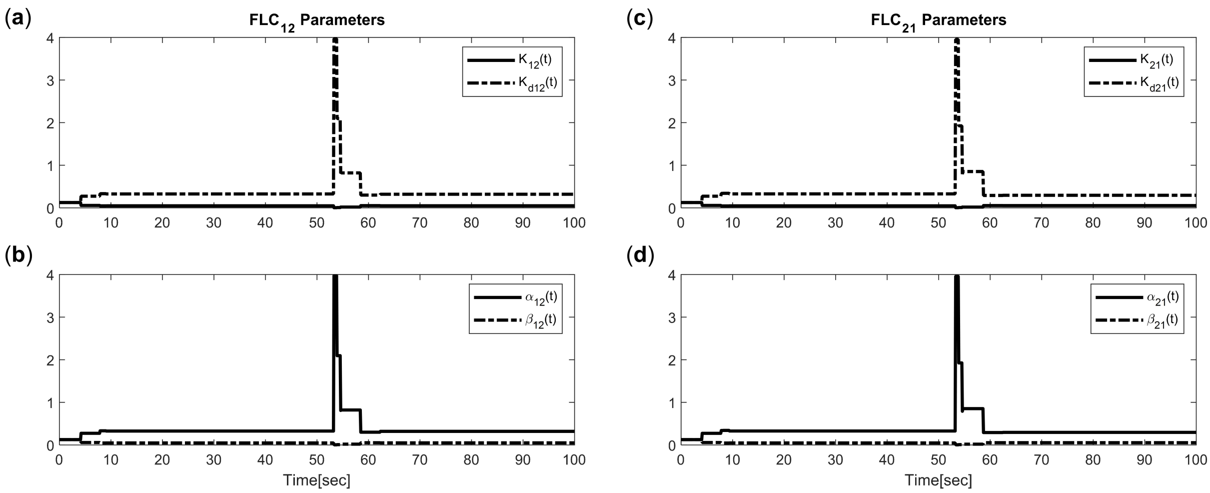

Figure 15. Input scaling coefficients (**a**,**c**), and output scaling coefficients (**b**,**d**) for FLC$_{12}$ and FLC$_{21}$ (Disturbance Rejection Case

.

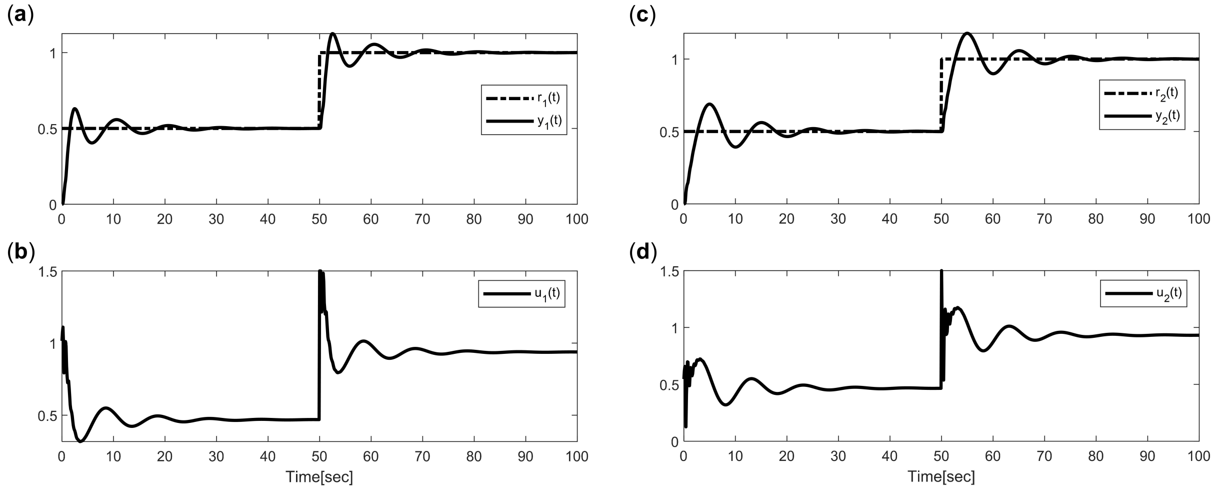

Figure 16. System outputs (**a**,**c**), control signals (**b**,**d**) for MIMO PID (Tracking Performance Case).

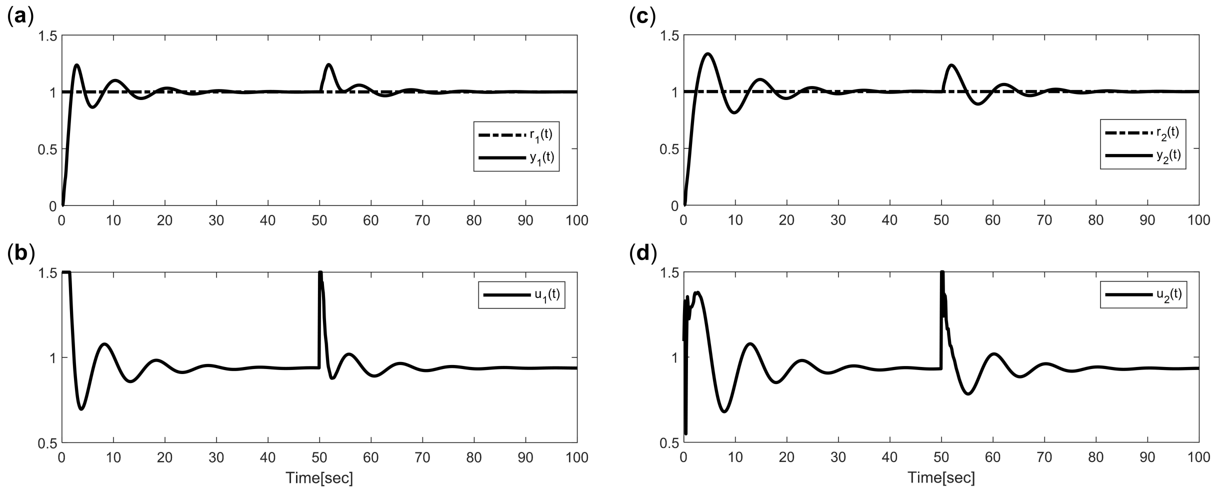

Figure 17. System outputs (**a**,**c**), control signals (**b**,**d**) for MIMO PID (Disturbance Rejection Case).

4.3. Disturbance rejection performance

In order to examine the robustness of the adaptation mechanism, a step type input disturbance is applied to the system at 50 seconds.

The disturbance rejection performance of the adaptation mechanism is illustrated in Figure 13. The adaptations of the controller parameters against the disturbance case are shown in Figures 14-15. The adaptation mechanism readjusts all controller parameters to suppress the disturbance.

As can be clearly seen from Figures 14-15, it can be observed that the coefficients of the derivative parts are very sensitive to disturbances. The introduced adaptation mechanism effectively rejects the step type input disturbances. The disturbance rejection performance of this structure is an open problem to be developed.

4.4. Comparison with conventional PID

The control performances of the non-adaptive fuzzy PID and peak observer based fuzzy PID are compared with the classical PID controller. Equivalent PID_{11} and PID_{22} values have been calculated with the help of the initial values of Fuzzy PID controllers in Table 4. The parameters of the coupling (PID_{12} and PID_{21}) controllers are chosen as 5 times the equivalent parameters obtained via Table 4. Thus, the parameters of MIMO PID are given in Table 5.

Table 5. MIMO PID controller parameters.

Parameters	PID_{11}	PID_{12}	PID_{21}	PID_{22}
K_p	1.25	0.78125	0.78125	1.25
K_i	0.9375	0.390625	0.390625	0.9375
K_d	0.3125	0.390625	0.390625	0.3125

In order to compare the controller performances, the following performance index function is utilized to constitute the comparison table in Table 6.

$$J_c = \int_{t=0}^{t_f} |e_1(t)| + \lambda_1 |\frac{du_1(t)}{dt}| + |e_2(t)| + \lambda_2 |\frac{du_2(t)}{dt}| \, dt \tag{8}$$

where $\lambda_1 = \lambda_2 = 20$ is chosen to minimize and limit the variation of the control signal.

Table 6. Performance comparisons(J_c).

Cases	FPID_{po}	FPID_{n-po}	MIMO PID
Nominal	28.033	31.832	180.422
Disturbance	48.393	48.393	201.04

The tracking and disturbance rejection performances of MIMO PID controller have been illustrated in Figure 16 and 17.

As can be seen from Figure 16, MIMO PID controller provokes too much oscillation and overshoot. As can be seen from Table 6, the performance of MIMO PID is the worst for both tracking and disturbance rejection performances. It is observed that the adaptation mechanism in FLC significantly improves the controller performance.

5. Conclusion

In this paper, an adaptation mechanism for MIMO fuzzy PID controller has been introduced for MIMO systems. The performance of the proposed mechanism is examined on tracking, stabilization and disturbance rejection problems. In order to examine the effect of the proposed adaptation structure in depth, it is compared with non-adaptive fuzzy PID and classical PID controller. The obtained results indicate that the introduced adjustment mechanism provides quite successful tracking, stabilization and disturbance rejection performances for the control of MIMO systems. As future works, the drawbacks of peak observer can be resolved by constantly observing the tracking error, not just at peak times. For this purpose, it is aimed to propose novel adaptive control architectures in which the tracking error is constantly deployed in the adaptation mechanism.

Acknowledgement

This work is supported by the Scientific and Technological Research Council of Turkey(TUBITAK)-BIDEB 2209/A University Students Research Projects Support Programme with the applied number 1919B012113187 (2021/2nd term).

References

[1] Qiao, W.Z. & Mizumoto, M. (1996). PID type fuzzy controller and parameters adaptive method. *Fuzzy Sets and Systems*, 78(1), 23–35.

[2] Chou, C.H. & Lu, H.C. (1994). A heuristic self-tuning fuzzy controller. *Fuzzy Sets and Systems*, 61(3), 249–264.

[3] Jung, C.H. Ham, C.S. & Lee, K.I. (1995). A real-time self-tuning fuzzy controller through scaling factor adjustment for the steam generator of NPP. *Fuzzy Sets and Systems*, 74(1), 53–60.

[4] Maeda, M. & Murakami, S. (1992). A Self-tuning fuzzy controller. *Fuzzy Sets and Systems*, 51(1), 29–40.

[5] Mudi, R.K. & Pal, N.R. (1999). A robust self-tuning scheme for PI- and PD-type fuzzy controllers. *IEEE Transactions on Fuzzy Systems*, 7(1), 2–16.

[6] Zheng, L. (1992). A practical guide to tune of proportional and integral (PI) like fuzzy controllers. *IEEE International Conference on Fuzzy Systems*, 633–640

[7] Chung, H.Y. Chen, B.C. & Lin, J.J. (1998). A PI-type fuzzy controller with self-tuning scaling factors. *Fuzzy Sets and Systems*, 93(1), 23–28.

[8] Chao, C.T. & Teng, C.C. (1997). A PD-like self-tuning fuzzy controller without steady-state error. *Fuzzy Sets and Systems*, 87(2), 141–154.

[9] Woo, Z.H., Chung, H.Y. & Lin, J.J. (2000). A PID type fuzzy controller with self-tuning scaling factors. *Fuzzy Sets and Systems*, 115(2), 321–326.

[10] Hu, B., Mann, G.K.I. & Gosine, R.G. (1999). New methodology for analytical and optimal design of fuzzy PID controllers. *IEEE Transactions on Fuzzy Systems*, 7(5), 521–539.

[11] Ketata, R., Geest, D.D. & Titli, A. (1995). Fuzzy controller: design, evaluation, parallel and hierarchical combination with a PID controller. *Fuzzy Sets and Systems*, 71(1), 113–129.

[12] Kim, B.J. & Chung, C.C. (2001). Design of fuzzy PID controller for tracking control. *Journal of Institute of Control*, 7(7), 1–7.

[13] Kien, C.V., Son, N.N. & Anh, H.P.H. (2020). Adaptive MIMO fuzzy controller for double coupled tank system optimizing by jaya algorithm. 5th International Conference on Green Technology and Sustainable Development (GTSD), Ho Chi Minh City, Vietnam, 495–499.

[14] Cherrat, N., Boubertakh, H. & Arioui, H. (2018). Adaptive fuzzy PID control for a class of uncertain MIMO nonlinear systems with dead-zone inputs' Nonlinearities. *Iranian Journal of Science and Technology, Transactions of Electrical Engineering*, 42, 21–39.

[15] Gil, P., Lucena, C., Cardoso, A. & Palma, L.B. (2015). Gain tuning of fuzzy PID controllers for MIMO systems: a performance-driven approach. *IEEE Transactions on Fuzzy Systems*, 23(4), 757–768.

[16] Yordanova, S., Yankov, V. & Jain, L. (2017). MIMO fuzzy logic supervisor-based adaptive control using the example of coupled-tanks levels control. International Journal of Innovative Computing, *Information and Control*, 13(2), 453–470.

[17] Pinto, M.B.B., Mota, J.G.R. & Almeida, O.M. (2010). PID self-adjustable fuzzy logic MIMO case: method and application. 9th IEEE/IAS International Conference on Industry Applications, Sao Paulo, Brazil, 1–6.

[18] Yeşil, E., Güzelkaya, M. & Eksin, I. (2003). Fuzzy PID controllers: an overview. 3rd Triennial ETAI International Conference on Applied Automatic Systems, Ohrid, Macedonia, 1–8.

[19] Kumar, V., Nakra, B.C. & Mittal, A. (2011). A review of classical and fuzzy PID controllers. *International Journal of Intelligent Control and Systems*, 16(3), 170–181.

[20] Güzelkaya, M., Eksin, I. & Yeşil, E. (2003). Self-tuning of PID-type fuzzy logic controller coefficients via relative rate observer. *Engineering Applications of Artificial Intelligence*, 16(3), 227–236.

[21] Karasakal, O., Yeşil, E., Güzelkaya, M. & Eksin, I. (2003). An implementation of peak observer based self-tuning fuzzy PID-type controller on PLC. 3rd International Conference on Electrical and Electronics Engineering, ELECO, Bursa, Turkey, 1–5.

[22] Yeşil, E., Kumbasar, T., Dodurka, M. & Sakallı, A. (2014). Peak observer based self-tuning of type-2 fuzzy PID controller. 10th IFIP International Conference on Artificial Intelligence Applications and Innovations (AIAI), Rhodes, Greece, 487–497.

[23] Uçak, K. & Günel, G.Ö. (2017). Generalized self-tuning regulator based on online support vector regression. *Neural Computing and Applications*, 28, S775–S801.

[24] Uçak, K. & Günel, G.Ö. (2017). Fuzzy PID type STR based on SVR for nonlinear systems. 10th International Conference on Electrical and Electronics Engineering (ELECO), Bursa, Turkey, 764–768.

[25] Arslanturk, B. & Uçak, K. (2022). An improved adaptive fuzzy PID controller based on peak observer for nonlinear dynamical systems. International ONLINE Conference on Mathematical Advances and Applications (ICOMAA-2022), Istanbul, Turkey, 85–91.

[26] Bouallegue, S., Haggege, J., Ayadi, M. & Benrejeb, M. (2012) PID-type fuzzy logic controller tuning based on particle swarm optimization. *Engineering Applications of Artificial Intelligence*, 25(3), 484–493.

[27] Karaman, K., Bekaroğlu, Y.T., Söylemez, M.T., Uçak, K. & Günel, G.Ö. (2015). Controlling 3-DOF helicopter via fuzzy PID controller. 9th International Conference on Electrical and Electronics Engineering (ELECO), Bursa, Turkey, 869–873.

Kemal Uçak *received his M.Sc. and Ph.D. degree in Control and Automation Engineering from Istanbul Technical University in 2012 and 2016 respectively. He has been a member of the faculty at Istanbul Technical University, and Muğla Sıtkı Koçman University where currently he is an Assistant Professor in the Department of Electrical and Electronics Engineering. He carried out his postdoctoral studies at Massachusetts Institute of Technology (MIT) in 2020. His research interests pertain to adaptive control, artificial intelligence, machine learning, and robust control. Dr. Uçak is a member of IEEE and IFAC.*

https://orcid.org/0000-0001-7005-7940

Beyza Nur Arslantürk *is a graduate student in Electrical and Electronics Engineering at Muğla Sıtkı Koçman University. Her research interests are adaptive control, adaptive fuzzy control architectures, and fuzzy system identification.*

https://orcid.org/0000-0001-5358-8811

An International Journal of Optimization and Control: Theories & Applications
ISSN: 2146-0957 eISSN: 2146-5703
Vol.13, No.2, pp.151-160 (2023)
https://doi.org/10.11121/ijocta.2023.1354

RESEARCH ARTICLE

Optimal C-type filter design for wireless power transfer system by using support vector machines

Haris Calgan *

Department of Electrical-Electronics Engineering, Balikesir University, Turkey
haris.calgan@balikesir.edu.tr

ARTICLE INFO

Article history:
Received: 18 January 2023
Accepted: 31 March 2023
Available Online: 9 July 2023

Keywords:
C-type power filter
Support vector machine
Optimization
Wireless power transfer
Electrical vehicle

AMS Classification 2010:
68Q32, 68T01, 62J02

ABSTRACT

The rapid increase in the number of Electrical Vehicles (EVs) will bring difficulties in the management of charging process and pose serious grid problems at low voltage levels. Particularly, with employment of wireless power transfer (WPT) system in a charging station, harmonic interference will increase. The main reason of that poor power quality lies on high frequency square wave output of transmitter side of WPT. In this study, a support vector machine (SVM) is proposed to design an optimal C-type passive filter in order to mitigate voltage and current total harmonic distortions (THD) of WPT system. Hereby, SVM-based model is constructed which consists of THD indices and power factor (PF) as outputs whereas filter parameters are inputs. The main aim of optimization process is minimization of distortions and correction of PF while searching the filter parameters. Particle swarm optimization (PSO) algorithm is employed to find the optimal filter parameters. To show the efficiency of proposed method, simulation studies are carried out on Matlab®/Simulink™ environment. It is observed that voltage total harmonic distortion (THD_v) and current total harmonic distortion (THD_i) are calculated as 1.03%, 2.23%, respectively, and the power factor is improved to 0.995% when the designed C-type filter is utilized.

1. Introduction

In recent years, carbon-based energy generation systems that cause environmental damage such as global warming, air pollution, water pollution, etc. have begun to replace systems that produce electrical energy through renewable and environmental friendly [1]. In addition, vehicles using carbon-based fuels are one of the important causes of environmental pollution. In order to solve this problem, it is great importance that vehicles working with electric energy should become widespread. In the event that the use of electric vehicle (EV) becomes widespread, another problem, which is efficient charging station design and easy access to stations, comes to the fore. According to the IEC61851 standard prepared for electric vehicle charging stations (EVCS), it is allowed to draw currents up to 32 A in residential uses and draw up to 250 A in alternating current in different charging modes. However, the rapid increase in the number of EVs will bring difficulties in the management of the charging process and pose serious grid problems at low voltage levels [2, 3]. Increasing load demand will create the need for additional facility investment. By using various heuristic algorithms, the effects of EVs on the distribution grid can be reduced and the load profile can be slightly smoothed [4]. However, it is still difficult to meet the desired electrical energy need without a facility investment.

Wireless charging methods, on the other hand, have come as a major innovation to the EV industry. Compared to conventional charging units, they do not require power connection. Wireless power transfer (WPT) is divided into static and dynamic structures. Static wireless power transfer systems by placing a single coil under a parked vehicle were proposed by General Motors in 1998 [5]. WPT is a safer and more convenient method for electrical charging due to its cable-free structure and resistant to environmental factors such as water and dust. When the reported studies are examined, it is seen that WPT is frequently employed in charging EVs. Li and Mi [6] present a study on magnetic coupling design in wireless power

*Corresponding author

transfer for EVs. They show the circuit compensation with power control via converters. Musavi and Eberle [7] compared the current wireless charging technologies for EVs on the basis of values such as efficiency, cost, capacity, and system complexity. They present two different wireless/built-in fast charging circuit models which are integrated into the vehicle, separately for passenger cars and large public transportation vehicles. Sun et al. [8] review existing wireless charging technologies for EVs and their applications. They examine different types of wireless charging applications for EVs and their economic feasibility is analyzed. In addition, electromagnetic field shielding methods for WPTs are also investigated.

Most of the aforementioned WPT applications include DC-DC or AC-DC converters. In fact, AC-DC converters in WPT systems are more convenient for grid-connected applications [9]. However, these converters contain high-frequency triggering and induce harmonic distortion on the voltage and current waveforms. These harmonics may cause unexpected impacts on the equipment in the system such as heating, malfunction on the actuator and line loss of the network [10]. Therefore, filters are generally designed in order to cope with these harmonics. Among the power filter types, passive filters are easy to implement and cost-effective. So, they are widely employed in power systems. Further, they are preferred to handle the harmonics particularly in electrical vehicle charging station. In this regards, Yang et al. [11] design a single-tuned passive filter which combines reactance and capacitor and creates a low resistance channel for specific order harmonics. According to their analyses, they find that the fifth and seventh orders are the most part of harmonics of EVCS. By using the designed single-tuned filter they decrease the THD_i to a low level. Zao and Yue [12] take the effects of the electric vehicle six-pulse rectifier charger into account and design single-tuned filter as well as high pass filter. Their simulation results show that a good harmonic suppression is achieved with the presented passive filter. Khudher et al. [13] present the design of output filter with shunt passive filters to decrease impact of electrical car charging stations on power grid harmonics. They reduce the THD_i from 46.19% to 3.73% by combining the double-tuned filters with high pass filter.

Alongside the conventional filters such as combination of single-tuned LC and high pass filter, parallel resonance can be avoided in the system by using C-type passive filter. Furthermore, it has lower loss than high-pass filter at fundamental frequency [14]. Due to these advantages, it is widely used in different applications such as loading capability improvement of transformers under non-sinusoidal conditions [15], filtration of higher harmonics injected into the transfer system by arc furnaces [16] and capacity reduction of hybrid power quality conditioner in co-phase traction power system [17].

According to the author's knowledge, there is lack of study in the implementation of C-type passive filter for WPT system which is the main contribution of this study. However, an optimal design of a C-type filter requires the analysis of system with single-phase equivalent circuit. Therefore, most of the equivalent circuit parameters such as linear impedance parameters of load and Thevenin equivalents have to be known. However, some studies construct a model between THD values and specified input parameters. In this context, Response Surface Method [18] and comparison of artificial neural network and SVM [19] are reported. However, in [19], SVM method is employed only for harmonic estimation.

In this study, SVM-based optimal design of C-type passive filter is proposed for an EVCS which contains AC-DC converter, a high frequency single phase inverter and WPT. The main advantage of the proposed method is no need of equivalent circuit parameters of the system while determining the model. THD_v, THD_i and PF are chosen as output parameters of the model whereas the filter parameters are assigned as input parameters. Afterwards, a traditional PSO method is applied on that model to minimize THD_v and THD_i as well as to maximize PF.

The organization of this manuscript is as follows: Section 2 describes EVCS with WPT. Section 3 defines the main problem of this study with THD indices. Section 4 explains C-type passive filter design. Section 5 details SVM-based modeling and PSO based optimization studies. Section 6 contains results and discussion. Section 7 is the conclusion.

2. Description EVCS with WPT system

The proposed EVCS basically contains three-phase rectifier, DC-link buffer, full-bridge resonant inverter, series-resonant LC tank, vehicle-side rectifier. Figure 1 shows the general scheme of system with C-type filter which is detailed in the next sections. In this system, proposed resonant inverter is grouped as Class D and is most popular for practical WPT systems [20].

As shown in Figure 1, proposed EVCS has series-series compensation topology. In this method, L_p, C_p, L_s and C_s stand for primary, secondary coils and compensated capacitors, respectively. If the primary and secondary coil currents are defined as I_p and I_s, effect of the secondary impedance to the primary side is expressed as in Eq. (1)

$$Z_r = \frac{-j\omega M I_s}{I_p} = \frac{\omega^2 M^2}{Z_s} \tag{1}$$

where M denotes the mutual inductance and calculated by

$$M = k\sqrt{L_p L_s} \tag{2}$$

where k is the coupling coefficient and ranged between 0 and 1 ($0 < k \le 1$). The impedance of the secondary side Z_s is determined as in Eq. (3).

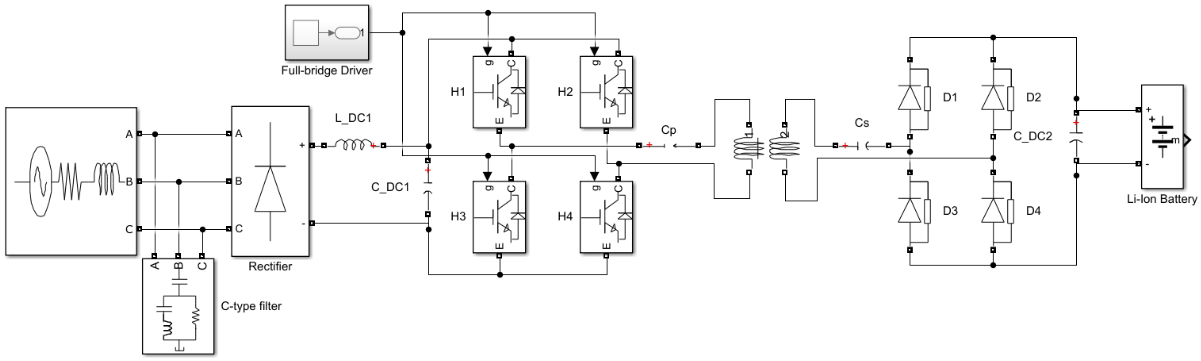

Figure 1. Block scheme of the EVCS

$$Z_s = j\omega L_s + \frac{1}{j\omega C_s} + R_L \quad (3)$$

where R_L is the load resistance and resonant frequency is calculated by $\omega_r = 1/\sqrt{L_s C_s}$. Consequently, the equivalent load impedance on the primary side is determined as in Eq. (4).

$$Z_s = j\omega L_p + \frac{1}{j\omega C_p} + Z_r \quad (4)$$

Alongside the WPT of EVCS, 3-phase, 380 V, 50 Hz AC grid voltage is rectified to 360 V_{dc} on the DC bus. Afterwards, it is inverted to 360 V, 30 kHz square wave AC voltage by means of full bridge resonant inverter. This signal is transferred to secondary side wirelessly. Lastly, vehicle-side converter rectifies the AC voltage to 360 V DC voltage in order to charge the lithium-ion batteries. Equivalent circuit parameters of the designed WPT system are given in Table 1. With given circuit parameters, resonant frequency is calculated as 30 kHz, approximately.

Table 1. The equivalent circuit parameters of WPT

Parameter	Value
C_p	105.74e^{-9} F
C_s	109.69e^{-9} F
L_p	266.16e^{-6} H
L_s	256.79e^{-6} H
M	85.46e^{-6} H

3. Problem definition

Regarding the presented EVCS, full-bridge resonant inverter converts the 360 V DC input into 360 V AC square wave output. The Fourier transform of the converted square wave is given by Eq. (5) [21].

$$U_{TX} = \frac{4}{\pi} U_{DC} \sum_{n=1,3,5}^{\infty} \frac{1}{n} \sin(n\omega_r t) \quad (5)$$

where U_{TX} is the output voltage of full-bridge resonant inverter as well as the input voltage of the WPT transmitter side. U_{DC} is the input of inverter when ω_r is chosen as resonant frequency and n is the harmonic order. It can be seen from Eq. (5) that U_{TX} includes harmonics. According to the harmonic analysis of WPT system given in [21], despite the harmonic current is reduced effectively by adjusting Q value of the resonant circuit, in some cases, harmonic current required to be reduced. So, the balance between Q value and harmonic voltage loaded on the transmitter coil should be adjusted accurately. Moreover, fundamental energy to harmonic energy ratio is given by Eq. (6).

$$\frac{P_{Harmonic}}{P_{Fundamental}} = \frac{1}{n^2} \frac{1}{\left(n\omega_r \frac{L}{R}\right)^2 (k - \frac{1}{k})^2 + \frac{1}{k^2}} \quad (6)$$

It can be deduced from Eq. (6) that the energy of harmonic transmission decreases since the k decreases. However, when the k is chosen around 0.9, maximum harmonic transmission ratio is observed [21]. It is also proven that when the harmonic-related reactive power accumulation increases, efficiency of the inverter-driven WPT system decreases. So, an appropriate control for inverter can overcome the harmonic related reactive power accumulation [22]. Additionally, aforementioned studies generally employ DC source and focus on harmonics on the WPT side. Since the EVCS is fed by the grid, the energy consumed via WPT draws non-sinusoidal currents from the grid. THD_i and THD_v can be calculated as in Eqs. (7) and (8) considering the fundamental frequency active power (P_1), reactive power (Q_1), fundamental frequency RMS current (I_1) and sinusoidal-rated supply voltage (V_1) [23].

$$THDi = \frac{\sum_{n \neq 1} I_n^2}{I_1} \quad (7)$$

$$THDv = \frac{\sum_{n \neq 1} V_n^2}{V_1} \quad (8)$$

where I_n and V_n stand for n^{th} harmonic current and voltage. Additionally, PF can be calculated as in Eq. (9) in terms of both powers.

$$PF = \frac{P_1}{V_1 I_1} = \cos\varphi_1 \quad (9)$$

where φ_1 denotes phase angle difference between fundamental frequency voltage and current. To avoid drawing of harmonically contaminated currents and improve PF, C-type passive filter is designed to fulfill the desired criteria which are minimization of THD_v, THD_i as well as maximizing the PF.

4. C-type passive filter design

Circuit of the typical C-type passive filter is given in Figure 2. Design procedure of the filter begins with the determination of reactive power Q_t at fundamental frequency f_0, which is 50 Hz, regarding to nominal voltage U_n and tuning frequency f_n.

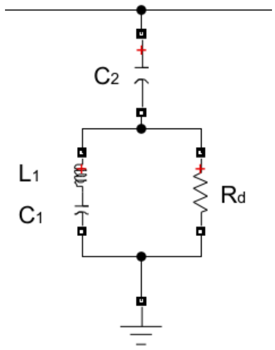

Figure 2. Circuit of the C-type filter

After specifying the necessary parameters, C_2 should be chosen large enough in order to meet the desired reactive power of the system. Afterwards, C_1 is calculated by means of following equation [24].

$$C_1 = C_2\left[\left(\frac{f_n}{f_0}\right)^2 - 1\right] \tag{10}$$

Then, series L_1-C_1 are tuned to f_0 as follows:

$$f_0 = \frac{1}{2\pi\sqrt{L_1 C_1}} \tag{11}$$

From Eq. (11), L_1 value is calculated since the tuning is realized. In order to have more effective filter a low value quality factor Q at the designed frequency f_n is chosen within 2 or 3. Damping resistance R_d is specified as in Eq. (12).

$$R_d = \frac{2\pi f_n L_1}{Q} \tag{12}$$

It is seen from Eqs. (10), (11) and (12) that the design problem of a C-type passive filter can be solved via foreknowledge of the system characteristics. In this study, without knowledge of these parameters an optimal filter design is aimed which employs a support vector machine-based modeling technique. Note that, alongside the C-type passive filter a serial connected input inductance L_i is also employed in the system.

5. Support vector machine-based optimization of C-type passive filter

This study intends to find optimal C-type passive filter parameters. While searching filter parameters, THD_v, THD_i values are aimed to be minimized and PF values is aimed to be close to 1. Hence, SVM regression method is utilized to model the system, PSO is operated to reach optimal filter parameters. The entire modeling and optimization processes are given as flowchart in Figure 3. The proposed method mainly targets to obtain optimal C-type filter parameters. But, modeling with high accuracy is the key procedure. Since the SVM is not able to well perform in estimation, PSO algorithm will not give the best filter parameters. Therefore, high accuracy in modeling is necessary to be succesful in optimization. After ensuring the model certainty, for a given search space, PSO is employed to reach desired metrics by means of calculating the best filter parameters. The details of modeling and optimization are reported in subsections.

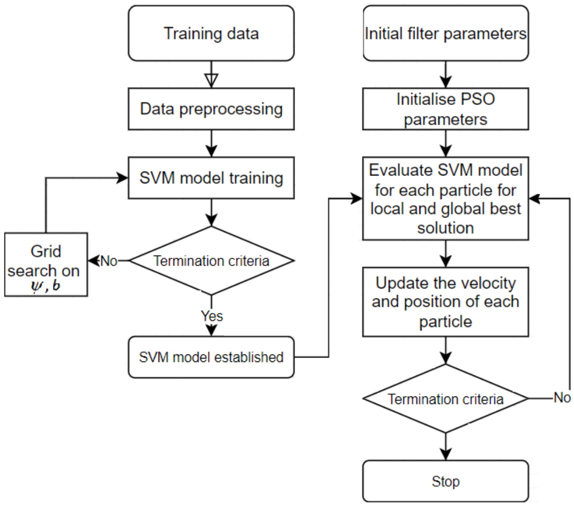

Figure 3. Flowchart of SVM-based optimization of C-type filter parameters

5.1. Support vector machine-based modelling

There are lots of machine learning-based modeling method in literature such as RSM [25], Artificial Neural Network [26] and Long Short-term Memory [27]. Support vector machine is also one of a machine learning methods and was proposed presented in 1995 by Cortes and Vapnik [28]. The general structure of an SVM is given in Figure 4. It is widely employed in the literature for the purpose of estimation, analysis and regression problems [19]. The main advantage of SVM is showing better performance against getting stuck with local minimum problem [29].

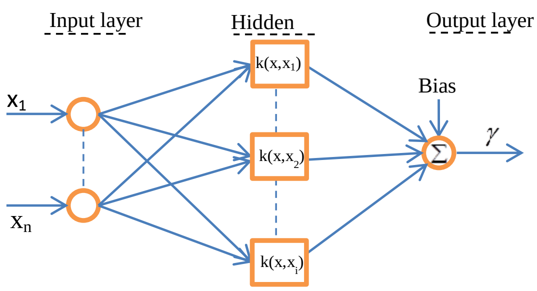

Figure 4. General scheme of SVM

Support vector regression (SVR) is an utilization of SVM and uses distinct kernel functions such as polynomial, radial basis function, sigmoid and linear. Since a training dataset contains input vector x_i and output vector γ_o, regression model can be formed as given in Eq. (13).

$$\gamma_o - \psi^T \theta(x_i) + b \quad (13)$$

where ψ, b, $\theta()$ stand for weighting vector, bias and nonlinear mapping function, respectively. In order to determine weighting parameters of regression model, the distance between margin and input vector that lie on the wrong side must be measured. Furthermore, the confidence interval and the empirical risk should be adjusted by penalty parameters. These two requirements yield a minimization problem as given in Eq. (14) to be solved [30].

$$\frac{1}{2}\psi^2 + k_p \sum_{i=1}^{N} \xi_i + \xi_1^{(*)} \quad (14)$$

where ξ_i denotes the slack variable and k_p is a constant penalization parameter. Weighting parameters are calculated when the function given in Eq. (14) is minimized. Lastly, Lagrange multipliers are introduced to solve the support vector regression problem.

Since this study aims to determine optimal C-type passive filter, input-output data of SVM are appointed as filter parameters and harmonic values, respectively. To elaborate more, filter parameters which are given in Eqs. (10), (11) and (12) are denoted as inputs, THD_v, THD_i and PF values are specified as outputs. Training dataset is formed by input-output data which is derived from simulation studies. Matlab®/Simulink™ program is chosen as simulation platform and min-max values of inputs are determined as given in Table 2. Considering the increment (step) values, simulation is run 180 times and THD_v, THD_i and PF values are recorded to be used in modeling procedure.

Table 2. Filter parameters constraints

Parameter	min	step	max
C_2	$1.2e^{-4}$	$2e^{-5}$	$2e^{-4}$
f_n/f_0	3	2	7
Q	3	2	7
L_i	$5e^{-3}$	$5e^{-3}$	$2e^{-2}$

After constructing the input-output training data set Matlab® '*fitrsvm*' command is employed to train SVM regression model. Note that normalization pre-process on the dataset is applied before training by using maximum values of each parameter as given in Table 2. Data mapping is occurred with Gaussian kernel functions and all elements of the predictor matrix divided by the value of appropriate KernelScale (auto). Using the chosen specifications, SVM model is obtained with 0.94 r-squared (R^2). To summarize, SVM predicts harmonic distortions and power factor with the high accuracy for the given filter parameters. It proves that the model can be used in optimization precisely.

5.2. Particle swarm optimization

PSO method is used for different applications in industry such as renewable energy [31], automation [32] and adaptive wireless power transfer [33]. Specifying the C-type filter parameters is a complex problem due to the nonlinearity of the EVCS. The performance of the filter can be improved by reducing THD_i and THD_v likewise by approximating to 1 in terms of PF. Additionally, it is well-known fact that THD_i and THD_v should be kept under limitation defined by IEEE Standard 519-2014 [34]. The THD_i limit is recommended as 8% when the ratio between maximum short-circuit current (ISC) and maximum demand load current (IL) at common coupling point (PCC) is less than 20. On the other hand, THD_v limit is defined as 5% since the bus voltage is less than 1 kV. Considering these limitations and handling PF as a percentage, the fitness function (FF) is designed by taking the limits equal to each other as 5%. Therefore, in this study, after well modeling of the EVCS with SVM, a fitness function is identified to be minimized and as given in Eq. (15). Note that, THD_i, THD_v and PF values given in Eq. (15) are predicted by SVM during the optimization process.

$$FF = w_1.THD_i + w_2.THD_v + w_3(1 - PF) \quad (15)$$

where w_1, w_2, w_3 are weightings of each parameter. As shown in Eq. (15), optimization problem has two parameters to be minimized and third parameter to be maximized which yields multi-objective optimization problem. However, considering the significance and goal value of each parameter, the problem can be converted to a single objective optimization by choosing the weightings equal. Hereby, minimization of THD values and maximization of PF can be done with equal importance. A set of lower and upper bounds on the design variables are given in Table 2. The optimization problem to get mentioned values under predefined constraints can be summarized as given in Eq. (16).

In this problem, search space is defined by Ω. The problem has four filter parameters to be optimized, where their general form can be indicated as $fp_{\min} \le fp \le fp_{\max}$. Note that C_1 and R_d are not included in optimization problem. Because, these two parameters are calculated by Eqs. (10) and (12), since the given parameters are determined.

$$\underset{fp \in \Omega}{Min}\ FF(fp)$$
$$subject\,to:\Omega \begin{cases} 1.2e^{-4} \le \quad C_2 \quad \le 2e^{-4} \\ 3 \le f_n / f_0 \le 7 \\ 1e^{-3} \le \quad Q \quad \le 7 \\ 5e^{-3} \le \quad L_i \quad \le 2e^{-2} \end{cases} \quad (16)$$

Classical PSO algorithm of Matlab® is used in this study. The parameters of PSO are given in Table 3. As mentioned before, applied SVM is done with normalized dataset during the modelling step. Therefore, each parameter of *fp* is normalized using the same method. After several optimization processes, best *FF* is obtained as 3.27 when the filter parameters are calculated as given in Table 4. By using ‘rng’ function of Matlab®, random number generation is controlled for reproducibility. Hereby, it is confirmed in each trial that, PSO is started with different initialization which yields not trapping by a local minimum solution.

Table 3. PSO tuning parameters

Parameter	Value
Function tolerance	$1e^{-6}$
Initial swarm span	2000
Min neighbors fraction	0.25
Self-adjustment weight	1.49
Swarm size	[100,300]

Table 4. Obtained filter parameters

Parameter	Value
C_2	$1.6e^{-4}$ F
C_1	$9.6e^{-3}$ F
L_1	$1.1e^{-3}$ H
L_i	$2e^{-2}$ H
R_d	121 Ω

Regarding to the obtained C-type filter, performance of the system is analyzed in the next section.

6. Results and discussion

This section presents and compares numerical results obtained by simulating EVCS with and without C-type passive filter. Matlab®/Simulink™ environment is employed for simulation studies. For the simulated EVCS, the equivalent circuit parameters are chosen as descripted in Section 2. Additionally, lithium-ion battery with a rectifier is connected to the secondary side of WPT. The system is supplied by three phase grid voltage which is 400 V in fundamental frequency and specifications of battery are as follows; nominal voltage=360 V, rated capacity=100 Ah, initial state-of-charge (SoC)=50%, battery response time=10 s, battery internal resistance=0.036 Ω.

Initially, the system is simulated without passive filter. Figure 5 shows the charging current and state of charge of lithium-ion battery. It is seen from figure that battery drawn around 15 A from DC link and keep being charged. It is clear that charging process works effectively.

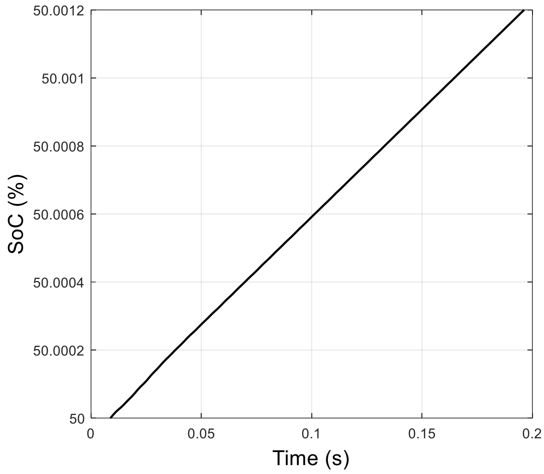

(a) State of charge

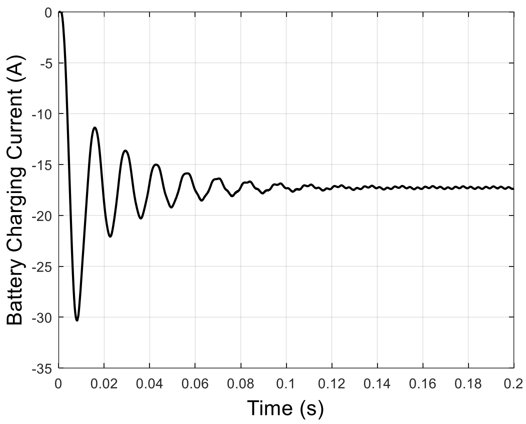

(b) Change in charging current

Figure 5. Charging of the battery without C-type filter

In the case of operating the EVCS without filter, waveform of the voltage at the point of common coupling is demonstrated in Figure 6a with harmonic spectrum. The magnitude and harmonic spectrum of current drawn from the grid is obtained as illustrated in Figure 6b. It is seen from Figure 6 that THD_v and THD_i are measured as 13.99% and 22.23%, respectively. The system has also low PF which is measured as 0.91. It is clear that THD values are above the limits and should be mitigated. Moreover, mitigation of harmonics may increase the effectiveness of the WPT and may accelerate the battery charging process.

Measured voltage and current with harmonic spectrums are illustrated in Figure 7 when the system is operated with designed C-type filter. In this case, voltage and current harmonics are reduced to 1.03% and 2.23%, respectively. PF is improved to 0.995. The absolute differences between the results show that the designed C-type filter keeps the THD_v, THD_i indices and PF within limits defined by IEEE Standard 519-2014. So, the results show that optimal C-type filter is determined effectively by using the SVM-based approach.

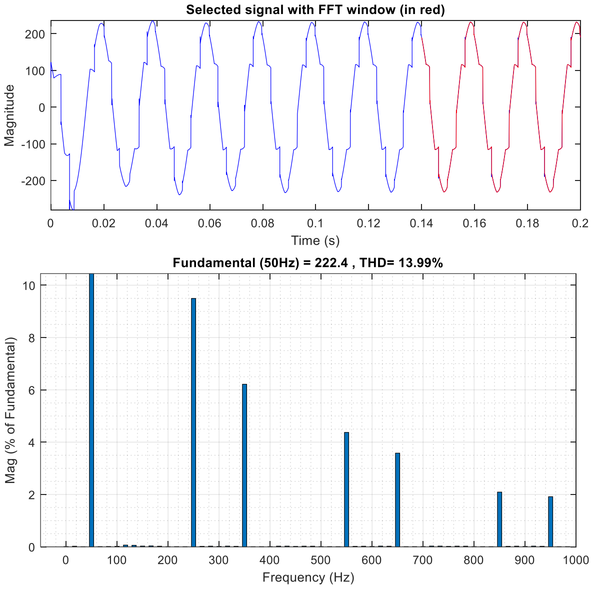

(a) Supply voltage and THD_v

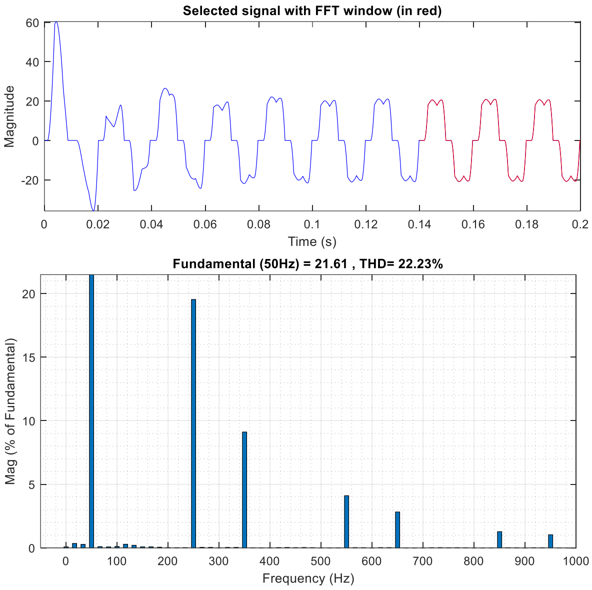

(b) Supply current and THD_i

Figure 6. THD values without C-type filter

Figure 8 indicates that performance of the battery charging process enhances as compared to without filter operation. As mentioned in [35], after compensation and harmonic elimination, the dc voltage may be higher for an uncontrolled rectifier. A slight increase in V_{dc} yields a large increase in the output power. It is clearly seen from the Figure 9 that with the mitigation of harmonics and power factor improvement, output voltage of converter structure increases from 388.4 to 388.58 V_{dc} on average. This observation is reflected in battery charging current too, while the input power is maintained constant, charging current increases from 18 A to 23 A on average. The small change in charging voltage (0.18 V_{dc}) leads an increase of 5 A which can be calculated by change in V_{dc} / battery internal resistance (0.18 V_{dc}/0.036 Ω). It can be concluded that speed of the battery charging process under the same operation conditions increases by 21% in case of using C-type filter. Therefore, the SoC curve as shown in Figure 8a goes up faster than without filter operation during the charging (Figure 5a).

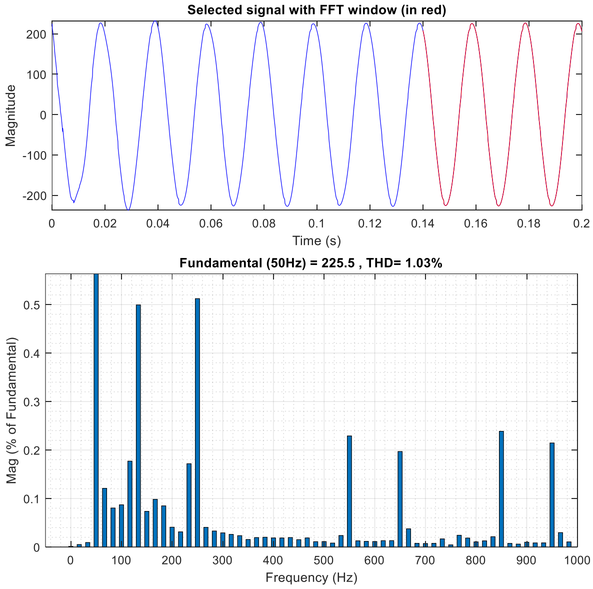

(a) Supply voltage and THD_v

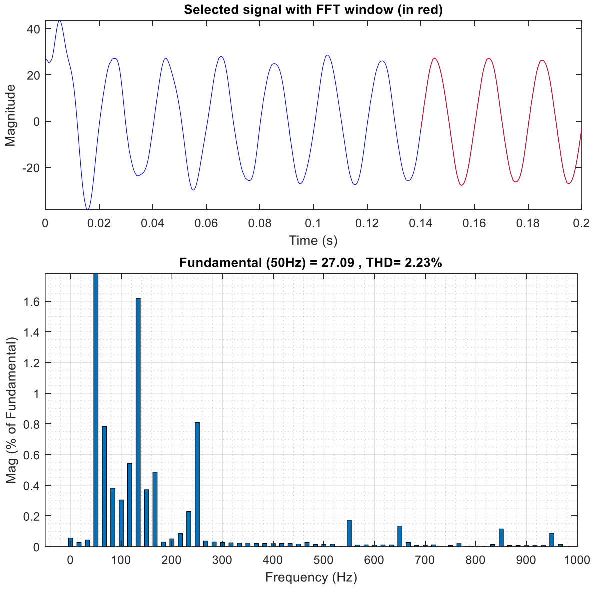

(b) Supply current and THD_i

Figure 7. THD values with C-type filter

7. Conclusion

WPT systems are widely employed in EVCS. However, structure of WPT causes current with harmonics and thus causes non-sinusoidal voltage drops. In this study, SVM-based optimal C-type passive filter design problem is taken into account in order to mitigate these harmonics and to increase PF. Therefore, firstly modeling of EVCS is realized by utilizing filter coefficients as inputs where THD_i, THD_v, PF are chosen as outputs. Secondly, PSO algorithm is employed on the SVM to find best filter parameters.

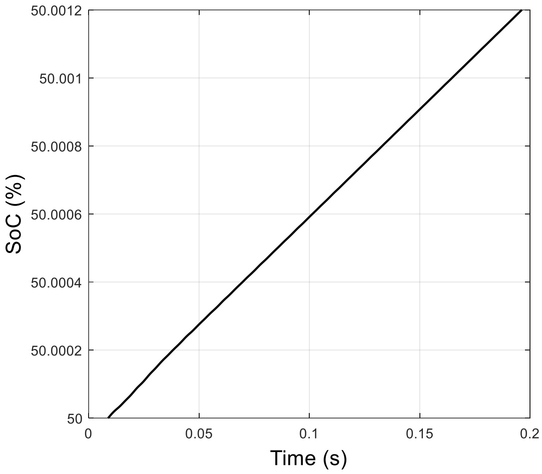

(a) State of charge

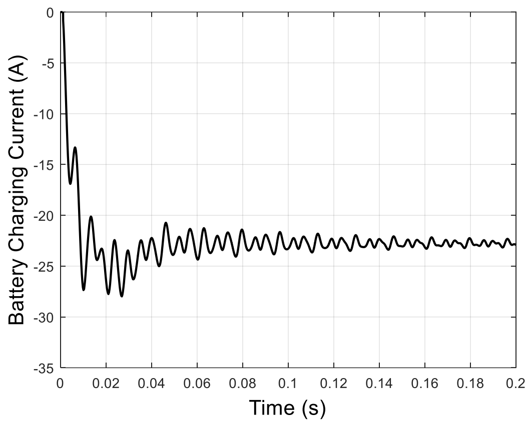

(b) Change in charging current

Figure 8. Charging of the battery with C-type filter

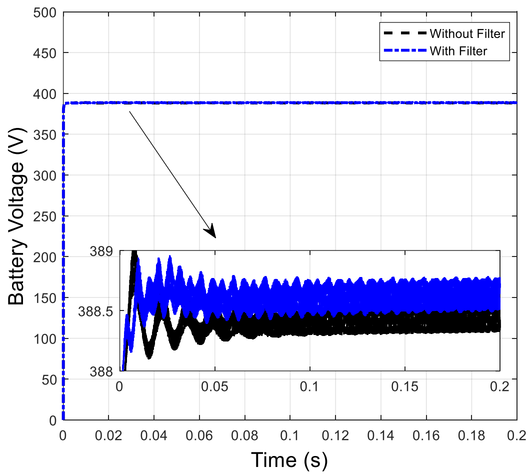

Figure 9. Comparison of charging voltage values with and without filter operation

The main advantage of the presented method is that it does not require any equivalent circuit parameters of the WPT system while determining the filter parameters. However, a single-output FF is employed in this study which is the main drawback of the method. It does not have the capability to find solutions in all objective contributions. After successful modelling and optimization process, the designed filter is employed in EVCS by using Matlab®/Simulink™ environment. Simulation results prove that THD_v and THD_i decrease under the limits defined by IEEE Standard 519-2014 and PF approaches to 1. Future works will be directed to compare different types of passive filter structures as well as various optimization methods such as chaotic PSO for the purpose of mitigating harmonics in WPT system.

Acknowledgments

The author would like to thank the anonymous reviewers for their valuable comments. This work was funded by Balikesir University under research grant BAP 2022/079.

References

[1] Demirtas, M., Calgan, H., & Ilten, E. (2022). Elektrikli Araçlar için Şebekeden bağımsız Kablosuz Şarj İstasyonu Tasarımı, *Mühendislikte Araştırma ve Değerlendirmeler*. Gece Kitaplığı, 241–266.

[2] Yağcıtekin, B., Uzunoğlu, M. & Karakaş, A. (2011). Elektrikli araçların şarjı ve dağıtım sistemi üzerine etkileri. *Elektronik ve Bilgisayar Sempozyumu, Fırat Üniversitesi-Elazığ*, 316-320.

[3] Güneş, D., Tekdemir, İ. G., Karaarslan, M. Ş., & Alboyacı, B. (2018). Assessment of the impact of electric vehicle charge station loads on reliability indices. *Journal of the Faculty of Engineering and Architecture of Gazi University*, 33(3), 1073-1084.

[4] Alonso, M., Amaris, H., Germain, J. G., & Galan, J. M. (2014). Optimal charging scheduling of electric vehicles in smart grids by heuristic algorithms. *Energies*, 7(4), 2449-2475.

[5] Spaur, C. W. , Braitberg, M. F., Kennedy, P. J., & Hatcher, L. B. (1998). Mobile portable wireless communication system. Google Patents.

[6] Li, S., & Mi, C. C. (2014). Wireless power transfer for electric vehicle applications. *IEEE Journal of Emerging and Selected Topics in Power Electronics*, 3(1), 4-17.

[7] Musavi, F., & Eberle, W. (2014). Overview of wireless power transfer technologies for electric vehicle battery charging. *IET Power Electronics*, 7(1), 60-66.

[8] Sun, L., Ma, D., & Tang, H. (2018). A review of recent trends in wireless power transfer technology and its applications in electric vehicle wireless charging. *Renewable and Sustainable Energy Reviews*, 91, 490-503.

[9] Liu, J., Xu, F., Sun, C., & Loo, K. H. (2022). A Compact Single-Phase AC–DC Wireless Power Transfer Converter With Active Power Factor Correction. *IEEE Transactions on Industrial Electronics*, 70(4), 3685-3696.

[10] Gündüz, H., Demirtas, M., Ilten, E., & Calgan, H. (2020). Paralel aktif güç filtresi için bulanık

uyarlamalı kesirli PI denetleyici tasarımı. *Düzce Üniversitesi Bilim ve Teknoloji Dergisi*, 8(3), 1975-1994.

[11] Yang, W., Wang, J., Zhang, Z., & Gao, Y. (2012). Simulation of electric vehicle charging station and harmonic treatment. In *2012 International Conference on Systems and Informatics* (pp. 609-613).

[12] Zhao, G., & Yue, Y. (2017). Harmonic analysis and suppression of electric vehicle charging station. *IEEE International Conference on Mechatronics and Automation* (pp. 347-351).

[13] Khudher, S. M., Aris, I. B., Othman, M., & Mailah, N. (2021). Output-Input Hybrid Passive Filter Design for Electric Vehicle Charging Station. *Al-Rafidain Engineering Journal (AREJ)*, 26(2), 132-142.

[14] Balci, M. E. (2014). Optimal C-type filter design to maximize transformer's loading capability under non-sinusoidal conditions. *Electric Power Components and Systems*, 42(14), 1565-1575.

[15] Karadeniz, A., & Balci, M. E. (2018). Comparative evaluation of common passive filter types regarding maximization of transformer’s loading capability under non-sinusoidal conditions. *Electric Power Systems Research*, 158, 324-334.

[16] Lange, A. G., & Redlarski, G. (2020). Selection of C-type filters for reactive power compensation and filtration of higher harmonics injected into the transmission system by arc furnaces. *Energies*, 13(9), 2330.

[17] Habibolahzadeh, M., Mahdinia Roudsari, H., Jalilian, A., & Jamali, S. (2021). Using C-type filter with partial compensation method for capacity reduction of hybrid power quality conditioner in co-phase traction power system. *IET Power Electronics*, 14(14), 2350-2373.

[18] Balci, M. E., & Karaoglan, A. D. (2013). Optimal design of C-type passive filters based on response surface methodology for typical industrial power systems. *Electric Power Components and Systems*, 41(7), 653-668.

[19] Ozdemir, S., Demirtas, M., & Aydin, S. (2016). Harmonic Estimation Based Support Vector Machine For Typical Power Systems. *Neural Network World*, 26(3), 233-252.

[20] Koizumi, H., & Kurokawa, K. (2007). Analysis of the class DE inverter with thinned-out driving patterns. *IEEE Transactions on Industrial Electronics*, 54(2), 1150-1160.

[21] Hu, J., & Zhao, J. (2020). Design of wireless power transfer system with inputfilter. *IET Power Electronics*, 13(7), 1393-1402.

[22] Sis, S. A., & Akca, H. (2020). Maximizing the efficiency of wireless power transfer systems with an optimal duty cycle operation. *AEU-International Journal of Electronics and Communications*, 116, 153081.

[23] Calgan, H., Ilten, E., & Demirtas, M. (2020). Thyristor controlled reactor-based voltage and frequency regulation of a three-phase self-excited induction generator feeding unbalanced load. *International Transactions on Electrical Energy Systems*, 30(6), e12387.

[24] Xiao, Y., Zhao, J., & Mao, S. (2004). Theory for the design of C-type filter. *11th International Conference on Harmonics and Quality of Power*, (pp. 11-15).

[25] Ilten, E., & Demirtas, M. (2016). Off-Line Tuning of Fractional Order PIλ Controller by Using Response Surface Method for Induction Motor Speed Control. *Journal of Control Engineering and Applied Informatics*, 18(2), 20–27.

[26] Demirtas, M., Ilten, E., & Calgan, H. (2019). Pareto-based multi-objective optimization for fractional order PIλ speed control of induction motor by using Elman neural network. *Arabian Journal for Science and Engineering*, 44(3), 2165-2175.

[27] Ilten, E., Calgan, H., & Demirtas, M. (2022). Design of induction motor speed observer based on long short-term memory. *Neural Computing and Applications*, 34(21), 18703-18723.

[28] Cortes, C., & Vapnik, V. (1995). Support-vector networks. *Machine Learning*, 20, 273-297.

[29] Pala, M. A., Çimen, M. E., Akgül, A., Yıldız, M. Z., & Boz, A. F. (2022). Fractal dimension-based viability analysis of cancer cell lines in lens-free holographic microscopy via machine learning. *The European Physical Journal Special Topics*, 231(5), 1023-1034.

[30] Türkan, Y. S., Aydoğmuş, H. Y., & Erdal, H. (2016). The prediction of the wind speed at different heights by machine learning methods. An International Journal of Optimization and Control: Theories & Applications (IJOCTA), 6(2), 179-187.

[31] Taibi, D., Amieur, T., Laamayad, T., & Sedraoui, M. (2022). Improvement of the Standard Perturb & Observe MPPT control strategy by the proposed Fuzzy Logic Mechanism for a Cascade Regulation of a PMSM-based PV pumping system. *Arabian Journal for Science and Engineering*, 1-17.

[32] Ilten, E. (2022). Conformable fractional order controller design and optimization for sensorless control of induction motor. *COMPEL: Int Journal for Computation and Mathematics in Electrical and Electronic Engineering*, 41(5), 1528-1541.

[33] Kilic, F., Sezen, S., & Sis, S. A. (2020). A misalignment-adaptive wireless power transfer system using PSO-based frequency tracking. An International Journal of Optimization and Control: Theories & Applications (IJOCTA), 10(2), 206-217.

[34] I. F. II (2014). IEEE Recommended Practice and Requirements for Harmonic Control in Electric Power Systems, in *IEEE Std 519-2014* (Revision of

IEEE Std 519-1992).

[35] Balcı, M. E., &. Emanuel, A. E. (2011). Apparent power definitions: a comparison study. *International Review of Electrical Engineering*, 6, 2713–2722.

Haris Calgan *received Ph.D. Degree in Electrical-Electronics Engineering from Balikesir University (Turkey) in 2020. His research interests are robust control, artificial intelligence, renewable energy. From 2014 till now, he is working as research assistant at Balikesir University (Turkey).*

http://orcid.org/0000-0002-9106-8144

An International Journal of Optimization and Control: Theories & Applications
ISSN:2146-0957 eISSN:2146-5703
Vol.13, No.2, pp.161-170 (2023)
http://doi.org/10.11121/ijocta.2023.1286

RESEARCH ARTICLE

On the regional boundary observability of semilinear time-fractional systems with Caputo derivative

Khalid Zguaid, Fatima Zahrae El Alaoui*

TSI Team, Faculty of Sciences, Moulay Ismail University, Meknès, Morocco
k.zguaid@edu.umi.ac.ma, f.elalaoui@umi.ac.ma

ARTICLE INFO

Article History:
Received 7 July 2022
Accepted 24 April 2023
Available 9 July 2023

Keywords:
Regional boundary observability
HUM approach
Fixed point
Semilinear fractional systems
Caputo derivative
Control theory

AMS Classification 2010:
93B07; 26A33; 93C20

ABSTRACT

This paper considers the regional boundary observability problem for semilinear time-fractional systems. The main objective is to reconstruct the initial state on a subregion of the boundary of the evolution domain of the considered fractional system using the output equation. We proceed by providing a link between the regional boundary observability of the considered semilinear system on the desired boundary subregion, and the regional observability of its linear part, in a well chosen subregion of the evolution domain. By adding some assumptions on the nonlinear term appearing in the considered system, we give the main theorem that allows us to reconstruct the initial state in the well-chosen subregion using the Hilbert uniqueness method (HUM). From it, we recover the initial state on the boundary subregion. Finally, we provide a numerical example that backs up the theoretical results presented in this paper with a satisfying reconstruction error.

1. Introduction

The analysis of distributed parameter systems leads to the introduction of many useful concepts such as controllability, stability, detectability, and observability [1, 2]. These notions permit researchers to understand those systems and their behaviors, which enable us to manipulate them. In the nineties, the concept of regional analysis was brought to life in [3, 4], bringing with it many tools for investigating real-world problems [5]. In particular, the concept of regional observability, which consists of finding and reconstructing the initial state in a desired subregion of the evolution domain, has great importance in the domain of control theory [3, 6–8].

Fractional calculus (FC) is a field of mathematics that investigates the notions of integration and differentiation of arbitrary or non-integer order. By fractional systems, we mean systems in which a fractional derivative appears. FC is growing in a fast manner nowadays, and this is because fractional operators present a powerful tool for modeling real-world phenomena [9–11]. For example, in [12], authors have generalized the linear prediction (LP) to fractional linear prediction (FLP) and described it with applications to one-dimensional (1D) and two-dimensional (2D) signals. They presented some numerical simulations where, for the 1D case, authors considered standard test signals, namely the square wave, sine wave, sawtooth wave, and real data signals such as speech and electrocardiogram. As for the 2D case, they choose grayscale images. The authors stated that, for the 1D case, the proposed FLP has the same construction as the LP, i.e. it uses linear combinations of non-integer derivatives with non-identical orders of derivatives. As for the 2D case, the FLP model uses a linear combination of fractional derivatives in horizontal and vertical directions. After comparing the performance of LP and FLP, the authors concluded that FLP could be used in processing 1D and 2D signals due to

*Corresponding Author

the comparable or better performance, using the same or even smaller number of parameters.

Recently, FC started to penetrate the domain of control theory [10, 13, 14]; in particular, it is used to investigate the notion of regional observability; see [15–18] for linear fractional systems and [19, 20] for semilinear ones. In this paper, we investigate the notion of regional boundary observability, which is basically regional observability where the desired subregion is a part of the boundary of the evolution domain [21, 22]. The principal goal is to reconstruct the initial state of the considered system, on a desired boundary subregion B, of the evolution domain Ω. Our contribution can be summarized in the following: Firstly, we define a new internal subregion $\omega_p \subset \Omega$, such that $B \subset \partial\omega_p$, which enables us to give a link between regional boundary observability of the considered semilinear system on B, and the regional observability of its linear part in ω_p. Secondly, we develop a method, which is based on the Hilbert uniqueness method (HUM), in order to reconstruct the initial state in ω_p, and from it we extract the value of the initial state on B.

The proposed method can be applied to real-world situations; for instance, we can use it to determine the initial population for a certain species at the frontiers of some geographical place. The diffusive logistic population growth model is given in general by,

$$D^\alpha y(x,t) - \Delta y(x,t) = my(x,t)\left(1 - \frac{y(x,t)}{b}\right),$$

where x is the spacial variable, t is time and D^α is some type of a fractional derivative. The above system is given with some boundary conditions and an unknown initial state. The quantities m and b are positive constants that are given depending on the species under investigation.

This manuscript is organized as follows: In section (2), we lay out the considered system and its properties, we also give some basic definitions and recalls covering both the field of control theory and fractional calculus. Section (3) is reserved for showing the link between the regional boundary observability of the considered semilinear system and the regional observability of its linear part throughout the subregion ω_p. In section (4), we use an extension of the Hilbert uniqueness method to reconstruct the considered system's initial state in ω_p, which led us to give an algorithm that was implemented numerically and gave us some satisfying numerical results.

2. Considered system and problematic

Let Ω be a bounded domain of $\mathbb{R}^n$, $n \geq 2$, with smooth enough boundary $\partial\Omega$, let $[0,T]$ be a time interval and α an element of $]0,1]$. From now on, we denote $Q := \Omega\times]0,T[$ and $\Sigma := \partial\Omega\times]0,T[$. Let $X = H^1(\Omega)$ be the state space and $\mathcal{O}$ a Hilbert space called the observation space, we consider the following fractional system,

$$\begin{cases} {}^C D^\alpha_{0^+} y(x,t) = \mathcal{A}y(x,t) + Fy(x,t) & \text{in } Q, \\ \dfrac{\partial y}{\partial \nu_{\mathcal{A}}}(\xi,t) = 0 & \text{on } \Sigma, \\ y(x,0) = y_0(x) & \text{in } \Omega, \end{cases} \tag{1}$$

augmented with the output equation,

$$z(t) = Cy(.,t), \quad 0 \leq t \leq T, \tag{2}$$

where :
- $\mathcal{A}$ is a second order linear differential operator which generates a C_0-semigroup $\{R(t)\}_{t\geq 0}$ on X.
- F is a nonlinear, globally Lipschitz and continuous operator.
- $C : X \longrightarrow \mathcal{O}$ is the observation operator, considered to be bounded.

- ${}^C D^\alpha_{0^+} y(x,t) := \dfrac{1}{\Gamma(1-\alpha)} \displaystyle\int_a^t (t-s)^{-\alpha} \frac{\partial}{\partial s} y(x,s)ds$, is the left sided time-fractional derivative, of order α, of y in the sense of Caputo and $\Gamma(\alpha) = \displaystyle\int_0^{+\infty} t^{\alpha-1}e^{-t}dt$ is the Euler gamma function.
- $\dfrac{\partial y}{\partial \nu_{\mathcal{A}}}$ is the co-normal derivative of y with respect to $\mathcal{A}$, see [23].
- y_0 is the initial state in X, supposedly unknown.

Definition 1. *[20] A function $y \in C(0,T;X)$, is called a mild solution of (1), if it satisfies*

$$y(.,t) = (R_\alpha(t)y_0)(.) + \int_0^t (t-\tau)^{\alpha-1}\mathcal{W}_\alpha(t-\tau)Fy(.,\tau)d\tau, \tag{3}$$

in $[0,T]$, where $R_\alpha(t) = \displaystyle\int_0^\infty \varpi_\alpha(\theta)R(t^\alpha\theta)d\theta$ and $\mathcal{W}_\alpha(t) = \alpha \displaystyle\int_0^\infty \theta\varpi_\alpha(\theta)R(t^\alpha\theta)d\theta$.
In addition,

$$\varpi_\alpha(\theta) = \sum_{n=1}^\infty \frac{(-\theta)^{n-1}}{\Gamma(n)\Gamma(1-\alpha n)}, \quad \theta \geq 0, \tag{4}$$

is the Mainardi function.

Proposition 1. *[24] The operators R_α and $\mathcal{W}_\alpha$ are strongly continuous. Furthermore,*

$$\exists M > 0, \text{ such that } \|R_\alpha(t)\|_{\mathcal{L}(X)} \leq M. \tag{5}$$

For the sake of simplicity, we define the operator $K : L^2(0,T;X) \longrightarrow L^2(0,T;X)$ by

$$(Ky)(t) = \int_0^t (t-\tau)^{\alpha-1}\mathcal{W}_\alpha(t-\tau)y(.,\tau)d\tau,$$

$\forall y \in L^2(0,T;X)$, $\forall t \in [0,T]$.
For the rest of this paper and without any loss of generality, we denote $y(t) := y(.,t)$ and for every operator A we denote its adjoint by A^*.

Let B be a non empty subset of the boundary $\partial\Omega$ with positive Lebesgue measure. We recall the following operators,

- $\gamma_0 : H^1(\Omega) \longrightarrow H^{\frac{1}{2}}(\partial\Omega)$, the trace operator of order zero, from Ω, on $\partial\Omega$. It is defined by $\gamma_0 v = v_{|\partial\Omega}$.
- $\chi_B : H^{\frac{1}{2}}(\partial\Omega) \longrightarrow H^{\frac{1}{2}}(B)$, the restriction operator, from $\partial\Omega$, on B. It is defined by $\chi_B v = v_{|B}$.
- $H_\alpha : X \longrightarrow L^2(0,T;\mathcal{O})$, the observability operator which is defined as follows $(H_\alpha x)(t) = CR_\alpha(t)x$.

This manuscript aims to study the regional boundary observability of the system (1). In other words, we are looking to reconstruct the initial state of system (1) on the boundary subregion B; this is equivalent to recover the value of y_0 on B, which we denote by y_0^1. One can see that $y_0^1 = \chi_B\gamma_0 y_0$. Then, we give the following definition.

Definition 2. *We say that system* (1)*, augmented with* (2)*, is $\mathcal{B}$-observable on B ($\mathcal{B}$ stands for boundary), if it is possible to reconstruct y_0^1 using the output equation* (2)*.*

Remark 1. *An alternative way to define the regional boundary observability on B is that for two different measurements, $z_1(.)$ and $z_2(.)$, we obtain two different values of y_0^1 on B.*

We associate to the considered system (1) the following linear system,

$$\begin{cases} {}^C D^\alpha_{0^+} y(x,t) = \mathcal{A}y(x,t) & in\ Q, \\ \dfrac{\partial y}{\partial \nu_{\mathcal{A}}}(\xi,t) = 0 & on\ \Sigma, \\ y(x,0) = y_0(x) & in\ \Omega, \end{cases} \tag{6}$$

which plays an important role in achieving the goal of this paper. We formulate the problem of this work as follows.

Problem: Given any system (1) with the output equation (2), can we reconstruct y_0^1?

3. Link between boundary and internal observability

In this section, we design a method for linking the regional boundary observability on B and the regional internal observability in a well-chosen subregion $\omega \subset \Omega$, such that $B \subset \partial\omega$. After reconstructing y_0 in ω, we obtain y_0^1 by taking the restriction on B of the trace of the reconstructed initial state on $\partial\omega$.
For a sufficiently small number $p > 0$, we define

$$U_p = \bigcup_{\xi \in B} \overline{B(\xi,p)} \quad \text{and} \quad w_p = U_p \bigcap \Omega,$$

where $\overline{B(\xi,p)}$ is the closed ball of center ξ and radius p.

Remark 2. *Notice that $\omega_p \subset \Omega$ and $B \subset \partial\Omega \cap \partial\omega_p$.*

As we did for Ω, we recall, for ω_p, the following operators:

- $\chi_{\omega_p} : H^1(\Omega) \longrightarrow H^1(\omega_p)$, the restriction operator in ω_p, which is defined by $\chi_{\omega_p} v = v_{|\omega_p}$.
- $\tilde{\gamma}_0 : H^1(\omega_p) \longrightarrow H^{\frac{1}{2}}(\partial\omega_p)$, the trace operator of order zero, from ω_p, on $\partial\omega_p$. It is defined by $\tilde{\gamma}_0 v = v_{|\partial\omega_p}$.
- $\tilde{\chi}_B : H^{\frac{1}{2}}(\partial\omega_p) \longrightarrow H^{\frac{1}{2}}(B)$, the restriction operator, from $\partial\omega_p$, on B. It is defined by $\tilde{\chi}_B v = v_{|B}$.

Remark 3. *One can see that $y_0^1 = \chi_B\gamma_0 y_0 = \tilde{\chi}_B\tilde{\gamma}_0\chi_{\omega_p}y_0$.*

Remark 4. *The adjoint of χ_{ω_p} is given by*

$$\chi^*_{\omega_p} g = \begin{cases} g & in \quad \omega_p. \\ 0 & in \quad \Omega \setminus \omega_p. \end{cases}, \forall g \in H^1(\omega_p).$$

Definition 3. *[25] We say that the linear system* (6)*, augmented with* (2)*, is approximately ω_p-observable if, and only if,*

$$\mathcal{K}er\left(H_\alpha\chi^*_{\omega_p}\right) = \{0\}.$$

Remark (3) allows us to deduce that in order to reconstruct y_0^1, it is sufficient to reconstruct $\chi_{\omega_p}y_0$, which is the initial state in ω_p, after that, we take the restriction on B, of its trace on $\partial\omega_p$. In order to illustrate this, we have the following theorem.

Theorem 1. *If the linear system* (6)*, augmented with* (2)*, is approximately ω_p-observable, then the semilinear system* (1)*, augmented with* (2)*, is $\mathcal{B}-$observable on B, and y_0^1 is the restriction on B of the trace on $\partial\omega_p$ of the restriction in ω_p of a fixed point of the function ϕ at $t = 0$, where*

$\phi : L^2(0,T;X) \longrightarrow L^2(0,T;X)$ *is defined, for every* $(t,y) \in [0,T] \times L^2(0,T;X)$*, as follows:*

$$\phi(y)(t) = R_\alpha(t)\overline{y}_0 + (KFy)(t) + R_\alpha(t)\chi^*_{\omega_p}\left[H_\alpha\chi^*_{\omega_p}\right]^\dagger \Big(z(.) - (H_\alpha\overline{y}_0)(.) - C(KFy)(.)\Big), \tag{7}$$

with

$$\left[H_\alpha\chi^*_{\omega_p}\right]^\dagger := \left[\left(H_\alpha\chi^*_{\omega_p}\right)^*\left(H_\alpha\chi^*_{\omega_p}\right)\right]^{-1}\left(H_\alpha\chi^*_{\omega_p}\right)^*,$$

is the pseudo (generalized) inverse of $H_\alpha\chi^*_{\omega_p}$*. Moreover,* $\overline{y}_0$ *has the value of* y_0 *in* $\Omega \setminus \omega_p$ *and zero in* ω_p*.*

Proof. Taking into account remark (4), we see that equation (3) can be written as follows:

$$y(t) = R_\alpha(t)\chi^*_{\omega_p}\chi_{\omega_p}y_0 + R_\alpha(t)\overline{y}_0 + (KFy)(t), \tag{8}$$

Using equations (2) and (8), we have,

$$(H_\alpha\chi^*_{\omega_p}\chi_{\omega_p}y_0)(.) = z(.) - (H_\alpha\overline{y}_0)(.) - C\,(KFy)\,(.), \tag{9}$$

and since (6) is approximately ω_p-observable, then, by the same arguments in [2], the operator $H_\alpha\chi^*_{\omega_p}$ has a generalized inverse, denoted $\left[H_\alpha\chi^*_{\omega_p}\right]^\dagger$, hence:

$$\chi_{\omega_p}y_0 = \left[H_\alpha\chi^*_{\omega_p}\right]^\dagger\Big(z(.) - (H_\alpha\overline{y}_0)(.) - C\,(KFy)\,(.)\Big). \tag{10}$$

So, by substituting (10) in (8), we get that:

$$y(t) = R_\alpha(t)\overline{y}_0 + (KFy)(t) = \phi(y)(t) + R_\alpha(t)\chi^*_{\omega_p}\left[H_\alpha\chi^*_{\omega_p}\right]^\dagger\Big(z(.) - (H_\alpha\overline{y}_0)(.) - C\,(KFy)\,(.)\Big), \tag{11}$$

hence, y is a fixed point of ϕ and $y(0)_{|\omega_p} = \chi_{\omega_p}y_0$. Thus $y_0^1 = \tilde{\chi}_B\tilde{\gamma}_0 y(0)_{|\omega_p} = \tilde{\chi}_B\tilde{\gamma}_0\chi_{\omega_p}y_0$. □

4. Reconstruction method

In consequence of theorem (1) and the discussion in section (3), we shall reconstruct the initial state in ω_p. For that we use an extension of the Hilbert uniqueness method for fractional systems. Let's start by introducing the following set,

$$\mathcal{E} = \left\{h \in H^1(\Omega) \;\middle|\; h = 0 \quad in \quad \Omega \setminus \omega_p\right\},$$

in which we define the following semi-norm,

$$\|h\|_{\mathcal{E}} = \sqrt{\int_0^T \|CR_\alpha(t)h\|^2_{\mathcal{O}}dt} = \sqrt{\int_0^T \|(H_\alpha h)(t)\|^2_{\mathcal{O}}dt}.$$

Remark 5. *If* g *is in* $\mathcal{E}$*, then* $\chi^*_{\omega_p}\chi_{\omega_p}g = g$*.*

For every Θ_0 in $\mathcal{E}$, we consider the system,

$$\begin{cases} {}^C D^\alpha_{0^+}\Theta(x,t) = \mathcal{A}\Theta(x,t) + F\Theta(x,t) & in\ Q, \\ \dfrac{\partial\Theta}{\partial\nu_{\mathcal{A}}}(\xi,t) = 0 & on\ \Sigma, \\ \Theta(x,0) = \Theta_0(x) & in\ \Omega, \end{cases} \tag{12}$$

which has a unique mild solution, see [26], written as follows,

$$\Theta(t) = R_\alpha(t)\Theta_0 + (KF\Theta)(t), \quad in \quad [0,T], \tag{13}$$

which we decompose as follows $\Theta = \Theta_1 + \Theta_2$, where Θ_1 and Θ_2 are given by the two systems:

$$\begin{cases} {}^C D^\alpha_{0^+}\Theta_1(x,t) = \mathcal{A}\Theta_1(x,t) & in\ Q, \\ \dfrac{\partial\Theta_1}{\partial\nu_{\mathcal{A}}}(\xi,t) = 0 & on\ \Sigma, \\ \Theta_1(x,0) = \Theta_0(x) & in\ \Omega, \end{cases} . \tag{14}$$

and

$$\begin{cases} {}^C D^\alpha_{0^+}\Theta_2(x,t) = \mathcal{A}\Theta_2(x,t) & in\ Q, \\ \qquad +F\left(\Theta_1(x,t) + \Theta_2(x,t)\right) & \\ \dfrac{\partial\Theta_2}{\partial\nu_{\mathcal{A}}}(\xi,t) = 0 & on\ \Sigma, \\ \Theta_2(x,0) = 0 & in\ \Omega, \end{cases} \tag{15}$$

with solutions,

$$\Theta_1(t) = R_\alpha(t)\Theta_0, \quad in \quad [0,T], \tag{16}$$

and

$$\Theta_2(t) = R_\alpha(t)\Theta_0 + (KF[\Theta_1 + \Theta_2])(t), \quad in \quad [0,T]. \tag{17}$$

<u>*Assumption*</u> : We assume, for the rest of this manuscript, that system (14), augmented with (2), is approximately ω_p-observable.

Proposition 2. *[18] If the above Assumption is satisfied, then the semi-norm* $\|.\|_{\mathcal{E}}$ *becomes a norm on* $\mathcal{E}$*.*

We introduce the following auxiliary system

$$\begin{cases} {}^{RL} D^\alpha_{T^-}\Xi(x,t) = \mathcal{A}^*\Xi(x,t) & in\ Q, \\ \qquad -F\Xi(x,t) - C^*C\Theta_1(t) & \\ \dfrac{\partial\Xi}{\partial\nu_{\mathcal{A}^*}}(\xi,t) = 0 & on\ \Sigma, \\ \lim\limits_{t\to T^-}\mathcal{I}^{1-\alpha}_{T^-}\Xi(x,t) = 0 & in\ \Omega, \end{cases} \tag{18}$$

where

$$\mathcal{I}^\alpha_{T^-}y(x,t) := -\frac{1}{\Gamma(\alpha)}\int_t^T (s-t)^{\alpha-1}y(x,s)ds,$$

is the right sided Riemann-Liouville time-fractional integral of order α, and

$${}^{RL} D^\alpha_{T^-}y(x,t) := -\frac{1}{\Gamma(1-\alpha)}\frac{\partial}{\partial t}\int_t^T (s-t)^{-\alpha}y(x,s)ds,$$

is the right sided Riemann-Liouville time-fractional derivative, of order α.

If Θ_0 is chosen in $\mathcal{E}$ such that $CR_\alpha\Theta_0(.) = z(.)$, then (18) is considered to be the adjoint system of (12).

System (18) has a unique mild solution, given by:

$$\begin{aligned}\Xi(x,t) &= \int_t^T (s-t)^{\alpha-1}\mathcal{W}_\alpha^*(s-t)\left[-F\Xi(s)\right.\\ &\qquad \left.-C^*C\Theta_1(s)\right] ds,\end{aligned} \tag{19}$$

which we also decompose into $\Xi = \Xi_1 + \Xi_2$, where Ξ_1 and Ξ_2 are solutions of

$$\begin{cases} {}^{RL}D^\alpha_{T^-}\Xi_1(x,t) = \mathcal{A}^*\Xi_1(x,t) & \text{in } Q,\\ \qquad -C^*C\Theta_1(t) & \\ \dfrac{\partial\Xi_1}{\partial\nu_{\mathcal{A}^*}}(\xi,t) = 0 & \text{on } \Sigma,\\ \lim\limits_{t\to T^-} \mathcal{I}^{1-\alpha}_{T^-}\Xi_1(x,t) = 0 & \text{in } \Omega, \end{cases} \tag{20}$$

and

$$\begin{cases} {}^{RL}D^\alpha_{T^-}\Xi_2(x,t) = \mathcal{A}^*\Xi_2(x,t) & \text{in } Q,\\ \qquad -F[\Xi_1(x,t)+\Xi_2(x,t)] & \\ \dfrac{\partial\Xi_2}{\partial\nu_{\mathcal{A}^*}}(\xi,t) = 0 & \text{on } \Sigma,\\ \lim\limits_{t\to T^-} \mathcal{I}^{1-\alpha}_{T^-}\Xi_2(x,t) = 0 & \text{in } \Omega. \end{cases} \tag{21}$$

Furthermore, they are written as follows,

$$\Xi_1(x,t) = -\int_t^T (s-t)^{\alpha-1}\mathcal{W}_\alpha^*(s-t)C^*C\Theta_1(s)ds, \tag{22}$$

and

$$\Xi_2(x,t) = -\int_t^T (s-t)^{\alpha-1}\mathcal{W}_\alpha^*(s-t)F\left[\Xi_1(s)+\Xi_2(s)\right] ds. \tag{23}$$

Let's denote by $P_{\omega_p} := \chi^*_{\omega_p}\chi_{\omega_p}$ the projection operator in $\mathcal{E}$, we have:

$$\begin{aligned} P_{\omega_p}\left(\mathcal{I}^{1-\alpha}_{T^-}\Xi(0)\right) &= \Lambda\Theta_0 + L\Theta_0,\\ &:= P_{\omega_p}\left(\mathcal{I}^{1-\alpha}_{T^-}\Xi_1(0)\right) + P_{\omega_p}\left(\mathcal{I}^{1-\alpha}_{T^-}\Xi_2(0)\right), \end{aligned}$$

where:

$$\begin{aligned} \Lambda \ : \ \mathcal{E} &\longrightarrow \mathcal{E},\\ \Theta_0 &\longmapsto P_{\omega_p}\left(\mathcal{I}^{1-\alpha}_{T^-}\Xi_1(0)\right), \end{aligned}$$

and

$$\begin{aligned} L \ : \ \mathcal{E} &\longrightarrow \mathcal{E},\\ \Theta_0 &\longmapsto P_{\omega_p}\left(\mathcal{I}^{1-\alpha}_{T^-}\Xi_2(0)\right). \end{aligned}$$

Thus,

$$\Lambda\Theta_0 = P_{\omega_p}\left(\mathcal{I}^{1-\alpha}_{T^-}\Xi(0)\right) - L\Theta_0,$$

and, as proven in [18], since (14) is approximately ω_p-observable, then Λ is an isomorphism. Therefore,

$$\begin{aligned} \Theta_0 &= \Lambda^{-1}P_{\omega_p}\left(\mathcal{I}^{1-\alpha}_{T^-}\Xi(0)\right) - \Lambda^{-1}L\Theta_0,\\ &:= \mathcal{N}\Theta_0. \end{aligned} \tag{24}$$

Hence, in order to reconstruct the initial state in ω_p, it is sufficient to solve the fixed point problem (24). For that, we give the following theorem.

Theorem 2. *Under the following assumptions:*

- H_1 - *System* (14), *augmented with* (2), *is approximately* ω_p*-observable.*
- H_2 - $\exists c > 0$, *such that:*

$$\|Fu(t)\|_X \le c\|\mathcal{I}^{1-\alpha}_{T^-}u(t)\|_X, \ \forall u \in L^2(0,T;X).$$

The operator $\mathcal{N}$ has a unique fixed point which corresponds with the initial state in ω_p.

Before proving this last theorem, let us give the following proposition.

Proposition 3. *[18] Let α be in $]0,1]$, t in $[0,T]$ and f in $L^2(0,T;X)$, we have:*

$$\begin{aligned} &\mathcal{I}^{1-\alpha}_{T^-}\int_t^T (s-t)^{\alpha-1}\mathcal{W}_\alpha^*(s-t)f(s)ds\\ &\qquad = \int_t^T R_\alpha^*(s-t)f(s)ds. \end{aligned} \tag{25}$$

Proof. : of theorem (2)
We use Schauder's fixed point theorem in our proof. In other words, we need to show that $\mathcal{N}$ is compact and $\mathcal{N}(B(0,s)) \subseteq B(0,s)$ for some $s > 0$, where $B(0,s)$ is the open ball of center zero and radius s.
Remark that $\mathcal{N}$ is compact if, and only if, L is compact. The operator L is compact if,

$$L\left(B(0,r)\right) = \left\{L\Theta_0 = P_{\omega_p}\left(\mathcal{I}^{1-\alpha}_{T^-}\Xi_2(0)\right),\ \Theta_0 \in B(0,r)\right\},$$

is relatively compact, for every $r > 0$, and since

$$L\left(B(0,r)\right) \subset \mathcal{J}_p,$$

with

$$\mathcal{J}_p := \left\{P_{\omega_p}\left(\mathcal{I}^{1-\alpha}_{T^-}\Xi_2(t)\right),\ \Theta_0 \in B(0,r),\ t \in [0,T]\right\},$$

hence it is sufficient to prove that $\mathcal{J}_p$ is relatively compact.

Step 1: We show that $\mathcal{J}_p$ is uniformly bounded. From proposition (3) and (21), we have:

$$\mathcal{I}^{1-\alpha}_{T^-}\Xi_2(t) = -\int_t^T R_\alpha^*(s-t)F\left[\Xi_1(s)+\Xi_2(s)\right] ds,$$

which gives, by using the property (5) and H_2,

$$\|\mathcal{I}^{1-\alpha}_{T^-}\Xi_2(t)\|_X \le Mc\int_0^T \|\mathcal{I}^{1-\alpha}_{T^-}\Xi_1(s)\|_X ds$$

$$+Mc\int_0^T \|\mathcal{I}_{T^-}^{1-\alpha}\Xi_2(s)\|_X ds.$$

Furthermore, from (22) and proposition (3), we have:

$$\mathcal{I}_{T^-}^{1-\alpha}\Xi_1(t) = -\int_t^T R_\alpha^*(s-t)\left[C^*C\Theta_1\right]ds,$$

hence, by using Cauchy-Schwartz,

$$\begin{aligned}\|\mathcal{I}_{T^-}^{1-\alpha}\Xi_1(t)\|_X &\leq M\|C\|_{\mathcal{L}(X,\mathcal{O})}\int_0^T \|C\Theta_1\|_{\mathcal{O}} ds,\\ &\leq M\|C\|_{\mathcal{L}(X,\mathcal{O})}T^{\frac{1}{2}}\|\Theta_0\|_{\mathcal{E}},\end{aligned} \tag{26}$$

thus,

$$\|\mathcal{I}_{T^-}^{1-\alpha}\Xi_2(t)\|_X \leq M^2c\|C\|_{\mathcal{L}(X,\mathcal{O})}T^{\frac{3}{2}}\|\Theta_0\|_{\mathcal{E}} +Mc\int_0^T \|\mathcal{I}_{T^-}^{1-\alpha}\Xi_2(s)\|_X ds.$$

By Gronwall's inequality, we obtain,

$$\|\mathcal{I}_{T^-}^{1-\alpha}\Xi_2(t)\|_X \leq M^2c\|C\|_{\mathcal{L}(X,\mathcal{O})}T^{\frac{3}{2}}\|\Theta_0\|_{\mathcal{E}}e^{McT}. \tag{27}$$

Therefore, the set $\mathcal{J}_p$ is uniformly bounded.

Step 2: We show that $\mathcal{J}_p$ is equicontinuous. Let's consider $\varepsilon > 0$, for t_1 and t_2 in $[0,T]$, such that $t_2 > t_1$, we have:

$$\begin{gathered}\mathcal{I}_{T^-}^{1-\alpha}\Xi_2(t_1) - \mathcal{I}_{T^-}^{1-\alpha}\Xi_2(t_2)\\ =\\ \int_{t_2}^T R_\alpha^*(s-t_2)F\left[\Xi_1(s)+\Xi_2(s)\right]ds\\ -\int_{t_1}^T R_\alpha^*(s-t_1)F\left[\Xi_1(s)+\Xi_2(s)\right]ds\\ =\\ \underbrace{\int_{t_2}^T \left(R_\alpha^*(s-t_2)-R_\alpha^*(s-t_1)\right)F\left[\Xi_1(s)+\Xi_2(s)\right]ds}_{:=\mathcal{R}_1}\\ \underbrace{-\int_{t_1}^{t_2} R_\alpha^*(s-t_1)F\left[\Xi_1(s)+\Xi_2(s)\right]ds,}_{:=\mathcal{R}_2}\end{gathered}$$

thus,

$$\|\mathcal{I}_{T^-}^{1-\alpha}\Xi_2(t_1) - \mathcal{I}_{T^-}^{1-\alpha}\Xi_2(t_2)\|_X \leq \|\mathcal{R}_1\|_X + \|\mathcal{R}_2\|_X.$$

Since the operator R_α is strongly continuous, then for every $\varepsilon_1 > 0$, $\exists\sigma > 0$, such that,

$$|t_1-t_2| < \sigma \implies \|R_\alpha^*(s-t_2)-R_\alpha^*(s-t_1)\|_{\mathcal{L}(X)} \leq \varepsilon_1,$$

hence, by using (26) and (27), we get,

$$\begin{aligned}\|\mathcal{R}_1\|_X &\leq \varepsilon_1 c\int_0^T \|\mathcal{I}_{T^-}^{1-\alpha}\Xi_2(s)\|_X + \|\mathcal{I}_{T^-}^{1-\alpha}\Xi_2(s)\|_X ds,\\ &\leq \varepsilon_1 \times \underbrace{McT^{\frac{1}{2}}\|C\|_{\mathcal{L}(X,\mathcal{O})}\|\Theta_0\|_{\mathcal{E}}\left[1+McTe^{McT}\right]}_{:=Z_1},\end{aligned} \tag{28}$$

and

$$\begin{aligned}\|\mathcal{R}_2\|_X &\leq Mc\int_{t_1}^{t_2} \|\mathcal{I}_{T^-}^{1-\alpha}\Xi_2(s)\|_X + \|\mathcal{I}_{T^-}^{1-\alpha}\Xi_2(s)\|_X ds,\\ &\leq \sigma \times \underbrace{M^2cT^{\frac{1}{2}}\|C\|_{\mathcal{L}(X,\mathcal{O})}\|\Theta_0\|_{\mathcal{E}}\left[1+McTe^{McT}\right]}_{:=Z_2}.\end{aligned} \tag{29}$$

Since P_{ω_p} is a projection operator, then, from (28) and (29), we have

$$\begin{aligned}&\|P_{\omega_p}\left(\mathcal{I}_{T^-}^{1-\alpha}\Xi_2(t_1)\right) - P_{\omega_p}\left(\mathcal{I}_{T^-}^{1-\alpha}\Xi_2(t_2)\right)\|_X\\ &\leq \|\mathcal{I}_{T^-}^{1-\alpha}\Xi_2(t_1) - \mathcal{I}_{T^-}^{1-\alpha}\Xi_2(t_2)\|_X,\\ &\leq \varepsilon_1 Z_1 + \sigma Z_2,\end{aligned}$$

therefore, by taking $\varepsilon_1 \leq \dfrac{\varepsilon}{2Z_1}$ and $\sigma \leq \dfrac{\varepsilon}{2Z_2}$, we conclude that:

$$\begin{aligned}\|P_{\omega_p}\left(\mathcal{I}_{T^-}^{1-\alpha}\Xi_2(t_1)\right) - P_{\omega_p}\left(\mathcal{I}_{T^-}^{1-\alpha}\Xi_2(t_2)\right)\|_X &\leq \frac{\varepsilon}{2}+\frac{\varepsilon}{2},\\ &\leq \varepsilon.\end{aligned}$$

Thus, $\mathcal{J}_p$ is equicontinuous.

From step 1 and 2, we get that L is compact hence so does $\mathcal{N}$.

Step 3: We show that $\mathcal{N}\left(B(0,s)\right) \subseteq B(0,s)$ for some $s > 0$.

we have that

$$\|\mathcal{N}\Theta_0\|_X \leq \|\Lambda^{-1}\|\left(\|\mathcal{I}_{T^-}^{1-\alpha}\Xi(0)\|_X + \|\mathcal{I}_{T^-}^{1-\alpha}\Xi_2(0)\|_X\right).$$

We know that Ξ and Ξ_2 are in $C(0,T;X)$, then so does $\mathcal{I}_{T^-}^{1-\alpha}\Xi$ and $\mathcal{I}_{T^-}^{1-\alpha}\Xi_2$, which means that they are in $L^\infty(0,T;X)$. Thus, $\exists\beta_1,\beta_2 > 0$ such that,

$$\|\mathcal{N}\Theta_0\|_X \leq \|\Lambda^{-1}\|\left(\beta_1+\beta_2\right).$$

In other words, if we take $s > \|\Lambda^{-1}\|\left(\beta_1+\beta_2\right)$, we get that $\mathcal{N}\left(B(0,s)\right) \subseteq B(0,s)$.

By Schauder's fixed point theorem, $\mathcal{N}$ admits a fixed point.

Step 4: We show that the fixed point is unique.

Let $\tilde{\Theta}_0$ and $\overline{\Theta}_0$ be two fixed points of $\mathcal{N}$. Then, as discussed in the paragraph before equation (19), they satisfy

$$CR_\alpha(.)\overline{\Theta}_0 = CR_\alpha(.)\tilde{\Theta}_0 = z(.),$$

hence, using remark 5, we have:

$$CR_\alpha(.)\left(\tilde{\Theta}_0 - \overline{\Theta}_0\right) = CR_\alpha(.)\chi_{\omega_p}^*\chi_{\omega_p}\left(\tilde{\Theta}_0 - \overline{\Theta}_0\right) = 0,$$

and since (14) is approximately ω_p-observable, we obtain that:

$$\chi_{\omega_p}\left(\tilde{\Theta}_0 - \overline{\Theta}_0\right) = 0,$$

since $\tilde{\Theta}_0$ and $\overline{\Theta}_0$ are in $\mathcal{E}$, then:

$$\tilde{\Theta}_0 = \overline{\Theta}_0.$$

Finally, $\mathcal{N}$ has a unique fixed point. □

Now that we recovered the initial state in ω_p, we can apply, to the recovered function, the trace operator $\tilde{\gamma}_0$ and the restriction operator $\tilde{\chi}_B$ to obtain the initial state on B.

5. Algorithm and numerical Simulation

This section is reserved to give an algorithm that allows us to reconstruct the initial state in ω_p and back up our theoretical results by presenting a successful numerical simulation. Following the steps of the above method, we obtain the following algorithm.

5.1. Algorithm

1 - Initialization of : α, ω_p, $\varepsilon = 10^{-6}$, Θ_0.
2 - Solve (14) and get Θ_1.
3 - Solve (20) and get Ξ_1.
4 - Solve (21) and get Ξ_2.
5 - Do $\Xi = \Xi_1 + \Xi_2$.
7 - If $\|\Theta_0 - \mathcal{N}\Theta_0\| > \varepsilon$, then:
  - $\Theta_0 = \mathcal{N}\Theta_0$.
  - go back to step 2.
else
  - Stop.

The reconstructed initial state in ω_p is $\chi_{\omega_p}\Theta_0$. Therefore, $y_0^1 = \tilde{\chi}_B\tilde{\gamma}_0\chi_{\omega_p}\Theta_0$ is the reconstructed initial state on B.

5.2. Numerical simulation

Let us take for this example $\Omega = [0,\pi]\times[0,1]$, $T = 2$, $\alpha = 0.5$, and $B = \{0\}\times[0,1]$. The dynamic of the system, $\mathcal{A}$, is considered to be $\Delta = \dfrac{\partial^2}{\partial x_1^2} + \dfrac{\partial^2}{\partial x_2^2}$, which has a complete set of eigenfunctions,

$$\left\{\varphi_{ij}(x_1,x_2) = \frac{2}{\sqrt{\pi(1-\lambda_{ij})}}\cos(ix_1)\cos(j\pi x_2)\right\}_{i,j\geq 0},$$

which forms an orthonormal basis of X, associated with the set of eigenvalues $\left\{\lambda_{ij} = -\left(\frac{i^2}{\pi^2} + j^2\right)\pi^2\right\}_{i,j\geq 0}$. The nonlinear operator F is defined as follows :

$$Fy(x_1,x_2,t) = \sum_{i,j\geq 0}^{\infty} \langle \mathcal{I}_{T^-}^{1-\alpha} y(t), \varphi_{ij}\rangle_X^2 \varphi_{ij}(x_1,x_2).$$

After specifying all the needed parameters, we consider now the semilinear system,

$$\begin{cases} {}^{C}D_{0+}^{\alpha} y(x_1,x_2,t) = \Delta y(x_1,x_2,t) & in\ Q, \\ \qquad +Fy(x_1,x_2,t) & \\ \dfrac{\partial y}{\partial \nu_\Delta}(\xi_1,\xi_2,t) = 0 & on\ \Sigma, \\ y(x_1,x_2,0) = y_0(x_1,x_2) & in\ \Omega. \end{cases} \tag{30}$$

The output equation is given by a zonal sensor (D,f), where $D\subset\Omega$ is called the geometric support (location) of the sensor and $f\in L^2(D)$ is its spatial distribution. Note that $\mathcal{O} = \mathbb{R}$ and (2) takes the form:

$$z(t) = \langle y(t), f\rangle_{L^2(D)}, \quad 0\leq t\leq T.$$

We set $f\equiv 1$, $D = [1.2\ ,\ 2.4]\times[0.1\ ,\ 0.9]$, $B = \{0\}\times[0,1]$, $\omega_p = [0\ ,\ 0.09]\times[0,1]$, and

$$y_0(x_1,x_2) = \left(\left(\frac{x_1}{\pi}+1\right)\ln\left(\frac{x_1}{\pi}+1\right) - \frac{x_1}{\pi} - \ln\left(\frac{x_1}{\pi}+1\right)^2\right).\left((x_2+1)\ln(x_2+1) - x_2 - \ln(x_2+1)^2\right),$$

which we suppose to be unknown on B.

In order to solve the systems (14), (20), and (21), we use a combination of two methods. The first is the spectral method [27], where instead of solving a fractional partial differential equation, we solve multiple fractional ordinary differential equations. The second method, which we use to solve the fractional ordinary differential equations derived from the first method, is the predictor-corrector method presented in [28].

By applying the proposed algorithm, and after eight iterations, we obtained the Figures (1), (2), (3) and (4).

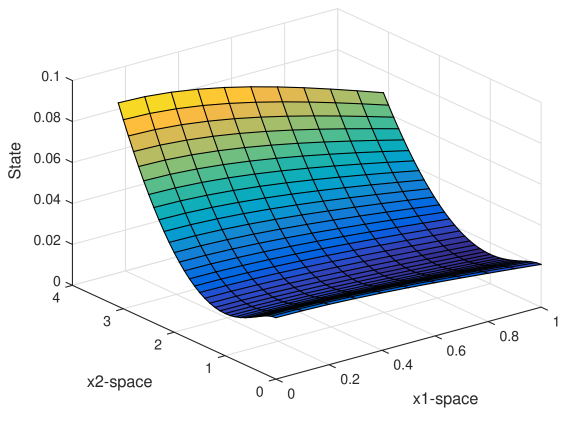

Figure 1. Initial state in Ω.

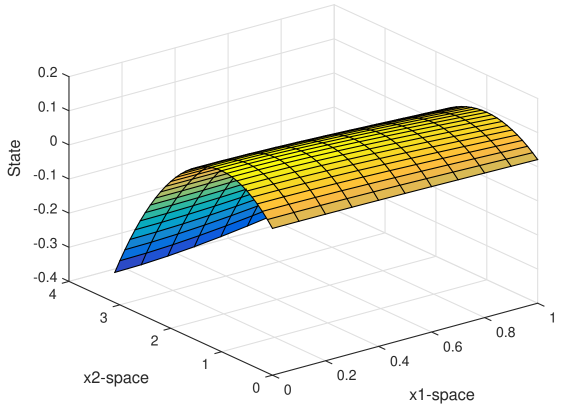

Figure 2. Reconstructed initial state in Ω.

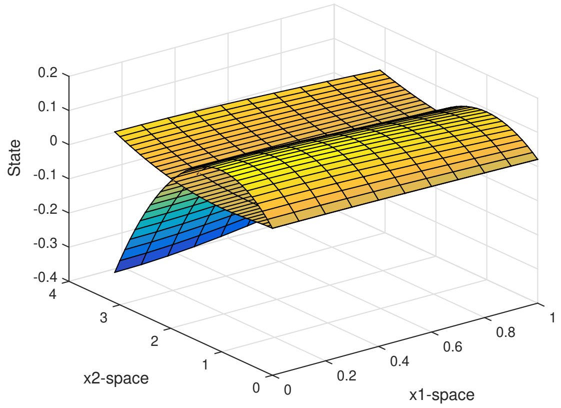

Figure 3. Initial state and the reconstructed one in Ω.

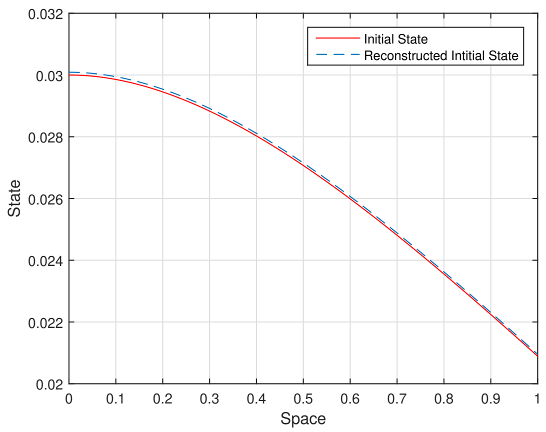

Figure 4. Initial state and the reconstructed one on in B.

Figures 1, 2, and 3 represent, respectively, the real initial state, the reconstructed initial state, and both of them in Ω. By taking a vertical cut in Figure 3 at $x_2 = 0$, we obtain Figure 4 where we can see the values of the two initial states on the boundary subregion B. It is clear, in Figure 4, that the initial state (y_0) is very close to the estimated initial one (Θ_0) on B. Furthermore, the reconstruction error is:

$$\|y_0 - \Theta_0\|^2_{L^2(B)} = 6.41 \times 10^{-9}.$$

In Figure 3, we remark that the two plots present very different behaviors unless in the desired boundary subregion, where they appear to be coinciding, which means that the proposed algorithm does not take into consideration other regions different than the desired one. This means that the cost and time needed to observe the system and reconstruct the initial state regionally is less than if we do it globally.

The efficiency of the proposed method is shown in Figure 4, where we can see that the plots of the initial state and the reconstructed one coincide. This is also backed up by the value of the reconstruction error, which is small.

Table 1 shows how the reconstruction error changes in the function of the sensor's location. We remark that the reconstruction error gets smaller as the area of B gets smaller. This proportionality proves that observing the initial state in a subregion is less expansive than observing it in the whole domain.

Table 1. Evolution of the reconstruction error with respect to the subregion B area.

Subregion B	Error $\|y_0 - \Theta_0\|^2_{L^2(B)}$
$\{0\} \times [0.00\ ,\ 1.00]$	6.41×10^{-9}
$\{0\} \times [0.05\ ,\ 0.95]$	5.80×10^{-9}
$\{0\} \times [0.10\ ,\ 0.90]$	5.18×10^{-9}
$\{0\} \times [0.15\ ,\ 0.85]$	4.55×10^{-9}
$\{0\} \times [0.20\ ,\ 0.80]$	3.92×10^{-9}
$\{0\} \times [0.25\ ,\ 0.75]$	3.27×10^{-9}
$\{0\} \times [0.30\ ,\ 0.70]$	2.63×10^{-9}
$\{0\} \times [0.35\ ,\ 0.65]$	1.67×10^{-9}
$\{0\} \times [0.40\ ,\ 0.60]$	1.32×10^{-9}
$\{0\} \times [0.45\ ,\ 0.55]$	6.59×10^{-10}

6. Conclusion

The present paper studied the regional boundary observability problem for time-fractional systems. We succeeded in reconstructing the initial state of the considered system in the desired boundary subregion by passing through an internal subregion and using the HUM approach. The method used in this work is very effective for regional boundary reconstruction problems. This is shown in the numerical simulation, where we obtained the initial state of a two-dimensional time-fractional diffusion system on the desired boundary subregion with a satisfying value of the reconstruction error. All along this paper, we worked with a bounded observation operator, but we opt to see what happens if we take an unbounded one for future works. We are also investigating the concept of regional gradient observability for fractional systems, where the goal is to reconstruct the gradient or flux of the initial state.

References

[1] Curtain, R.F., & Zwart, H. (1995). *An Introduction to Infinite-Dimensional Linear Systems Theory.* Springer-Verlag, New York.

[2] El Jai, A. (1997). *Capteurs et actionneurs dans l'analyse des systèmes distribués.* Elsevier Masson, Paris.

[3] Amouroux, M., El Jai A., & Zerrik, E. (1994). Regional observability of distributed systems. *International Journal of Systems Science*, 25(2), 301-313.

[4] El Jai, A., Somon, M.C., Zerrik, E. & Pritchard, A.J. (1995). Regional controllability of distributed parameter systems. *International Journal of Control,* 62(6), 1351-1365.

[5] El Jai, A., Afifi, L. & Zerrik, E. (2012). *Systems Theory: Regional Analysis of Infinite Dimensional Linear Systems.* Presses Universitaires de Perpignan, Perpignan.

[6] Boutoulout, A., Bourray, H. & El Alaoui, F.Z. (2013). Boundary gradient observability for semilinear parabolic systems: sectorial approach. *Mathematical Sciences Letters,* 2(1), 45-54.

[7] Boutoulout, A., Bourray, H., El Alaoui, F.Z., & Benhadid, S. (2014). Regional observability for distributed semi-linear hyperbolic systems. *International Journal of Control,* 87(5), 898-910.

[8] Zguaid, K., & El Alaoui, F.Z. (2022). Regional boundary observability for Riemann–Liouville linear fractional evolution systems. *Mathematics and Computers in Simulation,* 199, 272-286.

[9] Baleanu, D., & Lopes, A.M. (2019). *Handbook of Fractional Calculus with Applications: Applications in Engineering, Life and Social Sciences, Part A.* De Gruyter, Berlin, Boston.

[10] Petráš, I. (2019). *Handbook of Fractional Calculus with Applications: Applications in Control.* De Gruyter, Berlin, Boston.

[11] Tarasov, V.E. (2019). *Handbook of Fractional Calculus with Applications: Applications in Physics, Part A.* De Gruyter, Berlin, Boston.

[12] Skovranek, T., & Despotovic, V. (2019). Signal prediction using fractional derivative models. In: *Handbook of Fractional Calculus with Applications: Applications in Engineering, Life and Social Sciences, Part B.* De Gruyter, Berlin, Boston, 179–206.

[13] Sahijwani, N., & Sukavanam, N. (2023). Approximate controllability for systems of fractional nonlinear differential equations involving Riemann-Liouville derivatives. *An International Journal of Optimization and Control: Theories & Applications*, 13(1), 59-67.

[14] Pandey, R., Shukla, C., Shukla, A., Upadhyay, A., & Singh, A.K. (2023). A new approach on approximate controllability of Sobolev-type Hilfer fractional differential equations. *An International Journal of Optimization and Control: Theories & Applications*, 13(1), 130–138.

[15] Zguaid, K., El Alaoui, F.Z., & Torres D.F.M. (2023). Regional gradient observability for fractional differential equations with Caputo time-fractional derivatives. *International Journal of Dynamics and Control.* https://doi.org/10.1007/s40435-022-01106-0

[16] Zguaid, K., & El Alaoui, F.Z. (2022). Regional boundary observability for linear time-fractional systems. *Partial Differential Equations in Applied Mathematics*, 6, 100432.

[17] Zguaid, K., El Alaoui, F.Z., & Boutoulout, A. (2021). Regional Observability of Linear Fractional Systems Involving Riemann-Liouville Fractional Derivative. In: Z. Hammouch, H. Dutta, S. Melliani, and M. Ruzhansky, eds. *Nonlinear Analysis: Problems, Applications and Computational Methods,* Springer International Publishing, 164–178.

[18] Zguaid, K., El Alaoui, F.Z., & Boutoulout, A. (2021). Regional observability for linear time fractional systems. *Mathematics and Computers in Simulation*, 185, 77–87.

[19] Zguaid, K., & El Alaoui, F.Z. (2023). Regional boundary observability for semilinear fractional systems with Riemann-Liouville derivative. *Numerical Functional Analysis and Optimization*, 44(5), 420–437.

[20] El Alaoui, F.Z., Boutoulout, A., & Zguaid, K. (2021). Regional reconstruction of semilinear Caputo type time-fractional systems using the analytical approach. *Advances in the Theory of Nonlinear Analysis and its Application,* 5(4), 580-599.

[21] Boutoulout, A., Bourray, H., & El Alaoui, F.Z. (2010). Regional boundary observability for semilinear systems approach and simulation. *International Journal of Mathematical Analysis*, 4(24), 1153–1173.

[22] Boutoulout, A., Bourray, H., & El Alaoui, F.Z. (2015). Regional boundary observability of semilinear hyperbolic systems: sectorial approach. *IMA Journal of Mathematical Control and Information*, 32(3), 497–513.

[23] Lions, J.L., & Magenes, E. (1972). *Non-Homogeneous Boundary Value Problems and Applications Vol. 1.* Springer-Verlag, Berlin.

[24] Mu, J., Ahmad, B., & Huang, S. (2017). Existence and regularity of solutions to time-fractional diffusion equations. *Computers & Mathematics with Applications*, 73(6), 985–996.

[25] Ge, F., Quan, Y.C., & Kou, C. (2018). *Regional Analysis of Time-Fractional Diffusion Processes.* Springer International Publishing, Switzerland.

[26] Tiomela, R.F., Norouzi, F., N'guérékata, G., & Mophou, G. (2020). On the stability and stabilization of some semilinear fractional differential

equations in Banach Spaces. *Fractional Differential Calculus*, 10(2), 267–290.

[27] Gottlieb, D., & Orszag, S.A. (1977). *Numerical Analysis of Spectral Methods*. Society for Industrial and Applied Mathematics, Philadelphia.

[28] Garrappa, R. (2018). Numerical solution of fractional differential equations: a survey and a software tutorial. *Mathematics*, 6(2), 16.

Khalid Zguaid *has obtained his PhD degree in Mathematics from the Faculty of Sciences, University Moulay Ismail, Meknes, Morocco in 2022. He is currently an affiliate researcher at TSI team at the Faculty of Sciences, University Moulay Ismail, Meknes, Morocco. His fields of research are: optimal control, regional observability, frational calculus.*

https://orcid.org/0000-0003-3027-8049

Fatima Zahrae El Alaoui *has obtained her PhD degree in Mathematics from the Faculty of Sciences, University Moulay Ismail, Meknes, Morocco in 2011. She is currently working as a Professor at the Department of Mathematics, Faculty of Sciences, University Moulay Ismail, Meknes, Morocco. Her fields of research are: optimal control, regional observability, regional controllability, fractional calculus, applied mathematics.*

https://orcid.org/0000-0001-8912-4031

An International Journal of Optimization and Control: Theories & Applications (http://www.ijocta.org)

An International Journal of Optimization and Control: Theories & Applications
ISSN: 2146-0957 eISSN: 2146-5703
Vol.13, No.2, pp.171-180 (2023)
https://doi.org/10.11121/ijocta.2023.1332

RESEARCH ARTICLE

Single-drone energy efficient coverage path planning with multiple charging stations for surveillance

Atalay Celik, Enes Ustaomer, Sule Itir Satoglu*

Industrial Engineering Department, Istanbul Technical University, Turkey
celika17@itu.edu.tr, ustaomer17@itu.edu.tr, onbaslis@itu.edu.tr

ARTICLE INFO

Article history:
Received: 23 October 2022
Accepted: 1 July 2023
Available Online: 13 Jul 2023

Keywords:
Coverage path planning
Drone
Energy consumption
Mathematical model
Scenario analysis

AMS Classification 2010:
90C05, 90C10

ABSTRACT

Drones have started to be used for surveillance within the cities, visually scanning the predefined zones, quickly detecting abnormal states such as fires, accidents, and pollution, or assessing the disaster zones. Coverage Path Planning (CPP) is a problem that aims to determine the most suitable path or motion plan for a vehicle to cover the entire desired area in the task. So, this paper proposes a novel two-dimensional coverage path planning (CPP) mathematical model with the fact that a single drone may need to be recharged within its route based on its energy consumption, and the obstacles must be avoided while constructing the route. Our study aims to create realistic routes for drones by considering multiple charging stations and obstacles for surveillance. We tested the model for a grid example based on the scenarios obtained by changing the layout, the number of obstacles and recharging stations, and area size using the Python Gurobi Optimization library. As a contribution, we analyzed the impact of the number of existing obstacles and recharging stations, the size and layout of the area to be covered on total energy consumption, and the total solution time of CPP in our study for the first time in the literature, through a detailed Scenario Analysis. Results show that the map size and the number of covered cells affect the total energy consumption, but different layouts with shuffled cells are not effective. The area size to be covered affects the total computation time, significantly. As the number of obstacles and recharging stations increases, the computation time decreases up to a certain limit, then stabilizes.

1. Introduction

Technological developments such as unmanned aerial vehicles (UAVs) have significantly affected all industries in recent years. UAVs, which were first used for military purposes [1-2], soon attracted the attention of the private sector and commercial industries. With the new regulations made for air traffic management, drone studies have been channeled and increased accordingly. According to researchers, drones (UAVs) are currently used mostly in outdoor areas [3], and outdoor applications tend to increase in the future.

When UAV technologies are examined under the title of sustainable cities, it aims to be a solution to the problems that come with sustainable cities [4]. It will be possible to use UAVs, which are expected to have an important role in the field of smart and sustainable cities, in city problems such as flood detection, disaster management, traffic management, health needs distribution, and last-mile delivery by connecting to all data links with IoT technology [5]. Otto et al. [6] also emphasized that UAVs may provide cost savings and capabilities for difficult-to-access infrastructure, environmental monitoring, and medical supplies distribution, and help save lives.

In this study, we developed a mathematical model for the two-dimensional Coverage Path Planning Problem, which aims to minimize total energy consumption while considering the drone's recharging and the obstacles to be avoided within the path plan. Our study has the following contributions: Unlike the existing models for other vehicle types, the specialized energy consumption function for the drone has been added to the two-dimensional Coverage Path Planning (CPP) model. Besides, recharging the drones in the predetermined stations is decided in the model to overcome battery drain problems, and the obstacles are avoided during the path planning.

Although the related CPP problem has been examined

*Corresponding author

from many perspectives, we analyzed the impact of the number of existing obstacles and recharging stations, the size and layout of the area to be covered on total energy consumption, and the total solution time in our study for the first time in the literature, through a Scenario Analysis. This is a unique aspect of our study. This comprehensive analysis brings useful insights to this field. To the best of our knowledge, none of the past studies included all these aspects in the two-dimensional Coverage Path Planning of drones.

The paper is organized as follows: In the following section, the related works are briefly explained. In Section 3, the CPP problem is introduced. In Section 4, the Proposed Mathematical Model is explained. Then, in Section 5, Scenario Analysis and application results are discussed in detail. Finally, the Conclusion and future work are presented.

2. Literature review

In this section, a brief overview of the civil applications of drones/UAVs will be made. Later, past studies regarding the CPP will be discussed, and the merit of our study in the current literature will be explained. Cai et al. [7] made a survey of advances in UAVs and future application prospects. Drone technologies were studied for different application areas such as logistics [8-9], manufacturing [10], surveillance [11], intralogistics [12-13], disaster management [14], inventory management [15-16], and agriculture [17-18]. Ozkan and Kaya [11] studied UAV path planning for border security and patrolling missions and solved the problem using a Genetic Algorithm-based Matheuristic for different scenarios based on departure basis, daily patrol numbers, and ranges of UAVs.

Besides, Otto et al. [6] performed a comprehensive review study of the optimization approaches for civil applications of drones/UAVs. Coverage path planning for full and partial coverage, as well as, coverage from stationary positions were discussed in detail [6]. Readers may refer to this study for a comprehensive literature review. Glock and Meyer [19] developed a unified view for path planning and vehicle routing studies from many different disciplines that aim at spatial coverage. This study is also an interesting one that discusses the similarities between and the solution methods of these two problem types.

The CPP problem has been studied for not only single-drone but also multiple drones [20]. Avellar et al. found the optimum number of drones required to cover the entire designated area and tried to execute the task with multiple drones in a minimum time [21]. In another study, a suitable covering path was created for the mapping task to determine post-disaster risk with more than one drone [22]. Besides, Wang et al. [23] developed a model that allowed drones to cover the area more than once each time by improving the only one-time coverage constraint. Zhang and Duan [24] added constraints for drones with different starting battery capacities to cover the space. The path routing problem for multiple drones that minimizes total traveling time was studied in an urban setting, considering battery limitations, obstacles, and recharging stations [25]. Although this study is like our work, one minimized total time spent during the route rather than total energy consumption.

In addition to 2-dimensional studies, there are also instances of 3-dimensional (3D) CPP articles [26-27]. Bircher et al. [26] developed the routing optimization model and mostly focused on 3D structure inspections; while Balasubramanian et al. [27] determined the optimum route by considering different 3D static obstacles.

Besides, there are some past studies that focused on energy-efficient CPP which is the main topic of this study. Balasubramanian et al. [27] used the ant colony optimization model to calculate the 3-dimensional energy-efficient route. Vasquez-Gomez et al. [28] developed an efficient route planning algorithm for the coverage of the convex regions of the drones, based on different starting and end points, but the algorithm did not guarantee optimality. Choi et al. [29] developed a column generation algorithm for solving the CPP based on a precise computation of the energy consumption during the missions. Aiello et al. [30] developed an energy-efficient algorithm for route planning of drones, but the authors did not consider the recharging stage within the routes. Modares et al. [31] formulated the energy-efficient CPP for multiple drones and minimized the maximum energy consumption among all of the UAVs paths. Shivgan and Dong [32] modeled the energy-efficient CPP in a similar way to the traveling salesman problem and solved it by means of Genetic and Greedy Algorithms. To sum up, algorithm-based past papers for energy-efficient CPP are more common, but these do not guarantee optimality. Most of them do not consider recharging needs. However, our study considers both recharging states in the route and the time spent during the route including flight time and recharging time.

Bezas et al. [33] studied the CPP for swarms of UAVs and solved the model considering paths of parallel lines and spiral coverage. Vazquez-Carmona et al. [34] developed an efficient algorithm for the CPP, especially for disinfecting the areas, and simulated the routes that they developed. Tevyashov et al.[35] solved the multi-drone CPP of the agricultural fields, by minimizing the maximum time needed to cover assigned areas. The common objectives of the CPP models are maximum area coverage, minimum energy consumption, and minimum time [36]. For a detailed survey of the CPP with drones/UAVs, the readers may refer to [20].

The impact of the number of existing obstacles and recharging stations, the size and layout of the area to be covered on total energy consumption, and the total solution time of the Energy-Efficient CPP were analyzed for the first time in the literature, using a comprehensive Scenario Analysis. This is a unique aspect of our study.

3. Problem definition

Coverage Path Planning (CPP) is a problem that reveals the appropriate motion plan for a vehicle to cover the entire desired area in the task [20]. The mentioned vehicle could be a human, robot, flying vehicle, or any other mechanism which can move and turn. In this study, the area to be covered is thought to be covered with a multi-rotor UAV, commonly known as a drone.

To properly construct the CPP problem, the area to be covered is identified as a certain map and it is assumed that the UAV knows the map beforehand. As also stated in the research, the problem logic is similar to the problem of TSP [32], in that the vehicle has to consecutively visit all of the nodes in the system. A similar type of this method is used in literature by dividing the space into grids for discretizing it, the only difference is that the CPP problem is turned into a VRP problem [37]. In the CPP problem, the map is divided into cells that have an equal area, and the cell is assumed to be covered when the drone is positioned in the center of the cell since the drone has a specific hovering height and the camera can capture an area at a time [31]**.** The area of the cell is proportionate to the camera angle of view and it is assumed to be a square view. UAV hovers at a specific height which makes the map a 2-D space. Because of the fixed hovering height, at all points of the map, the camera sees cells that have the same dimensions.

Different types of UAVs can perform different movement types. To define the problem much more strictly, the type of movement that the UAV can perform has to be decided. In the literature, there are two types of approaches called the Von-Neumann and Moore Neighborhood movements which can be seen in Figure 1 [38]. Since drones can make diagonal moves by changing the power of rotors and it is more realistic, the Moore Neighborhood approach is more suitable for the application.

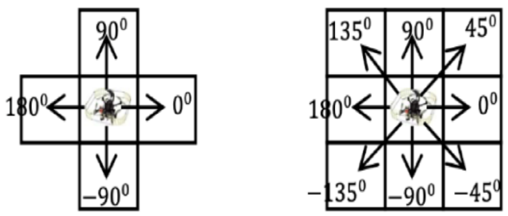

Figure 1. Von-Neumann movements (left) and Moore Neighborhood movements (right).

To make the application more realistic the map includes obstacle cells that UAV has to avoid and does not have to cover. These obstacles can range from no-fly zones to buildings. In the literature, multi-UAV applications [39] and single-UAV applications [40] are available. In this work, a single UAV is chosen. The drones are fit for the use areas. However, the main problem with drones is the low fly durations because of the battery [41]. To solve the problem of battery recharging stations that are spread across the map are added to the problem definition. To calculate the energy consumption a unit energy cost is defined per cell, and this consumption is correlated with the distance traveled. While straight movements cost one unit of energy, diagonal movements cost according to the distance traveled. Recharging stations allow the drone to fully charge its battery when it lands at the cell of the recharging station. Although technology development studies are conducted to achieve better energy management in electric vehicles [42], recharging station cells still must be covered in the path planning.

4. Mathematical model

We proposed a new mathematical model for the single-vehicle (i.e. UAV), energy-efficient two-dimensional CPP, in this study. The model consists of sub-elements such as assumptions, sets, parameters, variables, objective functions, and constraints that are expressed mathematically. Each element has been meticulously developed to validate that the model is sustainable and does not give infeasible solutions, and is explained in detail in the following sections:

Some assumptions have been made to reach feasible results and to increase the computational speed of the model. These assumptions are explained one by one in the following part:

- A drone is deployed from and returned to a predefined point inside the grid, called the base.
- If the area is not convex, it is converted into the convex hull of the area (square or rectangle).
- A drone is equipped with an onboard camera/sensor pointing down and has a square viewing aspect, which equals one-grid size.
- No external forces affecting the drones are considered, such as weather conditions (i.e. wind).
- The number of visiting recharging stations must be equal to 1 for the other cells. Cells that contain recharging stations are also considered to be covered.
- All coverage areas and recharging stations are at the same altitude; therefore, the problem is 2-dimensional.
- At any recharging station, the battery is charged to 100% battery level. In other words, no partial charging is allowed.
- The time spent at the charging stations varies according to the remaining charge of the drone.
- The spent time for landing and take-off movements from the starting and charging points is neglected in the model.
- Drone always moves at a constant speed, disregarding the extra time spent in turns.
- Total energy consumption is related to the distance traveled and unit energy consumption of the vehicle per meter.
- The battery needs to be always higher than a certain percent of its full battery level to provide enough energy to return home base in case of emergencies.

- The battery change times will not be included in the model since this is an energy-consumption-based model.

4.1. Sets

The sets that are used in the model are described below.

k: Step number (k = 0, 1, 2, …, K).

i: The cell that the drone is leaving (i = 1, 2, …, I).

j: The cell that the drone is entering (j = 1, 2, …, I) (i=j=1 represents depot/base).

OC: The set of cells that have an obstacle.

CC: The set of cells that needs to be covered.

SC: The set of cells that have a charging station.

4.2. Parameters

The parameters used in the construction of the model are described below.

p: Initial position of the drone.

d: Energy spent in the movement of one cell.

B: Full battery capacity of the drone.

I: Number of cells to be covered.

s_i: Whether cell i has a charging station or not. (s_i=1 ∀ i ∈ SC, s_i=0 ∀ i ∉ SC)

c_{ij}: Energy consumption between cell i and cell j.

r_{ij}: Time spent between cell i and cell j.

g: Total amount of time to fully charge the drone battery.

4.3. Decision variables

The decision variables that the model decides on are described below.

y_k: The battery of the drone at the end of step k.

h_k: The cumulative sum of energy consumption from step 1 to k.

u_i: Dummy variable for sub-tour constraints.

m_{ij}^k: Dummy multiplication variable.

t: The total time of flight for the drone to cover all cells.

x_{ij}^k={1, if the drone moves from cell i to cell j at step k; 0, otherwise} .

4.4. Mathematical model

The objective function of the model is as given in (1).

$$Minimize \ \sum_{i,j,k} c_{ij} x_{ij}^k \tag{1}$$

Subject to

$$\sum_i \ x_{ij}^k = \sum_i \ x_{ji}^{k+1}, \forall j, k, k \neq 0, k \neq K \tag{2}$$

$$\sum_i \ x_{ip}^K = 1 \tag{3}$$

$$x_{ij}^k = 0, \ \forall i, j, k, \ i = j \tag{4}$$

$$\sum_{i,k} x_{ij}^k \geq 1, \forall j, j \in CC \tag{5}$$

$$u_i - u_j + I \sum_k \ x_{ij}^k \leq I - 1, \forall i \neq j, i > 1, j > 1 \tag{6}$$

$$c_{ij} x_{ij}^k \leq d\sqrt{2} \ \forall i, j, k \tag{7}$$

$$\sum_k \ x_{ij}^k \leq 1, \forall i, j, i \neq j, k \neq 0 \tag{8}$$

$$x_{ij}^0 = 0, \forall i, j, i \neq j \tag{9}$$

$$\sum_{i,j} x_{ij}^k = 1, \forall k, k \neq 0 \tag{10}$$

$$h_k = h_{k-1} + \sum_{i,j} x_{ij}^k c_{ij}, \forall k, k \neq 0 \tag{11}$$

$$h_0 = 0 \tag{12}$$

$$h_k \leq h_{k+1}, \forall k, k \neq K \tag{13}$$

$$\sum_j \ x_{pj}^1 = 1 \tag{14}$$

$$y_0 = B \tag{15}$$

$$m_{ij}^k = s_i x_{ij}^k, \forall i, j, k \tag{16}$$

$$y_k = y_{k-1} - \sum_{i,j} x_{ij}^k c_{ij} + \sum_{i,j} m_{ij}^k (B - y_{k-1}) \ \forall k, k \neq 0 \tag{17}$$

$$t = \ \sum_{i,j,k} x_{ij}^k r_{ij} + \sum_{i,j,k; k \neq 0} g m_{ij}^k \, (B - y_{k-1})/B \tag{18}$$

$$y_k \geq \ 0.2B, \forall k \tag{19}$$

$$x_{ij}^k = \{0, 1\}, \forall i, j, k \tag{20}$$

$$m_{ij}^k = \{0, 1\}, \forall i, j, k \tag{21}$$

$$y_k, h_k, u_i, t \geq 0 \ \forall i, k \tag{22}$$

Objective (1) calculates the total energy consumption by the sum product of the given unit consumption cost and the decisions made by the model about the nodes to be visited at each step, considering all the decisions overall steps. Constraint in (2) applies the classical TSP approach by making sure that the number of elements that go into a cell goes out from it at all points. The only modification to the original equation is making sure the equality is according to the steps. With the constraint in (3) the UAV returns to its original position after covering every cell at the last step.

Constraint in (4) is a simple constraint that prohibits the movement from a cell to itself. The Constraint in (5) is the main constraint that ensures every single cell is covered. This is an inequality that is greater than or equal to one, and there can be some circumstances where the UAV has to visit the same cell twice. Here, the set CC does not contain the obstacle cells, which means obstacle cells must be avoided. Constraint in (6) is the sub-tour elimination constraint which is a well-known and standard constraint that prevents the system from going into a sub-tour and; thus, not being able to complete the whole path. Constraint in (7) ensures the drone movement is a type of Moore Neighborhood movement and other types of movements are not allowed. With the Constraint in (8) the same movement cannot be made in different steps. In other words, one movement can be made only in one step. Since the steps are defined starting from 0, the constraint in (9) ensures that there is no movement in step 0. Constraint in (10) ensures that one step includes only one movement. Constraint in (11) calculates the cumulative energy consumption to be used in the other constraints. Constraint in (12) initializes the sum of energy consumption to 0 at step 0. Constraint in (13) is the constraint that provides continuity to the model in terms of the steps. With this constraint, the order of steps is correctly evaluated in the model. Constraint in (14) ensures the UAV starts from the initial point *p* at step 1. Constraint in (15) is the initialization of battery level to B which is the maximum, at step 0. Constraint in (16) is added to the model as an intermediate calculation that calculates the auxiliary multiplication variable of whether the UAV is leaving the charging station or not. The Constraint in (17) is the battery update constraint which ensures the battery is lowered after a movement is made at any step. With the second part of the equation, the battery is fully charged if the UAV is exiting a charging station. The charging is made after the drone is done with its last step to ensure that there is no overplus of energy used when there is none. Constraint in (18) calculates the total flight time of the drone to fully cover all the cells that can be covered as well as the charging times in stations according to the amount of battery charged. Constraint (19) ensures that the battery is always more than 20% of full capacity [43]. Constraints in (20) and (21) are binary constraints for the variables x and m. Constraints in (22) are the nonnegativity constraints for the non-binary decision variables.

5. Experimental design

In this section, scenario analysis is performed to analyze the model under different circumstances. The effects of parameters such as layout, number of obstacles, area size, and number of recharging stations of the model are examined in detail with four different main scenarios.

The grid example shown below in Figure 2 illustrates the grid and cell design used by the model throughout the scenario analysis. While black cells represent barriers, the blue cell represents the recharging stations. Arrows also represent the optimal route that the model finds to cover all cells. As can be seen, the route manages to avoid obstacles while at the same time stopping by the charging station to avoid running out of battery. The battery needs to be always higher than 20% of its full battery level to provide enough energy to return home base in case of emergencies according to DJI which is one of the best drone producers [43].

As mentioned above, the model was examined under four different main scenarios. The changing parameters are as follows:

1. Layout Design
2. The number of Obstacles
3. Area Size
4. The number of Recharging Stations (RS)

There are also the fixed parameters of the model which are not changed across scenarios. The list of parameters and their values are given in Table 1. However, other than these, drone type, processor power, and battery type situations, which may vary in real life, are not considered in our analysis.

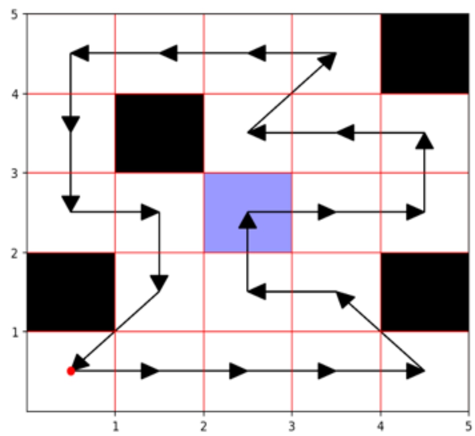

Figure 2. Grid example of the scenario analysis.

Table 1. Fixed-parameter values.

Parameter	Value
Starting Cell	1
Speed (Square/Unit Time)	1
Average Energy Consumption Per Cell	1
Maximum Battery Capacity (Unit Energy)	100

In addition to the fixed parameters above, each scenario has Controlled Parameters (C), Independent (Changing) Parameters (I), and Dependent Parameters (D). The controlled parameters have fixed values through the associated scenario runs. The Independent Parameters are the ones with changing values within different runs of the associated scenario. The dependent parameters are the ones whose values may change according to the change of the Independent Parameters. The matrix of the scenarios and parameters is presented in Table 2. The dependent *variables* to be observed were determined as total energy consumption, average energy consumption, and computation time. In Scenario 1, area size, the number of obstacles, the number of covered cells, and the number of recharging stations were kept constant to observe the impact of the layout change, by shuffling only their places. In Scenario 1, ten different layouts were considered. In scenario 2, only one new obstacle is added each time, keeping the previous obstacle positions constant while increasing the number of obstacles. The layout is not shuffled every time. As the number of obstacles increased from two to eleven at each run, the number of covered cells decreased.

Table 2. Parameters of the scenarios.

	Number of Cells Covered	Layout	Number of obstacles	Area Size	Number of Recharge Stations
S-1	C	I	C	C	C
S-2	D	C	I	C	C
S-3	D	C	C	I	C
S-4	C	C	C	C	I

In scenario 3, only the area size is increased by keeping the numbers and position of all obstacles and recharging stations constant. Accordingly, the number of coverable cells has increased. Six different area sizes changing from 3*3 to 8*8 were considered, at different runs. In scenario 4, the number of obstacles and area size are fixed. One new recharging station is added in each run, keeping the previous recharging stations' positions constant. The number of charging stations was increased from one to six at each iteration. The layout is not shuffled.

6. Scenario results and discussion

After deciding on the scenario setup, inputs, and outputs, the mathematical model was run by changing the parameter values at each scenario, iteratively, through the Gurobi Optimization Library. Recorded outputs were further prepared as bar/combo charts for each scenario. Throughout the analysis, the code for the model was compiled on the Gurobi Optimization Library in Python 3.8. The Gurobi version 9.1.2 was used to run the algorithm. The computer which was used to run the scenarios had a microprocessor of Intel(R) Core (TM) i7-7700HQ, and a total of four physical cores, and eight logical processors were used to run the scenarios with eight threads. We shared the Python codes of the mathematical model in [44].

For the study, the total energy consumption which is the objective of the model is the primary concern in terms of the outputs. As shown in the scenario details, since some of the models included different numbers of cells, the total energy consumption would not provide accurate or meaningful results. Hence, not to lose any type of information and to better interpret the results, the average energy consumption per cell was also logged. Lastly, for any scenario application of the mathematical model, the total computational time was recorded and a chart of the computation time was created.

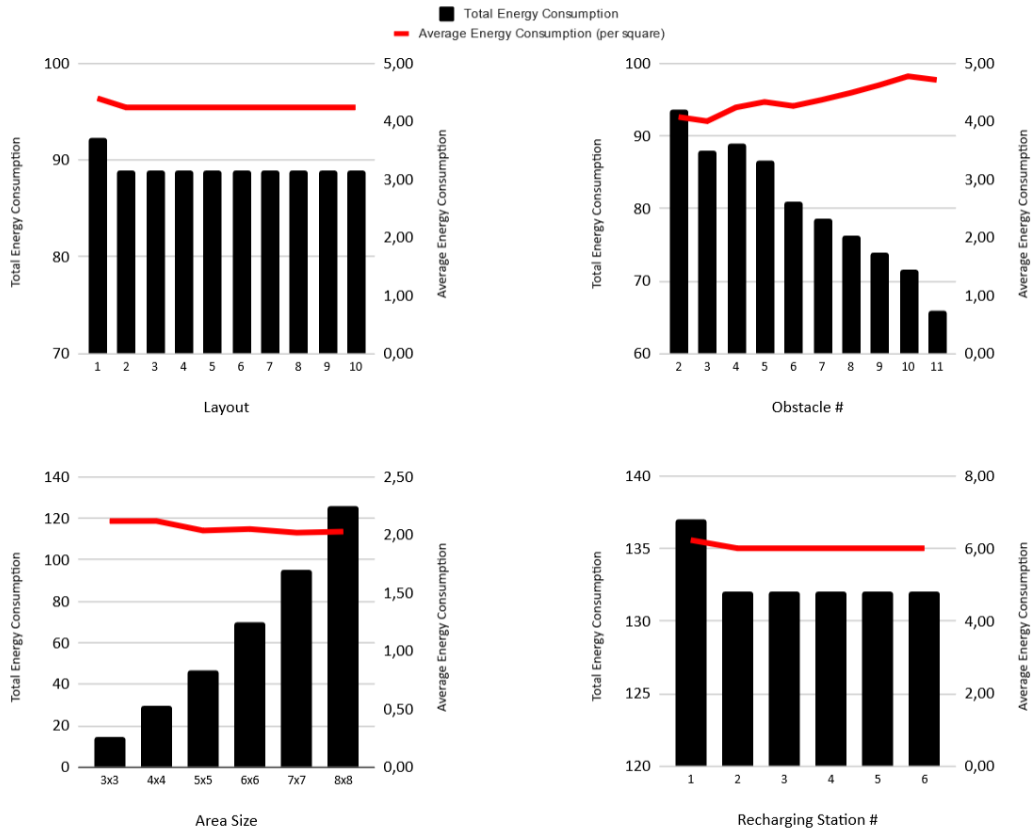

Figure 3. Scenario results for energy consumption.

6.1. Total energy consumption analysis

With the possible applications in mind, the most important performance metric in the covering mission is energy consumption. Drones are inadequate in terms of their battery capacity. Hence, utmost importance is given to the energy consumption. The four different scenarios have resulted as shown in Figure 3. The bars show the total energy consumption, whereas the red lines show the average energy consumption per cell.

The first scenario was constructed to observe if the total energy consumption changes in different layouts. The model was found to be resilient for different types of layouts by having similar results in terms of both total and average energy consumption. This shows that the model accomplishes what it was constructed for. In scenario 2, as the number of obstacles increases, the total energy consumption decreases. However, if average energy consumption per cell is observed (that is plotted in red), it increases as the number of obstacle cells increases. This indicates that the movements of the drone become more inefficient as the area becomes more restricted. In scenario 3, if there are more cells present on the map, the total energy consumption increases since the total area to be covered increases. The average energy consumption decreases slightly when the map size increases, but no significant changes are observed. Scenario 4 depicts the cases where the number of recharging stations increases in the same map setup (layout). The drone behaves differently and changes its path until a certain number of recharging stations. After that, the drone follows the same path since the battery does not become its primary concern. This behavior can be seen in Figure 3. After increasing the number of recharging stations beyond two, the model gives the same result in terms of total energy consumption.

As a result, in different scenarios, the model manages the battery of the drone as efficiently as possible, while covering the whole area. The map size, the number of covered cells, and to a certain extent the number of recharging stations affect the total energy consumption. However, different layouts with shuffled cells do not affect the total energy consumption.

6.2. Computation time analysis

We illustrate the computational times spent in each scenario, in Figure 4. In Scenario 3, the computation time is affected at most, since the number of cells increases exponentially. Scenario 1 has similar computation times through different layouts with some variation. This shows that the model acts efficiently in different layouts. In the second scenario, except for the model that has three obstacles, the computation time decreases. This decrease can be due to the decrease in the total cells that need to be covered. In the fourth scenario, the computation time decreases until the saturation point of the charging stations. After that, the computation time stabilizes. To sum up, the area size to be covered affects the total computation time, significantly. As the number of obstacles and recharging stations increases, the computation time decreases up to a certain limit, then stabilizes. The layout does not much affect the computational time.

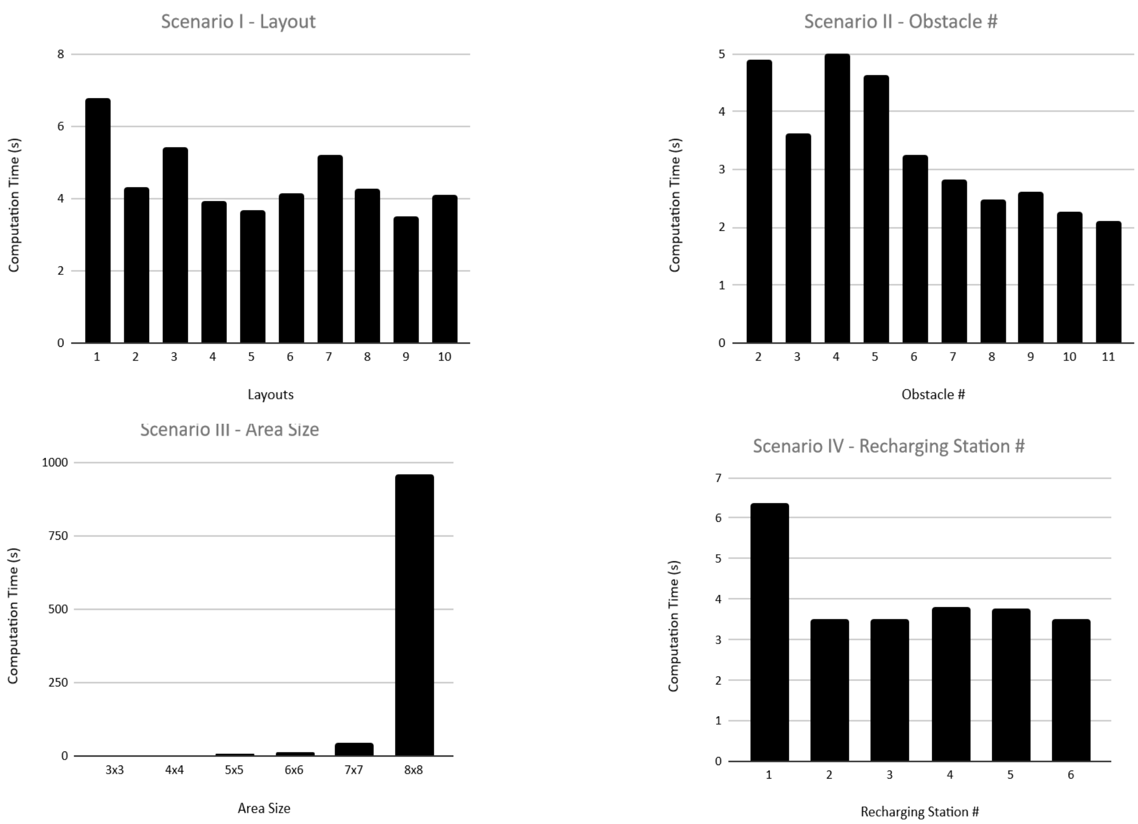

Figure 4. Scenario results for computational time

7. Conclusion

In this study, a novel mathematical model was proposed for the single-drone two-dimensional Coverage Path Planning that minimized the total energy consumption. The specialized energy consumption function for the drone has been defined in the objective. Besides, the model builds the path and decides at which step the battery must be recharged in the predetermined recharging stations while avoiding obstacles during the path planning. In addition, the impacts of the number of existing obstacles and recharging stations, the size and layout of the area to be covered on the total and average energy consumption, and total computational time were examined using a comprehensive Scenario Analysis. We explained our findings and proposed some insights. Some of the practical implications of this study are as follows:

- Disaster commanders and local government officials may employ the proposed model embedded in a software platform to plan the route of the UAVs, in order to assess the impact of the disaster and determine the affected disaster zones.
- For very big-size disasters, the area to be covered may be broken into segments, and the model can be solved, in shorter computational times.
- The availability of charging stations is a significant issue, especially for electric vehicles' adaptation. The total flight time results of our model can be exploited for the new recharging stations' location decisions.

To give perspectives for future studies in this field, more detailed studies can be performed on battery, algorithm, time, camera parameters, and movement. Firstly, the model can be modified to allow partial battery charging. In this way, it will provide more convenient routing for a drone that needs a limited time at the charging station or needs a partial charge to complete the route. Secondly, while dividing the areas where CPP will be applied, the real camera angle can be considered and the grid can be created accordingly. In this way, a more realistic routing matrix will be obtained.

Third, an objective function such as minimum time or latency can be written instead of energy consumption. In this way, the task assigned to the drone can be completed in a certain time instead of with minimum energy. Besides, the existing constraints in the model can be simplified, or some heuristic models can be developed for a faster solution. Because of the current complexity, serious computational power and time are needed. Lastly, the turning, accelerating, or decelerating movement of the drone can be added to make the work more realistic and applicable. For more advanced work, there could be an expansion by transitioning the 2-D space to a 3-D space with different obstacles, which could be buildings of different heights in the smart city application.

Acknowledgments

The authors gratefully acknowledge the academic support provided by Istanbul Technical University.

References

[1] Sifton, J. (2012). A Brief History of Drones, *The Nation*, 7, 325-335.

[2] Hassanalian, M., Abdelkefi, A. (2017). Classifications, applications, and design challenges of drones: A review. *Progress in Aerospace Sciences*, 91, 99-131.

[3] Goldman Sachs (2016). Drones: reporting for work, Goldman Sachs Research, 2016.

[4] Idries, M.F., Mohamed, A. N., Al-Jaroodi, J., & Jawhar, I. (2014). UAVs for smart cities: Opportunities and challenges. In 2014 International Conference on Unmanned Aircraft Systems (ICUAS), 267-273.

[5] Alam, M., Chamoli, A., & Hasan, N. (2022). Smart Cities and the Internet of Drones. *The Internet of Drones: AI Applications for Smart Solutions*, CRC Press, 295-323.

[6] Otto, A., Agatz, N., Campbell, J., Golden, B., & Pesch, E. (2018). Optimization approaches for civil applications of unmanned aerial vehicles (UAVs) or aerial drones: A survey. *Networks*, 72(4), 411-458.

[7] Cai, G., Dias, J., & Seneviratne, L. (2014). A survey of small-scale unmanned aerial vehicles: Recent advances and future development trends. *Unmanned Systems*, 2(2), 175-199.

[8] Torabbeigi, M., Lim, G. J., & Kim, S. J. (2018). Drone delivery schedule optimization considering the reliability of drones. In 2018 International Conference on Unmanned Aircraft Systems (ICUAS), 1048-1053.

[9] Gijseghem W., Agarwal, U. (2020). Drone Delivery Multi-Agent Routing Optimization. In AIAA Aviation 2020 Forum, https://doi.org/10.2514/6.2020-3208.

[10] Maghazei O., Netland, T. (2020). Drones in manufacturing: exploring opportunities for research and practice, *Journal Manufacturing Technology Management*, 31(6), 1237–1259.

[11] Ozkan, O., Kaya, M. (2021). UAV routing with genetic algorithm based matheuristic for border security missions. *An International Journal of Optimization and Control: Theories & Applications (IJOCTA)*, 11(2), 128-138.

[12] Amza, C.G., Cantemir, D., Oikonomoula,A., Cantemir, I., Poterucha, P., & Salucci, G. (2018). Guidelines on Industry 4.0 and Drone Entrepreneurship for VET Students, Danmar Computers LLC, Rzeszów.

[13] Ham, A. (2019). Drone-Based Material Transfer System in a Robotic Mobile Fulfillment Center, *IEEE Transactions on Automation Science and Engineering*, 17(2), 957-965.

[14] Erdelj, M., Natalizio, E. (2016). UAV-assisted disaster management: Applications and open issues. In 2016 international conference on computing, networking and communications (ICNC), Hawaii, USA.

[15] Wawrla, L., Maghazei, O. & Netland, T. (2019). Applications of drones in warehouse operations, Whitepaper. ETH Zurich, D-MTEC, www.pom.ethz.ch.

[16] Companik, E., Gravier, M. & Farris, M. (2018). Feasibility of Warehouse Drone Adoption and Implementation, *Journal of Transportation Management*, 28(2), 31-48.

[17] Abdullahi, H. S., Mahieddine, F., & Sheriff, R. E. (2015). Technology impact on agricultural productivity: A review of precision agriculture using unmanned aerial vehicles. In International conference on wireless and satellite systems, 388-400 Springer, Cham.

[18] Frankelius, P., Norrman, C., & Johansen, K. (2019). Agricultural Innovation and the Role of Institutions: Lessons from the Game of Drones, *Journal of Agricultural and Environmental Ethics*, 32, 681–707.

[19] Glock, K., Meyer, A. (2022). Spatial coverage in routing and path planning problems. *European Journal of Operational Research*, 305(1), 1-20.

[20] Cabreira, T. M., Brisolara, L. B., & Paulo R, F. J. (2019). Survey on coverage path planning with unmanned aerial vehicles. *Drones*, 3(1), 4-41.

[21] Avellar, G., Pereira, G., Pimenta, L., & Iscold, P. (2015). Multi-UAV Routing for Area Coverage and Remote Sensing with Minimum Time, *Sensors*, 15, 27783-27803.

[22] Nedjati, A., Izbirak, G., Vizvari, B. & Arkat, J. (2016). Complete Coverage Path Planning for a Multi-UAV Response System in Post-Earthquake Assessment, *Robotics*, 5(4), 26-40.

[23] Wang, Y., Kirubarajan, T., Tharmarasa, R., Jassemi-Zargani, R., & Kashyap, N. (2018). Multiperiod Coverage Path Planning and Scheduling for Airborne Surveillance, *IEEE Transactions on Aerospace and Electronic Systems*, 54(5), 2257–2273.

[24] Zhang, X., Duan, L. (2020). Energy-Saving Deployment Algorithms of UAV Swarm for Sustainable Wireless Coverage, *IEEE Transactions on Vehicular Technology*, 69(9), 10320-10335.

[25] Bahabry, A, Wan, X., Ghazzai, H., Menouar, H., Vesonder, G., & Massoud, Y. (2019). Low-Altitude Navigation for Multi-Rotor Drones in Urban Areas, *IEEE Access*, 7, 87716-87731.

[26] Bircher, A., Kamel, M., Alexis, K. et al. (2016). Three-dimensional coverage path planning via viewpoint resampling and tour optimization for aerial robots. *Autonomous Robots*, 40, 1059-1078.

[27] Balasubramanian, E., Elangovan, E., Tamilarasan, P., Kanagachidambaresan, G. R., & Chutia, D. (2022). Optimal energy efficient path planning of UAV using hybrid MACO-MEA* algorithm: theoretical and experimental approach. *Journal of Ambient Intelligence and Humanized Computing*, 1-21.

[28] Vasquez-Gomez, J. I., Marciano-Melchor, M., Valentin, L., & Herrera-Lozada, J. C. (2020). Coverage path planning for 2d convex regions. *Journal of Intelligent & Robotic Systems*, 97(1), 81-94.

[29] Choi, Y., Choi, Y., Briceno, S., & Mavris, D. N. (2020). Energy-constrained multi-UAV coverage path planning for an aerial imagery mission using column generation. *Journal of Intelligent & Robotic Systems*, 97(1), 125-139.

[30] Aiello, G., Valavanis, K. P., & Rizzo, A. (2022). Fixed-wing uav energy efficient 3d path planning in cluttered environments. *Journal of Intelligent & Robotic Systems*, 105(3), 1-13.

[31] Modares, J., Ghanei, F., Mastronarde, N., & Dantu, K. (2017, May). Ub-anc planner: Energy efficient coverage path planning with multiple drones. In 2017 IEEE international conference on robotics and automation (ICRA), 6182-6189).

[32] Shivgan, R., & Dong, Z. (2020, May). Energy-efficient drone coverage path planning using genetic algorithm. In 2020 IEEE 21st International Conference on High Performance Switching and Routing (HPSR), 1-6.

[33] Bezas, K., Tsoumanis, G., Angelis, C. T., & Oikonomou, K. (2022). Coverage Path Planning and Point-of-Interest Detection Using Autonomous Drone Swarms, *Sensors*, 22(19), 7551-7569.

[34] Vazquez-Carmona, E. V., Vasquez-Gomez, J. I., Herrera-Lozada, J. C., & Antonio-Cruz, M. (2022). Coverage path planning for spraying drones. *Computers & Industrial Engineering*, 168, 108125-108134.

[35] Tevyashov, G. K., Mamchenko, M. V., Migachev, A. N., Galin, R. R., Kulagin, K. A., Trefilov, P. M., & Goloburdin, N. V. (2022). Algorithm for Multi-drone Path Planning and Coverage of Agricultural Fields. In Agriculture Digitalization and Organic Production: Proceedings of the First International Conference, ADOP 2021, St. Petersburg, Russia, June 7–9, 299-310, Springer Singapore.

[36] Bae, H., Moon, I. (2016). Multi-depot vehicle routing problem with time windows considering delivery and installation vehicles, *Applied Mathematical Modelling*, 40(13), 6536–6549.

[37] Baras, N., Dasygenis, M., & Ploskas, N. (2019, May). Multi-robot coverage path planning in 3-dimensional environments. In 2019 8th International Conference on Modern Circuits and Systems Technologies, (MOCAST), 1-4.

[38] Nam, L. H., Huang, L., Li, X. J., & Xu, J. F. (2016). An approach for coverage path planning for UAVs. In the 2016 IEEE 14th international workshop on advanced motion control (AMC), 411-416.

[39] Kyriakakis, N. A., Marinaki, M., Matsatsinis, N., & Marinakis, Y. (2022). A cumulative unmanned aerial vehicle routing problem approach for humanitarian coverage path planning. *European Journal of Operational Research*, 300(3), 992-1004.

[40] Shen, Z., Song, J., Mittal, K., & Gupta, S. (2021). CT-CPP: Coverage Path Planning for 3D Terrain Reconstruction Using Dynamic Coverage Trees. *IEEE Robotics and Automation Letters*, 7(1), 135-142.

[41] Di Franco, C., & Buttazzo, G. (2015). Energy-aware coverage path planning of UAVs. In 2015 IEEE international conference on autonomous robot systems and competitions, 111-117.

[42] Keskin, K., Urazel, B. (2021). Fuzzy control of dual storage system of an electric drive vehicle considering battery degradation. *An International Journal of Optimization and Control: Theories & Applications (IJOCTA),* 11(1), 30-40.

[43] DJI. (2022). DJI Mini 3 Pro User Manual. Shenzhen, China. https://dl.djicdn.com/downloads/DJI_Mini_3_Pro/UM/DJI_Mini_3_Pro_user_manual_v1.0_en.pdf

[44] CPP Python Codes https://docs.google.com/document/d/1CjSqz_9I30zEI3AHbZweJXocJGjowV4qVUcNogJHqu4/edit?usp=sharing

Atalay Celik *graduated from Istanbul Technical University and earned a bachelor's degree in Industrial Engineering in 2022. He graduated from the university with a GPA of 3.8 ranked 4th in the department. In the third year of university period, he has been in Delft University of Technology, Netherlands, through the Erasmus Exchange program. He worked on drone coverage path planning optimization problem during his graduation thesis project. Currently, he has been pursuing graduate studies in Big Data and Business Analytics Master's program, in Istanbul Technical University. He has been also working in TUBITAK BILGEM which is one of the biggest information technology research centers in Türkiye, as a Data Analyst.*

http://orcid.org/0000-0003-4876-6657

Enes Ustaomer *has been currently pursuing Big Data & Business Analytics MSc Degree at Istanbul Technical University (ITU). Previously, he completed a Bachelor's Degree in Industrial Engineering at ITU, and was ranked 1st with a 3.91/4.00 GPA. He worked in the defense industry for over two years as an Integrated Logistics Support Analytics Engineer about the technologies such as data analytics, RPA, machine learning, optimization, and text mining. He is mainly focused on optimization, mission route planning, and deep reinforcement algorithms.*

http://orcid.org/0000-0002-7941-0242

Sule Itir Satoglu *earned her Master's and PhD degrees from Istanbul Technical University (ITU). She has been working as a professor of Industrial Engineering Department, at ITU. Her research interests include supply chain management and analytics, optimization algorithms, sustainability, and humanitarian logistics in disasters.*

http://orcid.org/0000-0003-2768-4038

An International Journal of Optimization and Control: Theories & Applications
ISSN:2146-0957 eISSN:2146-5703
Vol.13, No.2, pp.181-192 (2023)
http://doi.org/10.11121/ijocta.2023.1398

RESEARCH ARTICLE

Theoretical and numerical analysis of a chaotic model with nonlocal and stochastic differential operators

Ilknur Koca,[a*] Abdon Atangana[b,c]

[a] *Department of Accounting and Financial Management, Seydikemer High School of Applied Sciences, Mugla Sıtkı Kocman University, Mugla 48300, Turkey*
[b] *Institute for Groundwater Studies, Faculty of Natural and Agricultural Sciences, University of the Free State, Bloemfontein, 9301, South Africa*
[c] *Department of Medical Research, China Medical University Hospital, China Medical University, Taichung, Taiwan*
ilknurkoca@mu.edu.tr, AtanganaA@ufs.ac.za

ARTICLE INFO

Article History:
Received 25 April 2023
Accepted 31 May 2023
Available 19 July 2023

Keywords:
Nonlinear model
Chaotic number
Stochastic effect
Numerical analysis

AMS Classification 2010:
26A33; 34A34; 35B44; 65M06

ABSTRACT

A set of nonlinear ordinary differential equations has been considered in this paper. The work tries to establish some theoretical and analytical insights when the usual time-deferential operator is replaced with the Caputo fractional derivative. Using the Caratheodory principle and other additional conditions, we established that the system has a unique system of solutions. A variety of well-known approaches were used to investigate the system. The stochastic version of this system was solved using a numerical approach based on Lagrange interpolation, and numerical simulation results were produced.

1. Introduction

Systems of nonlinear ordinary differential and integral equations make up a significant class of nonlinear equations because they have been discovered to be effective at simulating challenging real-world issues that come up in various branches of science, technology, and engineering [1–10]. We will emphasize that a variety of differential operators, including the most recent one proposed in the literature, piecewise derivatives, fractional derivatives, and classical derivatives, have been employed to reflect the intricacies of nature. In fact, no viable analytical solution that can be solved analytically has been proposed in recent years. Therefore, to arrive at numerical solutions to these nonlinear systems of equations, researchers frequently used numerical techniques. Conditions do exist, nevertheless, in which they acknowledge the need for exact solutions. However, it was also recently reported that certain of these differential equations may not be able to accurately depict complicated processes with crossover tendencies when only utilizing a single differential operator. A notion known as the piecewise differential operator was proposed as a solution and successfully applied in various significant applications [11,12]. In this study, we intend to investigate a model that has been studied in a number of significant works a modified system of nonlinear equations. Following that, we'll use various differential operator types and offer some numerical and stability analyses.

2. Definitions of derivatives

In this section, we summarized some basic fractional order definitions in the next section [11,13, 14].

*Corresponding Author

Definition 1. *Caputo fractional derivative of order $\gamma > 0$ of a function $f : (0, \infty) \to R$, according to Caputo, the fractional derivative of a continuous and differentiable function f is given as :*

$$ {}^{C}D_t^{\gamma} f(t) = \frac{1}{\Gamma(1-\gamma)} \int_0^t (t-x)^{-\gamma} \frac{d}{dx} f(x) dx, \quad (1)$$

where $0 < \gamma \leq 1$.

Definition 2. *Let f be differentiable, then a piece-wise derivative with classical and fractional derivative with power-law kernel is given as*

$$ {}_0^{PC}D_t^{\gamma} f(t) = \begin{cases} f'(t), & \text{if } 0 \leq t \leq t_1 \\ {}_{t_1}^{C}D_t^{\gamma} f(t), & \text{if } t_1 \leq t \leq T \end{cases} \quad (2)$$

where ${}_0^{PC}D_t^{\gamma}$ represents classical derivative on $0 \leq t \leq t_1$ and Caputo fractional derivative on $t_1 \leq t \leq T$.

Definition 3. *The Riemann-Liouville fractional integral of order $\gamma > 0$ of a function $f : (0, \infty) \to R$, according to Riemann-Liouville, the fractional integral is considered as anti-fractional derivative of a function f is :*

$$ I_t^{\gamma} f(t) = \frac{1}{\Gamma(\gamma)} \int_0^t (t-x)^{\gamma-1} f(x) dx, \quad x > 0. \quad (3)$$

Definition 4. *Let f be continuous and $\gamma > 0$ then a piece-wise integral of f is given as*

$$ {}^{PPL}J_t^{\gamma} f(t) = \begin{cases} \int_0^t f(\tau) d\tau, & \text{if } 0 \leq t \leq t_1 \\ \frac{1}{\Gamma(\gamma)} \int_{t_1}^t (t-\tau)^{\gamma-1} f(\tau) d\tau, & \text{if } t_1 \leq t \leq T \end{cases} . \quad (4)$$

where ${}^{PPL}J_t^{\gamma} f(t)$ represents classical integral on $0 \leq t \leq t_1$ and the integral with power-law kernel on $t_1 \leq t \leq T$.

3. Model derivation

Fractional order models are very important for studying natural problems. It is well known that the nature of the trajectory of the fractional order derivatives is non-local, which describes that the fractional order derivative has a memory effect, meaning that the future states depend on the present as well as the past states. With this motivation in 2012, Ozalp and Koca have considered Barley and Cherifs deterministic model as fractional order dynamic [15, 16]. In this work, we extended the fractional-order nonlinear model by adding λx_2^2 and λx_1^2 factors where λ is 1 or 0. We find these components sufficient to make relevant practical conclusions. The model can be more complex later, once that is shown to be necessary. With these assumptions, the complete model is given as

$$\begin{aligned} {}_{t_1}^{C}D_t^{\alpha} x_1(t) &= -\alpha_1 x_1 + \beta_1 x_2 - \beta_1 \varepsilon x_2^3 \\ &\quad + \lambda x_2^2, \ 0 < \alpha \leq 1 \\ {}_{t_1}^{C}D_t^{\alpha} x_2(t) &= -\alpha_2 x_2 + \beta_2 x_1 - \beta_2 \varepsilon x_1^3 + \lambda x_1^2, \\ x_1(0) &= 0 \ , \ x_2(0) = 0. \end{aligned} \quad (5)$$

Positive values for the model show positive conscious experience, while negative values show negative conscious experience. Other parameters are oblivion, reaction, and attraction constants. Stochastic modeling is used in many places, from statistics to biology, from economics to physics. We know that deterministic modeling is predictable, so we know the future for sure, while stochastic modeling is random, so we cannot predict the future for sure. So we say that stochastic models can give rise to deterministic behavior. In particular, we can construct a sequence of models with a decreasing level of detail, from a deterministic model to a stochastic model or vice versa. Stochastic modeling is random in nature, and uncertain factors are included in the model. So in this paper with a numerical part, we will consider the fractional-order deterministic interaction model as a fractional order stochastic model with an added noise piece.

$$\begin{aligned} dx_1(t) &= \left(-\alpha_1 x_1 + \beta_1 x_2 - \beta_1 \varepsilon x_2^3 + \lambda x_2^2\right) dt \\ &\quad + \sigma_1 x_1 dB_1(t), \\ dx_2(t) &= \left(-\alpha_2 x_2 + \beta_2 x_1 - \beta_2 \varepsilon x_1^3 + \lambda x_1^2\right) dt \\ &\quad + \sigma_2 x_2 dB_2(t), \end{aligned} \quad (6)$$

We believe that this nonlinear stochastic model will explain the stochastic rates and factors (ecological, historical, cultural and community conditions) better than its deterministic version

4. Chaotic number for modified nonlinear model

The concept of mathematical modeling is used to analyze the between at least two variables. People who are in communication are aware of each other, and their connection with each other is conscious. In this section, we search for the chaotic number (C_0), which has been worked on by some researchers recently [17]. So we can have an idea about the future of communication. The function F will be obtained from the nonlinear part of the model, and the function V will be obtained from the linear part of the model. Here we recall our nonlinear model including classical derivative.

$$\begin{aligned}\frac{dx_1(t)}{dt} &= -\alpha_1 x_1 + \beta_1 x_2 - \beta_1 \varepsilon x_2^3 + \lambda x_2^2,\\ \frac{dx_2(t)}{dt} &= -\alpha_2 x_2 + \beta_2 x_1 - \beta_2 \varepsilon x_1^3 + \lambda x_1^2,\end{aligned} \tag{7}$$

with initial conditions $x_1(0) = 0$ and $x_2(0) = 0$. We note that in analysis we take $\lambda = 1$.

To begin, we divide the system into two sections.

$$\begin{bmatrix} x_1' \\ x_2' \end{bmatrix} = f - v. \tag{8}$$

Here f is given as

$$f = \begin{bmatrix} -\beta_1 \varepsilon x_2^3 + x_2^2 \\ -\beta_2 \varepsilon x_1^3 + x_1^2 \end{bmatrix} \tag{9}$$

and v is given as

$$v = \begin{bmatrix} \alpha_1 x_1 - \beta_1 x_2 \\ \alpha_2 x_2 - \beta_2 x_1 \end{bmatrix}. \tag{10}$$

Let us take partial derivatives of f and v then we get F and V which are given as below

$$F = \begin{bmatrix} 0 & -3\beta_1 \varepsilon x_2^2 + 2x_2 \\ -3\beta_2 \varepsilon x_1^2 + 2x_1 & 0 \end{bmatrix}, \tag{11}$$

and

$$V = \begin{bmatrix} \alpha_1 & -\beta_1 \\ -\beta_2 & \alpha_2 \end{bmatrix}. \tag{12}$$

To obtain Chaotic number (C_0), we have to calculate $N_G = F.V^{-1}$ matrice which is named as Next-Generation matrix of the system. Then (C_0) will be obtained from the spectral radius of the matrix of N_G.

First, we need to calculate V^{-1}. If V is

$$V = \begin{bmatrix} \alpha_1 & -\beta_1 \\ -\beta_2 & \alpha_2 \end{bmatrix}, \tag{13}$$

then

$$V^{-1} = \frac{1}{\alpha_1\alpha_2 - \beta_1\beta_2} \begin{bmatrix} \alpha_2 & \beta_1 \\ \beta_2 & \alpha_1 \end{bmatrix}. \tag{14}$$

So we get

$$\begin{aligned} F.V^{-1} = &\begin{bmatrix} 0 & -3\beta_1 \varepsilon x_2^2 + 2x_2 \\ -3\beta_2 \varepsilon x_1^2 + 2x_1 & 0 \end{bmatrix} \\ &\times \begin{bmatrix} \frac{\alpha_2}{\alpha_1\alpha_2-\beta_1\beta_2} & \frac{\beta_1}{\alpha_1\alpha_2-\beta_1\beta_2} \\ \frac{\beta_2}{\alpha_1\alpha_2-\beta_1\beta_2} & \frac{\alpha_1}{\alpha_1\alpha_2-\beta_1\beta_2} \end{bmatrix} \end{aligned} \tag{15}$$

$$F.V^{-1} = \begin{bmatrix} \frac{\beta_2\left(-3\beta_1\varepsilon x_2^2+2x_2\right)}{\alpha_1\alpha_2-\beta_1\beta_2} & \frac{\alpha_1\left(-3\beta_1\varepsilon x_2^2+2x_2\right)}{\alpha_1\alpha_2-\beta_1\beta_2} \\ \frac{\alpha_2\left(-3\beta_2\varepsilon x_1^2+2x_1\right)}{\alpha_1\alpha_2-\beta_1\beta_2} & \frac{\beta_1\left(-3\beta_2\varepsilon x_1^2+2x_1\right)}{\alpha_1\alpha_2-\beta_1\beta_2} \end{bmatrix}.$$

Now we calculate the eigenvalues by solving

$$\det\left(F.V^{-1} - \lambda I\right) = 0, \tag{16}$$

so we get

$$\begin{aligned} &\det\left(F.V^{-1} - \lambda I\right) \\ &= \det \begin{vmatrix} \frac{\beta_2\left(-3\beta_1\varepsilon x_2^2+2x_2\right)}{\alpha_1\alpha_2-\beta_1\beta_2} - \lambda & \frac{\alpha_1\left(-3\beta_1\varepsilon x_2^2+2x_2\right)}{\alpha_1\alpha_2-\beta_1\beta_2} \\ \frac{\alpha_2\left(-3\beta_2\varepsilon x_1^2+2x_1\right)}{\alpha_1\alpha_2-\beta_1\beta_2} & \frac{\beta_1\left(-3\beta_2\varepsilon x_1^2+2x_1\right)}{\alpha_1\alpha_2-\beta_1\beta_2} - \lambda \end{vmatrix}. \end{aligned} \tag{17}$$

Here we need simplification as

$$\begin{aligned} l_1 &= -3\beta_2\varepsilon x_1^2 + 2x_1,\\ l_2 &= -3\beta_1\varepsilon x_2^2 + 2x_2,\\ k &= \alpha_1\alpha_2 - \beta_1\beta_2. \end{aligned} \tag{18}$$

So start from forming a new matrix by subtracting λ from the diagonal entries of the given matrix we have

$$\begin{aligned} &\det\left(F.V^{-1} - \lambda I\right) = \det \begin{vmatrix} \frac{\beta_2 l_2}{k} - \lambda & \frac{\alpha_1 l_2}{k} \\ \frac{\alpha_2 l_1}{k} & \frac{\beta_1 l_1}{k} - \lambda \end{vmatrix} = 0,\\ &= \left(\frac{\beta_2 l_2}{k} - \lambda\right)\left(\frac{\beta_1 l_1}{k} - \lambda\right) - \frac{\alpha_1\alpha_2 l_2 l_1}{k^2} = 0,\\ &= \lambda^2 - \lambda\left(\frac{\beta_2 l_2}{k} + \frac{\beta_1 l_1}{k}\right) - \frac{l_2 l_1}{k^2}\left(\alpha_1\alpha_2 - \beta_1\beta_2\right) = 0. \end{aligned} \tag{19}$$

We can have two roots from the last equality

$$\lambda_1 = \frac{\beta_1 l_1 + \beta_2 l_2 + \sqrt{\beta_1^2 l_1^2 - 2 l_2 l_1 \beta_1\beta_2 + 4\alpha_1\alpha_2 l_2 l_1 + \beta_2^2 l_2^2}}{2\alpha_1\alpha_2 - \beta_1\beta_2} \tag{20}$$

and

$$\lambda_2 = \frac{\beta_1 l_1 + \beta_2 l_2 - \sqrt{\beta_1^2 l_1^2 - 2 l_2 l_1 \beta_1\beta_2 + 4\alpha_1\alpha_2 l_2 l_1 + \beta_2^2 l_2^2}}{2\alpha_1\alpha_2 - \beta_1\beta_2}. \tag{21}$$

We know that the maximum eigenvalue is the spectral radius of the matrix, so the chaotic number is found for this model as

$$C_0 = \frac{\beta_1 l_1+\beta_2 l_2+\sqrt{\beta_1^2 l_1^2-2l_2 l_1\beta_1\beta_2+4\alpha_1\alpha_2 l_2 l_1+\beta_2^2 l_2^2}}{2\alpha_1\alpha_2-\beta_1\beta_2}. \tag{22}$$

5. Global stability results for nonlinear model

Explicit solutions to a given differential equation are often difficult to find. In such cases, trying to understand how the solutions of the system behave as time goes to infinity can give a lot of information about the system. Equilibrium points are very important for systems because all solutions converge on these fixed points. To achieve this, we can use the Lyapunov method, which was introduced by Aleksandr Mikhailovich Lyapunov in 1982. So here, the Lyapunov function theory will be used to investigate the global stability of the system. Let us consider the model again.

$$\begin{aligned} \frac{dx_1(t)}{dt} &= -\alpha_1 x_1+\beta_1 x_2-\beta_1\varepsilon x_2^3+x_2^2,\\ \frac{dx_2(t)}{dt} &= -\alpha_2 x_2+\beta_2 x_1-\beta_2\varepsilon x_1^3+x_1^2, \end{aligned} \tag{23}$$

with initial conditions $x_1(0)=0$ and $x_2(0)=0$.

Theorem 1. *If $C_0 \geq 1$, the equilibrium point of model $E^*(x_1^*, x_2^*)$ is globally asymptotically stable.*

Proof. We prove this using the idea of the Lyapunov function. We start by defining the Lyapunov function associated with the system as below:

$$\begin{aligned} L(E^*(x_1^*,x_2^*)) = &\left(x_1-x_1^*+x_1^*\log\frac{x_1^*}{x_1}\right)\\ &+\left(x_2-x_2^*+x_2^*\log\frac{x_2^*}{x_2}\right). \end{aligned} \tag{24}$$

By the derivative of Lyapunov function with respect to t, we get

$$\frac{dL(t)}{dt} = \left(\frac{x_1-x_1^*}{x_1}\right)\frac{dx_1(t)}{dt}+\left(\frac{x_2-x_2^*}{x_2}\right)\frac{dx_2(t)}{dt}. \tag{25}$$

Now we put values in the above equation for derivatives

$$\begin{aligned} \frac{dL(t)}{dt} = &\left(1-\frac{x_1^*}{x_1}\right)\left(-\alpha_1 x_1+\beta_1 x_2-\beta_1\varepsilon x_2^3+x_2^2\right)\\ &+\left(1-\frac{x_2^*}{x_2}\right)\left(-\alpha_2 x_2+\beta_2 x_1-\beta_2\varepsilon x_1^3+x_1^2\right). \end{aligned} \tag{26}$$

Now we divide all items into positive and negative parts,

$$\frac{dL(t)}{dt} = L_1 - L_2, \tag{27}$$

Here

$$\begin{aligned} L_1 &= \beta_1 x_2 + x_2^2 + x_1^*\alpha_1 + \frac{x_1^*\beta_1\varepsilon x_2^3}{x_1}+\beta_2 x_1 + x_1^2\\ &\quad + x_2^*\alpha_2 + \frac{x_2^*\beta_2\varepsilon x_1^3}{x_2},\\ L_2 &= \alpha_1 x_1 + \beta_1\varepsilon x_2^3 + \frac{x_1^*\beta_1 x_2}{x_1}\\ &\quad + \frac{x_1^* x_2^2}{x_1} + \alpha_2 x_2 + \beta_2\varepsilon x_1^3 + \frac{x_2^*\beta_2 x_1}{x_2} + \frac{x_2^* x_1^2}{x_2}. \end{aligned} \tag{28}$$

Therefore if

$$\begin{aligned} &L_1 - L_2 > 0 \text{ then } \frac{dL(t)}{dt} > 0,\\ &L_1 - L_2 = 0 \text{ then } \frac{dL(t)}{dt} = 0,\\ &L_1 - L_2 < 0 \text{ then } \frac{dL(t)}{dt} < 0. \end{aligned} \tag{29}$$

□

5.1. Second derivative of Lyapunov

The Lyapunov function is used for reporting the global stability of systems. The sign of the first derivative of the Lyapunov function may not be enough to say whether we are talking about the local maximum or the local minimum. So we can proceed with analysis to determine the sign of the second derivative of the Lyapunov function. With the following inequality, we obtain the second derivative of the Lyapunov function for our model:

$$\begin{aligned} \frac{d}{dt}\left(\frac{dL(t)}{dt}\right) &= \frac{d}{dt}\left(\left(\frac{x_1-x_1^*}{x_1}\right)\frac{dx_1(t)}{dt}+\left(\frac{x_2-x_2^*}{x_2}\right)\frac{dx_2(t)}{dt}\right),\\ &= \left(\frac{x_1'}{x_1}\right)^2 x_1^* + \left(\frac{x_2'}{x_2}\right)^2 x_2^* + \left(\frac{x_1-x_1^*}{x_1}\right)\frac{d^2x_1(t)}{dt^2}\\ &\quad+\left(\frac{x_2-x_2^*}{x_2}\right)\frac{d^2x_2(t)}{dt^2} \end{aligned} \tag{30}$$

Here we need first and second-order derivative counterparts of equations.

$$\begin{aligned} \frac{dx_1(t)}{dt} &= -\alpha_1 x_1+\beta_1 x_2-\beta_1\varepsilon x_2^3+x_2^2,\\ \frac{dx_2(t)}{dt} &= -\alpha_2 x_2+\beta_2 x_1-\beta_2\varepsilon x_1^3+x_1^2,\\ \frac{d^2x_1(t)}{dt^2} &= -\alpha_1\frac{dx_1(t)}{dt}+\beta_1\frac{dx_2(t)}{dt}-3\beta_1\varepsilon x_2^2\frac{dx_2(t)}{dt}+2x_2\frac{dx_2(t)}{dt},\\ \frac{d^2x_2(t)}{dt^2} &= -\alpha_2\frac{dx_2(t)}{dt}+\beta_2\frac{dx_1(t)}{dt}-3\beta_2\varepsilon x_1^2\frac{dx_1(t)}{dt}+2x_1\frac{dx_1(t)}{dt}. \end{aligned} \tag{31}$$

If we arrange the last two derivatives

$$\begin{aligned}\frac{d^2x_1(t)}{dt^2} &= \alpha_1^2x_1+\alpha_1\beta_1\varepsilon x_2^3+\beta_1\beta_2x_1+\beta_1x_1^2+3\beta_1\varepsilon\alpha_2x_2^3\\ &+3\beta_1\beta_2\varepsilon^2x_2^2x_1^3+2\beta_2x_1x_2+2x_2x_1^2\\ &-(\alpha_1\beta_1x_2+\alpha_1x_2^2+\beta_1\alpha_2x_2+\beta_1\beta_2\varepsilon x_1^3+3\beta_1\beta_2\varepsilon x_2^2x_1\\ &+3\beta_1\varepsilon x_2^2x_1^2+2\alpha_2x_2^2+2x_2\beta_2\varepsilon x_1^3),\end{aligned}\tag{32}$$

and

$$\begin{aligned}\frac{d^2x_2(t)}{dt^2} &= \alpha_2^2x_2+\alpha_2\beta_2\varepsilon x_1^3+\beta_1\beta_2x_2+\beta_2x_2^2+3\beta_2\varepsilon\alpha_1x_1^3\\ &+3\beta_1\beta_2\varepsilon^2x_1^2x_2^3+2x_2x_1\beta_1+2x_1x_2^2\\ &-(\alpha_2\beta_2x_1+\alpha_2x_1^2+\beta_2\alpha_1x_1+\beta_1\beta_2\varepsilon x_2^3+3\beta_1\beta_2\varepsilon x_1^2x_2\\ &+3\beta_2\varepsilon x_2^2x_1^2+2\alpha_1x_1^2+2x_1\beta_1\varepsilon x_2^3).\end{aligned}\tag{33}$$

Let us consider

$$\begin{aligned}\frac{d^2x_1(t)}{dt^2} &= A_1+A_2,\\ \frac{d^2x_2(t)}{dt^2} &= B_1+B_2.\end{aligned}\tag{34}$$

Here A_1 and B_1 are positive part and taken as

$$\begin{aligned}A_1 = {} & \alpha_1^2x_1+\alpha_1\beta_1\varepsilon x_2^3+\beta_1\beta_2x_1+\beta_1x_1^2+3\beta_1\varepsilon\alpha_2x_2^3\\ &+3\beta_1\beta_2\varepsilon^2x_2^2x_1^3+2\beta_2x_1x_2+2x_2x_1^2,\\ B_1 = {} & \alpha_2^2x_2+\alpha_2\beta_2\varepsilon x_1^3+\beta_1\beta_2x_2+\beta_2x_2^2+3\beta_2\varepsilon\alpha_1x_1^3\\ &+3\beta_1\beta_2\varepsilon^2x_1^2x_2^3+2x_2x_1\beta_1+2x_1x_2^2\end{aligned}\tag{35}$$

and A_2 and B_2 are negative part and taken as

$$\begin{aligned}A_2 = {} & -(\alpha_2\beta_2x_1+\alpha_2x_1^2+\beta_2\alpha_1x_1+\beta_1\beta_2\varepsilon x_2^3+3\beta_1\beta_2\varepsilon x_1^2x_2\\ &+3\beta_1\varepsilon x_2^2x_1^2+2\alpha_2x_2^2+2x_2\beta_2\varepsilon x_1^3),\\ B_2 = {} & -(\alpha_2\beta_2x_1+\alpha_2x_1^2+\beta_2\alpha_1x_1+\beta_1\beta_2\varepsilon x_2^3+3\beta_1\beta_2\varepsilon x_1^2x_2\\ &+3\beta_2\varepsilon x_2^2x_1^2+2\alpha_1x_1^2+2x_1\beta_1\varepsilon x_2^3).\end{aligned}\tag{36}$$

So we have

$$\begin{aligned}\frac{d^2L(t)}{dt^2} = {} & \left(\frac{\overset{\prime}{x_1}}{x_1}\right)^2x_1^*+\left(\frac{\overset{\prime}{x_2}}{x_2}\right)^2x_2^*\\ &+A_1+A_2-\frac{x_1^*}{x_1}A_1-\frac{x_1^*}{x_1}A_2\\ &+B_1+B_2-\frac{x_2^*}{x_2}B_1-\frac{x_2^*}{x_2}B_2.\end{aligned}\tag{37}$$

Now we divide normalsize all items with positive and negative parts

$$\frac{d^2L(t)}{dt^2} = \Phi_1-\Phi_2,\tag{38}$$

Here the positive part of equality is given as

$$\Phi_1 = \left(\frac{\overset{\prime}{x_1}}{x_1}\right)^2x_1^*+\left(\frac{\overset{\prime}{x_2}}{x_2}\right)^2x_2^*+A_1+B_1+\frac{x_1^*}{x_1}A_2+\frac{x_2^*}{x_2}B_2,\tag{39}$$

and the negative part of equality is given as

$$\Phi_2 = A_2+B_2-\frac{x_1^*}{x_1}A_1-\frac{x_2^*}{x_2}B_1.\tag{40}$$

Therefore if

$$\begin{aligned}&\Phi_1-\Phi_2>0 \text{ then } \frac{d^2L(t)}{dt^2}>0,\\ &\Phi_1-\Phi_2=0 \text{ then } \frac{d^2L(t)}{dt^2}=0,\\ &\Phi_1-\Phi_2<0 \text{ then } \frac{d^2L(t)}{dt^2}<0.\end{aligned}\tag{41}$$

6. Existence and uniqueness of system solution

In the last past years, several authors have devoted their attention to developing conditions under which nonlinear differential equations admit unique solutions, in particular for the case of classical derivatives. Several extensions have been done within the framework of fractional derivation with singular and non-singular kernels. We shall state one of the important on here, which will be used.

Theorem 2. *Let $I_T=[0,T]$, the function $f: \underset{(t,y)\to}{I\times R}\to \underset{f(t,y)}{R}$ is such that, $f(t,y)$ is measurable for $y\in R$ and $y\to f(t,y)$ is continuous for each $t\in I_T$. If there exists on $M\in L^2[I_T,R]$ such that*

$$|f(t,y)|^2\le M\left(1+|y|^2\right),\ \forall(t,y)\in I_T\times R\tag{42}$$

then there exists a continuous $u(t)$ such that

$$u(t)=\int_0^t f(\tau,u(\tau))\,d\tau.\tag{43}$$

If in addition, one have

$$|f(t,y)-f(t,\overline{y})|<K|y-\overline{y}|^2,\ \forall y,\overline{y}\in R\tag{44}$$

then the solution is unique.

Indeed the existence can be achieved via sequence by constructing the Picard, Tonelli other sequences [18, 19]. The main task is to show that under the above condition, the sequence is equicontinuous uniformly and bounded uniformly. The Peano-Cauchy theorem helps us to secure the existence [20]. The Gronwall inequality helps us obtain uniqueness within the framework of fractional calculus, there is an extra condition on the fractional order. It's required that $\alpha > \frac{1}{2}$ since

$$\begin{aligned}
&\left|\frac{1}{\Gamma(\alpha)}\int_0^t (t-\tau)^{\alpha-1} f(\tau, y(\tau))\, d\tau\right|^2 \quad (45)\\
\leq\ & \frac{1}{\Gamma^2(\alpha)}\int_0^t (t-\tau)^{2\alpha-2} \left|f(\tau, y(\tau))\right|^2 d\tau\\
\leq\ & \frac{1}{\Gamma^2(\alpha)}\int_0^t (t-\tau)^{2\alpha-2} d\tau \int_0^t \left|f(\tau, y(\tau))\right|^2 d\tau\\
\leq\ & \frac{t^{2\alpha-1}}{(2\alpha-1)\Gamma^2(\alpha)} \left\|f(., y(.))\right\|^2_{L^2[0,T]}
\end{aligned}$$

Thus $\alpha > \frac{1}{2}$.

The existence and uniqueness of the solution of a differential equation are the most important parts of the theory of differential equations. There are various proofs on this subject. Here we will do our proof by obtaining the necessary conditions via Linear growth and Lipschitz for our model [21].

$$\begin{aligned}
\frac{dx_1(t)}{dt} &= -\alpha_1 x_1 + \beta_1 x_2 - \beta_1 \varepsilon x_2^3 + x_2^2, \quad (46)\\
\frac{dx_2(t)}{dt} &= -\alpha_2 x_2 + \beta_2 x_1 - \beta_2 \varepsilon x_1^3 + x_1^2,
\end{aligned}$$

with initial conditions $x_1(0) = 0$ and $x_2(0) = 0$.

Let us find the necessary conditions for the existence and uniqueness, we must prove that $\forall\ [0, T_1]$ and $f_i(x_1, x_2)$ for $i = 1, 2$ satisfy

1)Linear growth condition

$$\left|f_i(x_i, t)\right|^2 \leq s_i(1 + |x_i|^2) \quad \text{for } i = 1, 2. \quad (47)$$

2)The Lipschitz condition

$$\left|f_i(x_i, t) - f_i(\overline{x}_i, t)\right|^2 \leq \overline{s}_i \left|x_i - \overline{x}_i\right|^2 \quad \text{for } i = 1, 2. \quad (48)$$

Now we define the norm $\|\varphi\|_\infty = \sup_{t\in D_\varphi} |\varphi(t)|$. Now we put the existence and uniqueness of the solution for $[0, T_1]$. For $[0, T_1]$, there exist 2 positive constant M_1 and $M_2 < \infty$ such that

$$\begin{aligned}
\|x_1\|_\infty &< M_1, \quad (49)\\
\|x_2\|_\infty &< M_2.
\end{aligned}$$

Let us write the system as below:

$$\left\{\begin{array}{l} \dot{x_1} = f_1(x_1, x_2), \\ \dot{x_2} = f_2(x_1, x_2), \end{array}\right. \text{if } 0 \leq t \leq T_1. \quad (50)$$

For proof, we consider the function

$$\begin{aligned}
\left|f_1(x_1, x_2)\right|^2 &= \left|-\alpha_1 x_1 + \beta_1 x_2 - \beta_1 \varepsilon x_2^3 + x_2^2\right|^2,\\
&\leq 4\alpha_1^2 |x_1|^2 + 4\beta_1^2 |x_2|^2\\
&+ 4\beta_1^2\varepsilon^2 \left|x_2^3\right|^2 + 4\left|x_2^2\right|^2\\
&\leq 4\alpha_1^2 |x_1|^2 + 4\beta_1^2 \sup_{t\in[0,T_1]} |x_2|^2\\
&+ 4\beta_1^2\varepsilon^2 \sup_{t\in[0,T_1]} \left|x_2^3\right|^2 + 4\sup_{t\in[0,T_1]} \left|x_2^2\right|^2\\
&\leq 4\alpha_1^2 |x_1|^2 + 4\beta_1^2 \|x_2\|^2_\infty + 4\beta_1^2\varepsilon^2 \left\|x_2^3\right\|^2_\infty\\
&+ 4\left\|x_2^2\right\|^2_\infty,\\
&\leq 4\beta_1^2 \|x_2\|^2_\infty + 4\beta_1^2\varepsilon^2 \left\|x_2^3\right\|^2_\infty\\
&+ 4\left\|x_2^2\right\|^2_\infty \times\\
&\left(1 + \frac{4\alpha_1^2 |x_1|^2}{4\beta_1^2 \|x_2\|^2_\infty + 4\beta_1^2\varepsilon^2 \left\|x_2^3\right\|^2_\infty + 4\left\|x_2^2\right\|^2_\infty}\right)\\
&\leq s_1(1 + |x_1(t)|^2)
\end{aligned} \quad (51)$$

Here

$$s_1 = 4\beta_1^2 \|x_2\|^2_\infty + 4\beta_1^2\varepsilon^2 \left\|x_2^3\right\|^2_\infty + 4\left\|x_2^2\right\|^2_\infty \quad (52)$$

and under the condition that

$$\frac{\alpha_1^2}{\beta_1^2 \|x_2\|^2_\infty + \beta_1^2\varepsilon^2 \left\|x_2^3\right\|^2_\infty + \left\|x_2^2\right\|^2_\infty} < 1, \quad (53)$$

then we have

$$\left|f_1(x_1, x_2)\right|^2 \leq s_1(1 + |x_1(t)|^2). \quad (54)$$

Using the same routine

$$\begin{aligned}
\left|f_2(x_1, x_2)\right|^2 &= \left|-\alpha_2 x_2 + \beta_2 x_1 - \beta_2 \varepsilon x_1^3 + x_1^2\right|^2,\\
&\leq 4\alpha_2^2 |x_2|^2 + 4\beta_2^2 |x_1|^2 + 4\beta_2^2\varepsilon^2 \left|x_1^3\right|^2 + 4\left|x_1^2\right|^2,\\
&\leq 4\alpha_2^2 |x_2|^2 + 4\beta_2^2 \sup_{t\in[0,T_1]} |x_1|^2\\
&+ 4\beta_2^2\varepsilon^2 \sup_{t\in[0,T_1]} \left|x_1^3\right|^2 + 4\sup_{t\in[0,T_1]} \left|x_1^2\right|^2\\
&\leq 4\alpha_1^2 |x_2|^2 + 4\beta_2^2 \|x_1\|^2_\infty + 4\beta_1^2\varepsilon^2 \left\|x_1^3\right\|^2_\infty\\
&+ 4\left\|x_1^2\right\|^2_\infty,\\
&\leq 4\beta_2^2 \|x_1\|^2_\infty + 4\beta_1^2\varepsilon^2 \left\|x_1^3\right\|^2_\infty + 4\left\|x_1^2\right\|^2_\infty \times\\
&\left(1 + \frac{4\alpha_1^2 |x_2|^2}{4\beta_2^2 \|x_1\|^2_\infty + 4\beta_1^2\varepsilon^2 \left\|x_1^3\right\|^2_\infty + 4\left\|x_1^2\right\|^2_\infty}\right)\\
&\leq s_2(1 + |x_2(t)|^2)
\end{aligned} \quad (55)$$

Here

$$s_2 = 4\beta_2^2 \|x_1\|_\infty^2 + 4\beta_1^2\varepsilon^2 \left\|x_1^3\right\|_\infty^2 + 4 \left\|x_1^2\right\|_\infty^2 \quad (56)$$

and under the condition

$$\frac{\alpha_1^2}{\beta_2^2 \|x_1\|_\infty^2 + \beta_1^2\varepsilon^2 \left\|x_1^3\right\|_\infty^2 + \left\|x_1^2\right\|_\infty^2} < 1 \quad (57)$$

Therefore the condition of linear growth is verified if

$$\max\left\{ \begin{array}{c} \frac{\alpha_1^2}{\beta_1^2\|x_2\|_\infty^2+\beta_1^2\varepsilon^2\left\|x_2^3\right\|_\infty^2+\left\|x_2^2\right\|_\infty^2}, \\ \frac{\alpha_1^2}{\beta_2^2\|x_1\|_\infty^2+\beta_1^2\varepsilon^2\left\|x_1^3\right\|_\infty^2+\left\|x_1^2\right\|_\infty^2}, \end{array} \right\} < 1. \quad (58)$$

The first part of proof is completed. Now we have to verify Lipschitz condition for equations. If we have $\forall x_1, \overline{x}_1 \in R^2$ and $t \in [0, T_1]$, for the function $f_1(x_1, x_2)$,

$$\begin{aligned} |f_1(x_1, x_2) - f_1(\overline{x}_1, x_2)| &\leq \alpha_1^2 |x_1 - \overline{x}_1|, \quad (59) \\ &\leq \overline{s}_1 |x_1 - \overline{x}_1|. \end{aligned}$$

If we have $\forall x_2, \overline{x}_2 \in R^2$ and $t \in [0, T_1]$ for the function $f_2(x_1, x_2)$,

$$\begin{aligned} |f_2(x_1, x_2) - f_2(x_1, \overline{x}_2)| &\leq \alpha_2^2 |x_2 - \overline{x}_2|, \quad (60) \\ &\leq \overline{s}_2 |x_2 - \overline{x}_2|. \end{aligned}$$

We verified the Lipschitz condition, which completes the proof.
Finally, we consider the following fractional order model as below;

$$\begin{aligned} &{}_{t_0}^{C}D_t^\alpha x_1(t) = f_1(t, x_1(t)), \quad \text{if } t > 0 \quad (61) \\ &{}_{t_0}^{C}D_t^\alpha x_2(t) = f_2(t, x_2(t)), \\ &x_1(t_0) = x_{10},\ x_2(t_0) = x_{20} \quad \text{if } t = 0. \end{aligned}$$

We can write the system above as

$$\begin{aligned} {}_{t_0}^{C}D_t^\alpha X(t) &= F(t, X(t)), \quad (62) \\ X(t_0) &= X_0, \end{aligned}$$

where

$$X(t) = \left\{ \begin{array}{l} x_1(t), \\ x_2(t) \end{array} \right., \ X(t_0) = \left\{ \begin{array}{l} x_1(t_0), \\ x_2(t_0) \end{array} \right.,$$
$$F(t, X(t)) = \left\{ \begin{array}{l} f_1(t, x_1(t)), \\ f_2(t, x_2(t)) \end{array} \right. . \quad (63)$$

Now applying the fractional integral on both sides

$$X(t) = \frac{1}{\Gamma(\alpha)} \int_0^t F(\tau, X(\tau)) (t-\tau)^{\alpha-1} d\tau. \quad (64)$$

At the previous section we showed that $f_1(t, x_1(t))$ and $f_2(t, x_2(t))$ satisfy the Lipschitz condition and are bounded in $[a, b]$. Using the Picard iteration for above , then we have that

$$X_{n+1}(t) = \frac{1}{\Gamma(\alpha)} \int_{t_0}^t F(\tau, X_n(\tau)) (t-\tau)^{\alpha-1} d\tau. \quad (65)$$

For the existence theory, we define Banach space $\Phi = X \times X$ where $X = C[0, T_1]$ under the following norm

$$\|X\| = \max_{t\in[0,T_1]} |x_1(t), x_2(t)|. \quad (66)$$

So we have

$$\begin{aligned} \|X_{n+1}\| &= \max_{t\in[0,T_1]} \left| \frac{1}{\Gamma(\alpha)} \int_{t_0}^t F(\tau, X_n(\tau)) (t-\tau)^{\alpha-1} d\tau \right| \\ &\leq \frac{1}{\Gamma(\alpha)} \int_{t_0}^t s(1 + \|X_n\|) (t-\tau)^{\alpha-1} d\tau \\ &\leq \frac{s(1 + \|X_n\|)}{\Gamma(\alpha)} \frac{(t-t_0)^\alpha}{\alpha}. \end{aligned} \quad (67)$$

So we have that $\forall t \in [a, b]$

$$\|X_{n+1}\| \leq \frac{s(1 + \|X_n\|)}{\Gamma(\alpha+1)} (b - t_0)^\alpha \quad (68)$$

But $\forall n > 0$, $\exists c \in [x_0 - c, x_0 + c]$ then

$$\begin{aligned} &\frac{s(1 + \|X_n\|)}{\Gamma(\alpha+1)} (b - t_0)^\alpha < c, \\ &b < \left(\frac{c\Gamma(\alpha+1)}{s(1 + \|X_n\|)} \right)^{\frac{1}{\alpha}} + t_0. \end{aligned} \quad (69)$$

Under the above condition $X_n(t)$ for $n \geq 0$ is uniformly bounded and well-defined. For equicontinuity of X, let us take $t_1 < t_2 < T_1$, then consider

$$\|X_n(t_1) - X_n(t_2)\|$$

$$= \frac{1}{\Gamma(\alpha)} \max \left| \begin{array}{l} \int_{t_0}^{t_1} F(\tau, X_{n-1}(\tau)) (t_1-\tau)^{\alpha-1} d\tau \\ -\int_{t_0}^{t_2} F(\tau, X_{n-1}(\tau)) (t_2-\tau)^{\alpha-1} d\tau \end{array} \right|$$

$$= \frac{1}{\Gamma(\alpha)} \max \left| \begin{array}{l} \int_{t_0}^{t_2} F(\tau, X_{n-1}(\tau)) (t_1-\tau)^{\alpha-1} d\tau \\ -\int_{t_0}^{t_2} F(\tau, X_{n-1}(\tau)) (t_2-\tau)^{\alpha-1} d\tau \\ +\int_{t_2}^{t_1} F(\tau, X_{n-1}(\tau)) (t_1-\tau)^{\alpha-1} d\tau \end{array} \right|$$

$$\leq \frac{1}{\Gamma(\alpha)} \int_{t_0}^{t_2} \|F(\tau, X_{n-1}(\tau))\| \left\{ (t_1-\tau)^{\alpha-1} - (t_2-\tau)^{\alpha-1} \right\} d\tau$$
$$+ \frac{1}{\Gamma(\alpha)} \int_{t_2}^{t_1} \|F(\tau, X_{n-1}(\tau))\| (t_1-\tau)^{\alpha-1} d\tau$$
$$\leq \frac{s(1+\|X_n\|)}{\Gamma(\alpha)} \left\{ \frac{(t_1-t_0)^\alpha}{\alpha} - \frac{(t_2-t_0)^\alpha}{\alpha} - \frac{(t_1-t_2)^\alpha}{\alpha} \right\}$$
$$+ \frac{s(1+\|X_n\|)}{\Gamma(\alpha)} \left\{ \frac{(t_1-t_2)^\alpha}{\alpha} \right\}$$
$$\leq \frac{s(1+\|X_n\|)}{\Gamma(\alpha+1)} \{(t_1-t_0)^\alpha - (t_2-t_0)^\alpha\}. \tag{70}$$

Noting that the $(t-t_0)^\alpha$ is differentiable, by the Mean Value theorem we can find $c \in [t_1-t_0, t_2-t_0]$ such that

$$\alpha (c-t_0)^{\alpha-1} (t_1-t_2) = (t_1-t_0)^\alpha - (t_2-t_0)^\alpha. \tag{71}$$

So we have

$$\begin{aligned} \|X_n(t_1) - X_n(t_2)\| &\leq \frac{s(1+\|X_n\|)}{\Gamma(\alpha+1)} \alpha (c-t_0)^{\alpha-1} (t_1-t_2) \\ &\leq \frac{s(1+\|X_n\|)}{\Gamma(\alpha+1)} \alpha (c-t_0)^{\alpha-1} \|t_1-t_2\| \\ &< \varepsilon \end{aligned} \tag{72}$$

then $\forall \varepsilon > 0$, we must find $\exists \delta > 0$ such that

$$\delta < \frac{\varepsilon \Gamma(\alpha)}{s(1+\|X_n\|) \alpha (c-t_0)^{\alpha-1}}. \tag{73}$$

So under the condition above $X_n(t)$ is uniformly equicontinuous.

Beside the Caratheodory principle verified above, one can demonstrate the existence and uniqueness of the system solutions of the considered system.

We have that

$$\begin{aligned} {}_0^C D_t^\alpha x_1(t) &= f_1(t, x_1(t)), \quad \text{if } t > 0 \\ {}_0^C D_t^\alpha x_2(t) &= f_2(t, x_2(t)). \end{aligned} \tag{74}$$

It is sufficient to show that $\forall t \in I_b = [0, b]$ the associate Jacobian matrix is differentiable continuous. The Jacobian associated to this system is given as

$$J(x_1, x_2) = \begin{bmatrix} -\alpha_1 & \beta_1 - 3\varepsilon\beta_1 x_2^2 + 2\lambda x_2 \\ \beta_2 - 3\varepsilon\beta_2 x_1^2 + 2\lambda x_1 & -\alpha_2 \end{bmatrix}. \tag{75}$$

The above is continuous for $\forall (x, y)$ which completes the proof.

7. Model with piecewise concept

It indeed above model can be used to replicate some interpersonal interaction, one will notice that the current mathematical model show only one process, for example with the Caputo one can only describe the relation following the power-law behavior. Whereas in normal situations, interpersonal interaction undergoes piecewise behaviors, where the relation change as function of time in the case of ordinary differential equation and space time in the case of partial differential equation. In this section, we shall consider the model with two to three processes, including classical behaviors, then power law behaviors or power law and stochastic with piecewise idea [11]. In these cases, the following mathematical systems are constructed

$$\begin{aligned} \frac{dx_1(t)}{dt} &= -\alpha_1 x_1 + \beta_1 x_2 - \beta_1 \varepsilon x_2^3 + \lambda x_2^2, \text{ if } 0 \leq t \leq t_1 \\ \frac{dx_2(t)}{dt} &= -\alpha_2 x_2 + \beta_2 x_1 - \beta_2 \varepsilon x_1^3 + \lambda x_1^2, \\ {}_{t_1}^C D_t^\alpha x_1(t) &= -\alpha_1 x_1 + \beta_1 x_2 - \beta_1 \varepsilon x_2^3 + \lambda x_2^2, \text{ if } t_1 \leq t \leq T \\ {}_{t_1}^C D_t^\alpha x_2(t) &= -\alpha_2 x_2 + \beta_2 x_1 - \beta_2 \varepsilon x_1^3 + \lambda x_1^2, \end{aligned} \tag{76}$$

or

$$\begin{aligned} \frac{dx_1(t)}{dt} &= -\alpha_1 x_1 + \beta_1 x_2 - \beta_1 \varepsilon x_2^3 + \lambda x_2^2, \text{ if } 0 \leq t \leq t_1 \\ \frac{dx_2(t)}{dt} &= -\alpha_2 x_2 + \beta_2 x_1 - \beta_2 \varepsilon x_1^3 + \lambda x_1^2, \\ dx_1(t) &= \left(-\alpha_1 x_1 + \beta_1 x_2 - \beta_1 \varepsilon x_2^3 + \lambda x_2^2\right) dt + \sigma_1 x_1 dB_1(t), \\ &\quad \text{if } t_1 \leq t \leq T \\ dx_2(t) &= \left(-\alpha_2 x_2 + \beta_2 x_1 - \beta_2 \varepsilon x_1^3 + \lambda x_1^2\right) dt + \sigma_2 x_2 dB_2(t). \end{aligned} \tag{77}$$

Obviously the above system can not be solved analytically indeed due to non linearity, therefore we will present some existence and uniqueness conditions for the two systems. Indeed by putting

$$\begin{aligned}
\frac{dx_1(t)}{dt} &= f_1\left(t, x_1, x_2\right), \text{ if } 0 \leq t \leq t_1 \\
\frac{dx_2(t)}{dt} &= f_2\left(t, x_1, x_2\right), \\
{}_{t_1}^{C}D_t^{\alpha} x_1(t) &= f_1\left(t, x_1, x_2\right), \text{if } t_1 \leq t \leq T \\
{}_{t_1}^{C}D_t^{\alpha} x_2(t) &= f_2\left(t, x_1, x_2\right).
\end{aligned} \tag{78}$$

The following Picard system of sequence can be defined

$$\begin{aligned}
&x_{1n+1}(t) = x_1(0) + \int_0^t f_1\left(\tau, x_{1n}, x_{2n}\right) d\tau, \text{ if } 0 \leq t \leq t_1 \\
&x_{2n+1}(t) = x_2(0) + \int_0^t f_2\left(\tau, x_{1n}, x_{2n}\right) d\tau, \\
&x_{1n+1}(t) = x_1(t_1) + \int_{t_1}^t \frac{(t-\tau)^{\alpha-1}}{\Gamma(\alpha)} f_1\left(\tau, x_{1n}, x_{2n}\right) d\tau, \\
&\qquad \text{if } t_1 \leq t \leq T \\
&x_{2n+1}(t) = x_2(t_1) + \int_{t_1}^t \frac{(t-\tau)^{\alpha-1}}{\Gamma(\alpha)} f_2\left(\tau, x_{1n}, x_{2n}\right) d\tau,
\end{aligned} \tag{79}$$

and

$$\begin{aligned}
&x_{1n+1}(t) = x_1(0) + \int_0^t f_1\left(\tau, x_{1n}, x_{2n}\right) d\tau, \text{ if } 0 \leq t \leq t_1 \\
&x_{2n+1}(t) = x_2(0) + \int_0^t f_2\left(\tau, x_{1n}, x_{2n}\right) d\tau, \\
&x_{1n+1}(t) = x_1(t_1) + \int_{t_1}^t f_1\left(\tau, x_{1n}, x_{2n}\right) d\tau + \sigma_1 \int_{t_1}^t x_{1n} dB_1(t), \\
&\qquad \text{if } t_1 \leq t \leq T \\
&x_{2n+1}(t) = x_2(t_1) + \int_{t_1}^t f_2\left(\tau, x_{1n}, x_{2n}\right) d\tau + \sigma_2 \int_{t_1}^t x_{2n} dB_2(t), \\
&\qquad \text{if } t_1 \leq t \leq T.
\end{aligned} \tag{80}$$

The above sequences are Picard sequences that indeed satisfying indeed under some conditions uniform equicontinuity and bounded, this lead to the existence of a unique system of solutions. The detailed proof will not be presented here. However, a numerical scheme will be used to solve numerically the above equation. For the classical case, we shall adopt Heun's method

$$\begin{aligned}
&\widetilde{x}_{1n+1} = x_{1n} + h\left[f_1\left(t_n, x_{1n}, x_{2n}\right)\right], \\
&\widetilde{x}_{2n+1} = x_{2n} + h\left[f_2\left(t_n, x_{1n}, x_{2n}\right)\right], \\
&x_{1n+1} = x_{1n} + \frac{h}{2}\left[f_1\left(t_n, x_{1n}, x_{2n}\right) + f_1\left(t_{n+1}, \widetilde{x}_{1n+1}, \widetilde{x}_{2n+1}\right)\right], \\
&x_{2n+1} = x_{2n} + \frac{h}{2}\left[f_2\left(t_n, x_{1n}, x_{2n}\right) + f_2\left(t_{n+1}, \widetilde{x}_{1n+1}, \widetilde{x}_{2n+1}\right)\right],
\end{aligned} \tag{81}$$

replacing $\widetilde{x}_{1n+1}$ and $\widetilde{x}_{2n+1}$, we get

$$\begin{aligned}
x_{1n+1} = x_{1n} + \frac{h}{2}&[f_1\left(t_n, x_{1n}, x_{2n}\right) \\
&+ f_1\left(t_{n+1}, x_{1n} + hf_1\left(t_n, x_{1n}, x_{2n}\right)\right)], \\
x_{2n+1} = x_{2n} + \frac{h}{2}&[f_2\left(t_n, x_{1n}, x_{2n}\right) \\
&+ f_2\left(t_{n+1}, x_{2n} + hf_2\left(t_n, x_{1n}, x_{2n}\right)\right)].
\end{aligned}$$

For the Caputo type, to avoid confusion, we define

$$\begin{aligned}
x_1(t_{n+1}) &= x_{1n+1}, \\
x_2(t_{n+1}) &= x_{2n+1}, \\
x_1(t_0) &= x_{10}, \\
x_2(t_0) &= x_{20}.
\end{aligned} \tag{82}$$

$$\begin{aligned}
&x_{1n+1} = x_{10} + \frac{1}{\Gamma(\alpha)} \sum_{j=0}^{n} \int_{t_j}^{t_{j+1}} f_1\left(\tau, x_1, x_2\right)\left(t_{n+1}-\tau\right)^{\alpha-1} d\tau, \\
&x_{2n+1} = x_{20} + \frac{1}{\Gamma(\alpha)} \sum_{j=0}^{n} \int_{t_j}^{t_{j+1}} f_2\left(\tau, x_1, x_2\right)\left(t_{n+1}-\tau\right)^{\alpha-1} d\tau, \\
&x_{1n+1} = x_{10} + \frac{1}{2\Gamma(\alpha)} \sum_{j=0}^{n} \int_{t_j}^{t_{j+1}} [f_1\left(t_j, x_{1j}, x_{2j}\right) \\
&\qquad + f_1\left(t_{j+1}, x_{1j+1}, x_{2j+1}\right)]\left(t_{n+1}-\tau\right)^{\alpha-1} d\tau, \\
&x_{2n+1} = x_{20} + \frac{1}{2\Gamma(\alpha)} \sum_{j=0}^{n} \int_{t_j}^{t_{j+1}} [f_2\left(t_j, x_{1j}, x_{2j}\right) \\
&\qquad + f_2\left(t_{j+1}, x_{1j+1}, x_{2j+1}\right)]\left(t_{n+1}-\tau\right)^{\alpha-1} d\tau
\end{aligned} \tag{83}$$

$$\begin{aligned}
&x_{1n+1} = x_{10} + \frac{h^{\alpha}}{2\Gamma(\alpha+1)} \sum_{j=0}^{n-1} \left[f_1\left(t_j, x_{1j}, x_{2j}\right) + f_1\left(t_{j+1}, x_{1j+1}, x_{2j+1}\right)\right] \\
&\qquad \left\{(n-j+1)^{\alpha} - (n-j)^{\alpha}\right\} \\
&\qquad + \frac{h^{\alpha}}{2\Gamma(\alpha+1)}\left[f_1\left(t_n, x_{1n}, x_{2n}\right) + f_1\left(t_{n+1}, \widetilde{x}_{1n+1}, \widetilde{x}_{2n+1}\right)\right], \\
&x_{2n+1} = x_{20} + \frac{h^{\alpha}}{2\Gamma(\alpha+1)} \sum_{j=0}^{n-1} \left[f_2\left(t_j, x_{1j}, x_{2j}\right) + f_2\left(t_{j+1}, x_{1j+1}, x_{2j+1}\right)\right] \\
&\qquad \left\{(n-j+1)^{\alpha} - (n-j)^{\alpha}\right\} \\
&\qquad + \frac{h^{\alpha}}{2\Gamma(\alpha+1)}\left[f_2\left(t_n, x_{1n}, x_{2n}\right) + f_2\left(t_{n+1}, \widetilde{x}_{1n+1}, \widetilde{x}_{2n+1}\right)\right],
\end{aligned} \tag{84}$$

where

$$\widetilde{x}_{1n+1} = x_{10} + \frac{h^\alpha}{\Gamma(\alpha+1)} \sum_{j=0}^{n} f_1(t_j, x_{1j}, x_{2j}) \{(n-j+1)^\alpha - (n-j)^\alpha\},$$

$$\widetilde{x}_{2n+1} = x_{20} + \frac{h^\alpha}{\Gamma(\alpha+1)} \sum_{j=0}^{n} f_2(t_j, x_{1j}, x_{2j}) \{(n-j+1)^\alpha - (n-j)^\alpha\}. \tag{85}$$

Finally for the stochastic part, the following numerical solution can be obtained

$$\begin{aligned}
\widetilde{x}_{1n+1} &= x_{1n} + h f_1(t_n, x_{1n}, x_{2n}) + \sigma_1 x_{1n} [B_{1n+1} - B_{1n}], \\
\widetilde{x}_{2n+1} &= x_{2n} + h f_2(t_n, x_{1n}, x_{2n}) + \sigma_2 x_{2n} [B_{2n+1} - B_{2n}], \\
x_{1n+1} &= x_{1n} + \frac{h}{2} [f_1(t_n, x_{1n}, x_{2n}) + f_1(t_{n+1}, \widetilde{x}_{1n+1}, \widetilde{x}_{2n+1})] \\
&\quad + \sigma_1 x_{1n} [B_{1n+1} - B_{1n}], \\
x_{2n+1} &= x_{2n} + \frac{h}{2} [f_2(t_n, x_{1n}, x_{2n}) + f_2(t_{n+1}, \widetilde{x}_{1n+1}, \widetilde{x}_{2n+1})] \\
&\quad + \sigma_2 x_{2n} [B_{2n+1} - B_{2n}].
\end{aligned} \tag{86}$$

8. Numerical simulations

In this section, we will deal with the numerical simulation of the interpersonal model with the piecewise differential operators and the numerical scheme where the Lagrange polynomial interpolation is used [22]. In the numerical scheme, the first part is classical, the second part is stochastic and the last part is fractional. The numerical simulations are shown in Fig. 1 for $\alpha = 1$, Fig. 2 for $\alpha = 0.97$, Fig. 3 for $\alpha = 0.98$, and Fig. 4 is obtained for chaos for $\alpha = 1$, Fig. 5 is obtained for chaos for $\alpha = 0.97$, Fig. 6 is obtained for chaos for $\alpha = 0.98$. For all figures, density of randomness are taken as $\sigma_1 = 0.09$, and $\sigma_2 = 0.09$. Also figures including the initial conditions as $x_1(0) = -0.1$, $x_2(0) = 0.8$. Also, for the numerical simulations of the system we consider the values of the parameters as follows:

$$\alpha_1 = 0.1, \alpha_2 = 0.01, \beta_1 = 5.7, \beta_2 = -1, \varepsilon = 0.01$$

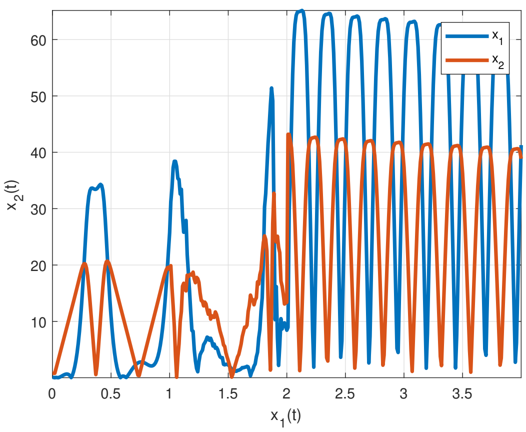

Figure 1. Numerical solutions for $\alpha = 1$.

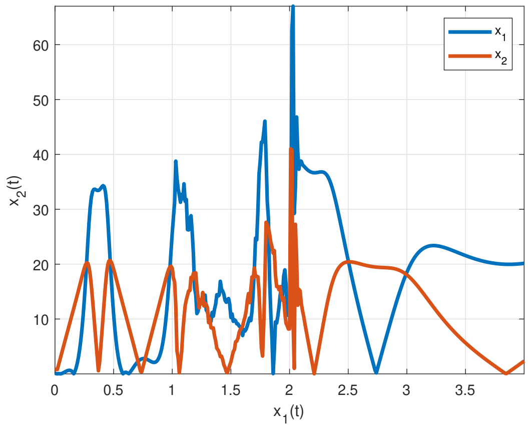

Figure 2. Numerical solutions for $\alpha = 0.97$.

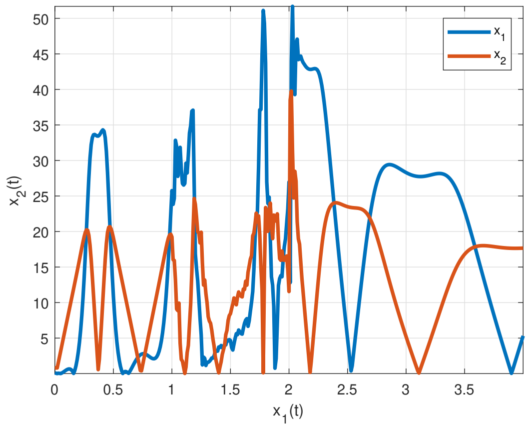

Figure 3. Numerical solutions for $\alpha = 0.98$.

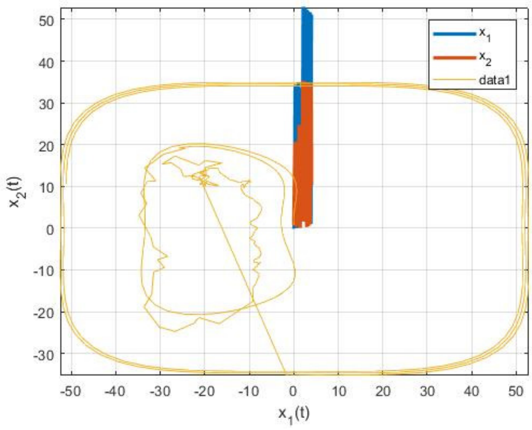

Figure 4. Numerical solutions for $\alpha = 1$.

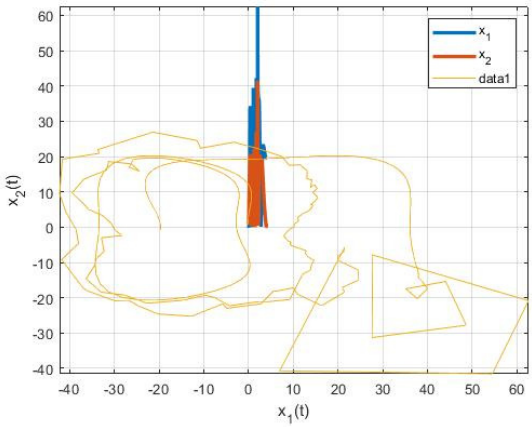

Figure 5. Numerical solutions for $\alpha = 0.97$.

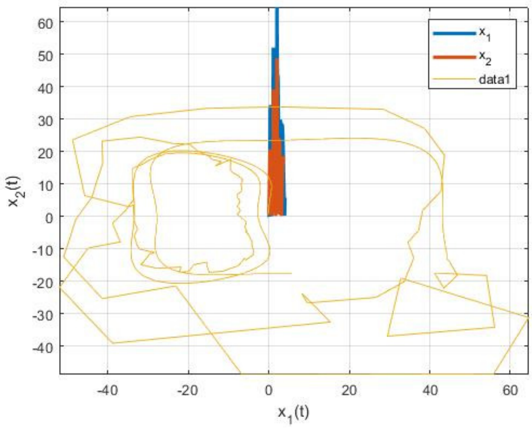

Figure 6. Numerical solutions for $\alpha = 0.98$.

9. Conclusion

In this work, a nonlinear differential equation was taken into consideration, and the Caputo, stochastic process, and piecewise differential operators were used in place of the classical differential operators. Through this work, we have looked into the associated equilibrium points' general approach to stability. We have derived the conditions under which the system admits a singular, unique system of solutions using the linear growth and Lipschitz requirements. To solve this problem numerically in the Caputo, stochastic, and piecewise cases, a numerical approach was adopted.

Acknowledgments

The authors express their gratitude to the anonymous reviewers and the editor for their insightful comments and suggestions.

References

[1] Uçar, E., Özdemir, N., & Altun, E. (2023). Qualitative analysis and numerical simulations of new model describing cancer. *Journal of Computational and Applied Mathematics,* 422, 114899.

[2] Zhang X-H, Algehyne E.A., Alshehri M.G., Bilal, M, Khan, M.A., & Muhammad, T. (2021). The parametric study of hybrid nanofluid flow with heat transition characteristics over a fluctuating spinning disk. *Plos One*. 16(8), e0254457.

[3] Wang, B., Jahanshahi, H., Volos, C., Bekiros, S., Khan, M.A., Agarwal, P., & Aly, A.A. (2021). A new RBF neural network-based fault-tolerant active control for fractional time-delayed systems. *Electronics*. 10(12), 1501.

[4] Abdullah, F.A., Islam, T., Gómez-Aguilar, J.F., & Akbar, A. (2023). Impressive and innovative soliton shapes for nonlinear Konno-Oono system relating to electromagnetic field. *Optical and Quantum Electronics*, 55, 69.

[5] Attia, R.A.M., Tian, J., Lu, L., Gómez-Aguilar, J.F., & Khater, M.M.A. (2022). Unstable novel and accurate soliton wave solutions of the nonlinear biological population model. *Arab Journal of Basic and Applied Sciences*. 29(1), 19-25.

[6] Sheergojri A., Iqbal P., Agarwal P., & Ozdemir N. (2022). Uncertainty-based Gompertz growth model for tumor population and its numerical analysis. *An International Journal of Optimization and Control: Theories & Applications (IJOCTA)*, 12, 137-150.

[7] Sene, N. (2022). Theory and applications of new fractional-order chaotic system under Caputo operator. *An International Journal of Optimization and Control: Theories & Applications*, 12(1), 20-38.

[8] Evirgen, F. (2023). Transmission of Nipah virus dynamics under Caputo fractional derivative. *Journal of Computational and Applied Mathematics*, 418, 114654.

[9] Evirgen, F., Ucar, E., Ucar, S., & Ozdemir, N. (2023). Modelling Influenza A disease dynamics under Caputo-Fabrizio fractional derivative with distinct contact rates. *Mathematical Modelling and Numerical Simulation with Applications,* 3(1), 58-72.

[10] Dokuyucu, M.A., & Dutta H. (2020). A fractional order model for Ebola Virus with the new Caputo fractional derivative without singular kernel. *Chaos, Solitons & Fractals*, 134, 109717.

[11] Atangana A., & Araz Igret S. (2021). New concept in calculus: Piecewise differential and integral operators. *Chaos, Solitons & Fractals,* 145, 110638.

[12] Koca I. & Atangana A. (2022). Some Chaotic mathematical models with stochastic resetting. *Fractals,* 30(8), 2240212.

[13] Miller, K.S., & Ross, B. (1993). *An Introduction to the Fractional Calculus and Fractional Differential Equations*, Wiley Hoboken, NJ, USA.

[14] Podlubny, I. (1998). *Fractional differential equations: an introduction to fractional derivatives, fractional differential equations, to methods of their solution and some of their applications.* Vol. 198. Elsevier.

[15] Cherif, A., Barley, K. (2011). Stochastic nonlinear dynamics of interpersonal and romantic relationships. *Applied Mathematics and Computation*, 217(13), 6273–6281.

[16] Ozalp, N., & Koca, I. (2012). A fractional order nonlinear dynamical model of interpersonal relationships. *Advances in Differential Equations*, (2012)189.

[17] Atangana, A., & Koca, I. (2023). Analytical and numerical investigation of the Hindmarsh-Rose model neuronal activity. *Mathematical Biosciences and Engineering*, 20(1), 1434-1459.

[18] Robin, W.A. (2010). Solving differential equations using modified Picard iteration. *International Journal of Mathematical Education in Science and Technology*, 41(5).

[19] Tonelli, L. (1928). Sulle equazioni funzionali del tipo di Volterra. *Bull. of the Calcutta Math. Soc.* 20, 31-48.

[20] Peano, G. (1890). Demonstration de l'integrabilite des equations differentielles ordinaires. *Mathematische Annalen.* 37(2), 182–228.

[21] Atangana, A. (2021). Mathematical model of survival of fractional calculus, critics and their impact: How singular is our world?. *Advances in Difference Equations,* (1), 1-59.

[22] Toufik M, & Atangana A. (2017). New numerical approximation of fractional derivative with non-local and non-singular kernel: application to chaotic models. *The European Physical Journal Plus*, 132(10) 444.

Ilknur Koca *received the B.Sc. and M.Sc. degrees in 2007 and 2009 from the Department of Mathematics from Ankara University, Turkey respectively. She received her Ph.D. degree from the same university in 2013. She is working as an Associate Professor at the Department of Accounting and Financial Management, Seydikemer High School of Applied Sciences, Mugla Sıtkı Kocman University, Mugla, Turkey. Her research interests are methods and applications of partial and ordinary differential equations, fractional differential equations, and iterative methods.*
https://orcid.org/0000-0003-4393-1588

Abdon Atangana *is a professor at the University of the Free State, Bloemfontein, South Africa.*
https://orcid.org/0000-0002-1886-3125

An International Journal of Optimization and Control: Theories & Applications
ISSN:2146-0957 eISSN:2146-5703
Vol.13, No.2, pp.193-204 (2023)
http://doi.org/10.11121/ijocta.2023.1348

RESEARCH ARTICLE

A study on the approximate controllability results of fractional stochastic integro-differential inclusion systems via sectorial operators

Kalimuthu Kaliraj [a*], Kothandapani Muthuvel [a,b]

[a] *Ramanujan Institute for Advanced Study in Mathematics, University of Madras, Chennai 600 005, Tamil Nadu, India*
[b] *Department of Mathematics, Guru Nanak College, Chennai 600 042, Tamil Nadu, India*
kaliraj@unom.ac.in, muthuvel1729@gmail.com

ARTICLE INFO

Article History:
Received 23 December 2022
Accepted 24 April 2023
Available 19 July 2023

Keywords:
Fractional derivatives and integrals
Approximate controllability
Sectorial operators
Fixed point techniques
Fractional stochastic system

AMS Classification 2010:
26A33; 93B05; 47B12; 37C25; 93E03

ABSTRACT

The study deals with the findings of the outcome of the approximate controllability results of inclusion type fractional stochastic system in Banach space with the order of the fractional system $\varrho \in (1, 2)$. At first, we implement Bohnenblust-Karlin's fixed point technique to deduce the required conditions on which the fractional system with inital conditions is approximately controllable, and there by, we postulate the sufficient conditions for extending the obtained results to the system with nonlocal conditions.

1. Introduction

The recent development in the area of fractional theory plays an important role in mathematics. It is well understood by physical interpretation of differential equations that many of the realistic systems are better modeled by fractional order derivatives than integer order. Hence, there has been a huge growth in the fractional research field. The progress of this particular theory has a wide range of application in electro-magnetic, viscoelasticity, image processing, signal processing, control theory, diffusion, porous media, fluid flow and other fields. For more noteworthy contributions of fractional field the readers are referred to the books [1–5] and the research papers [6–14]. Moreover fractional integro-differential equations are used in various scientific domains such as control theory, medicine, biology and ecology etc. In the following research articles the above discussed concepts are well explained [6, 10, 11, 15, 16].

Inclusion type differential equation establishes a relation of the type $\dot{x} \in F(x)$ in such a way that the map F assigns any point $x \in R^n$ to a set $F(x) \subset R^n$. To put in simple terms, the generalization of the differential function $\dot{x} = F(x)$ is termed as differential inclusion. In 1995, El-Sayed and Ibrahim extended the theory of integer order differential inclusion to fractional order [17]. Differential inclusion of fractional order acts as a key technique in analyzing differential equation with discontinuous right hand side which basically arises while modelling dynamical system which involves friction and impact problem. A sectorial operator is a type of linear operator that maps functions from one Banach space to another. It is a type of operator that is widely used in the study of partial differential equations and their associated boundary value problems. Sectorial

*Corresponding Author

operators play an important role in the analysis of differential calculus, especially in the study of well-posedness and stability of boundary value problems. They are also used in the theory of semigroups of operators and in the study of evolution equations. In [18] Kazufumi Ito et. al. analyzed the various secorial properties of Caputo derivative of order $\varrho \in (1,2)$. In [19] JinRong Wang et. al. investigated the existence of piece wise mild solutions of nonlocal impusive fractional differential inclusions with fractional sectorial operator on Banach spaces. The readers can refer to [12, 20–24] for present qualitative research topics in differential equations of inclusion type. In [13, 14, 25, 26] the authors studied the existence and solvability of mild solution for various fractional order systems with sectorial operator of the type $(P, \eta, \varrho, \gamma)$.

In general, while dealing with complicated differential systems such as growth modeling, economics, biology and quantum field theory the random noise or stochastic perturbation is unavoidable. Therefore there are numerous ongoing research in analyzing the existence and uniqueness of stochastic control models using various fixed point methods. The concept of stochastic fractional control system has been well developed with the help of different kinds of fixed point approaches in [6, 13, 27, 28]. The weaker notion of control theory is called as approximate controllability. This type of controllable system ensures that the system is steered to any random small neighborhood of the final state. Recently, the approximate controllability of control systems defined by impulsive functional inclusions and neutral integro-differential systems are well discussed in the research publications [6, 8, 10, 12, 29–32].

Very recently the autors in [10] investigated the following existence results for Caputo fractional mixed Volterra Fredholm-type integro differential inclusions of order $\varrho \in (1,2)$ with sectorial operators. Further in the past few years the application of nonlocal condition in fractional differential equations has emerged as a magnificient area of investication since it describes the evolution of the system in an efficient way. Therfore we extend out theoritical result of the Caputo fractional stochastic integro-differential inclusions system to nonlocal conditions with sectorial operators.

$$
\begin{aligned}
{}^{C}D^{\varrho}_{\zeta}z(\zeta) \in & Az(\zeta) + G\Big(\zeta, z(\zeta), \int_0^{\zeta} f(\zeta,\nu,z(\nu)), \\
& \int_0^T f(\zeta,\nu,z(\nu))d\nu\Big),\ \zeta \in V=[0,T], \\
& z(0)=z_0,\ z'(0)=z_1.
\end{aligned}
$$

Being motivated by the above works, in this paper we establish the sufficient conditions for the approximate controllability of Caputo fractional stochastic integro-differential inclusions with sectorial operators of the form

$$
\begin{aligned}
{}^{C}D^{\varrho}_{\zeta}z(\zeta) \in Az(\zeta) + G\Big(\zeta, z(\zeta), \int_0^T f(\zeta,\nu,z(\nu))d\nu\Big) \\
\frac{dW(\zeta)}{d\zeta} + \mathbb{B}x(\zeta),\ \zeta \in V=[0,T], \qquad (1) \\
z(0)=z_0,\ z'(0)=z_1.
\end{aligned}
$$

where $\varrho \in (1,2)$, the sectorial operator A is a mapping from $D(A) \subset \mathcal{X}$ to $\mathcal{X}$ of type $(P, \eta, \varrho, \gamma)$ in Banach space $\mathcal{X}$. $W(\zeta)$ be a standard cylindrical Wiener process in $\mathcal{X}$ defined on a stochastic space $\big(\Omega, \Im, \{\Im_\zeta\}_{\zeta\geqslant 0}, \mathbb{P}\big)$. The nonempty, closed, convex and bounded multivalued function $G: V \times \mathcal{X} \times \mathcal{X} \to 2^{\mathcal{X}} \setminus \{\emptyset\}$ and f be a mapping from $V \times V \times \mathcal{X}$ into $\mathcal{X}$, $x \in L^2(V, \mathcal{H})$, where $\mathcal{H}$ stand for Banach space. In addition, the linear operator $\mathbb{B}: \mathcal{H} \to \mathcal{X}$ is bounded.

The article contains the following parts:

Part 2 : Consists of the preliminaries and definitions.

Part 3 : The controllability results for the chosen fractional inclusion systems (1) are derived by using fixed point technique.

Part 4 : The outcome of approximate controllability results derived for system (1) is extended to fractional nonlocal system.

Part 5: Appropriate illustrations for the obtained results have been established.

Part 6: Conclusion and future works of the presented system are discussed.

2. Preliminaries

Consider the Hilbert spaces $\mathcal{X}$, $\mathbb{K}$ and the complete probability space (CPS) $\big(\Omega, \Im, \mathbb{P}\big)$ outfitted with a normal filtration $\{\Im_\zeta, \zeta \in V\}$ satisfies the regular conditions ($\Im_\zeta$ is a increasing right continuous family such that $\Im_\zeta \subseteq \Im$, $\Im_0$ contains all $\mathbb{P}$-null set). Let $E(.)$ denotes the expectation with respect to the measure $\mathbb{P}$. Let $\{e_j\}_{j=1}^{\infty}$ be a complete orthonormal basis of $\mathbb{K}$. Suppose that $W = (W_\zeta)_{\zeta\geqslant 0}$ is a cylindrical $\mathbb{K}$-valued Wiener process defined on the CPS $\big(\Omega, \Im, \mathbb{P}\big)$ with covariance operator $Q \geqslant 0$, such that $Trace(Q) = \sum_{j=1}^{\infty} \lambda_j = \lambda < \infty$, and $Qe_j = \lambda_j e_j$. Then $W(\zeta) = \sum_{j=1}^{\infty} \sqrt{\lambda_j} W_j(\zeta)$, with $W_j(\zeta)$, $j = 1$ to ∞

are mutually independent one-dimensional standard Wiener processes. We consider that $\Im_\zeta = T\{W(s) : 0 \leqslant s \leqslant \zeta\}$ is the sigma algebra generated by W and $\Im_\zeta = \Im$. Let $L(\mathbb{K}, \mathcal{X})$ be a bounded linear operator space with the usual operator norm $\|\cdot\|$. For $\varphi \in L(\mathbb{K}, \mathcal{X})$ we define $\|\varphi\|^2 = Trace(\varphi Q \varphi^*) = \sum_{j=1}^{\infty} \|\sqrt{\lambda_j}\varphi e_j\|^2$. If $\|\varphi\|^2 < \infty$ then φ is called $Q-$Hilbert-Schmidt operator and the space of such operators is denoted by $L_Q(\mathbb{K}, \mathcal{X})$. The completion $L_Q(\mathbb{K}, \mathcal{X})$ of $L(\mathbb{K}, \mathcal{X})$ w.r.t the topology induced by the norm $\|.\|_Q$ where $\|\varphi\|_Q^2 = (\varphi, \varphi)$ is a Hilbert space with the above norm topology.

The Banach space $L_2(\Omega, \Im_T, \mathcal{X})$ is the collection of all square-integrable, strongly measurable, $\Im_\zeta-$ adapted, $\mathcal{X}-$ valued random variables. Also take

$$C\big(V, L_2(\Omega, \Im_T, \mathcal{X})\big) = \big\{z : V \to L_2(\Omega, \Im_T, \mathcal{X}) \mid z \text{ is continuous and } \sup_{\zeta \in V} E\|z(\zeta)\|^2 < \infty\big\}$$

be a Banach space. Finally, we define the set

$$\mathcal{C} = \big\{z \in C\big(V, L_2(\Omega, \Im_T, \mathcal{X})\big) \mid z \text{ is measurable, } \Im_\zeta - \text{adapted } \mathcal{X} \text{ valued functions}\big\}$$

be a closed subspace of $C\big(V, L_2(\Omega, \Im_T, \mathcal{X})\big)$ with norm $\|z\| = \sup_{\zeta \in V} E\|z(\zeta)\|^2$, E determine the integration w.r.t the probability measure.

Definition 1. *[3] The Riemann-Liouville fractional integral of order β having the lower limit 0 for a function g mapping $[0, \infty)$ into $\mathbb{R}^+$ is defined as*

$$I^\beta g(\zeta) = \frac{1}{\Gamma(\beta)} \int_0^\zeta \frac{g(\nu)}{(\zeta - \nu)^{1-\beta}} d\nu, \quad \zeta > 0, \ \beta \in \mathbb{R}^+.$$

Definition 2. *[3] The Riemann-Liouville fractional derivative of order β employing the lower limit 0 for a function g is defined as*

$$^{RL}D^\beta g(\zeta) = \frac{1}{\Gamma(j-\beta)} \frac{d^j}{d\zeta^j} \int_0^\zeta g^{(j)}(\nu)(\zeta - \nu)^{j-\beta-1} d\nu, \quad \zeta > 0, \ j-1 < \beta < j, \ \beta \in \mathbb{R}^+, \ j \in \mathbb{N}.$$

Definition 3. *[3] Caputo fractional derivative of order β employing the lower limit 0 for a function g is defined as*

$$^C D^\beta g(\zeta) = {}^L D^\beta \left(g(\zeta) - \sum_{i=0}^{j-1} \frac{g^{(i)}(0)}{i!} \zeta^i \right), \quad \zeta > 0, \ j-1 < \beta < j, \ \beta \in \mathbb{R}^+, \ j \in \mathbb{N}.$$

Definition 4. *[14] The closed and linear operator A mapping from D into $\mathcal{X}$ is called sectorial operator of type $(P, \eta, \varrho, \gamma)$ provided that there exist γ belongs to $\mathbb{R}$, η belongs to $(0, \frac{\pi}{2})$ and $P > 0$ such that the ϱ-resolvent of A exists outside the sector*

$$\gamma + \mathcal{S}_\eta = \{\eta + \mu^\varrho : \mu \text{ in } C(V, \mathcal{X}), \ |Arg(-\mu^\varrho)| < \eta\}$$

$$\|(\mu^\varrho I - A)^{-1}\| \le \frac{P}{|\mu^\varrho - \gamma|}, \ \mu^\varrho \notin \gamma + \mathcal{S}_\eta.$$

Further, throughout the paper we assume that A is a sectorial operator of type $(P, \eta, \varrho, \gamma)$, hence it is easy to establish that A stands for infinitesimal generator of a ϱ-resolvent family $\{\mathcal{W}_\varrho(\zeta)\}_{\zeta \ge 0}$ which belongs to Banach space, where

$$\mathcal{W}_\varrho(\zeta) = \frac{1}{2\pi i} \int_c e^{\mu\varrho} \mathscr{R}(\mu^\varrho, A) \, d\mu.$$

Definition 5. *[14] Let $G : V \times \Omega \to L(\mathbb{K}, \mathcal{X})$ be the strongly measurable mapping such that $\int_0^T E\|G(\zeta)\|^p_{L(\mathbb{K},\mathcal{X})} d\zeta < \infty$ then $E\| \int_0^\zeta G(\nu) dW(\nu)\|^p \leqslant L_g \int_0^\zeta E\|G(\nu)\|^p_{L(\mathbb{K},\mathcal{X})} d\nu$, for all $\zeta \in J$ and $p \geqslant 2$, where L_g is a constant.*

Definition 6. *[14] A function z belongs to $C(V, \mathcal{X})$ is called mild solution of (1) provided that it fulfills the operator equation*

$$z(\zeta) = \mathcal{K}_\varrho(\zeta) z_0 + \mathcal{Q}_\varrho(\zeta) z_1 + \int_0^\zeta \mathcal{W}_\varrho(\zeta - \nu) g(\nu) dW(\nu) + \int_0^\zeta \mathcal{W}_\varrho(\zeta - \nu) \mathbb{B} x(\nu) d\nu.$$

In the above

$$\mathcal{K}_\varrho(\zeta) = \frac{1}{2\pi i} \int_c e^{\mu\varrho} \mu^{\varrho-1} \mathscr{R}(\mu^\varrho, A) d\mu, \ \mathcal{Q}_\varrho(\zeta) = \frac{1}{2\pi i} \int_c e^{\mu\varrho} \mu^{\varrho-2} \mathscr{R}(\mu^\varrho, A) d\mu,$$

$$\mathcal{W}_\varrho(\zeta) = \frac{1}{2\pi i} \int_c e^{\mu\varrho} \mathscr{R}(\mu^\varrho, A) d\mu,$$

with c being a suitable path such that $\mu^\varrho \notin \gamma + \mathcal{S}_\eta$ for φ belongs to C.

Theorem 1. *[14, 33] If A is a sectorial operator then the following hold on $\|\mathcal{K}_\varrho(\zeta)\|$:*

(i) *Take $\gamma \ge 0$ and $0 < \chi < \pi$, then*

$$\|\mathcal{K}_\varrho(\zeta)\| \le \frac{M_1(\eta, \chi) P e^{[M_1(\eta,\chi)(1+\gamma\zeta^\varrho)]^{\frac{1}{2}} \left[\left(1 + \frac{\sin\chi}{\sin(\chi-\eta)} \right)^{\frac{1}{\varrho}} - 1 \right]}}{\pi \sin^{1+\frac{1}{\varrho}} \eta} (1 + \eta\zeta^\varrho) + \frac{\Gamma(\varrho) P}{\pi(1 + \gamma\zeta^\varrho) |\cos\frac{\pi-\chi}{\varrho}|^\varrho \sin\eta \sin\chi},$$

where, $\zeta > 0, M_1(\eta, \chi) = \max\left\{ \dfrac{\sin\chi}{\sin(\chi - \eta)}, 1 \right\}.$

(ii) *Take $\gamma < 0$ and $0 < \chi < \pi$ then for $\zeta > 0$*

$$\|\mathcal{K}_\varrho(\zeta)\| \leq \frac{1}{1+|\gamma|\zeta^\varrho} \left(\frac{eP[(\sin\chi+1)^{\frac{1}{\varrho}}-1]}{\pi|\cos\chi|^{1+\frac{1}{\varrho}}} + \frac{\Gamma(\varrho)P}{\pi|\cos\chi|\,|\cos\frac{\pi-\chi}{\varrho}|^\varrho} \right).$$

Theorem 2. *[14, 33] If A is a sectorial operator then the following hold for $\|\mathcal{W}_\varrho(\zeta)\|$ and $\|\mathcal{Q}_\varrho(\zeta)\|$:*

(i) *Take $\gamma \geq 0$ and $0 < \chi < \pi$ then $\zeta > 0$*

$$\|\mathcal{W}_\varrho(\zeta)\| \leq \frac{P\left[\left(1+\frac{\sin\chi}{\sin(\chi-\eta)}\right)^{\frac{1}{\varrho}}-1\right]}{\pi\sin\eta} \times (1+\eta\zeta^\varrho)^{\frac{1}{\varrho}}\zeta^{\varrho-1}e^{[M_1(\eta,\chi)(1+\gamma\zeta^\varrho)]^{\frac{1}{\varrho}}} + \frac{P\zeta^{\varrho-1}}{\pi(1+\gamma\zeta^\varrho)|\cos\frac{\pi-\chi}{\varrho}|^\varrho\sin\eta\sin\chi},$$

$$\|\mathcal{Q}_\varrho(\zeta)\| \leq \frac{P\left[\left(1+\frac{\sin\chi}{\sin(\chi-\eta)}\right)^{\frac{1}{\varrho}}-1\right]M_1(\eta,\chi)}{\pi\sin\eta^{\frac{\varrho+2}{\varrho}}} (1+\eta\zeta^\varrho)^{\frac{\varrho-1}{\varrho}}\zeta^{\varrho-1}e^{[M_1(\eta,\chi)(1+\gamma\zeta^\varrho)]^{\frac{1}{\varrho}}} + \frac{P\varrho\Gamma(\varrho)}{\pi(1+\gamma\zeta^\varrho)|\cos\frac{\pi-\chi}{\varrho}|^\varrho\sin\eta\sin\chi},$$

where $M_1(\eta,\chi) = \max\left\{1, \frac{\sin\eta}{\sin(\chi-\eta)}\right\}$.

(ii) *Take $\gamma < 0$ and $0 < \chi < \pi$ then*

$$\|\mathcal{W}_\varrho(\zeta)\| \leq \frac{\zeta^{\varrho-1}}{1+|\gamma|\zeta^\varrho} \left(\frac{eP[(\sin\chi+1)^{\frac{1}{\varrho}}-1]}{\pi|\cos\chi|} + \frac{P}{\pi|\cos\frac{\pi-\chi}{\varrho}|\,|\cos\chi|} \right).$$

$$\|\mathcal{Q}_\varrho(\zeta)\| \leq \left(\frac{eP[(\sin\chi+1)^{\frac{1}{\varrho}}-1]t}{\pi|\cos\chi|^{1+\frac{2}{\varrho}}} + \frac{\varrho\Gamma(\varrho)P}{\pi|\cos\frac{\pi-\chi}{\varrho}|\,|\cos\chi|} \right) \frac{1}{1+|\gamma|\zeta^\varrho}, \text{ for } \zeta > 0.$$

Let $(\mathcal{X}, d)$ be a metric space. The following expressions are used in this article:

- $\mathcal{N}(\mathcal{X}) = \{H \in \mathcal{P}(\mathcal{X}) : H \neq \emptyset\}$,
- $\mathcal{N}_{cl}(\mathcal{X}) = \{H \in \mathcal{N}(\mathcal{X}) : H \text{ closed}\}$,
- $\mathcal{N}_b(\mathcal{X}) = \{H \in \mathcal{N}(\mathcal{X}) : H \text{ bounded}\}$,
- $\mathcal{N}_{cp}(\mathcal{X}) = \{H \in \mathcal{N}(\mathcal{X}) : H \text{ compact}\}$,
- $\mathcal{N}_c(\mathcal{X}) = \{H \in \mathcal{N}(\mathcal{X}) : H \text{ convex}\}$.

For the multivalued map $\mathscr{K} : \mathcal{C} \to 2^{\mathcal{C}} \setminus \{\emptyset\}$ the following definition holds. Additional information on multivalued maps can be found in the books [34].

Definition 7. *[35] If for all $z \in \mathcal{C}$, $\mathscr{K}(z)$ is closed(convex) then the map $\mathscr{K}$ is closed(convex). For every bounded set C of $\mathcal{C}$, $\mathscr{K}(C) = \bigcup_{z\in\mathcal{C}}\mathscr{K}(z)$ is bounded in $\mathcal{C}$ then $\mathscr{K}$ is bounded on bounded sets.*

Definition 8. *[35] $\mathscr{K}$ is known as upper semi continuous (u.s.c) on $\mathcal{C}$ if the following conditions holds:*

(i) *For all $z_0 \in \mathcal{C}$ the set $\mathscr{K}(z_0) \neq \phi$ and it is closed.*
(ii) *For all open set $C \in \mathcal{C}$ such that $C \supset \mathscr{K}(z_0)$ then there exist an open neighborhood $\mathscr{K}(\mathcal{W}) \subseteq C$.*

Definition 9. *[35] If $\mathscr{K}(C)$ is a relatively compact, for all bounded subset C of $\mathcal{C}$ then $\mathscr{K}$ is completely continuous.*

Definition 10. *[35] If the completely continuous map $\mathscr{K}$ has a nonempty values then $\mathscr{K}$ is u.s.c if and only if $\mathscr{K}$ has a closed graph i.e., $z^k \to z^*$, $u^k \to u^*$, u^k such that $\mathscr{K}z^k$ signify $u^* \in \mathscr{K}z^*$. Moreover , if there exists $z \in Y$ such that $z \in \mathscr{K}(z)$ then $\mathscr{K}$ has a fixed point.*

An u.s.c function $\mathscr{K} : \mathcal{X} \to \mathcal{X}$ is said to be condensing if for all bounded subset $\mathscr{C} \subseteq \mathcal{X}$ having $\iota(\mathscr{C}) \neq 0$, where ι stands for the Kuratowski measure of non compactness, we get

$$\iota(\mathscr{K}(\mathscr{C})) < \iota(\mathscr{C}).$$

Definition 11. *[35] G mapping from $V \times \mathcal{X} \times \mathcal{X}$ into $\mathcal{N}_{b,cl,cp}(L(\mathbb{K},\mathcal{X}))$ is called L^1-Caratheodory provided that*

(i) *$\zeta \to G(\zeta, z, x, y)$ is measurable for all z, x, y belongs to $\mathcal{X}$.*
(ii) *$(z, x, y) \to G(\zeta, z, x, y)$ is u.s.c for all ζ belongs to V.*
(iii) *For all $p > 0$, there exist j_p belongs to $L^1(V, \mathbb{R}^+)$ such that*

$$E\|G(\zeta,z,x,y)\|^2 \leq \sup\{E\|g\|^2 : g \in G(\zeta,z,x,y)\} \leq j_p(\zeta), \text{ for all } \zeta \in V.$$

For further information on multivalued functions refer the books [34]. Detail analysis in multivalued maps are presended in this work. The following are two suitable operators and their underlying assumptions:

$$\Gamma_0^T = \int_0^T \mathcal{W}_\varrho(\zeta-\nu)\mathbb{B}\mathbb{B}^*\mathcal{W}_\varrho^*(\zeta-\nu)d\nu : \mathcal{X} \to \mathcal{X},$$

$$\mathscr{R}(\hbar, \Gamma_0^T) = (\hbar I + \Gamma_0^T)^{-1} : \mathcal{X} \to \mathcal{X}.$$

In the above $\mathcal{W}_{\varrho}^{*}(\zeta-\nu)$ and $\mathbb{B}^{*}$ stands for adjoints of $\mathcal{W}_{\varrho}(\zeta-\nu)$ and $\mathbb{B}$ respectively and Clearly Γ_0^T is the bounded linear operator.

To begin, evaluate the below assumptions:

($\mathbf{H_0}$) In the strong operator topology, $\hbar\mathscr{R}(\hbar,\Gamma_0^T)\to 0$ as $\hbar\to 0^+$.

Consider the accompanying linear inclusions of fractional system

$$\begin{cases} {}^{C}D_{\zeta}^{\varrho}z(\zeta)\in Az(\zeta)+\mathbb{B}x(\zeta),\ \zeta\in V=[0,T],\\ z(0)=z_0,\ z'(0)=z_1,\end{cases}$$

is approximately controllable on V.

Lemma 1. *[16]. Suppose V is a compact real interval and the collection of all nonempty, bounded, closed and convex subsets of $\mathcal{X}$ is called $\mathcal{N}_{b,cl,cp}(\mathcal{X})$. Consider multivalued function G mapping from $V\times\mathcal{X}$ into $\mathcal{N}_{b,cl,cp}(\mathcal{X})$ is measurable to ζ for all fixed z belongs to $\mathcal{X}$, upper continuous to z for all ζ belongs to V and for all z belongs to $\mathcal{C}$,*

$$S_{G,z}=\left\{g\in L^1(V,\mathcal{X}):g(\zeta)\in G\left(\zeta,z(\zeta),\int_0^T f(\zeta,\nu,z(\nu))d\nu\right),\ \zeta\in V\right\}$$

is nonempty. Assume that $\mathcal{M}:L^1(V,\mathcal{X})\to\mathcal{C}$ is a linear continuous function, next

$$\mathcal{M}\circ S_G:\mathcal{C}\to\mathcal{N}_{b,cl,cp}(\mathcal{C})$$
$$z\to(\mathcal{M}\circ S_G)(z)=\mathcal{M}(S_{G,z})$$

is a closed graph operator belongs to $\mathcal{C}\to\mathcal{C}$.

Lemma 2. *[36] Suppose H is a subset of $\mathcal{X}$ which is nonempty, bounded, closed and convex, assume $\mathcal{D}:H\to 2^{\mathcal{X}}\setminus\{\emptyset\}$ is u.s.c with closed, convex values such that $\mathcal{D}(H)\subset H$ where $\mathcal{D}(H)$ is compact, then $\mathcal{D}$ has a fixed point.*

3. Approximate controllability

The section explicitly focuses on the articulation of mild solution for the above mentioned system (1). We now present the required hypothesis for proving the main theorem:

($\mathbf{H_1}$) $\mathcal{K}_{\varrho}(\zeta)$, $\mathcal{Q}_{\varrho}(\zeta)$ and $\mathcal{W}_{\varrho}(\zeta)$ are compact ϱ-resolvent families generated by the sectorial operator A. For all ζ belongs to V, there exist $\widehat{P}>0$ such that

$$\sup_{0\le\zeta\le T}\|\mathcal{K}_{\varrho}(\zeta)\|\le\widehat{P},$$
$$\sup_{0\le\zeta\le T}\|\mathcal{Q}_{\varrho}(\zeta)\|\le\widehat{P},$$
$$\sup_{0\le\zeta\le T}\|\mathcal{W}_{\varrho}(\zeta)\|\le\widehat{P}.$$

($\mathbf{H_2}$) The functions $g(\zeta,s,.),h(\zeta,s,.):\mathcal{X}\longrightarrow\mathcal{X}$ are continuous for all $(\zeta,s)\in\Delta$ and for all $z\in\mathcal{X}$ the function $g(.,.,z),h(.,.,z):\Delta\longrightarrow\mathcal{X}$ are strongly measurable.

($\mathbf{H_3}$) The multivalued map $G:V\times\mathcal{X}\times\mathcal{X}\to\mathcal{N}_{b,cl,cp}(L(K,\mathcal{X}))$ is an L^2- caratheordy function such that for all $\zeta\in V$, the function $G(\zeta,.,.):\mathcal{X}\times\mathcal{X}\to\mathcal{N}_{b,cl,cp}(L(K,\mathcal{X}))$ is u.s.c and for all $(s,z)\in\times\mathcal{X}\times\mathcal{X}$ the set

$$S_{G,z}=\left\{g\in L^2(J,L(K,\mathcal{X})):g(\zeta)\text{ in }G\left(\zeta,z(\zeta),\int_0^T f(\zeta,\nu,z(\nu))d\nu\right)\text{ for a.e }\zeta\in V\right\}$$

is nonempty.

($\mathbf{H_4}$) There exists a function $L_{g,p}:\mathcal{X}\to R^+$ such that.

$$\sup\left\{E\|g\|^2:g(\zeta)\in G\left(\zeta,z(\zeta),\int_0^T f(\zeta,\nu,z(\nu))d\nu\right)\right\}\le L_{g,p}(\zeta),$$

for almost every $\zeta\in V$.

($\mathbf{H_5}$) The function $\nu\to(\zeta-\nu)^{T-1}L_{g,p}(\zeta)\in L^1(V,\mathbb{R}^+)$ such that there exist $\varphi>0$ such that

$$\lim_{p\to\infty}\inf\frac{\int_0^\zeta\nu^{\mu-1}L_{g,p}(\nu)d\nu}{p}=\varphi<+\infty.$$

($\mathbf{H_6}$) If $g:C([0,T],\mathcal{X})\to\mathcal{X}$ is continues then there exists some constant M_g such that $E\|g(x)\|^2\le\|x\|^2$.

Now, we can show that the system (1) is controllable approximately on the given interval. That is there exist a mild solution $z\in\mathcal{C}$ satisfies the requirements of approximate controllability, where

$$\begin{aligned}z(\zeta)&=\mathcal{K}_{\varrho}(\zeta)z_0+\mathcal{Q}_{\varrho}(\zeta)z_1\\&\quad+\int_0^\zeta\mathcal{W}_{\varrho}(\zeta-\nu)g(\nu)dW(\nu)\\&\quad+\int_0^\zeta\mathcal{W}_{\varrho}(\zeta-\nu)\mathbb{B}x(\nu)d\nu,\ g\in S_{G,z},\end{aligned}$$

$$x(\zeta)=\mathbb{B}^*\mathcal{W}_{\varrho}^*(\zeta-\nu)\mathscr{R}(\hbar,\Gamma_0^T)q(z(\cdot)).$$

In the above

$$\begin{aligned}q(z(\cdot))&=z_T-\mathcal{K}_{\varrho}(T)z_0-\mathcal{Q}_{\varrho}(T)z_1\\&\quad-\int_0^T\mathcal{W}_{\varrho}(\zeta-\nu)g(\nu)dW(\nu).\end{aligned}$$

Theorem 3. *On considering the hypothesis* $(\mathbf{H_0})-(\mathbf{H_6})$ *are fulfilled then* (1) *contains at least one mild solution on V if*

$$4\widehat{P}^2\left[1+\frac{(\widehat{P}P_{\mathbb{B}})^4}{\hbar}\right]\varphi<1$$

with $P_{\mathbb{B}} = \|\mathbb{B}\|$.

Proof. The main aim of this theorem is to nd conditions for solvability of system (1) to be resolvable for $\hbar > 0$. Now we prove that the mapping Φ from $\mathcal{C}$ into $2^{\mathcal{C}}$ given by

$$\Phi(z) = \Big\{ z \in \mathcal{C}.\ m(\zeta) = \mathcal{K}_\varrho(\zeta)z_0 + \mathcal{Q}_\varrho(\zeta)z_1 + \int_0^\zeta \mathcal{W}_\varrho(\zeta-\nu)g(\nu)dW(\nu) + \int_0^\zeta \mathcal{W}_\varrho(\zeta-\nu)\mathbb{B}x(\nu)d\nu,\ g \in S_{G,z} \Big\},$$

has a fixed point.

Step 1: For all $\hbar > 0$, $\Phi(z)$ is convex for all z belongs to $\mathcal{C}$. Let $m_1, m_2 \in \mathcal{C}$, then there exists g_1, g_2 belongs to $S_{G,z}$ such that ζ belongs to V, we obtain

$$\begin{aligned} m_i(\zeta) = {} & \mathcal{K}_\varrho(\zeta)z_0 + \mathcal{Q}_\varrho(\zeta)z_1 \\ & + \int_0^\zeta \mathcal{W}_\varrho(\zeta-\nu)g_i(\nu)dW(\nu) \\ & + \int_0^\zeta \mathcal{W}_\varrho(\zeta-\nu)\mathbb{B}\mathbb{B}^*\mathcal{W}_\varrho^*(\zeta-\nu)\mathscr{R}(\hbar,\Gamma_0^T) \\ & \times \Big[z_T - \mathcal{K}_\varrho(T)z_0 - \mathcal{Q}_\varrho(T)z_1 \\ & - \int_0^T \mathcal{W}_\varrho(T-\tau)g_i(\tau)dW(\tau)\Big](\nu)d\nu,\ i = 1, 2. \end{aligned}$$

Let $\kappa \in [0, 1]$, then for all ζ belongs to V, now we have

$$\begin{aligned} (\kappa m_1 + (1-\kappa)m_2)(\zeta) = {} & \mathcal{K}_\varrho(\zeta)z_0 \\ & + \mathcal{Q}_\varrho(\zeta)z_1 + \int_0^\zeta \mathcal{W}_\varrho(\zeta-\nu)[\kappa g_1(\nu) + (1-\kappa)g_2(\nu)]d\nu \\ & + \int_0^\zeta \mathcal{W}_\varrho(\zeta-\nu)\mathbb{B}\mathbb{B}^*\mathcal{W}_\varrho^*(\zeta-\nu)\mathscr{R}(\hbar,\Gamma_0^T) \\ & \times \Big[z_T - \mathcal{K}_\varrho(T)z_0 - \mathcal{Q}_\varrho(T)z_1 - \int_0^T \mathcal{W}_\varrho(T-\tau)[\kappa g_1(\tau) \\ & + (1-\kappa)g_2(\tau)]dW(\tau)\Big](\nu)d\nu. \end{aligned}$$

Since $S_{G,z}$ is convex, $\kappa m_1 + (1-\kappa)m_2$ belongs to $S_{G,z}$. Hence $\kappa m_1 + (1-\kappa)m_2$ belongs to $\Phi(z)$.

Step 2: Assume that

$$\mathcal{B}_p = \{ z \in \mathcal{C} | \|z\|_{\mathcal{C}} \le p \},\ \text{for}\, p > 0.$$

Clearly $\mathcal{B}_p$ is convex, closed and bounded subset of $\mathcal{C}$. For $\hbar > 0$, our assumption is there exist $p > 0$ such that

$$\Phi(\mathcal{B}_p) \subset \mathcal{B}_p.$$

If not, then for all $p > 0$, there exist z^p belongs to $\mathcal{B}_p$, but $\Phi(z^p) \notin \mathcal{B}_p$, i.e,

$$\|\Phi(z^p)\|_{\mathcal{C}} = \sup\{ \|m^p\|_{\mathcal{C}} : m^p \in \Phi(z^p)\} > p,$$

and

$$\begin{aligned} m^p(\zeta) = {} & \mathcal{K}_\varrho(\zeta)z_0 + \mathcal{Q}_\varrho(\zeta)z_1 \\ & + \int_0^\zeta \mathcal{W}_\varrho(\zeta-\nu)g^p(\nu)dW(\nu) \\ & + \int_0^\zeta \mathcal{W}_\varrho(\zeta-\nu)\mathbb{B}\mathbb{B}^*\mathcal{W}_\varrho^*(\zeta-\nu)\mathscr{R}(\hbar,\Gamma_0^T) \\ & \times \Big[z_T - \mathcal{K}_\varrho(T)z_0 - \mathcal{Q}_\varrho(T)z_1 \\ & - \int_0^T \mathcal{W}_\varrho(T-\tau)g^p(\tau)dW(\tau)\Big](\nu)d\nu, \end{aligned}$$

for some g^p belongs to S_{G,z^p}.

By referring $(\mathbf{H_3})$, we get

$$\begin{aligned} E\|x^p(\zeta)\|^2 = {} & E\Big\| \mathbb{B}^*\mathcal{W}_\varrho^*(T-\tau)\mathscr{R}(\hbar,\Gamma_0^T) \\ & \Big[z_T - \mathcal{K}_\varrho(T)z_0 - \mathcal{Q}_\varrho(T)z_1 \\ & - \int_0^T \mathcal{W}_\varrho(T-\tau)g^p(\tau)dW(\tau)\Big]\Big\|^2 \\ \le {} & E\|\mathbb{B}^*\|^2 E\|\mathcal{W}_\varrho^*(T-\tau)\|^2 E\|\mathscr{R}(\hbar,\Gamma_0^T)\|^2 \\ & \times E\Big\|\Big[z_T - \mathcal{K}_\varrho(T)z_0 - \mathcal{Q}_\varrho(T)z_1 \\ & - \int_0^T \mathcal{W}_\varrho(T-\tau)g^p(\tau)dW(\tau)\Big]\Big\|^2 \\ \le {} & \widehat{P}^2 P_{\mathbb{B}}^2 \frac{1}{\hbar}\Big[4E\|z_T\|^2 \\ & + 4E\|\mathcal{K}_\varrho(T)z_0\|^2 + 4E\|\mathcal{Q}_\varrho(T)z_1\|^2 \\ & + 4L_g \int_0^T E\|\mathcal{W}_\varrho(T-\tau)g^p(\tau)\|^2 d\tau \Big] \\ \le {} & \frac{\widehat{P}^2 P_{\mathbb{B}}^2}{\hbar}\Big[4E\|z_T\|^2 + 4\widehat{P}^2E\|z_0\|^2 + 4\widehat{P}^2E\|z_1\|^2 \\ & + 4\widehat{P}^2 L_g \int_0^T \|g^p(\tau)\|^2 d\tau \Big]. \end{aligned}$$

Now for $\hbar > 0$,

$$\begin{aligned} p < {} & E\|(\Phi z^p)(\zeta)\|^2 \le 4E\|\mathcal{K}_\varrho(\zeta)z_0\|^2 \\ & + 4E\|\mathcal{Q}_\varrho(\zeta)z_1\|^2 \\ & + 4L_g \int_0^\zeta E\|\mathcal{W}_\varrho(\zeta-\nu)g^p(\nu)\|^2 d\nu \\ & + 4\int_0^\zeta E\|\mathcal{W}_\varrho(\zeta-\nu)\mathbb{B}x^p(\nu)\|^2 d \\ \le {} & 4\widehat{P}^2E\|z_0\|^2 + 4\widehat{P}^2E\|z_1\|^2 \\ & + 4\widehat{P}^2 L_g \int_0^\zeta E\|g^p(\nu)\|^2 d\nu \\ & + 4\widehat{P}^2 \int_0^\zeta E\|\mathbb{B}x^p(\nu)\|^2 d\nu \end{aligned}$$

$$\begin{aligned}
&\leq 4\widehat{P}^2 E\|z_0\|^2 + 4\widehat{P}^2 E\|z_1\|^2 \\
&\quad + 4\widehat{P}^2 L_g \int_0^\zeta L_{g,p}(\nu) d\nu \\
&\quad + 4\widehat{P}^2 P_{\mathbb{B}}^2 \int_0^\zeta \left(\frac{\widehat{P}^2 P_{\mathbb{B}}^2}{\hbar} \Big[E\|z_T\|^2 + \widehat{P}^2 E\|z_0\|^2 \right. \\
&\quad \left. + \widehat{P}^2 E\|z_1\|^2 + \widehat{P}^2 L_g \int_0^T L_{g,p}(\tau) d\tau \Big] \right) d\nu \\
&\leq 4\widehat{P}^2 E\|z_0\|^2 + 4\widehat{P}^2 E\|z_1\|^2 \\
&\quad + 4\widehat{P}^2 L_g \int_0^\zeta L_{g,p}(\nu) d\nu \\
&\quad + 4\frac{(\widehat{P}^2 P_{\mathbb{B}}^2)^2}{\hbar} \Big[4E\|z_T\|^2 + 4\widehat{P}^2 E\|z_0\|^2 \\
&\quad + 4\widehat{P}^2 E\|z_1\|^2 + 4\widehat{P}^2 L_g \int_0^T L_{g,p}(\tau) d\tau \Big].
\end{aligned}$$

Dividing the above equation by p and as $p \to \infty$ we obtain

$$4\widehat{P}^2 \Big[1 + 4\frac{(\widehat{P}^2 P_{\mathbb{B}}^2)^2}{\hbar} \Big] \varphi \geq 1,$$

which contradicts to our assumption.

Step 3: We check that $\{\Phi(z) : z \in \mathcal{B}_p\}$ is equicontinuous.

For all m belongs to $\Phi(z)$ and z belongs to $\mathcal{B}_p$, there exist $g \in S_{G,z}$ such that

$$\begin{aligned}
m(\zeta) &= \mathcal{K}_\varrho(\zeta) z_0 + \mathcal{Q}_\varrho(\zeta) z_1 + \int_0^\zeta \mathcal{W}_\varrho(\zeta - \nu) g(\nu) d\nu \\
&\quad + \int_0^\zeta \mathcal{W}_\varrho(\zeta - \nu) \mathbb{B} x(\nu) d\nu.
\end{aligned}$$

Suppose $0 \leq \zeta_1 < \zeta_2 \leq T$. In addition,

$$\begin{aligned}
&E\|m(\zeta_2) - m(\zeta_1)\|^2 = E\|\mathcal{K}_\varrho(\zeta_2) z_0 + \mathcal{Q}_\varrho(\zeta_2) z_1 \\
&\quad + \int_0^{\zeta_2} \mathcal{W}_\varrho(\zeta_2 - \nu) g(\nu) dW(\nu) \\
&\quad + \int_0^{\zeta_2} \mathcal{W}_\varrho(\zeta_2 - \nu) \mathbb{B} x(\nu) d\nu - \mathcal{K}_\varrho(\zeta_1) z_0 - \mathcal{Q}_\varrho(\zeta_1) z_1 \\
&\quad - \int_0^{\zeta_1} \mathcal{W}_\varrho(\zeta_1 - \nu) g(\nu) dW(\nu) \\
&\quad - \int_0^{\zeta_1} \mathcal{W}_\varrho(\zeta_1 - \nu) \mathbb{B} x(\nu) d\nu\|^2 \\
&\leq 6E\|[\mathcal{K}_\varrho(\zeta_2) - \mathcal{K}_\varrho(\zeta_1)] z_0\|^2 \\
&\quad + 6E\|[\mathcal{Q}_\varrho(\zeta_2) - \mathcal{Q}_\varrho(\zeta_1)] z_1\|^2 \\
&\quad + 6L_g^2 \int_{\zeta_1}^{\zeta_2} E\|\mathcal{W}_\varrho(\zeta_2 - \nu) g(\nu)\|^2 d\nu \\
&\quad + L_g^2 \int_0^{\zeta_1} E\|[\mathcal{W}_\varrho(\zeta_2 - \nu) - \mathcal{W}_\varrho(\zeta_1 - \nu)] g(\nu)\|^2 d\nu \\
&\quad + \int_{\zeta_1}^{\zeta_2} E\|\mathcal{W}_\varrho(\zeta_2 - \nu) \mathbb{B} x(\nu)\|^2 d\nu \\
&\quad + \int_0^{\zeta_1} E\|[\mathcal{W}_\varrho(\zeta_2 - \nu) - \mathcal{W}_\varrho(\zeta_1 - \nu)] \mathbb{B} x(\nu)\|^2 d\nu \\
&\leq 6E\|\mathcal{K}_\varrho(\zeta_2) - \mathcal{K}_\varrho(\zeta_1)\|^2 E\|z_0\|^2 \\
&\quad + 6E\|\mathcal{Q}_\varrho(\zeta_2) - \mathcal{Q}_\varrho(\zeta_1)\|^2 E\|z_1\|^2 \\
&\quad + 6L_g^2 \widehat{P}^2 \int_{\zeta_1}^{\zeta_2} L_{g,p}(\nu) d\nu \\
&\quad + 6L_g^2 \int_0^{\zeta_1} E\|\mathcal{W}_\varrho(\zeta_2 - \nu) - \mathcal{W}_\varrho(\zeta_1 - \nu)\|^2 L_{g,p}(\nu) d\nu \\
&\quad + 6\widehat{P}^2 P_{\mathbb{B}}^2 \int_{\zeta_1}^{\zeta_2} E\|x(\nu)\|^2 d\nu \\
&\quad + 6P_{\mathbb{B}}^2 \int_0^{\zeta_1} E\|\mathcal{W}_\varrho(\zeta_2 - \nu) - \mathcal{W}_\varrho(\zeta_1 - \nu)\|^2 \\
&\quad \times E\|x(\nu)\|^2 d\nu.
\end{aligned}$$

In the above aforementioned inequality the right hand side $\to 0$ as $\zeta_2 \to \zeta_1$ by using the continuity of functions $\zeta \to \|\mathcal{K}_\varrho(\zeta)\|, \zeta \to \|\mathcal{Q}_\varrho(\zeta)\|$ and $\zeta \to \|\mathcal{W}_\varrho(\zeta)\|$. Therefore, $\Phi(\mathcal{B}_p)$ is equicontinuous.

Step 4: We show that $\mathcal{H}(\zeta) = \{m(\zeta) : m \in \Phi(B_p)\}$ is relatively compact belongs in $\mathcal{X}$. For $\zeta = 0$, result is trivial, hence $\mathcal{H}(\zeta) = \{z_0\}$. For some fixed ζ belongs to V. Assume that $0 < \epsilon < \zeta$, z belongs to $\mathcal{B}_p$ and introduce the operator m^ϵ by

$$\begin{aligned}
m^\epsilon(\zeta) &= \mathcal{K}_\varrho(\zeta) z_0 + \mathcal{Q}_\varrho(\zeta) z_1 \\
&\quad + \int_0^{\zeta - \epsilon} \mathcal{W}_\varrho(\zeta - \nu) g(\nu) dW(\nu) \\
&\quad + \int_0^{\zeta - \epsilon} \mathcal{W}_\varrho(\zeta - \nu) \mathbb{B} x(\nu) d\nu.
\end{aligned}$$

Hence $\mathcal{Q}(\epsilon)$, $\epsilon > 0$ is a compact operator, then $\mathcal{H}^\epsilon(\zeta) = \{m^\epsilon(\zeta) : m^\epsilon \in \Phi(B_p)\}$ is relatively compact belongs to $\mathcal{X}$, $0 < \epsilon < \zeta$. Further, for all z belongs to $\mathcal{B}_p$, we get

$$\begin{aligned}
E\|m(\zeta) - m^\epsilon(\zeta)\|^2 &= E\| \int_0^\zeta \mathcal{W}_\varrho(\zeta - \nu) g(\nu) dW(\nu) \\
&\quad + \int_0^\zeta \mathcal{W}_\varrho(\zeta - \nu) \mathbb{B} x(\nu) d\nu \\
&\quad - \int_0^{\zeta - \epsilon} \mathcal{W}_\varrho(\zeta - \nu) g(\nu) dW(\nu) \\
&\quad - \int_0^{\zeta - \epsilon} \mathcal{W}_\varrho(\zeta - \nu) \mathbb{B} x(\nu) d\nu\|^2, \\
&\leq 2 \int_{\zeta - \epsilon}^\zeta L_g^2 E\|\mathcal{W}_\varrho(\zeta - \nu) g(\nu)\|^2 d\nu \\
&\quad + 2 \int_{\zeta - \epsilon}^\zeta E\|\mathcal{W}_\varrho(\zeta - \nu) \mathbb{B} x(\nu)\|^2 d\nu \\
&\leq 2L_g^2 \widehat{P}^2 \int_{\zeta - \epsilon}^\zeta L_{g,p}(\nu) d\nu
\end{aligned}$$

$$+2\widehat{P}^2 P_{\mathbb{B}}^2 \int_{\zeta-\epsilon}^{\zeta} E\|x(\nu)\|^2 d\nu.$$

We see that $E\|m(\zeta) - m^{\epsilon}(\zeta)\|^2 \to 0$ as $\epsilon \to 0^+$. Thus there exist relatively compact set and it is arbitrarily close to $\mathcal{H}(\zeta) = \{m(\zeta) : m \in \Phi(B_r)\}$ and the set $\mathcal{H}(\zeta)$ is relatively compact in $\mathcal{X}$ for all $\zeta \in [0,T]$. At $\zeta = 0$ it is compact, hence $\mathcal{H}(\zeta)$ is relatively compact belongs to $\mathcal{X}$ for all $\zeta \in [0,T]$.

Step 5: Φ has a closed graph.

Consider $z^n \to z^*$ and $m^n \to m^*$ as $n \to \infty$. We will prove $m^* \in \Phi(z^*)$. Since $m^n \in \Phi(z^n)$, such that g^n belongs to S_{G,z^n} such that

$$\begin{aligned} m^n(\zeta) &= \mathcal{K}_\varrho(\zeta)z_0 + \mathcal{Q}_\varrho(\zeta)z_1 \\ &+ \int_0^\zeta \mathcal{W}_\varrho(\zeta-\nu)g^n(\nu)dW(\nu) \\ &+ \int_0^\zeta \mathcal{W}_\varrho(\zeta-\nu)\mathbb{B}\mathbb{B}^*\mathcal{W}_\varrho^*(\zeta-\nu)\mathscr{R}(\hbar,\Gamma_0^T) \\ &\times \Big[z_T - \mathcal{K}_\varrho(T)z_0 - \mathcal{Q}_\varrho(T)z_1 \\ &- \int_0^T \mathcal{W}_\varrho(T-\tau) \times g^n(\tau)dW(\tau)\Big](\nu)d\nu. \end{aligned}$$

We need to show there exist g^* belongs to S_{G,z^*} such that for all ζ belongs to V,

$$\begin{aligned} m^*(\zeta) &= \mathcal{K}_\varrho(\zeta)z_0 + \mathcal{Q}_\varrho(\zeta)z_1 \\ &+ \int_0^\zeta \mathcal{W}_\varrho(\zeta-\nu)g^*(\nu)dW(\nu) \\ &+ \int_0^\zeta \mathcal{W}_\varrho(\zeta-\nu)\mathbb{B}\mathbb{B}^*\mathcal{W}_\varrho^*(\zeta-\nu)\mathscr{R}(\hbar,\Gamma_0^T) \\ &\times \Big[z_T - \mathcal{K}_\varrho(T)z_0 - \mathcal{Q}_\varrho(T)z_1 \\ &- \int_0^T \mathcal{W}_\varrho(T-\tau)g^*(\tau)dW(\tau)\Big](\nu)d\nu. \end{aligned}$$

Clearly,

$$\begin{aligned} E\Big\|\Big(& m^n(\zeta) - \mathcal{K}_\varrho(\zeta)z_0 - \mathcal{Q}_\varrho(\zeta)z_1 \\ &- \int_0^\zeta \mathcal{W}_\varrho(\zeta-\nu)\mathbb{B}\mathbb{B}^*\mathcal{W}_\varrho^*(\zeta-\nu)\mathscr{R}(\hbar,\Gamma_0^T) \\ &\times \Big[z_T - \mathcal{K}_\varrho(T)z_0 - \mathcal{Q}_\varrho(T)z_1 \\ &- \int_0^T \mathcal{W}_\varrho(T-\tau)g^n(\tau)dW(\tau)\Big](\nu)d\nu\Big) \\ &- \Big(m^*(\zeta) - \mathcal{K}_\varrho(\zeta)z_0 - \mathcal{Q}_\varrho(\zeta)z_1 \\ &- \int_0^\zeta \mathcal{W}_\varrho(\zeta-\nu)\mathbb{B}\mathbb{B}^*\mathcal{W}_\varrho^*(\zeta-\nu)\mathscr{R}(\hbar,\Gamma_0^T) \\ &\times \Big[z_T - \mathcal{K}_\varrho(T)z_0 - \mathcal{Q}_\varrho(T)z_1 \\ &- \int_0^T \mathcal{W}_\varrho(T-\tau)g^*(\tau)dW(\tau)\Big](\nu)d\nu\Big)\Big\|^2 \to 0, \end{aligned}$$

as $n \to \infty$. Assume that $\mathcal{T} : L^1(V,\mathcal{X}) \to \mathcal{C}$,

$$\begin{aligned} (\mathcal{T}g)(\zeta) &= \int_0^\zeta \mathcal{W}_\varrho(\zeta-\nu)g(\nu)dW(\nu) \\ &+ \int_0^\zeta \mathcal{W}_\varrho(\zeta-\nu)\mathbb{B}\mathbb{B}^*\mathcal{W}_\varrho^*(\zeta-\nu)\mathscr{R}(\hbar,\Gamma_0^T) \\ &\times \Big[\int_0^T \mathcal{W}_\varrho(T-\tau)g(\tau)dW(\tau)\Big](\nu)d\nu. \end{aligned}$$

We can conclude that the operator $\mathcal{T} \circ S_{G,z}$ is a closed graph by using Lemma 1. Then, in view of $\mathcal{T}$ we can see that

$$\begin{aligned} \Big(& m^n(\zeta) - \mathcal{K}_\varrho(\zeta)z_0 - \mathcal{Q}_\varrho(\zeta)z_1 \\ &- \int_0^\zeta \mathcal{W}_\varrho(\zeta-\nu)\mathbb{B}\mathbb{B}^*\mathcal{W}_\varrho^*(\zeta-\nu)\mathscr{R}(\hbar,\Gamma_0^T) \\ &\times \Big[z_T - \mathcal{K}_\varrho(T)z_0 - \mathcal{Q}_\varrho(T)z_1 \\ &- \int_0^T \mathcal{W}_\varrho(T-\tau)g^*(\tau)dW(\tau)\Big](\nu)d\nu\Big) \in \mathcal{T}(S_{G,z^n}). \end{aligned}$$

Since $g^n \to g^*$, as n tends to zero, it follows that for all ζ belongs to V, we obtain

$$\begin{aligned} \Big(& m^*(\zeta) - \mathcal{K}_\varrho(\zeta)z_0 - \mathcal{Q}_\varrho(\zeta)z_1 \\ &- \int_0^\zeta \mathcal{W}_\varrho(\zeta-\nu)\mathbb{B}\mathbb{B}^*\mathcal{W}_\varrho^*(\zeta-\nu)\mathscr{R}(\hbar,\Gamma_0^T) \\ &\times \Big[z_T - \mathcal{K}_\varrho(T)z_0 - \mathcal{Q}_\varrho(T)z_1 \\ &- \int_0^T \mathcal{W}_\varrho(T-\tau)g^*(\tau)dW(\tau)\Big](\nu)d\nu\Big) \\ &\in \mathcal{T}(S_{G,z^*}). \end{aligned}$$

As a result, Φ is a closed graph.

Thus Φ is multivalued map which is completely continuous and hence as a result of the previous steps and Ascoli-Arzela theorem it is easily see that Φ is u.s.c. As a result, which has a fixed point $z(\zeta)$ on $\mathcal{B}_p$ and by referring to Lemma 2, which is the mild solution of (1). □

Definition 12. *The fractional integro-differential inclusions* (1) *is called approximately controllable on* $[0,T]$ *provide that* $\overline{\mathscr{R}(T,z_0)} = \mathcal{X}$, *where* $\mathscr{R}(T,z_0) = \{z_T(z_0;z) : z(\zeta)$ *in* $L^2(V,\mathcal{X})\}$ *is a mild solution of* (1).

The following assumptions are required for proving the main results.

H7 The function $G : V \times \mathcal{X} \times \mathcal{X} \to \mathcal{N}_{b,cl,cp}(L(K,\mathcal{X}))$ is uniformly bounded for all $\zeta \in V$ and $z \in \mathcal{X}$

Theorem 4. *Suppose* $(\mathbf{H_0}) - (\mathbf{H_7})$ *are fulfilled. Further there exist* $\mathscr{I}$ *belongs to* $L^1(V,[0,+\infty))$ *such that* $\sup_{z\in\mathcal{X}} \|G(\zeta, z(\zeta), \int_0^T f(\zeta,\nu,z(\nu))d\nu)\| \le \mathscr{I}(\zeta)$ *for a.e.* ζ *belongs to* V. *In addition,* (1) *is approximately controllable.*

Proof. Let $z^\alpha(.) \in B_p$ be a fixed point of the operator Φ, by Theorem 3.1 any fixed point of Φ is a mild solution of 1. This means that there is $z^\alpha \in \Phi(z^\alpha)$, i.e. by the Fubini theorem there is $g^\alpha \in S_{G,z^*}$ such that for all $\zeta \in V$.

$$\begin{aligned} z^\alpha(\zeta) &= \mathcal{K}_\varrho(\zeta)z_0 - \mathcal{Q}_\varrho(\zeta)z_1 \\ &\quad - \int_0^\zeta \mathcal{W}_\varrho(\zeta-\nu)\mathbb{B}\mathbb{B}^*\mathcal{W}_\varrho^*(\zeta-\nu)\mathscr{R}(\hbar,\Gamma_0^T) \\ &\quad \times \Big[z_T - \mathcal{K}_\varrho(T)z_0 - \mathcal{Q}_\varrho(T)z_1 \\ &\quad - \int_0^T \mathcal{W}_\varrho(T-\tau)g^*(\tau)dW(\tau)\Big](\nu)d\nu\Big). \end{aligned}$$

Define

$$\begin{aligned} P(g^\alpha) &= z_\alpha - \mathcal{K}_\varrho(T)z_0 - \mathcal{Q}_\varrho(T)z_1 \\ &\quad - \int_0^T \mathcal{W}_\varrho(T-\nu)g^\alpha(\nu)dW(\nu), \end{aligned}$$

for some $g^\alpha \in S_{G,z^*}$.
Noting that $I - \Gamma_0^T\mathscr{R}(\hbar,\Gamma_0^T) = \alpha\mathscr{R}(\hbar,\Gamma_0^T)$,
i.e we get $z^\alpha(b) = z_T - \alpha\mathscr{R}(\hbar,\Gamma_0^T)P(g^\alpha)$.
By assumption (H7),

$$\begin{aligned} E\|\int_0^T g^\alpha(\nu)dW(\nu)\|^2 &\le L_g^2 \int_0^T E\|g^\alpha(\nu)\|^2 d\nu \\ &\le L_g^2 l_r(\zeta)T \le L_g^2 l_r T. \end{aligned}$$

Subsequently, the sequence $\{g^\alpha\}$ is uniformly bounded in $L^2(V,\mathcal{X})$. Hence we can find a subsequence of $\{g^\alpha\}$ which is still denoted by $\{g^\alpha\}$ that converges weakly to $g \in L^2(V,\mathcal{X})$
Denoting $h = z_T - \mathcal{K}_\varrho(T)z_0 - \mathcal{Q}_\varrho(T)z_1 - \int_0^T \mathcal{W}_\varrho(T-\nu)g^*(\nu)dW(\nu)$.

We see that

$$\begin{aligned} &E\|P(g^\alpha) - h\|^2 \\ &= E\left\|\int_0^T \mathcal{W}_\varrho(T-\nu)[g^*(\nu) - g(\nu)]dW(\nu)\right\|^2 \\ &\le L_g^2 \int_0^T E\|\mathcal{W}_\varrho(\zeta-\nu)[g^\alpha(\nu) - g(\nu)]\|^2 d\nu \\ &\le \sup_{0\le t\le T} \int_0^\zeta E\|\mathcal{W}_\varrho(\zeta-\nu)[g^\alpha(\nu) - g(\nu)]\|^2 d\nu. \end{aligned}$$

Using Ascoli-Arzela theorem, we can see that the linear operator, $\int_0^{(\cdot)} (.,-\nu)^{\mu-1}\mathcal{W}_\varrho(.-\nu)g(\nu)d\nu : L^2(V,\mathcal{X}) \to C(V,\mathcal{X})$ is compact. Therefore, we get $E\|P(g^\alpha) - h\|^2 \to 0$ as $\alpha \to 0$.
Hence,

$$\begin{aligned} &E\|z^\alpha(b) - z_T\|^2 = E\|\mathscr{R}(\alpha,\Gamma_0^T)P(g^\alpha)\|^2 \\ &\le 2E\|\mathscr{R}(\alpha,\Gamma_0^T)(h)\|^2 + 2E\|\mathscr{R}(\alpha,\Gamma_0^T)(P(g^\alpha) - h)\|^2 \\ &\le 2E\|\mathscr{R}(\alpha,\Gamma_0^T)(h)\|^2 + \|(P(g^\alpha) - h)\|^2 \to 0 \\ &\text{as } \alpha \to 0^+. \end{aligned}$$

This proves the approximate controllability of system (1) □

4. Nonlocal conditions

The idea of nonlocal initial conditions of the differential systems were inspired by physical concerns. The result pertaining to approximate controllability is extended to Hilbert space in [37]. In contrary, to local conditions Byszewski et. al [38] interrogated the abstract Cauchy with nonlocal conditions in Banach spaces. For more details on nonlocal conditions refer [13, 14, 39, 40]. Consider the fractional systems of order $\varrho \in (1,2)$ with nonlocal conditions:

$$\begin{cases} {}^C D_\zeta^\varrho z(\zeta) \in Az(\zeta) + G(\zeta, z(\zeta), \\ \int_0^T f(\zeta,\nu,z(\nu))d\nu)\frac{dW(\nu)}{d\nu} \\ +\mathbb{B}x(\zeta),\ \zeta \in V = [0,T], \\ z(0) = z_0 + w_1(z),\ z'(0) = z_1 + w_2(z). \end{cases} \tag{2}$$

In the above, w_1, w_2 is appropriate functions and it is mapping from $V \times \mathcal{X}$ into $\mathcal{X}$ which fulfill the subsequent condition:

$(\mathbf{H_8})$ The completely continuous functions w_1, w_2 belongs to $C(V,\mathcal{X})$ and there exists $c, d, e, k > 0$ such that

$$\begin{aligned} &E\|w_1(z)\|^2 \le cE\|z\|^2 + d, \\ &E\|w_2(z)\|^2 \le eE\|z\|^2 + k, \quad \text{for all } z \in \mathbb{Y}. \end{aligned}$$

Definition 13. *A function z belongs to $\mathcal{C}$ is called a mild solution of (2) provide that*

$$z(\zeta) = \mathcal{K}_\varrho(\zeta)[z_0 - w_1(z)] + \mathcal{Q}_\varrho(\zeta)[z_1 - w_2(z)] + \int_0^\zeta \mathcal{W}_\varrho(\zeta-\nu)g(\nu)dW(\nu) + \int_0^\zeta \mathcal{W}_\varrho(\zeta-\nu)\mathbb{B}x(\nu)d\nu.$$

Theorem 5. *Provide that* $(\mathbf{H_0})$-$(\mathbf{H_8})$ *are fulfilled and if*

$$\widehat{P}^2\left[1+\frac{(\widehat{P^2P_{\mathbb{B}}^2})^2}{\hbar}\right]\varphi + \widehat{P}^2(c+e) \times \left[1+\frac{(\widehat{P}^2P_{\mathbb{B}}^2)^2}{\hbar}\right]\varphi < 1$$

where $P_{\mathbb{B}} = \|\mathbb{B}\|$ then (2) *has at least one mild solution on* $[0,T]$ *and is approximately controllable.*

Proof. Since the theoretical proof of the theorem much similar to that of Theorem 3, we neglect the proof. □

5. Application

To illustrate our finding we consider the following fractional integro-differential system

$$\begin{cases} \frac{\partial^\varrho}{\partial\zeta^r}z(\zeta,s) \in \frac{\partial^2}{\partial s^2}z(\zeta,s) + \mathscr{J}\Big(\zeta, z(\zeta,s), \\ \int_0^\zeta e(\zeta,\nu,z(\nu,s))d\nu\Big)\frac{dW(\nu)}{d\nu} + w(\zeta,s), \\ z(\zeta,0) = z(\zeta,1) = 0, \ \zeta \in V, \\ z(0,s) = z_0(s), \\ z'(0,s) = z_1(s), \ s \in [0,\pi]. \end{cases} \quad (3)$$

In the above the order of fractional system $\varrho = \frac{3}{2}$, $\mathscr{J} : [0,1]\times\mathcal{X}\times\mathcal{X} \to 2^{\mathcal{X}}\setminus\{\emptyset\}$ and the continuous function e mapping from $[0,1]\times[0,1]\times\mathcal{X}$ into $\mathcal{X}$. Let us consider $\mathcal{X} = \mathcal{H} = L^2([0,\pi])$ and let $W(\zeta)$ be a standard cylindrical Wiener process in $\mathcal{X}$ defined on a stochastic space $\big(\Omega, \Im, \{\Im_\zeta\}_{\zeta\geqslant 0}, \mathbb{P}\big)$, $D^\varrho z = \frac{\partial^\varrho z}{\partial\zeta^\varrho}$ is the Caputo fractional derivative of order $1 < \beta < 2$.

$$D(A) = \{z \in \mathcal{X} : z, \ z' \text{ are absolutely continuous}, \ z'' \in \mathcal{X}, \ z(0) = z(\pi) = 0\}.$$

Now there exist a sequence $\{e_j\}_{j\geqslant 1}$ of eigenvectors of $\mathcal{A}$ such that. $\{e_j\}_{j\geqslant 0}$ is a complete orthonormal and $e_j(y) = \sqrt{\frac{2}{\pi}}\, sin\, y$. Furthermore $\mathcal{A}$ is dense in $\mathcal{X}$ and A is the infinitesimal generator of a resolvent family $\{\mathcal{W}(\zeta), \ \zeta \geq 0\}$ belongs to $\mathcal{X}$, according to [14].

Put $z(\zeta) = z(\zeta,\cdot)$, ζ belongs to $[0,1]$ and $x(\zeta) = \omega(\zeta,\cdot)$. The linear bounded operator $\mathbb{B} : \mathcal{H} \to \mathcal{X}$ defined by $\mathbb{B}x(\zeta)(s) = w(\zeta,s)$. Then

$$e(\zeta,\nu,z)(s) = f(\zeta,\nu,z(s)),$$

and

$$G(\zeta,z,\wp_1)(s) = \mathscr{J}(\zeta, z(s), \wp_1(s))$$

for ζ,ν belongs to $[0,1]$, $z,\wp_1$ belongs to $\mathcal{X}$ and s belongs to $[0,\pi]$. The above mentioned fractional partial differential system (3) can be consider as the exact representation of the problem (1) with the functions our preferred choices. Then it can be easily viewed that all the requirements of the Theorem 3 satisfied and hence we can ensure the approximate controllability of (3) on $[0,T]$.

6. Conclusion

The findings of this research analyze the outcome results of approximate controllability of Stochastic fractional integro-differential equation considered in Banach space. Bohnenblust-Karlin's fixed point technique is used as the key factor to establish the required conditions for our chosen fractional system (1) to be controllable approximately. The above mentioned procedure to establish the approximate controllability is extended to fractional nonlocal system. In future the present work can be extended by analysing the controllability results of stochastic integro fractional differential inclusion system with impulsive conditions.

References

[1] Kilbas, A.A., Srivastava, H.M., & Trujillo, J.J. (2006). Theory and applications of fractional differential equations, *Elsevier*, Amsterdam.

[2] Miller, K.S., & Ross, B. (1993). *An Introduction to the Fractional Calculus and Fractional Differential Equations*, Wiley, New York.

[3] Podlubny, I. (1999). *Fractional differential equations: An introduction to fractional derivatives, fractional differential equations, to method of their solution and some of their applications*, San Diego, CA: Academic Press.

[4] Zhou, Y. (2014). *Basic Theory of Fractional Differential Equations*, World Scientific, Singapore. https://doi.org/10.1142/10238.

[5] Zhou, Y. (2015). *Fractional Evolution Equations and Inclusions: Analysis and Control*, Elsevier, New York.

[6] Dineshkumar, C., Nisar, K.S., Udhayakumar, R., & Vijayakumar, V. (2021). New discussion about the approximate controllability of fractional stochastic differential inclusions with order $1 < r < 2$. *Asian Journal of Control*, 1-15. https://doi.org/10.1002/num.22698.

[7] Kaliraj, K., Lakshmi Priya, P.K., & Ravichandran, C. (2022). An explication of finite-time stability for fractional delay model with neutral impulsive conditions. *Qualitative Theory of Dynamical Systems*, 21, 1-17. Doi:10.1007/s12346-022-00694-8.

[8] Kavitha, K., Vijayakumar, V., Udhayakumar, R., & Ravichandran, C. (2021). Results on controllability of Hilfer fractional differential equations with infinite delay via measures of noncompactness. *Asian Journal of Control*, 24, 1-10. https://doi.org/10.1002/asjc.2549.

[9] Lakshmi Priya, P.K., & Kaliraj, K. (2022). An application of fixed point technique of Rothe's-type to interpret the controllability criteria of neutral nonlinear fractional order impulsive system. *Chaos, Solitons & Fractals*, 164, 112647.

[10] Mohan Raja, M., & Vijayakumar, V. (2022). Existence results for Caputo fractional mixed Volterra-Fredholm-type integrodifferential inclusions of order $r \in (1,2)$ with sectorial operators. *Chaos, Solitons & Fractals*, 159, 1-8. https://doi.org/10.1016/j.chaos.2022.112127.

[11] Mohan Raja, M., Vijayakumar, V., Shukla, A., Nisar, K.S., & Baskonus, H.M. (2022). On the approximate controllability results for fractional integrodifferential systems of order $1 < r < 2$ with sectorial operators. *Journal of Computational and Applied Mathematics*, 415, 1-12. https://doi.org/10.1016/j.cam.2022.114492.

[12] Sakthivel, R., Ganesh, R., & Anthoni, S.M. (2013). Approximate controllability of fractional nonlinear differential inclusions. *Applied Mathematics and Computation*, 225, 708-717. https://doi.org/10.1016/j.amc.2013.09.068.

[13] Shu, L., Shu, X.B., & Mao, J. (2019). Approximate controllability and existence of mild solutions for Riemann-Liouville fractional stochastic evolution equations with nonlocal conditions of order $1 < \alpha < 2$. *Fractional Calculus & Applied Analysis*, 22, 1086-1112. https://doi.org/10.1515/fca-2019-0057.

[14] Shu, X.B., & Wang, Q. (2012). The existence and uniqueness of mild solutions for fractional differential equations with nonlocal conditions of order $1 < \alpha < 2$. *Computers and Mathematics with Applications*, 64, 2100-2110. https://doi.org/10.1016/j.camwa.2012.04.006.

[15] Mohan Raja, M., Vijayakumar, V., & Udhayakumar, R. (2020). Results on the existence and controllability of fractional integro-differential system of order $1 < r < 2$ via measure of noncompactness. *Chaos, Solitons & Fractals*, 139, 110299. https://doi.org/10.1016/j.chaos.2020.110299.

[16] Wang, J., & Zhou, Y. (2011). Existence and controllability results for fractional semilinear differential inclusions. *Nonlinear Analysis*, 12, 3642-3653. https://doi.org/10.1016/j.nonrwa.2011.06.021.

[17] El-Sayed, A.M.A., & Ibrahim, A.G. (1995). Multivalued fractional differential equations of arbitrary orders. *Applied Mathematics and Computation*, 68, 15-25. https://doi.org/10.1016/0096-3003(94)00080-N.

[18] Ito, K., Jin, B., & Takeuchi, T. (2015), On the sectorial property of the Caputo derivative operator. *Applied Mathematics Letters*, 47, 43-46.

[19] Wang, J.R., Ibrahim, A.G., & Feckan, M. (2015). Nonlocal impulsive fractional differential inclusions with fractional sectorial operators on Banach spaces. *Applied Mathematics and Computation*, 257, 103-118. https://doi.org/10.1016/j.amc.2014.04.093.

[20] Agarwal, R.P., Bashir, A., Alsaedi, A., & Shahzad, N. (2012). On the dimension of the solution set for semilinear fractional differential inclusions. *Abstract and Applied Analysis*, 10, 1-10. https://doi.org/10.1155/2012/305924.

[21] Benchohra, M., & Ziane, M. (2013). Impulsive evolution inclusions with state-dependent delay and multivalued jumps. *Electronic Journal of Qualitative Theory of Differential Equations*, 42, 1-21. https://doi.org/10.14232/ejqtde.2013.1.42.

[22] He, J.W., Liang, Y., Ahmad, B., & Zhou, Y. (2019). Nonlocal fractional evolution inclusions of order $\alpha \in (1,2)$. *Mathematics*, 209, 1-17. https://doi.org/10.3390/math7020209.

[23] Mohan Raja, M., Vijayakumar, V., & Udhayakumar, R. (2020). A new approach on approximate controllability of fractional evolution inclusions of order $1 < r < 2$ with infinite delay. *Chaos Solitons & Fractals*, 141, 110343. https://doi.org/10.1016/j.chaos.2020.110343

[24] Mohan Raja, M., Vijayakumar, V., Udhayakumar, R., & Zhou, Y. (2020). A new approach on the approximate controllability of fractional differential evolution equations of order $1 < r < 2$ in Hilbert spaces. *Chaos Solitons & Fractals*, 141, 110310. https://doi.org/10.1016/j.chaos.2020.110310.

[25] Dhayal, R., Malik, M., & Abbas, S. (2021). Solvability and optimal controls of non-instantaneous impulsive stochastic fractional differential equation of order $q \in (1,2)$. *Stochastics*, 93(5), 780–802. http://www.aimspress.com/article/10.3934/math.2019.3.663.

[26] Shu, X.B., Lai, Y., & Chen, Y. (2011). The existence of mild solutions for impulsive fractional partial differential equations. *Nonlinear Analysis*, 74, 2003-2011. https://doi.org/10.1016/j.na.2010.11.007.

[27] Dineshkumar, C., Nisar, K.S., Udhayakumar, R., & Vijayakumar, V. (2021). A discussion on approximate controllability of Sobolev-type Hilfer neutral fractional stochastic differential inclusions. *Asian Journal of Control*, 1-17. https://doi.org/10.1016/j.chaos.2020.110472.

[28] Singh, A., Shukla, A., Vijayakumar, V., & Udhayakumar, R. (2021). Asymptotic stability of fractional order (1,2] stochastic delay differential equations in Banach spaces. *Chaos Solitons & Fractals*, 150, 111095. https://doi.org/10.1016/j.chaos.2021.111095.

[29] Kavitha, K., Vijayakumar, V., Anurag, S., Nisar, K.S., & Udhayakumar, R. (2021). Results on approximate controllability of Sobolev-type fractional neutral differential inclusions of Clarke subdifferential type. *Chaos Solitons & Fractals*, 151, 111264. https://doi.org/10.1016/j.chaos.2021.111264.

[30] Ma, Y.K., Kavitha, K., Albalawi, W., Shukla, A., Nisar, K.S., & Vijayakumar, V. (2022). An analysis on the approximate controllability of Hilfer fractional neutral differential systems in Hilbert spaces. *Alexandria Engineering Journal*, 61(9), 7291-7302.

[31] Shukla, A., Sukavanam, N., & Pandey, D.N. (2015). Complete controllability of semi-linear stochastic system with delay. *Rendicondi del Circolo Matematico di Palermo*, 64, 209–220. https://doi.org/10.1007/s12215-015-0191-0.

[32] Vijayakumar, V., Nisar, K.S., Chalishajar, D., Shukla, A., Malik, M., Alsaadi, A., & Aldosary, S.F. (2022). A note on approximate controllability of fractional semilinear integrodifferential control systems via resolvent operators. *Fractal and Fractional*, 6(2). https://doi.org/10.3390/fractalfract6020073.

[33] Shu, X.B., & Xu, F. (2014). Upper and lower solution method for factional evolution equations with order $1 < \alpha < 2$. *Korean Mathematical Society*, 51, 1123-1139. https://doi.org/10.4134/JKMS.2014.51.6.1123.

[34] Deimling, K. (1992). *Multivalued Differential Equations*. De Gruyter, Berlin, https://doi.org/10.1515/9783110874228.

[35] Chang, Y., & Nieto, J.J. (2009). Existence of solutions for impulsive neutral integro-differential inclusions with nonlocal initial conditions via fractional operators. *Numerical Functional Analysis and Optimization*, 30, 227–244. https://doi.org/10.1080/01630560902841146.

[36] Bohnenblust, H.F., & Karlin, S. (1950). On a theorem of Ville, Contributions to the theory of games. *Annals of Mathematics Studies*, 24, Princeton University Press, Princeton, N. J., 155–160. DOI: 10.4236/am.2013.47A008.

[37] Mahmudov, N.I. (2001). Controllability of linear stochastic systems in Hilbert spaces. *Journal of Mathematical Analysis and Applications*, 259(1), 64-82. https://doi.org/10.1006/jmaa.2000.7386.

[38] Byszewski, L., & Akca, H. (1997). On a mild solution of a semilinear functional-differential evolution nonlocal problem. *Journal of Applied Mathematics and Stochastic Analysis*, 10, 265–271. https://doi.org/10.1155/S1048953397000336.

[39] Mohan Raja, M., & Vijayakumar, V. (2022). Optimal control results for Sobolev-type fractional mixed Volterra-Fredholm type integrodifferential equations of order $1 < r < 2$ with sectorial operators. *Optimal Control Applications and Methods*, 43, 1-17, https://doi.org/10.1002/oca.2892.

[40] Wang, X., & Shu, X.B. (2015). The existence of positive mild solutions for fractional differential evolution equations with nonlocal conditions of order $1 < \alpha < 2$. *Advances in Difference Equations*, 159, 1-15. https://doi.org/10.1186/s13662-015-0461-3.

Kalimuthu Kaliraj *working as an Assistant Professor of Mathematics at Ramanujan Institute for Advanced Study in Mathematics, University of Madras, Chepauk, Chennai, Tamil Nadu State, INDIA. His area of research topics are fractional calculus, Mathematical Biology, Control problems, and Mathematical Modeling. He completed his Ph. D. from Anna University, Chennai. He has published more than 40 research papers in Scopus/SCI-indexed journals.*
https://orcid.org/0000-0003-0902-3842

Kothandapani Muthuvel *received the B.Sc. and M.Sc. degree in mathematics from the University of Madras, Chennai in 2005 and 2007, respectively. He completed his M.Phil., degree in mathematics in 2009 at Ramanujan Institute for Advanced Study in Mathematics, University of Madras. Since 2013, he has been working as an assistant professor at the Department of Mathematics, Guru Nanak College, Chennai, India. His research interests focus on the relative controllability of the dynamical systems in fractional calculus.*
https://orcid.org/0009-0000-5358-2364

An International Journal of Optimization and Control: Theories & Applications
ISSN: 2146-0957 eISSN: 2146-5703
Vol.13, No.2, pp.205-213 (2023)
https://doi.org/10.11121/ijocta.2023.1260

RESEARCH ARTICLE

Fractional fuzzy PI controller using particle swarm optimization to improve power factor by boost converter

Metin Demirtas*, Farhan Ahmad

Department of Electrical and Electronics Engineering, Balikesir University, Turkey
mdtas@balikesir.edu.tr, engrfarhan27@outlook.com

ARTICLE INFO

Article history:
Received: 29 April 2022
Accepted: 7 May 2023
Available Online: 27 July 2023

Keywords:
DC-DC boost converter
PI and fuzzy logic controller
Fractional order PI controller
Power factor
Particle swarm optimization

AMS Classification 2010:
93B52, 94C30, 94C60, 94C05

ABSTRACT

The power circuit of AC voltage controller capable of operating at a leading, lagging, and unity power factor is studied by a lot of researchers in the literature. Circuits working with high switching frequency are known as power factor correctors (PFCs). The single-phase boost converter has become the most popular topology for power factor correction (PFC) in general purpose power supplies. Power factor correction circuit provides conventional benefits to electric power systems. The benefits are the reduction of power factor penalty and utility bill and power loss. Therefore, a boost converter power factor correction scheme is presented in this paper. A PI, fuzzy logic PI and fractional order PI (FOPI) controllers are used to fix an active shaping of input current of the circuit and to improve the power factor. The controller parameters (coefficients) are optimized using the Particle Swarm Optimization (PSO) algorithm. Average current mode control (ACMC) method is used in the circuit. The converter circuit consists of a single-phase bridge rectifier, boost converter, transformer and load. A mathematical model of the plant is required to design the PI controller. A model for power factor correction circuit is formed in MATLAB/Simulink toolbox and a filter is designed to reduce THD value. The proposed model is simulated using a combination of PI, fuzzy logic and FOPI controllers. The control scheme is applied to 600 Watt PFC boost converter to get 400 Volt DC output voltage and 0.99 power factor. The input voltage is 230 V_{RMS} with 50 Hz. The combination of FOPI and PI controller has the best solution to control the power factor according to PI and fuzzy controllers.

1. Introduction

With the recent advancement in industrial equipments, power electronic components have gained popularity due to energy crises in the world and power converters for renewable energy (solar, wind) have become more important. AC-DC converters are played a vital role in power supplies such as different level power charging, mobile charging and battery charging unit.

The advantage of semiconductor switches has dramatically increased the DC-DC boost converter [1]. One of the major applications is power factor correction. Using of switched mode power supply (SMPS) has increased in some industrial applications such as robotics, air/space craft, see vehicles etc. [2].

If a non-linear load is connected to grid, there will be a voltage distortion in side of the grid. Power factor correction (PFC) is required to eliminate the distortions. Generally, a high power factor is required in power systems connected to grid to reduce the harmonics occurring by high switching frequency. If a nonlinear load such as rectifier or converter is tied to grid, the harmonics with different frequency happen in the current waveform. They are multiplies of the input frequency. Therefore, the less average power is transferred to load. Limits of power factor and input current harmonics are determined according to international standard IEC 61003-2 and IEE/ANSI519, respectively [3].

PFC correction circuits are widely used in the input part of electronic circuits to decrease the rective power drawn from the grid [4]. The aim of this study is to reduce reactive power consumption and obtain better performance in the circuit by improvement of power factor. When line current with high power factor is

*Corresponding author

drawn by SMPS, total harmonic distortion (THD) decreases in side of grid and a filter is designed to reduce the THD value on grid side. The performance of power factor correction is depended on the current and voltage controllers. There are different control modes such as average current mode control (ACMC), peak current mode control and inductor hysteric control. Various small signal modelling analysis and pulse width modulation (PWM) control techniques has been proposed in early 1970's. The most common method is the average technique [5]. The distinctive feature of ACMC is a good tracking of average current [2].

Many researchers have been directed to apply nonlinear circuit techniques to dynamic control of circuit. The average current mode control method is used to sense and control the peak voltage across inductor in power supplies. This method eliminates the noise, immunity, slope compensation and peak to average current errors [6]. Cascade control structure is presented for the converter with PSO-based FOPI controller as inner current and outer voltage controllers for PFC and load voltage regulation. The main contribution of this paper is to correct the PFC and output voltage using Fuzzy+FOPI controllers with together. The paper is concerted in the following manner: Section 1 describes the introduction, section 2 illustrates the average current control method, section 3 illustrates the boost converter model, fuzzy logic controller, classic PI controller, FOPI controller, selection of voltage controller, selection of current controller, measuring of power factor and THD values, section 4 describes the results and discussions, and section 5 prescribes the conclusion.

2. Average current control method

In DC-DC Converters, average current control method is very popular due to simplicity of implimentation and good performance. In this method, the value of current is sensed by a shunt resistor R_s [7]. The output voltage are subratracted from the reference voltages to gain the output voltage and this signal is used for the multiplication block. The inverse of square input value of voltage is taken and multiply by the with the input voltage to gain the reference curent. Afterwards, the current flowing from the inductor is measured using the R_s and it is subtrachted from the reference current. This signal is used to control the MOSFET to get the output voltage as well as to for the PFC [3].

3. Boost converter model

Boost converters are step-up converters. It is one of the simplest type of switch-mode converter. Its duty is to increase the voltage at the input of circuit at the output of circuit. An ideal circuit of boost converter is shown in Figure 1. It is utilized in regulation of DC power supplies and bidirectional DC power supplies. When the switch Q is on state (close), the diode is reverse biased. The output resistance is isolated from source and the energy is transferred from the source to the inductor L. In the steady-state analysis, the capacitor C is supposed too large to maintain a constant output voltage $v_o(t) \cong v_o$.

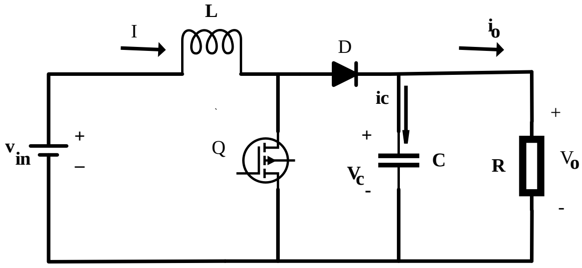

Figure 1. Ideal DC-DC boost converter circuit topology

There are two different operation modes of the circuit depending on the switch position u. When Kirchhoff's Law is applied to the circuit with switch off (u=0) and the derived equations for voltage and current are written as below.

$$L\frac{di_L}{dt} = v_{in} - v_o \tag{1}$$

$$i_C = C\frac{dv_o}{dt} = i_L - \frac{v_o}{R} \tag{2}$$

When the switch position is on (u=1), Eq. (3) and Eq. (4) for the circuit can be written as below

$$L\frac{di_L}{dt} = v_{in} \tag{3}$$

$$C\frac{dv_o}{dt} = -\frac{v_o}{RC} \tag{4}$$

Where V_{in} , I_L and V_o are the input voltage, inductor current and output voltage, respectively. The output voltage is equal to the capacitor voltage because the capacitor is connected parallel with load and are selected as state variables depending on *u* for a period, the state space equations for boost converter by combining the above equations are written as shown in Eq. (5) and Eq. (6).

$$\frac{di_L}{dt} = \frac{v_{in}}{L} - \frac{v_o}{L} + \frac{v_o}{L}u \tag{5}$$

$$\frac{dv_o}{dt} = \frac{i_L}{C} - \frac{i_L}{C}u - \frac{v_o}{RC} \tag{6}$$

3.1 Fuzzy logic controller

Fuzzy Logic Controller (FLC) has been used in many industrial applications such as AC and DC drives, PWM inverter and DC-DC converters in past years. Many research articles has been written by using FLC but they did not defined any exact model for converters [4,5]. FLC is an application of fuzzy set theory [8]. This theory is about uncertainty. It enables one to use non precise, ill-defined concepts [9]. FLC has an advanced level of efficiency for nonlinear converters [10]. Many researchers approved FLC to become one of intelligent controller for their appliances and successfully implemented their tactics [11-14]. FLC does not require an accurate mathematical model of a circuit. Therefore, it is valid to a process where the circuit model is unknown or ill-defined. Fuzzy control is adaptive in nature and nonlinear. It gives smooth performance under variations of parameters and load disturbances [9]. FLC is completely based on linguistic control variables. FLC is like human thinking, so it lowers the gap between mathematical calculation of plant and human certainty. FLC algorithm consists of three steps. The first step is fuzzification, second step is inference and third is defuzzification [15]. The schematic diagram of FLC is shown in Figure 2. Fuzzy controller has two inputs. Comparing the reference value with output value at each interval, error (v) and change in error (Δv) are calculated. Here the reference voltage is r(k) and output voltage is y(K). Error voltage e (k) is calculated as shown in Eq. (8).

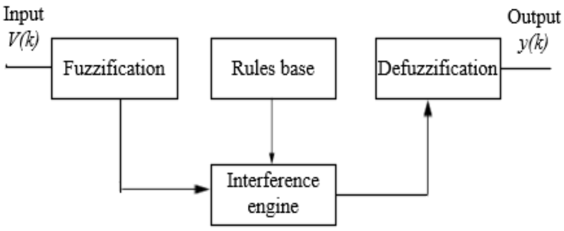

Figure 2. Block diagram of Fuzzy Logic Controller

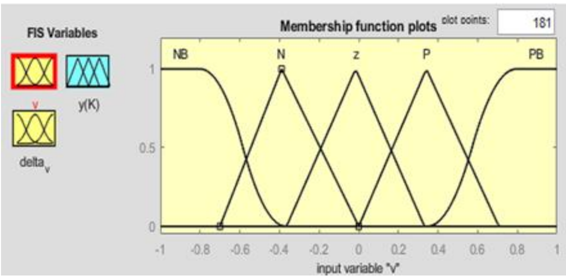

(a)

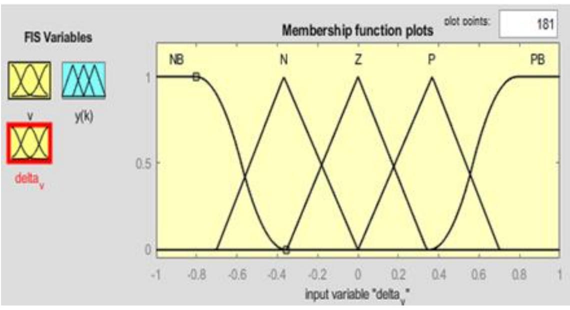

(b)

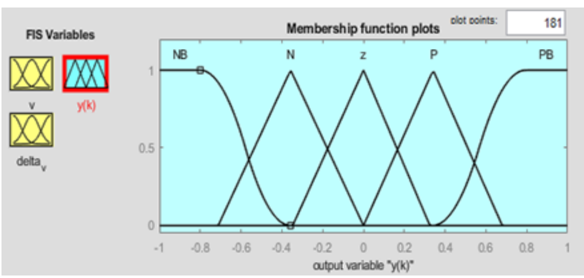

(c)

Figure 3. Designed membership functions (a) error MFs (b) change in error MFs (c) Defuzzification MFs

$$v(k) = r(k) - y(k) \quad (7)$$

$$\Delta v(k) = e(k) - e(k-1) \quad (8)$$

These are extended at the input of the controller for fuzzification. Fuzzy sets utilize linguistic terms and membership functions (MF's). The selected memberships are presented in Figure 3. MF's depend upon the impact of the linguist term regarding the output value.

The fuzzy rule editor is shown in Figure 4, in which rules are selected according to user visualizing. The membership functions are selected by taking account the system limits. The overall fuzzy logic designer representation is shown in Figure 5. Fuzzy rules contain 5 error voltage as well as change in error of voltage. The selected fuzzy rules are given in Table 1.

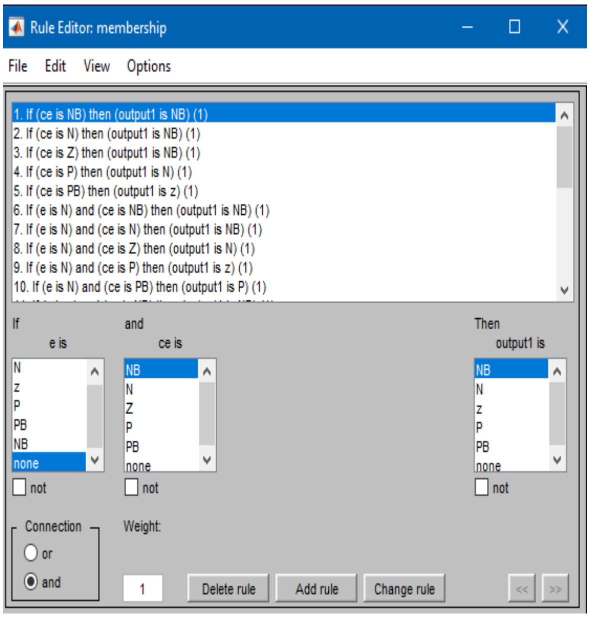

Figure 4. Fuzzy rules editor

Table 1. Fuzzy rules

v /Δv	NB	N	Z	P	PB
NB	NB	NB	NB	N	Z
N	NB	NB	N	Z	P
Z	NB	N	Z	P	PB
P	Z	Z	P	PB	PB
PB	N	P	PB	PB	PB

3.2 Classical PI controller

Classical PI controller is the simplest controller [16] which is frequently used in most of the circuits to control the output voltage and to meet the user's demand. These types of controllers are used mostly in situations where there are no load changes. The accuracy of classical PI controller can be disturbed when the load is varied frequently. Performance of classical PI controllers used in the inner loop and outer loop is also discussed in this section. The transfer function of classical PI controller is written as below.

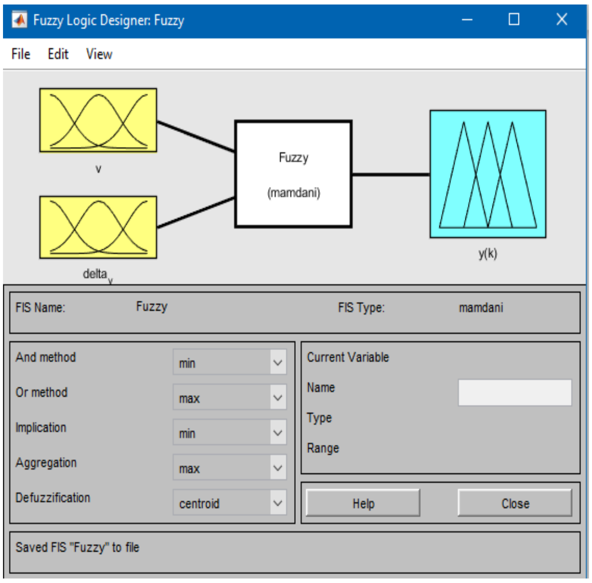

Figure 5. Overall fuzzy logic designer representation

$$G(s) = k_p + \frac{k_I}{s} \qquad (9)$$

Where K_P and K_I are gain coefficients of proportional and integral controller [17].

3.3 Fractional order PI$^{\lambda}$ controller

A generalization form of fractional calculus is classical integer order calculus, which consists of integral differential operators of fractional orders. Different approaches are executed to find optimum values of the three parameters of FOPD controller. One of the tuning rules of FOPID controller is Ziegler–Nichols method [18]. The mathematical expression of fractional derivatives defined by Grünwald-Letnikov is [19,20]:

$${}_cD_t^{\alpha} f(t) = \lim_{h \to 0} \frac{\sum_{k=1}^{\left[\frac{t-c}{h}\right]} (-1)^k \binom{\alpha}{k} f(t-kh)}{h^{\alpha}} \qquad (10)$$

This technique is used to calculate the transfer function of FOPI. It is described as below [21-26]:

$$G_c(S) = k_p + k_I s^{-\lambda} \qquad (11)$$

Here K_p is representing the proportional constant, K_I is representing the integral constant and λ is representing fractional integral constant.

3.4 Selection of voltage controller

The simulation of FLC circuit diagram on boost PFC using the average current control method is presented in Figure 6. In this paper, FLC is based on Mamdani fuzzy system which contains two inputs and one output. The circuit includes inner loop controller and outer loop controller. Inner controller is also known as current controller which controls the input current. Outer loop controller also called voltage controller controls the output voltage. Output voltage is compared with reference voltage. Here error (e) and change in error (Δe) are calculated at every interval, after it takes the derivative of change in error value. The voltage controller generates a signal which is transferred to the multiplier block. It multiplies the rectified voltage of circuit with the square of peak voltage of source v_{in}^2 [3]. Then signal goes towards the current controller after subtracting from reference current. After that PWM generator block leads this signal to the gate of switch IGBT or MOSFET. A shunt resistance (Rs) is used in simulations to sense the inductor current in the circuit.

In this paper, different controllers are used to determine the best performance of the circuit. Classical PI, Fuzzy and FOPI controllers are utilised to control the voltage and current in this study. To find the best controller for outer loop, different controllers are used at the outer loop while PI controller is only used in the inner loop.

3.5 Selection of current controller

The selection of inner loop controller is done by taking account the best performance of outer loop. It is performed by keeping the FOPI as the outer loop controller while the inner loop controller is changed. The boost converter PFC circuit diagram is shown in Figure 7. In this paper, FOPI controller is found as the best controller for the inner loop.

3.6 Measuring of power factor and THD values

Power factor is measured at the input side of circuit. To perform the Fourier analysis, Fourier block is used in the designed circuits with the help of MATLAB-Simulink, as shown in Figure 6 and Figure 7. Voltage distortion occurs when the current drawn by the load does not do remain sinusoidal form. Harmonics play a critical role for life of electrical and electronics systems. THD is the most common measured parameters of voltage and current of grid. THD is described as the root mean square (RMS) value of harmonics divided by the RMS value of fundamental and multiply by 100.

$$THD_I\,\% = \frac{\sqrt{I_{rms(2)} + \cdots + I_{rms(n)}}}{I_{rms(1)}} \times 100 \qquad (12)$$

Where $I_{rms(n)}$ is the RMS value of the nth harmonic current and $I_{rms(1)}$ is the RMS value of the fundamental component. If the THD value of current is below 5%, it is considered within acceptable limits according to international standards. If it is more than 10%, it causes problem for the equipment's and loads [27]. According to standards, the power factor should be between 0.90-0.99 or near to unity. So, both designed controllers show that the power factor is almost near to unity as shown in Figure 8. The designed filter capacitance value is 31.8 mF and resistance value is 1.5 Ω. The THD value of circuit is decreased to 4.72% as shown in Figure 10 when passive filter is used in the input side of rectifier.

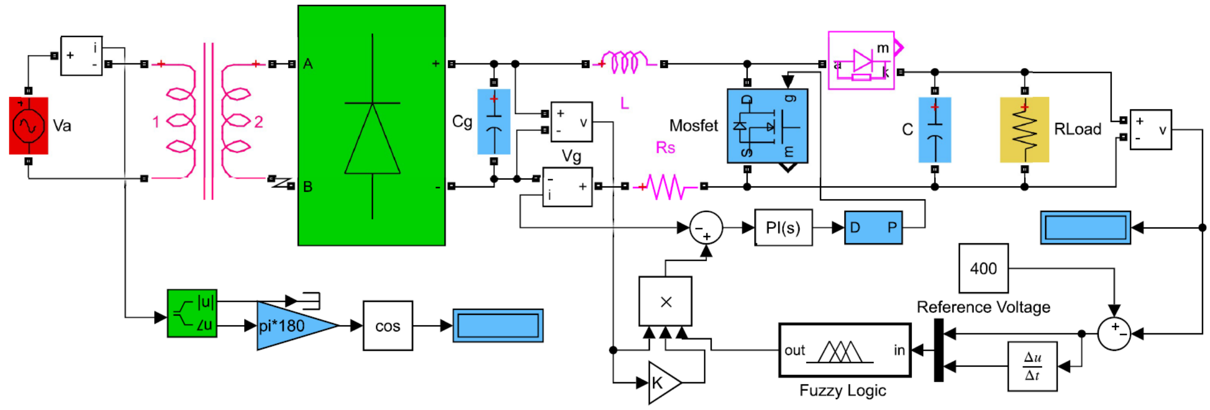

Figure 6. Simulation diagram for the selection of outer loop controller using FLC

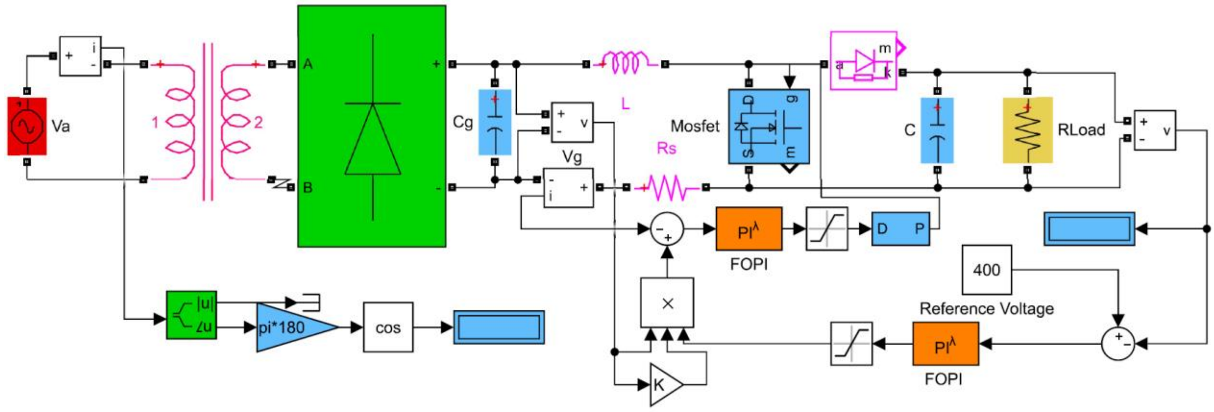

Figure 7. Simulation diagram for selection of inner loop controller

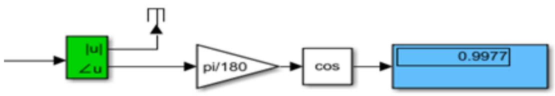

Figure 8. Power factor measuring

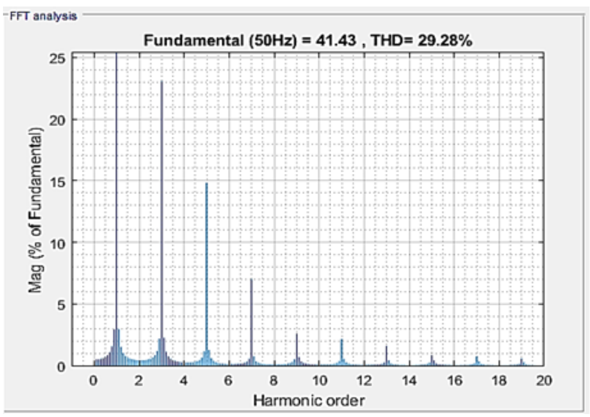

Figure 9. THD value of designed controller without filter

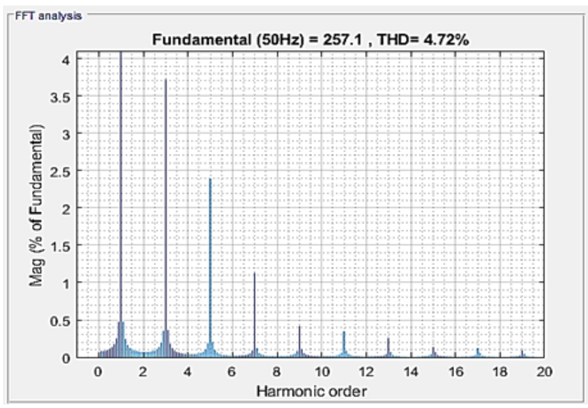

Figure 10. THD value of designed controller with filter

When the passive filter is not utilized in the input side of circuit, THD value is 29.28%. The current contains harmonics, and its waveform is distorted as shown in Figure 11.

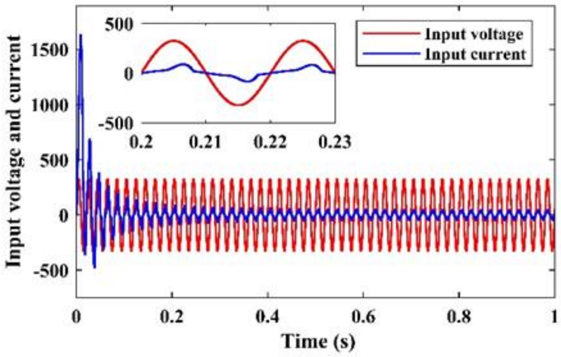

Figure 11. Input voltage and current without filter

As shown in Figure 10, THD value decreases from 29.28% to 4.72% when the passive filter is used in the output side of grid. The current drawn by the load contains lower harmonics and its waveform is closer to the sinusoidal waveform with distortion as given in Figure 10 when the passive filter is settled in the input side of circuit.

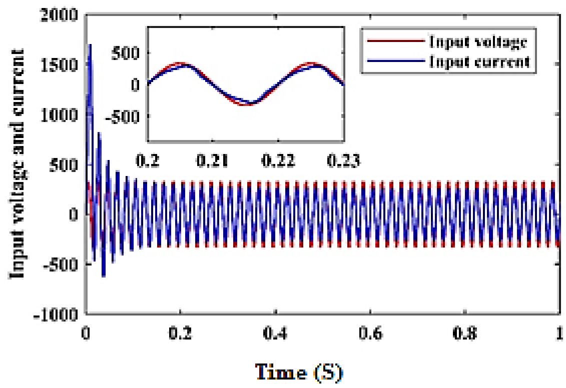

Figure 12. Input voltage and current with filter

4. Results and discussions

In this paper, the power factor correction is performed using the boost converter. The power factor is measured for each step by selecting the inner loop and outer loop controller. The simulations are done by using the DELL core I3 laptop. Nominal load is used as 266 Ω and a disturbance load is added to the circuit as 100 Ω. It can be seen in Figure 10 that the input current is not sinusoidal and have a THD like 29.28%. When the passive filter R-C is added to the circuit, the current waveform came into sinusoidal waveform and THD value becomes 4.72%. When the passive filter is added into a circuit, the harmonics come in a range of intentional standards. The output voltages for the selection of outer loop and inner loop controllers are shown in Figure 13 and Figure 14, respectively. It is seen from Figure 13, when FOPI controller is utilized in the outer loop while keeping PI controller in the inner loop, the system has a good response compared to reference voltage. When disturbance or variable load is added to the circuit for an interval of time, it does not maintain its accuracy and performance. As shown in Figure 13, FOPI controller is faster response than the other controllers. It also maintains its accuracy and performance according to the others.

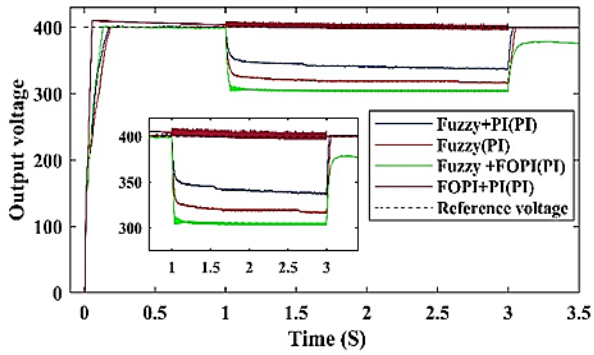

Figure 13. Output voltage for the selection of voltage controller

To select the inner loop controller (current controller), the best performance of voltage controller is obtained by FOPI controller. Therefore, FOPI controller for the outer loop is not changed when different controllers such as Fuzzy, PI, Fuzzy+PI structure are used in the inner loop to determine the best controller for the system. The output results of these controllers are shown in Figure 14. It can be seen that Fuzzy, PI and Fuzzy+PI achieve a good response at settling time. When the variable load is added into the system, FOPI controller is faster than the others in view of performance of current controller. The performance of current controllers is almost same when load change occurs in the system.

In the circuit, power factor correction and output voltage control are implemented at the same time. THD value is very high according to the international standard as the power factor value approaches to unity. To decrease THD value, passive filter R-C is used in the input side of circuit. Thus, unity power factor is adjusted 0,99 and THD value has been brought to international standard.

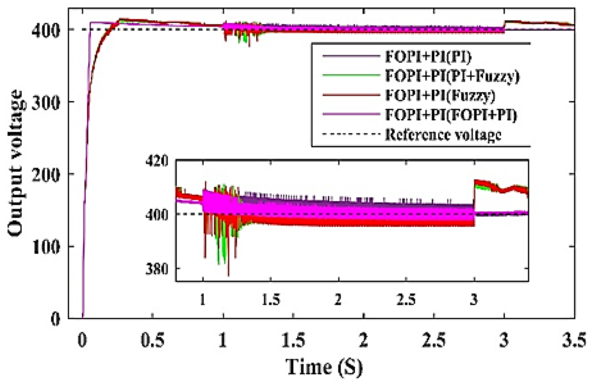

Figure 14. Output voltage for the selection of current controller

The selected parameters of designed circuit are shown in Table 2 and the optimized parameter using the PSO are shown in Table 3. For the optimization Integral Time Absolute Error (ITAE) function is used for optimization of controller parameters [21].

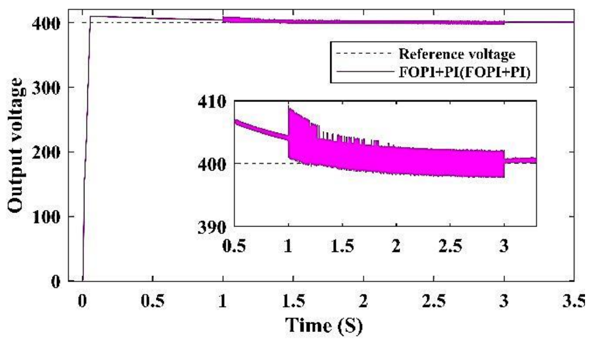

Figure 15. Output voltage for the FOPI+PI controller

The THD value of the designed circuit with filter is shown in Figure 16. It is clearly shown in the Figure 9 that without the filter, THD value was 29.28% while using the filter THD value is decreased to 4.27% as shown in Figure 16. This is acceptable according to IEE/ANSI519.

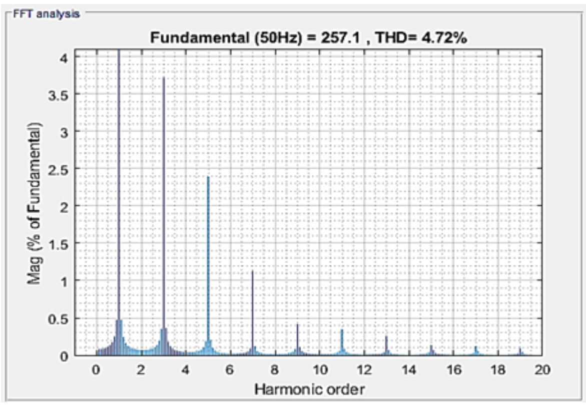

Figure 16. THD value of designed controller with filter

The designed parameters of discussed boost converter are calculated according to using Eqs. (13)-(16).
The value of the inductor is calculated using the Eq.(13).

$$L = \frac{D(1-D)^2 \times R}{2 \times f} \tag{13}$$

In practical application, the inductor value is selected 25% greater than this calculated for better performance. Here the R is the resistance/output load, f is the switching frequency, L is the inductor value calculated by Eq.(13) and the D is the duty cycle. The D is calculated according to Eq.(14)

$$D = 1 - \frac{v_{in}}{v_o} \tag{14}$$

Here the v_{in} is the input voltage and v_o is representing the output voltage. The value of output capacitor is calculated using the Eq.(15).

$$C_{out} \geq \frac{D}{R\left(\frac{\Delta v_o}{v_o}\right) \times f} \tag{15}$$

Here D is the duty cycle, f is the frequency and $\left(\frac{\Delta v_o}{v_o}\right)$ is representing the ripple factor of the output voltage which is taking 1% of the output voltage. The capacitor C_g value is selected maximum to remove the ripple of the input voltage.

$$C_g = \frac{I_{rms} \times I_{ripple}}{v_{rms} \times v_{ripple} \times 2\pi f} \tag{16}$$

Here the I_{rms}, V_{rms} is the RMS value of current and voltage representing respectively. I_{ripple} and V_{ripple} representing the ripple current and ripple voltage and their values are taken 5% and 1% respectively [17].

Table 2. The parameter values of designed circuit

Parameters	values
L	4.34 mH
C_{out}	600 µF
R_{Load}	266 Ω
V_{in}	230 V_{RMS}
Supply frequency	50 Hz
R_s	0.02 Ω
Cg	100 mF
V_{ref}	400 V
Switching frequency	1000 HZ

Table 3. Optimized parameter values of the designed controllers

Parameters	Values
FOPI	K_P=1.5981 K_I=1.5981 λ=1
Classic PI controller	K_P=4.1437 K_I=0.1

5. Conclusions

In this paper, fuzzy, PI and FOPI controllers and different variations of these controllers are applied to in the inner and outer loops to increase the power factor value and regulate the output voltage. The best performance of voltage and current controllers are assessed for the PFC using boost converter. When the FOPI contoller in the inner loop and PI controller in outer loop are used, the obtained results have faster and more smoothly responses. The results are compared with PI and fuzzy PI (FPI) controller. They show the FOFPI has less fluctuations, overshoot and settling time compared to FPI. The presented system can be used to provide electrical power to electronic devices in critical applications such as military, space craft, and sea vehicles.

Acknowledgment

The authors are supported by the BAP project no. 2022/012 of Balikesir University.

References

[1] Divya S. P. N., Sathik J., L. A, V. K, & Almakhles D. (2021). A comprehensive study on various dc–dc converter voltage-boosting topologies and their applications, *Circuit World*, 48(4), 529-549.

[2] K. Periyasamy (2012). Power factor correction based on Fuzzy Logic controller with average current-mode for DC-DC boost converter, *Elektronika ir Elektrotechnika*, 2(2), 67–72.

[3] Jensen C. H. K., Lind R. B., Hertel J. C., Ammar A. M., Knott, A. & Andersen M. A. E. (2019). A time-based control scheme for power factor correction boost converter, *IEEE Nord. Circuits Syst. Conf. NORCAS 2019 NORCHIP Int. Symp. Syst. SoC 2019 - Proc.*

[4] Kessal A., Rahmani L., Mostefai M., & Gaubert J. (2012). Power factor correction based on fuzzy logic controller with fixed switching frequency, *Elektronika ir Elektrotechnika*, 2(2), 67–72.

[5] Chung H. S. H., Tam E. P. W., & Hui S. Y. R. (1999). Development of a fuzzy logic controller for boost rectifier with active power factor correction, *PESC Rec. - IEEE Annu. Power Electron. Spec. Conf.*, 1, 149–154.

[6] Dixon L. (1991). Average Current Mode Control of Switching Power Supplies, *Proc. Intersoc. Energy Convers. Eng. Conf.*, 1, 218–223.

[7] Panov Y. & Jovanovic M. M. (2008). Loop gain measurement of paralleled DC-DC converters with average-current-sharing control, *2008 Twenty-Third Annual IEEE Applied Power Electronics Conference and Exposition*, 1048-1053.

[8] Ahmad Firdaus A.Z., Normahira M., Syahirah K.N. & Sakinah J. (2013). Design and simulation of Fuzzy Logic controller for boost converter in renewable energy application, *2013 IEEE International Conference on Control System, Computing and Engineering, 29 Nov. - 1 Dec. 2013, Penang, Malaysia*, 520-524.

[9] Lin B. R. & Hua C. (1993). Buck/boost converter control with fuzzy logic approach, *Proceedings of IECON '93 - 19th Annual Conference of IEEE Industrial Electronics-1* 1342-1346.

[10] Duranay Z. B., Guldemir H., & Tuncer S. (2018)., Fuzzy sliding mode control of DC-DC boost converter, *Engineering, Technology & Applied Science Research*, 8(3), 3054–3059.

[11] Ismail N. F. N., Musirin I., Baharom R. & Johari D. (2010). Fuzzy logic controller on DC/DC boost converter," *2010 IEEE International Conference on Power and Energy (PECon2010), Nov 29 - Dec 1, 2010, Kuala Lumpur, Malaysia,* 1-6.

[12] Ucak K. & Arslanturk B. N. (2023). Adaptive MIMO fuzzy PID controller based on peak observer, *An International Journal of Optimization and Control: Theories & Applications*, 13(2), 139-150.

[13] Sulaiman I. M. & Ghazal P. L. (2021). Shamanskii method for solving parameterized fuzzy nonlinear equations, A*n International Journal of Optimization and Control: Theories & Applications,* 11(1), 24-29.

[14] Kakran V. & Dhodiya J. (2022). A belief-degree based multi-objective transportation problem with multi-choice demand and supply, *An International Journal of Optimization and Control: Theories & Applications*, 12(2), 99-112.

[15] Saravanan S., Rani P. U. & Thakre M. P. (2022). Evaluation and improvement of a transformerless high-efficiency DC–DC converter for renewable energy applications employing a fuzzy logic controller, *MAPAN-Journal of Metrology Society of India*, 37(2), 291–310.

[16] Demirtas M., Calgan H., Amieur T. & Sedraoui M. (2021). Small-signal modeling and robust multi-loop PID and H ∞ controllers synthesis for a self-excited induction generator, *ISA Transactions,* 117, 234-250.

[17] Ahmad F. (2022). Power pactor correction in single phase AC/DC converters used for wireless energy transfer, *Master Thesis*, *Balikesir University*.

[18] Arpaci H., Ozguven O. F. & Can M. S. (2016). Fractional Model Reference Adaptive $PI^{\lambda}D^{\mu}$ Control, *Journal of New Results in Science.*, 5(11), 102–117.

[19] Ilten E. & Demirtas M. (2019). Fractional order super-twisting sliding mode observer for sensorless control of induction motor, *COMPEL-The international journal for computation and mathematics in electrical and electronic engineering*, 38(2), 878–892.

[20] Chafekar N., Mate U. M., Kurode S. R. & Vyawahare V. A. (2019). Design and implementation of fractional order sliding mode controller for DC-DC buck converter, *2019 Fifth Indian Control Conference (ICC),* 201–206.

[21] Calgan H. & Demirtas M. (2021). A robust LQR-$FOPI^{\lambda}D^{\mu}$ controller design for output voltage regulation of stand-alone self-excited induction generator, *Electric Power System Research*, 196, 1-16.

[22] Ilten, E. (2022). Conformable fractional order controller design and optimization for sensorless control of induction motor, *COMPEL - The international journal for computation and mathematics in electrical and electronic engineering,* 41(5), 1528-1541.

[23] Ilten, E. (2022). Conformable fractional order controller design and implementation for per-phase voltage regulation of three-phase SEIG under unbalanced load, *Electric Power Components and Systems*, 50(11-12), 636–648.

[24] Ilten, E. (2021). Conformable fractional order PI controller design and optimization for permanent magnet synchronous motor speed tracking system, *Düzce Üniversitesi Bilim ve Teknoloji Dergisi*, 9(3), 130-144.

[25] Ozyetkin M. M. & Birdane H. (2022). The processes with fractional order delay and PI controller design using particle swarm optimization, *An International Journal of Optimization and Control: Theories & Applications*, 13(1), 81-91.

[26] Tajadodi H., Jafari H. & Ncube M. N. (2022). Genocchi polynomials as a tool for solving a class of fractionaloptimal control problems, *An International Journal of Optimization and Control: Theories & Applications*, 12(2), 160-168.

[27] Grady W. M. & Santoso S. (2001). Understanding power system harmonics, *IEEE Power Engineering Review*, 21(11), 8–11.

Metin Demirtas *received Ph.D. degree in Electrical Engineering from Yıldız Technical University in 2002. He is a full professor of Electrical and Electronics Engineering Department at Balikesir University, Turkey. He is working on power electronics, electrical machines, and control.*

https://orcid.org/0000-0003-2622-5286

Farhan Ahmad *was born in Pakistan. He studied F.Sc (Pre-engineering) in GOVT Higher Secondary School Muridke. He graduated from one of the public sector of Pakistan; University of Gujrat, Gujrat in the department Electrical Engineering and technology at the program of BS Electrical Technology in 2015. He worked 3 years in semi-automatic plant of Steel Industry. He graduated from Electrical and Electronics MSc program at Balikesir University, Turkey. His specialization is in the field of power electronics.*

https://orcid.org/0000-0002-1338-4328

An International Journal of Optimization and Control: Theories & Applications
ISSN:2146-0957 eISSN:2146-5703
Vol.13, No.2, pp.214-223 (2023)
http://doi.org/10.11121/ijocta.2023.1269

RESEARCH ARTICLE

Prediction of anemia with a particle swarm optimization-based approach

Arshed A. Ahmad,[a] Khalid M. Saffer,[a] Murat Sari,[b*] Hande Uslu[c]

[a] *Department of Computer Science, University of Diyala, Iraq*
[b] *Department of Mathematical Engineering, Istanbul Technical University, Istanbul, Turkey*
[c] *Department of Mathematics, Yildiz Technical University, Istanbul, Turkey*
arshed980@gmail.com, kha2005ms@yahoo.com, muratsari@itu.edu.tr, usluh@yildiz.edu.tr

ARTICLE INFO

Article History:
Received 23 May 2022
Accepted 8 February 2023
Available 28 July 2023

Keywords:
Anemia
Particle swarm optimization
Support vector machine
Prediction

AMS Classification 2010:
93B52; 93C35; 93C40; 93C42

ABSTRACT

Healthcare enables the maintenance of health through some physical and mental care for the prevention, diagnosis and treatment of disease. Diagnosis of anemia, one of the most common health problems of the age, is also very ambitious. Whereas, pathological individuals could be predicted through various biomedical variables using some appropriate methods. In order to estimate these individuals just by taking into account biological data, particle swarm optimization (PSO) and support vector machine (SVM) clustering techniques have been merged (PSO-SVM). In this respect, the dataset provided has been divided into five clusters based on anemia types consisting of 539 subjects in total, and the anemia values of each subject have been recorded according to corresponding biomedical variables taken as independent parameters. The findings of the PSO-SVM method have been compared to the results of the SVM algorithm. The hybrid PSO-SVM method has proven to be quite effective, particularly in terms of the high predictability of clustered disease types. it is possible to lead the successful creation of appropriate treatment programs for diagnosed patients without overlooking or wasting time during treatment.

1. Introduction

In the past decade computer models have become very popular in the field of biomedicine due to exponentially increasing computer power. So, an efficient healthcare system using computer models can contribute to an important part of a country's economic development, and industrialization. Healthcare has traditionally been recognized as an important determinant in improving the overall physical and mental health and well-being of people around the world. Anemia is clinically defined as a below hemoglobin value from the appropriate reference range for an individual and it possibly leads to crucial blood diseases. Anemia types are determined depending on symptoms ranged from short episodes to chronic conditions [1–5].

Few have analyzed types of anemia, although it has received much attention recently because of epidemiological studies suggesting that anemia may be associated with worse outcomes in various diseases [5–9].

In the literature, there have been several methods [8–16] to analyze anemia types. Besides to their notable advantages, many common properties, such as being costly, difficulty in usage, time-consuming and having constraints in daily usage, lead to their drawbacks. In this case, optimization modeling should be taken into consideration alongside those methods.

It is obviously discovered that by taking into account the mechanics of computer hardware, it can be created novel hybrid approaches that are much more effective for certain calculations as outlined

*Corresponding Author

in the literature [17–24], even though these concepts may appear to be unrelated to physical limitations.

A more efficient algorithm can complete any computation much faster than any inefficient algorithm, even without changing the computer hardware. Therefore, advancements in algorithms can be used to make computers faster, such as precomputing parts of a problem or other solutions to improve computing efficiency.

Therefore, there are particular techniques for optimization, including particle swarm optimization (PSO) which is becoming increasingly popular as an effective method for many data processing tasks. In this work, the hybrid algorithm of PSO with another important optimization algorithm, support vector machine (SVM), has been created to predict types of anemia. To the best of the authors' knowledge, this is the first time a combination of PSO and SVM has been used to forecast anemia types using biological data, despite the fact that certain conventional methods are utilized for evaluating anemia types in the literature [7–15]. The PSO-SVM algorithm has been suggested for reliable data treatment and further analysis for interpretation due to its high level of flexibility and lack of requirement for specialized knowledge in statistics [25–27].

The PSO-SVM is a comprehensive optimization clustering technique as a consequence, enabling the estimation of different patterns using the data that is currently available in an area. By forecasting the clusters that are most likely to include individuals who have that form of anemia, it is able to predict anemia types. Investigating pathological individuals from a population was the goal of this study, and using advanced computers to implement the PSO-SVM technique has been attractive [10], [28].

2. Materials and methods

2.1. Biomedical data collection and study design

The dataset has been prepared from observations of anemia disease. The dataset that consists of the anemia measurements contains 5 classes and 539 subjects provided from the literature [9], [11], [12] whose main concerns are creating mathematical models that can predict the type of anemia based on various blood variables by only specific algorithms while in the current study, a hybrid algorithm has been developed using pathological individuals from a population and their corresponding blood variables. The data has been collected from individuals between aged 6 to 56 years. Each sample includes information from blood variables; Red Blood Cells (RBC), a portable protein Hemoglobin (HB) inside the RBC containing iron atoms which carry oxygen from the lungs to the body's tissues and return carbon dioxide from the tissues back to the lungs, Hematocrit (HCT) which shows the percentage of RBC in the blood, Mean Corpuscular Volume (MCV) which measures average size of the red cells in a sample and [8]. In addition to these, some biophysical variables, sex and age, have also been considered since natural HB in the body varies from male (1) to female (2) and natural HB in the body varies according to age.

The best four variables have been selected from the prediction of anemia through the PSO and machine learning, and are mentioned in Table 1 and Figures 1. The relationship between different parameter values of the subjects is illustrated in Figure 2.

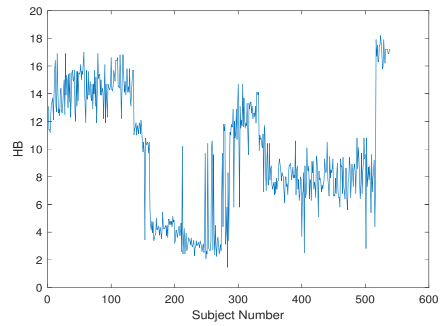

(a)

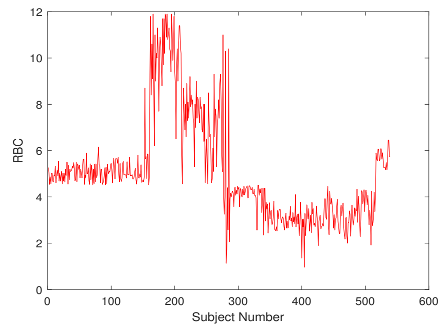

(b)

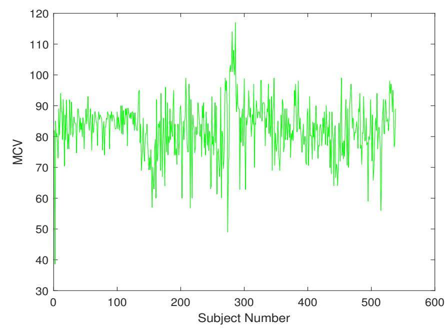

(c)

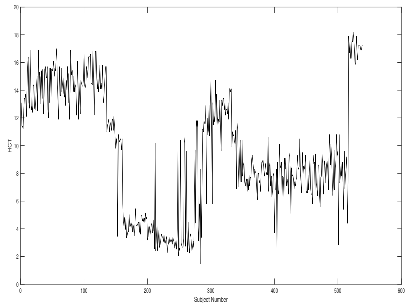

(d)

Figure 1. The parameter values of every subject.

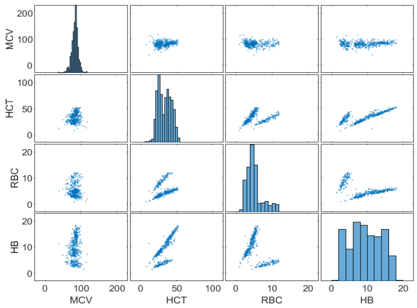

Figure 2. Relationship between parameter values of the subjects.

The goal of this research is to detect anemia in a population through the utilization of PSO-SVM algorithm and analysis of blood parameters. Since the hybrid algorithm is based on clustering principle, the five clusters have been generated by blood variables as detailed in Table 1 and Figure 3. This study has classified anemia types into five separate clusters based on common characteristics and danger levels. The attributes of anemia dataset can be seen in Table 2. The proposed approach has been implemented on the collected data to identification a healthy or infected person out of involved 539 subjects.

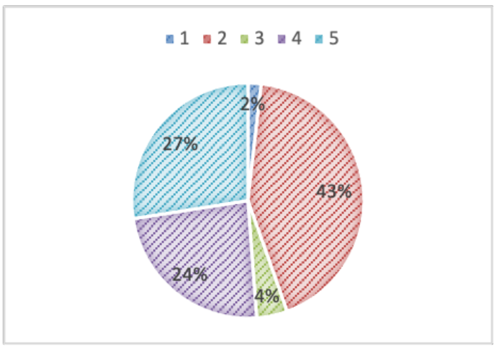

Figure 3. Dataset collected.

2.2. Particle swarm optimization

Kennedy and Eberhart developed an evolutionary and population-based optimization technique referred to as the particle swarm optimization (PSO) [29] by drawing inspiration from the collective behavior of birds and fish. So, these animals played an important role in the development of an algorithm by escaping dangerous situations and finding food. The PSO is much faster and more effective than other optimization techniques because it requires fewer parameters and is less likely to be stuck in local minimum points as a possible solution.

The PSO seeks to improve a solution to a problem by having each particle trace its coordinates in terms of the best solutions that have already been made. The particle keeps track of its own best, known as *pbest*, and the best solution in the near surroundings, known as *lbest*. If the particle considers the entire population for its topological neighbors, then the best value becomes the global best, or *gbest*. At every step, the particles' velocities are adjusted according to the *pbest* and *lbest* locations.

In the PSO, software agents known as particles move through the related space to find improved results. At each step, the randomly selected particles adjust their velocities using data from their local areas, their own neighborhoods and from randomness in order to search for better spots in the solution space. The position of a particle is an indication of a potential solution to the problem. At the conclusion of each cycle, all particles attempt to find more desirable locations in the search space by altering their speed. For each iteration, the position and velocity vectors have been determined as follows:

$$\begin{aligned} V_p^{new} = wV_p^{old} + c_1 rand_1 (Pbest - X_p^{old}) \\ + c_2 rand_2 (gbest - X_p^{old}) \end{aligned} \tag{1}$$

$$X_p^{new} = X_p^{old} + V_p^{new} \tag{2}$$

where w represents corresponding weights, c_1, c_2 are acceleration coefficients (cognitive parameter, social parameter), $rand_1, rand_2$ are uniformly distrubed random numbers between 0 and 1, V_p^{old} gives velocity of individual p at the iteration, X_p^{old} determines position of individual p at the current iteration, *Pbest* and *gbest* indicate the best local value of each particle and the best value of swarm, respectively [30], [31].

Table 1. Clusters and subject numbers.

Cluster no.	MCV	HCT	RBC	HB	Number of Subjects	Anemia Type
1	≥ 100	-	-	-	10	Deficiency B12
2	< 100	≥ 48	-	-	230	Thalassemia
3	<100	< 48	≤ 4.5	-	23	Sickle Cell
4	< 100	< 48	> 4.5	< 11	128	Iron deficiency
5	<100	< 48	> 4.5	≥ 11	148	Normal

Table 2. Attributes of anemia dataset.

Attribute	Attribute value	Attribute category
Age	6-56	0-13 Child, >13 Adult
Gender	1,2	1 = Male, 2 = Female
HB	1.46-18.2	$<$ 11 Severe, 11-15 Moderate
RBC	0.96-11.9	$<$ 4.5 Low, 4.5-6.5 Normal, $>$ 6.5 High
MCV	38.6-117	$<$ 80 Microcytic, 80-100 Normocytic, $\geq$ 100 Macrocytic
HCT	7.7-51.7	$<$ 35 Low, 35-48 Normal, $\geq$ 48 High

3. Support vector machine

Vladimir Vapnik began examining Support Vector Machines (SVMs) in the late 1970s, but in the late 1990s, the field began to gain extreme recognition [32]. The SVMs are supervised learning algorithms operated by statistical learning theory to identify patterns and perform suitable regression.

Statistical learning theory can accurately identify the components needed for successful learning of certain basic algorithms. However, due to the complexity of more intricate models and algorithms used in real-world applications, it is difficult to analyze them theoretically.

The SVMs can be thought of as a combination of learning theory and practicality, which is simple enough to be understood mathematically. This is due to the fact that an SVM can be regarded as a linear model in a high-dimensional space and the SVMs are able to go beyond the limitations of linear learning machines by incorporating a kernel function, allowing for the discovery of a nonlinear decision function [33].

4. The PSO-SVM algorithm

The process of feature selection can be regarded as a challenge of global combinatorial optimization in machine learning, wherein the amount of features is reduced and also unimportant, noisy and redundant information is eliminated to achieve a satisfactory classification accuracy. The significance of this method is immense in the fields of pattern recognition, medical data analysis, machine learning, and data mining. In order to increase processing rate, accuracy, and reduce incomprehensibility, a reliable feature selection method that takes into account the number of features studied for sample classification is necessary.

In this study, a binary version of the PSO algorithm has been used and the placement of each particle is indicated through a binary string that symbolizes the feature choice situation. The position and velocity of each particle is revised in accordance with the following equations:

$$\begin{aligned} V_{pd}^{new} &= wV_{pd}^{old} + c_1 rand_1 (Pbest_{pd} - X_{pd}^{old}) \\ &\quad + c_2 rand_2 (gbest_d - X_{pd}^{old}) \end{aligned} \tag{3}$$

$$S(V_{pd}^{new}) = \frac{1}{1 + e^{-V_{pd}^{new}}} \tag{4}$$

$$\begin{aligned} if(rand < S(V_{pd}^{new}))then \quad X_{pd}^{new} &= 1; \\ else \quad X_{pd}^{new} &= 0 \end{aligned} \tag{5}$$

where V_{pd}^{new} and V_{pd}^{old} are the particle velocities, X_{pd}^{old} shows the current position, and X_{pd}^{new} represents the updated position for the related solution. The values $Pbest_{pd}$ and $gbest_d$ are defined as local and global best fitness value. The $rand_1$ and $rand_2$ are randomly generated numbers between 0 to 1, whereas c_1 and c_2 are acceleration factors, usually chosen as $c_1 = c_2 = 2$. Velocities for each dimension have been tried to reach a maximum velocity V_{max}. If the combined velocities of a given dimension add up to more than the predetermined value of V_{max}, the velocity of that dimension will be restricted to V_{max}, which is a value set by the user.

After renewal, the new feature is calculated as in Eq. 4, where V_{pd}^{new} represents the velocity. If calculated value $S(V_{pd}^{new})$ is greater than a randomly generated number that is between $(0, 1)$, then its position value $F_n, n = 1, 2, \ldots, m$ is represented as 1 by meaning that this feature is chosen to be a required feature for the upcoming renewal. Otherwise, the value is represented as 0.

A one-layer SVM model has only the capability of distinguishing between two types of anemia, as it is a binary classifier. Because of this limitation, in this study, a four-layer SVM classifier, as illustrated in Figure 4, has been used to predict anemia, which includes four disease states and one normal state.

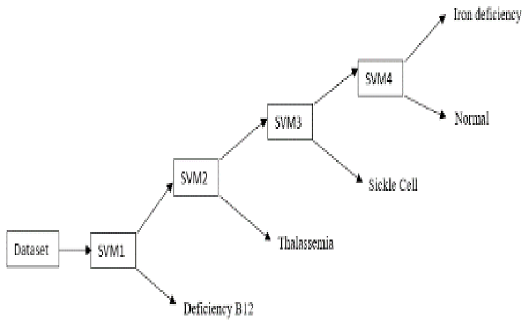

Figure 4. Four-layer SVM classifier.

The anemia dataset has been randomly split into two groups: 80% for training samples and 20% for testing samples. Before the application, the PSO algorithm has been used to determine the best combination of parameters $(c, \delta)$for each SVM based on the training samples. The testing samples have verified the effectiveness of the multi-layer SVM classifier.

An illustration of the setup of the PSO-SVM model for predicting anemia is presented in Figure 5.

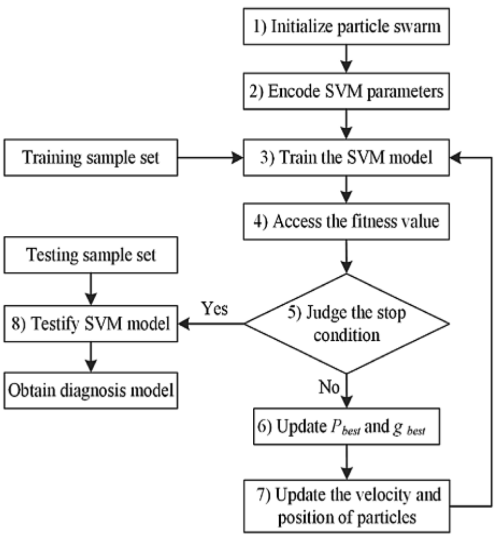

Figure 5. Flowchart of the prediction of anemia.

The results of the anemia prediction from the testing samples are presented in Table 3. Comparing the two models, the PSO-SVM exhibits a higher overall accuracy than the SVM.

5. Results and discussion

The developed PSO-SVM algorithm has intended to predict anemia outcomes based on the testing samples presented in Table 3 and Figure 6. It has greater overall accuracy than the SVM algorithm, and has been attempted to locate the blood variables of the clustered data for each type of anemia. The algorithm assesses whether the data for each anemia type is categorized precisely.

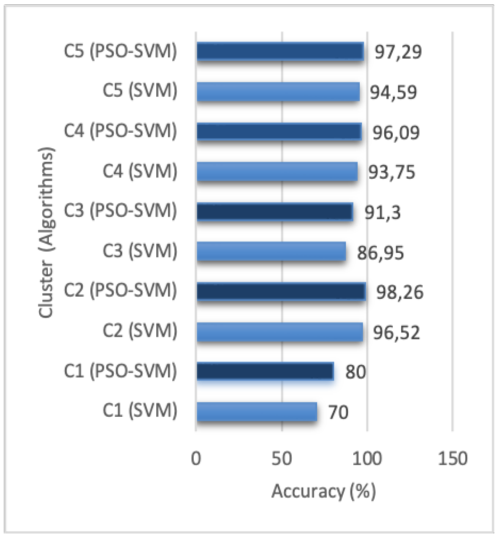

Figure 6. Comparison of the PSO-SVM and SVM algorithms by general accuracy (%).

It can be a wise move to observe the distribution of data both practically and computationally. The comparison between the computed results and the actual values has been displayed in Figures 7, 8. It is evident that the calculated results of all clusters are in agreement with the actual results.

As seen in Table 3 and Figure 6, the produced results of the PSO-SVM algorithm are generally good outperform with the results of the SVM algorithm. For example, the accuracy of the PSO-SVM and the SVM algorithms are 80% and 70% and success set 8 and 7 people for cluster 1, respectively. Similarly, in the same order, the algorithm's accuracy of the cluster 2 are 98.26% and 96.52% and success set 226 and 222 people. The two algorithms generated results of 21 and 20 individuals for Cluster 3, which is 3 lower than the actual number of 23, and so the accuracies are 91.3% and 86.95%, respectively. The success set of the algorithms in the cluster 4 are 123 and

Table 3. Comparison of the PSO-SVM and SVM algorithms by general accuracy (%)

Cluster	Algorithms	Test Set	Success Set	Fail Set	Accuracy (%)
C1	SVM	10	7	3	70
	PSO-SVM		8	2	80
C2	SVM	230	222	8	96.52
	PSO-SVM		226	4	98.26
C3	SVM	23	20	3	86.95
	PSO-SVM		21	2	91.3
C4	SVM	128	120	8	93.75
	PSO-SVM		123	5	96.09
C5	SVM	148	140	8	94.59
	PSO-SVM		144	4	97.29

120 people and the accuracies 96.09% and 93.75%. Also, for the cluster 5 the success set are 144 and 140 and the accuracies 97.29%, 94.59%, respectively.

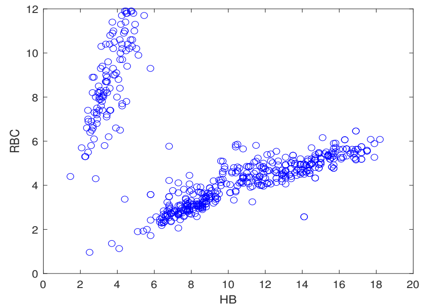

(a)

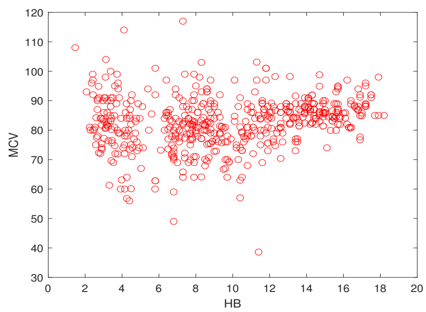

(b)

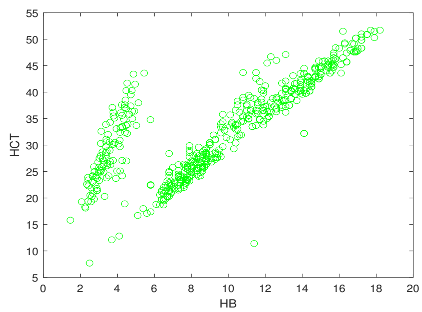

(c)

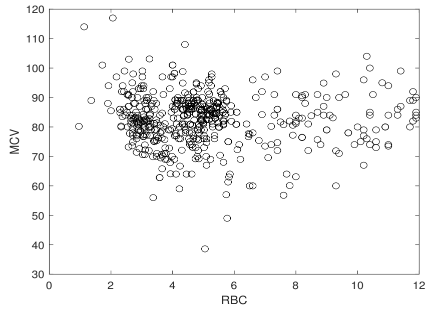

(d)

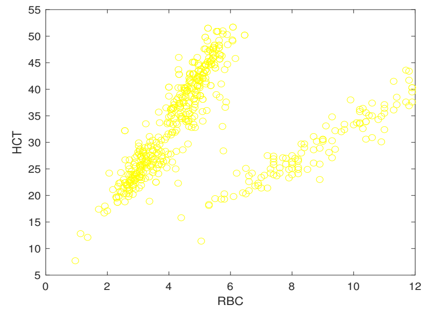

(e)

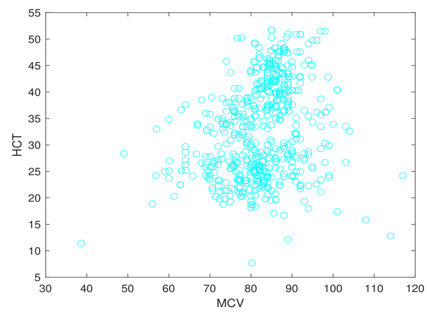

(f)

Figure 7. Five clusters (a) HB and RBC parameter, (b) HB and MCV parameter, (c) HB and HCT parameter, (d) RBC and MCV parameter, (e) RBC and HCT parameter, (f) MCV and HCT parameter of every subject without classification.

The five groups with different parameters without classification can be seen in Figure 7. On the other hand, the five groups with different parameters after classification can be seen in Figure 8.

The results of Figure 8 demonstrated that the algorithm used in the research was designed to determine the correct number of subjects in the clusters, as well as the anemia types in those clusters. By utilizing the PSO-SVM algorithm, the accuracy of the data clustering and the effects of biomedical information on the anemia types have been examined. In literature, various versions of the PSO-SVM algorithm have been developed for different issues in multiple scientific fields. In comparison to the literature, the PSO and SVM clustering algorithms have been observed to be extremely successful for their own concerns [29–31, 34–43]. This study successfully created a combined version of the algorithm, as well as its computer code.

In this study, the PSO and SVM algorithms and their combination have been used for the first time to detect anemia types. One of the most significant contributions of this study is its application of the algorithm to anemia data for the first time. It has been examined whether it would be successful in this area, like in other areas of science. The combination of the SVM and the PSO resulted in very effective outcomes in the investigation of the anemia types. This application in this field can assist clinicians in predicting the anemia types. The goal of the clustering was to distinguish the anemia types into normal or pathological classes accurately. The number of clusters for the algorithm was given by the user. Subjects were split into 5 clusters based on their blood variables. The performance of the hybrid algorithm was determined by using the blood variables to predict the anemia types. This demonstrates that the proposed algorithm has been seen to be more effective when there is a well-structured algorithm with a sufficient amount of data.

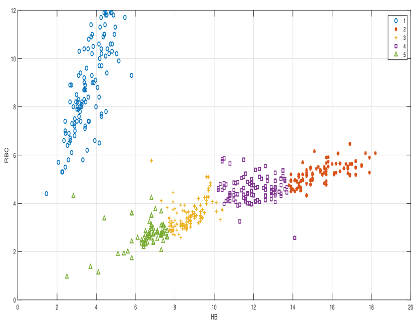

(a)

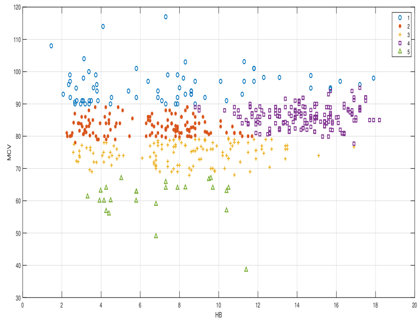

(b)

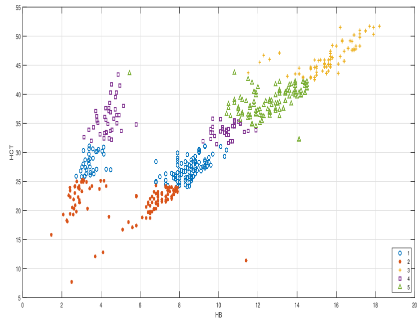

(c)

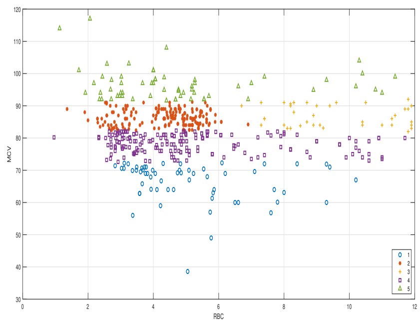

(d)

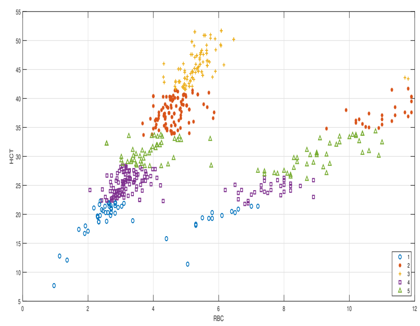

(e)

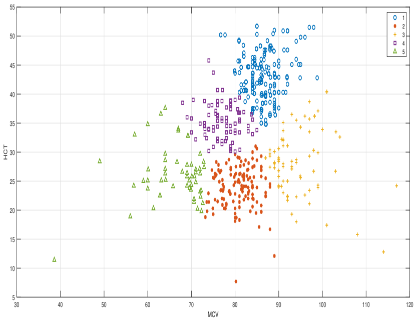

(f)

Figure 8. Five clusters (a) HB and RBC parameter, (b) HB and MCV parameter, (c) HB and HCT parameter, (d) RBC and MCV parameter, (e) RBC and HCT parameter, (f) MCV and HCT parameter of every subject with PSO-SVM.

6. Conclusions

This research has evaluated the feasibility of the PSO-SVM algorithm to predict anemia using biomedical variables. This was the first attempt to use this newly combined approach to predict anemia. The results generated by the PSO-SVM algorithm have been compared to the actual values and have been found to be highly effective in enhancing anemia predictions through biomedical factors. The findings suggest that this method could be clinically valuable for creating suitable treatment programs for patients. More clusters could be used for further research, as the current data structure is limited in terms of medical analysis point of view.

Acknowledgments

The fourth author thanks Dr Aniela Balacescu (Constantin Brancuşi University) for her hospitality throughout the conference. The authors also would like to thank the anonymous reviewers for their valuable comments.

References

[1] Janz T.G., Johnson R.L., & Rubenstein S.D. (2013). Anemia in the emergency department: evaluation and treatment. *Emergency Medicine Practice*, 15, 1-5.

[2] Ganesan J., & Saravanabavan V. (2018). Nutritional problems of anaemia disorders among the tea plantation labourers in nilgiris district–a geo medical study. *International Journal of Scientific Research in Science, Engineering and Technology*, 4, 1360-1366.

[3] WHO C. (2008). Worldwide Prevalence of Anaemia 1993–2005, WHO Global Database on Anaemia.

[4] Kern W.F. (2002). PDQ Hematology, PMPH-USA.

[5] Jiménez, C.V. (1993). Iron-deficiency anemia and thalassemia trait differentiated by simple hematological tests and serum iron concentrations. *Clinical Chemistry*, 39(11), 2271-2275.

[6] Foster, M., Nolan, R. L., & Lam, M. (2003). Prediction of anemia on unenhanced computed tomography of the thorax. *Journal-Canadian Association of Radiologists*, 54(1), 26-30.

[7] Yılmaz, Z., & Bozkurt, M.R. (2012). Determination of women iron deficiency anemia using neural networks. *Journal of Medical Systems*, 36(5), 2941-2945.

[8] Mohammed, S., Ahmad, A. A., & Sari, M., (2020). Analysis of anemia using data mining techniques with risk factors specification. *In 2020 International Conference for Emerging Technology (INCET)*, 1-5, IEEE.

[9] Ahmad, A. A., & Sari, M. (2020). Anemia prediction with multiple regression support in system medicinal internet of things. *Journal of Medical Imaging and Health Informatics*, 10(1), 261-267.

[10] Jaiswal, M., Srivastava, A., & Siddiqui, T.J. (2019). Machine learning algorithms for anemia disease prediction. *In Recent Trends in Communication, Computing, and Electronics*, Springer, Singapore, 463-469.

[11] Ahmad, A.A., & Sari, M. (2019). Parameter estimation to an anemia model using the particle swarm optimization. *Sigma: Journal of Engineering & Natural Sciences*, 37(4), 1331-1343.

[12] Ahmad, A.A., Sari, M., & Cosgun, T. (2020). A medical modelling using multiple linear regression. *In Mathematical Modelling and Optimization of Engineering Problems*, Springer, Cham, 71-87.

[13] Rivera, S. & Ganz, T. (2009). Animal models of anemia of inflammation. *In Seminars in Hematology*, 46(4), 351-357.

[14] Weiss, G. & Gasche, C. (2010). Pathogenesis and treatment of anemia in inflammatory bowel disease. *Haematologica*, 95(2), p.175.

[15] Sari, M., Ahmad, A.A. and Uslu, H. (2021). Medical model estimation with particle swarm optimization. *Communications Faculty of Sciences University of Ankara Series A1 Mathematics and Statistics*, 70(1), 468-482.

[16] Algarin, C., Nelson, C.A., Peirano, P., Westerlund, A., Reyes, S. & Lozoff, B. (2013). Iron-deficiency anemia in infancy and poorer cognitive inhibitory control at age 10 years. *Developmental Medicine & Child Neurology*, 55(5), 453-458.

[17] Aghabozorgi, S., Ying Wah, T., Herawan, T., Jalab, H.A., Shaygan, M.A. & Jalali, A. (2014). A Hybrid algorithm for clustering of time series data based on affinity search technique. *The Scientific World Journal*, Article ID 562194.

[18] Liv, C., Zhang, C., Lian, K., Ren, Y. & Meng, L. (2020). A Hybrid Algorithm for the Static Bike-Sharing Re-Positioning Problem Based on an Effective Clustering Strategy. *Transportation Research Part B: Methodological*, 140, p.1-21.

[19] Farnad, B., Jafarian, A. & Baleanu, D. (2018). A new hybrid algorithm for continuous optimization problem. *Applied Mathematical Modelling*, 55, 652-673.

[20] Taheri, G., Khonsari, A., Entezari-Maleki, R. & Sousa, L. (2020). A hybrid algorithm for task scheduling on heterogeneous multiprocessor embedded systems. *Applied Soft Computing*, 91, p.106202.

[21] Karimov, J. & Ozbayoglu, M. (2015). High quality clustering of big data and solving empty-clustering problem with an evolutionary hybrid algorithm. *In 2015 IEEE International Conference on Big Data (Big Data)*, 1473-1478, IEEE.

[22] Wahyono, I.D., Asfani, K., Mohamad, M.M., Rosyid, H.A. & Afandi, A.N. (2020). New hybrid algorithm implementation on spread wireless sensor to determine the point of fire in the building. *In 2020 7th International Conference on Information Technology, Computer, and Electrical Engineering (ICITACEE)*, 110-114, IEEE.

[23] Luo, Y., Pan, Y., Li, C. & Tang, H. (2020). A hybrid algorithm combining genetic algorithm and variable neighborhood search for process sequencing optimization of large-size problem. *International Journal of Computer Integrated Manufacturing*, 33(10-11), 962-981.

[24] Ahlawat, A. & Suri, B. (2016). Improving classification in data mining using hybrid algorithm. *In 2016 1st India International Conference on Information Processing (IICIP)*, 1-4, IEEE.

[25] Liu, X., & Fu, H. (2014). PSO-based support vector machine with cuckoo search technique for clinical disease diagnoses. *The Scientific World Journal*, Article ID 548483.

[26] Kennedy, J., & Eberhart, R. (1995). Particle swarm optimization. *In Proceedings of IEEE International Conference on Neural Networks*, 4, 1942-1948, IEEE.

[27] Soliman, O.S., & Aboelhamd, E. (2014). Classification of diabetes mellitus using modified particle swarm optimization and least squares support vector machine. *arXiv preprint arXiv:1405.0549.*

[28] Sari, M., Tuna, C., & Akogul, S. (2018). Prediction of tibial rotation pathologies using particle swarm optimization and K-means algorithms. *Journal of Clinical Medicine*, 7(4), 65.

[29] Kennedy, J. (2011). *Particle Swarm Optimization.* In Encyclopedia of Machine Learning, Springer: New York, NY, USA, 760–766.

[30] Alzaidi, K.M.S., Bayat, O. & Uçan, O.N. (2018). A heuristic approach for optimal planning and operation of distribution systems. *Journal of Optimization*, 2018.

[31] Bai, Q. (2010). Analysis of particle swarm optimization algorithm. *Computer and Information Science*, 3(1), 180.

[32] Burges, C.J. (1998). A tutorial on support vector machines for pattern recognition. *Data Mining and Knowledge Discovery*, 2(2), 121-167.

[33] Hearst, M.A., Dumais, S.T., Osuna, E., Platt, J. & Scholkopf, B. (1998). Support vector machines. *IEEE Intelligent Systems and Their Applications*, 13(4), 18-28.

[34] Cohen, S.C.M., & De Castro, L.N. (2006). Data clustering with particle swarms. *In Proceedings of the IEEE Congress on Evolutionary Computation (CEC 2006)*, Vancouver, BC, Canada, 1792–1798.

[35] Sarkar, S., Roy, A., & Purkayastha, B.S. (2013). Application of particle swarm optimization in data clustering: a survey. *International Journal of Computer Applications*, 65(25), 38-46.

[36] Mane, S. U., & Gaikwad, P.G. (2014). Hybrid particle swarm optimization (HPSO) for data clustering. *International Journal of Computer Applications*, 97(19).

[37] Ramyachitra, D., Sofia, M., & Manikandan, P. (2015). Interval-value based particle swarm optimization algorithm for cancer-type specific gene selection and sample classification. *Genomics Data*, 5, 46-50.

[38] Latchoumi, T.P., Ezhilarasi, T.P., & Balamurugan, K. (2019). Bio-inspired weighed quantum particle swarm optimization and smooth support vector machine ensembles for identification of abnormalities in medical data. *SN Applied Sciences*, 1(10), 1-10.

[39] Altinoz, O.T. (2018). Multiobjective PID controller design for active suspension system: scalarization approach. *An International Journal of Optimization and Control: Theories & Applications (IJOCTA)*, 8(2), 183-194.

[40] Wei-Jia, L., Liang, M. & Hao, C. (2017). Particle swarm optimisation-support vector machine optimised by association rules for detecting factors inducing heart diseases. *Journal of Intelligent Systems*, 26(3), 573-583.

[41] Yin, R., Li, Q., Li, P. & Lu, D. (2020). A novel method for matching reservoir parameters based on particle swarm optimization and support vector machine. *Mathematical Problems in Engineering*, 2020, 7542792.

[42] Erguzel, T.T. (2015). A hybrid PSO-PID approach for trajectory tracking application of a liquid level control process. *An International Journal of Optimization and Control: Theories & Applications (IJOCTA)*, 5(2), 63-73.

[43] Gong, C., Chen, H., He, W. & Zhang, Z. (2017). Improved multi-objective clustering algorithm using particle swarm optimization. *PloS One*, 12(12), p.e0188815.

Arshed A. Ahmad *born in Iraq in 1980. He is an Assistant Professor at the University of Diyala,*

Iraq. He received a Ph.D. degree from Yildiz Technical University in 2020. His research interests include mathematical modeling, applied mathematics, numerical analysis, and probability and statistics. He is the author of more than 14 research papers since 2008.
https://orcid.org/0000-0003-1393-1253

Khalid M. Saffer *born in Iraq in 1971. He is a lecturer at the University of Diyala, Iraq. He received a Ph.D. degree from Altinbas University in 2018. His research interests include optimization algorithms, information technology, image processing, information security, and database systems design and implementation. He is the author of more than 12 research papers since 2011.*
https://orcid.org/0000-0001-8670-4161

Murat Sari *is a Professor of the Department of Mathematical Engineering at Istanbul Technical University. He completed his Ph.D. in Mathematics from the University of South Wales, UK, in 2000. His current research interests include artificial intelligence modeling, simulation and computational methods, computational fluid dynamics, modeling of nonlinear behaviors, economical modeling, and biomechanical/biomedical modeling. He has about 100 high-quality scientific papers, over 50 conference proceedings, and has written various chapters in some books. He is a reviewer/editor for some international high-quality journals.*
https://orcid.org/0000-0003-0508-2917

Hande Uslu *is a Research Assistant in the Department of Mathematics at Yildiz Technical University, Istanbul, Turkey since 2017. She received her B.Sc degree in Mathematics from Bogazici University in 2015, and MSc degree in Applied Mathematics from Yildiz Technical University, in 2018. She is currently pursuing her Ph.D. studies in the thesis period in the Department of Mathematics at Yildiz Technical University. Her research interests are mathematical modeling, simulation techniques, stochastic processes, and artificial intelligence. She has six scientific papers and more than fifteen conference proceedings.*
https://orcid.org/0000-0002-1642-1120

An International Journal of Optimization and Control: Theories & Applications (http://www.ijocta.org)

An International Journal of Optimization and Control: Theories & Applications
ISSN:2146-0957 eISSN:2146-5703
Vol.13, No.2, pp.224-235 (2023)
http://doi.org/10.11121/ijocta.2023.1278

RESEARCH ARTICLE

Existence and stability analysis to the sequential coupled hybrid system of fractional differential equations with two different fractional derivatives

Mohamed Houas,[a] Jehad Alzabut,[b,c] Mahammad Khuddush[d*]

[a] *Laboratory FIMA, UDBKM, Khemis Miliana University, Algeria*
[b] *Department of Mathematics and Sciences, Prince Sultan University, 11586 Riyadh, Saudi Arabia*
[c] *Department of Industrial Engineering, OSTİM Technical University, Ankara 06374, Türkiye*
[d] *Department of Mathematics, Dr. Lankapalli Bullayya College of Engineering, Resapuvanipalem, Visakhapatnam, 530013, Andhra Pradesh, India*
m.houas.st@univ-dbkm.dz, jalzabut@psu.edu.sa, jehad.alzabut@ostimteknik.edu.tr, khuddush89@gmail.com

ARTICLE INFO

Article History:
Received 12 June 2022
Accepted 8 February 2023
Available 29 July 2023

Keywords:
Coupled systems
Hybrid differential equations
Boundary value problem
Fractional derivative
Ulam-Hyers stability

AMS Classification 2010:
26A33; 34A08; 47H10

ABSTRACT

In this paper, we discussed the existence, uniqueness and Ulam-type stability of solutions for sequential coupled hybrid fractional differential equations with two derivatives. The uniqueness of solutions is established by means of Banach's contraction mapping principle, while the existence of solutions is derived from Leray-Schauder's alternative fixed point theorem. Further, the Ulam-type stability of the addressed problem is studied. Finally, an example is provided to check the validity of our obtained results.

1. Introduction

Differential equations are essential for a mathematical description of Nature. Many of the general laws of Nature–in physics, chemistry, biology, economics, and engineering find their most natural expression in the language of differential equation. Differential equation (DE) allows us to study all kinds of evolutionary processes with the properties of finite-dimensionality and differentiability. Derivative of arbitrary order arises from many physical processes, such as a charge transport in amorphous semiconductors, electrochemistry and material science, where they are described by differential equations of arbitrary order, see [1–4]. Recently, many researchers have exposed attention in the field of fractional differential equations theory, which will be used to describe phenomena of real-world problems. For more details; we refer the reader to the papers [5–18]. On the other hand, hybrid differential equations have gained extensive attention from many scholars; see for example [19–21]. Hybrid differential equations and coupled hybrid systems involving fractional derivatives have also been investigated by scientific researchers; see for instance [22–28] and the references cited therein. In recent years, sequential fractional hybrid differential equations have been studied by several researchers [29–34]. On the other hand, the stability of solutions of differential equations is important in physical problems because if slight deviations from the mathematical model caused by unavoidable errors in measurement do not have a correspondingly slight effect on the solution, the mathematical equations describing the problem will not accurately predict the future outcome.

*Corresponding Author

For example, one of the difficulties in predicting population growth is the fact that it is governed by the equation $w(t) = ce^{at}$, which is an unstable solution of the equation $w'(t) = aw(t)$. Even if there are no unfavourable factors, very few inaccuracies in the initial population count (c) or breeding rate (a) will result in fairly significant errors in prediction. One of the interesting subjects in this area, is the investigation of the existence and stability of solutions, because the study of the existence of solution of the fractional differential equation(FDE) became important due to the lack of a general formula for solving nonlinear FDEs, see [29, 30, 32, 33]. Recently, Some scholars have discussed the existence, uniqueness, and different types of Ulam stability of solutions of fractional sequential hybrid differential equations [29,32,33] and the references cited therein. The classical form of hybrid differential equation [35] is given by the following differential equation

$$\begin{cases} \dfrac{d}{dt}\left[\dfrac{w(t)}{\psi(t, w(t))}\right] = \varphi(t, w(t)), \ 0 \le t \le T, \\ \qquad\qquad w(t_0) = \quad w_0, \ w_0 \in \mathbb{R}, \end{cases}$$

where $\psi \in C([0,T] \times \mathbb{R}, \mathbb{R} - \{0\})$ and $\varphi \in C([0,T] \times \mathbb{R} \to \mathbb{R})$. Many scientific researchers have studied different fractional types of the above hybrid differential equation. For example in [36], the authors have discussed the fractional hybrid differential equations involving Riemann-Liouville differential operators

$$\begin{cases} {}^{\mathtt{RL}}\mathtt{D}\left[\dfrac{w(t)}{\psi(t, w(t))}\right] = \varphi(t, w(t)), \ 0 \le t \le T, \\ \qquad\qquad w(0) = \quad 0, \end{cases}$$

where $0 << 1$, $\psi \in C([0,T] \times \mathbb{R}, \mathbb{R} - \{0\})$ and $\varphi \in C([0,T] \times \mathbb{R}, \mathbb{R})$.

In [37], the authors studied the existence and uniqueness of solutions of coupled hybrid fractional differential equations described by

$$\begin{cases} {}^{\mathtt{C}}\mathtt{D}\left[\dfrac{w(t)}{\psi_1(t, w(t), z(t))}\right] = \varphi(t, w(t), z(t)), \\ {}^{\mathtt{C}}\mathtt{D}\left[\dfrac{z(t)}{\psi_2(t, w(t), z(t))}\right] = \phi(t, w(t), z(t)), \\ w(0) = w(1) = 0, \quad z(0) = z(1) = 0, \end{cases}$$

where $t \in [0,1], 1 <\le 2, 1 <\le 2$, $\psi_j \in C([0,1] \times \mathbb{R}, \mathbb{R} - \{0\}), j = 1,2$ and $\varphi, \phi \in C([0,1] \times \mathbb{R}, \mathbb{R})$. The existence and uniqueness results were obtained by applying Leray-Schauder's alternative criterion and Banach's contraction mapping principle.

Motivated by above-mentioned works, in this paper, we discuss the existence, uniqueness and Ulam-Hyers-Rassias stability of solution for sequential coupled fractional hybrid system of the following form

$$\begin{cases} {}^{\mathtt{RL}}\mathtt{D}\left[{}^{\mathtt{C}}\mathtt{D}\left[\dfrac{w(t)}{\psi_1(t, w(t), z(t))}\right]\right] \\ \qquad = \displaystyle\sum_{i=1}^{k} \varphi_i(t, w(t), z(t)), \\ {}^{\mathtt{RL}}\mathtt{D}\left[{}^{\mathtt{C}}\mathtt{D}\left[\dfrac{z(t)}{\psi_2(t, w(t), z(t))}\right]\right] \\ \qquad = \displaystyle\sum_{i=1}^{k} \phi_i(t, w(t), z(t)), \\ w(0) = w(1) = 0, \ z(0) = z(1) = 0, \end{cases} \tag{1}$$

where $0 \le t \le 1, 0 <, < 1, + > 1, 0 <, < 1, + > 1$, ${}^{\mathtt{RL}}\mathtt{D}, \in \{,\}$ and ${}^{\mathtt{C}}\mathtt{D}, \in \{,\}$ are the Riemann-Liouville and Caputo fractional derivatives respectively, $\psi_j : [0,1] \times \mathbb{R}^2 \to \mathbb{R} - \{0\}, j = 1,2$ and $\varphi_i, \phi_i : [0,1] \times \mathbb{R}^2 \to \mathbb{R}, 1 \le i \le k$, are continuous functions.

We impose the following hypotheses throughout the paper:

- (H_1) For each $i = 1,2,...,k$, the functions $\varphi_i, \phi_i : [0,1] \times \mathbb{R}^2 \to \mathbb{R}$ are continuous and there exist constants $\pi_i > 0, \vartheta_i > 0$ such that for all $t \in [0,1]$ and $(w_1, z_1), (w_2, z_2) \in \mathbb{R}^2 \to \mathbb{R}$ are continuous and there exist constants $\pi_i > 0, \vartheta_i > 0$ such that for all $t \in [0,1]$ and $(w_1, z_1), (w_2, z_2) \in \mathbb{R}^2$,
$$|\varphi_i(t, w_1, z_1) - \varphi_i(t, w_2, z_2)| \le \pi_i(|w_1 - z_1| + |w_2 - z_2|),$$
and
$$|\phi_i(t, w_1, z_1) - \phi_i(t, w_2, z_2)| \le \vartheta_i(|w_1 - z_1| + |w_2 - z_2|)$$
for $i = 1, 2, \cdots, k$,
- (H_2) For all $j = 1,2$, the functions $\psi_j : [0,1] \times \mathbb{R}^2 \to \mathbb{R} - \{0\}$ are continuous and there exist constants $\Pi_j > 0$ such that
$$\psi_1(t, w, z) \le \Pi_1 \text{ and } \psi_2(t, w, z) \le \Pi_2,$$
for each $t \in [0,1]$ and $(w, z) \in \mathbb{R}^2$.
- (H_3) For each $i = 1,2,...,k$, the functions $\varphi_i, \phi_i : [0,1] \times \mathbb{R}^2 \to \mathbb{R}$ are continuous and

there exist constants $\gamma_i, \omega_i, \gamma_i^{'}, \omega_i^{'} \geq 0$ and $\lambda_i > 0, \lambda_i^{'} > 0$ such that for all $t \in J$ and $w, z \in \mathbb{R}$, we have

$\varphi_i(t, w, z) \leq \lambda_i + \gamma_i |w| + \omega_i |z|$,

and

$\phi_i(t, w, z) \leq \lambda_i^{'} + \gamma_i^{'} |w| + \omega_i^{'} |z|$.

The rest of the paper is organized in the following fashion. In Section 2, we introduce some basic definitions and lemmas which are useful in our main results. In Section 3, we establish a criteria for the existence and uniqueness of solutions to the boundary value problem (1) by applying the Leray-Schauder's alternative fixed point theorem and the Banach's contraction mapping principle in a Banach space. In section 4, we study Ulam-Hyers-Rassias stability of solutions to the problem (1). Finally, as an application, we demonstrate our results with example.

2. Preliminaries

In this section, we introduce some basic definitions and lemmas which are useful for our later discussions.

Definition 1. *[38] The Riemann-Liouville fractional integral of order > 0 for a function $f : (0,\infty) \to \mathbb{R}$ is defined as*

$$\mathtt{I}^{f}(t) = \frac{1}{\Gamma()} \int_0^t (t-s)^{-1} f(s) ds,$$

provided that the right side is pointwise defined on $(0,\infty)$.

Definition 2. *[38] The Riemann-Liouville fractional derivative of order > 0 for a continuous function $f : (0,\infty) \to \mathbb{R}$ is defined as*

$$\mathtt{D}^{f}(t) = \frac{1}{\Gamma(m-)} \left(\frac{d}{dt}\right)^m \int_0^t \frac{f(s)}{(t-s)^{-m-1}} ds,$$

where $m = [] + 1$, provided that the right side is pointwise defined on $(0,\infty)$.

Definition 3. *[38] For a function f given on the interval $[0,\infty)$, The Caputo derivative of fractional order γ for the function f continuous on $[0,\infty)$ is defined as*

$${}^{\mathtt{C}}\mathtt{D}^{f}(t) = \frac{1}{\Gamma(m-)} \int_0^t (t-s)^{m--1} f^{(m)}(s) ds,$$

$m = [] + 1$.

Lemma 1. *[12] Let $, > 0$ and $h \in L^1([0,1])$. Then $\mathtt{I}\mathtt{I}h(t) = \mathtt{I}^{+}h(t)$ and ${}^{\mathtt{RL}}\mathtt{D}\mathtt{I}h(t) = h(t)$.*

Lemma 2. *[12] Let $>> 0$ and $h \in L^1([0,1])$. Then ${}^{\mathtt{RL}}\mathtt{D}\mathtt{I}h(t) = \mathtt{I}^{-}h(t)$.*

Lemma 3. *[12] Let > 0. Then for $w \in C(0,1) \cap L^1(0,1)$ and ${}^{\mathtt{RL}}\mathtt{D}w \in C(0,1) \cap L^1(0,1)$, we have*

$$\mathtt{I}^{\mathtt{RL}}\mathtt{D}w(t) = w(t) + c_1 t^{-1} + c_2 t^{-2} + \cdots + c_n t^{-n},$$

where $c_i \in \mathbb{R}, i = 1, 2, ..., n,\ n = [] + 1$.

Lemma 4. *[12] Let > 0. Then*

$$\mathtt{I}\left[{}^{\mathtt{C}}\mathtt{D}w(t)\right] = w(t) + c_0 + c_1 t, + c_2 t^2 + ... + c_{n-1} t^{n-1},$$

for some $c_i \in \mathbb{R}, i = 0, 1, 2, ..., n-1, n-1 << n$.

Lemma 5. *For $g, h \in C([0,1], \mathbb{R})$ and $\psi_j \in C(([0,1] \times \mathbb{R}^2, \mathbb{R} - \{0\}), j = 1, 2$, the boundary value problem*

$$\begin{cases} {}^{\mathtt{RL}}\mathtt{D}\left[{}^{\mathtt{C}}\mathtt{D}\left[\dfrac{w(t)}{\psi_1(t, w(t), z(t))}\right]\right] = g(t), \\ {}^{\mathtt{RL}}\mathtt{D}\left[{}^{\mathtt{C}}\mathtt{D}\left[\dfrac{z(t)}{\psi_2(t, w(t), z(t))}\right]\right] = h(t), \\ w(0) = w(1) = 0, \quad z(0) = z(1) = 0, \end{cases} \tag{2}$$

where $0 \leq t \leq 1$, $0 <, < 1$, $+ > 1$, $0 <, < 1$, $+ > 1$, has a unique solution

$$w(t) = \psi_1(t, w(t), z(t)) \Bigg[\int_0^t \frac{(t-s)^{+-1}}{\Gamma(+)} g(s) ds - t^{+-1} \int_0^1 \frac{(1-s)^{+-1}}{\Gamma(+)} g(s) ds\Bigg], \tag{3}$$

and

$$z(t) = \psi_2(t, w(t), z(t)) \Bigg[\int_0^t \frac{(t-s)^{+-1}}{\Gamma(+)} g(s) ds - t^{+-1} \int_0^1 \frac{(1-s)^{+-1}}{\Gamma(+)} g(s) ds\Bigg]. \tag{4}$$

Proof. Using Lemma 3, we can write

$$\frac{w(t)}{\psi_1(t, w(t), z(t))} = \mathtt{I}g(t) + a_1 t^{-1},$$
$$\frac{z(t)}{\psi_2(t, w(t), z(t))} = \mathtt{I}h(t) + b_1 t^{-1},$$

where $a_1, b_1 \in \mathbb{R}$. Now by Lemma 4, we have

$$
\begin{aligned}
w(t) = \psi_1(t, w(t), z(t)) \Big[& \mathtt{I}^{+} g(t) \\
& + \frac{a_1 \Gamma()}{\Gamma(+)} t^{+-1} + a_2 \Big],
\end{aligned} \tag{5}
$$

$$
\begin{aligned}
z(t) = \psi_2(t, w(t), z(t)) \Big[& \mathtt{I}^{+} h(t) \\
& + \frac{b_1 \Gamma()}{\Gamma(+)} t^{+-1} + b_2 \Big],
\end{aligned} \tag{6}
$$

where $a_2, b_2 \in \mathbb{R}$. Using boundary conditions $w(0) = w(1) = z(0) = z(1) = 0$, we obtain $a_2 = b_2 = 0$,

$$
a_1 = -\frac{\Gamma(+)}{\Gamma()} \int_0^1 (1-s)^{+-1} g(s)\, ds,
$$

and

$$
b_1 = -\frac{\Gamma(+)}{\Gamma()} \int_0^1 (1-s)^{+-1} h(s)\, ds.
$$

Substituting the values of $a_j, b_j, j = 1, 2$ in (5) and (6), we get (3) and (4). □

3. Existence and uniqueness of solutions to the sequential coupled hybrid system

We will use the standard fixed point theorems, to study the fractional hybrid system (1). In this regard, we define the space

$$
\mathtt{W} \times \mathtt{Z} = \{(w, z) : w, z \in C([0,1], \mathbb{R})\},
$$

endowed with the norm $\|(w,z)\|_{\mathtt{W}\times\mathtt{Z}} = \|w\| + \|z\|$, where $\|w\| = \sup\{|w(t)| : t \in [0,1]\}$. It is clear that $(\mathtt{W} \times \mathtt{Z}, \|.\|_{\mathtt{W}\times\mathtt{Z}})$ is a Banach space. Define an operator $\mathtt{O} : \mathtt{W} \times \mathtt{Z} \to \mathtt{W} \times \mathtt{Z}$ by

$$
\mathtt{O}(w,z)(t) = (\mathtt{O}_1(w,z)(t),\ \mathtt{O}_2(w,z)(t)),\ t \in [0,1],
$$

where

$$
\mathtt{O}_1(w,z)(t) = \psi_1(t, w(t), z(t))\, \mathfrak{N}_1(t), \tag{7}
$$

in which

$$
\begin{aligned}
\mathfrak{N}_1(t) = & \sum_{i=1}^{k} \int_0^t \frac{(t-s)^{+-1}}{\Gamma(+)} \varphi_i(s, w(s), z(s))\, ds \\
& - \sum_{i=1}^{k} \int_0^1 \frac{[t(1-s)]^{+-1}}{\Gamma(+)} \varphi_i(s, w(s), z(s))\, ds,
\end{aligned}
$$

and

$$
\mathtt{O}_2(w,z)(t) = \psi_2(t, w(t), z(t))\, \mathfrak{N}_2(t), \tag{8}
$$

in which

$$
\begin{aligned}
\mathfrak{N}_2(t) = & \sum_{i=1}^{k} \int_0^t \frac{(t-s)^{+-1}}{\Gamma(+)} \phi_i(s, w(s), z(s))\, ds \\
& - \sum_{i=1}^{k} \int_0^1 \frac{[t(1-s)]^{+-1}}{\Gamma(+)} \phi_i(s, w(s), z(s))\, ds \Big].
\end{aligned}
$$

Now, we prove the existence of solutions of the fractional hybrid system (1) by applying Leray-Schauder nonlinear alternative [39].

Lemma 6. *(Leray-Schauder alternative). Let $F : E \to E$ be a completely continuous operator (i.e.,a map that restricted to any bounded set in E is compact). Let*

$$
(F) = \{u \in E : u = \lambda F(u) \ \textit{for some}\ 0 < \lambda < 1\}.
$$

Then either the set (F) is unbounded, or F has at least one fixed point.

Theorem 1. *Assume that hypotheses $(H_j)_{j=2,3}$ are satisfied. Furthermore, assume that*

$$
\sum_{i=1}^{k} \left(\frac{\Pi_1 \gamma_i}{\Gamma(++1)} + \frac{\Pi_2 \gamma_i'}{\Gamma(++1)} \right) < \frac{1}{2},
$$

and

$$
\sum_{i=1}^{k} \left(\frac{\Pi_1 \omega_i}{\Gamma(++1)} + \frac{\Pi_2 \omega_i'}{\Gamma(++1)} \right) < \frac{1}{2}.
$$

Then the system (1) has at least one solution on $[0,1]$.

Proof. In the first step, we show that the operator $\mathtt{O} : \mathtt{W} \times \mathtt{Z} \to \mathtt{W} \times \mathtt{Z}$ is completely continuous. By continuity of the functions $\psi_j, \varphi_i, \phi_i, j = 1, 2, i = 1, 2, ..., k$, it follows that the operator $\mathtt{O}$ is continuous.

Let $\Sigma \subset \mathtt{W} \times \mathtt{Z}$ be bounded. Then we can find positive constants $A_i, B_i, i = 1, 2, ..., k$ such that

$$
|\varphi_i(t, w(t), z(t))| \le A_i, |\varphi_i(t, w(t), z(t))| \le B_i
$$

for all $(w,z) \in \Sigma$. Then for any $(w,z) \in \Sigma$ we have

$$
\begin{aligned}
& \|\mathtt{O}_1(w,z)\| \\
& \le \Pi_1 \Big[\frac{1}{\Gamma(+)} \sum_{i=1}^{k} \int_0^t (t-s)^{+-1} |\varphi_i(s, w(s), z(s))|\, ds \\
& \quad + \frac{t^{+-1}}{\Gamma(+)} \sum_{i=1}^{k} \int_0^1 (1-s)^{+-1} |\varphi_i(s, w(s), z(s))|\, ds \Big] \\
& \le \sum_{i=1}^{k} \frac{2 \Pi_1 A_i}{\Gamma(++1)},
\end{aligned}
$$

which yields

$$\|\mathtt{O}_1(w,z)\| \leq \sum_{i=1}^{k} \frac{2\Pi_1 A_i}{\Gamma(+ + 1)} < +\infty. \tag{9}$$

Also,

$$\|\mathtt{O}_2(w,z)\| \leq \sum_{i=1}^{k} \frac{2\Pi_2 B_i}{\Gamma(+ + 1)} < +\infty. \tag{10}$$

Hence, by (9) and (10), we deduce that the operator $\mathtt{O}$ is uniformly bounded.

Next, we show that $\mathtt{O}$ is equicontinuous. For all $0 \leq t_2 < t_1 \leq 1$, we have

$$\begin{aligned}&\left|\mathtt{O}_1(w,z)(t_1) - \mathtt{O}_1(w,z)(t_2)\right| \\ &\leq \sum_{i=1}^{k} \frac{\Pi_1 A_i}{\Gamma(+ + 1)}\Big(\left[(t_1 - t_2)^{+} + \left|t_1^{+} - t_2^{+}\right|\right] \\ &\quad + \left|t_1^{+-1} - t_2^{+-1}\right|\Big),\end{aligned} \tag{11}$$

and

$$\begin{aligned}&\left|\mathtt{O}_2(w,z)(t_1) - \mathtt{O}_2(w,z)(t_2)\right| \\ &\leq \sum_{i=1}^{k} \frac{\Pi_2 B_i}{\Gamma(+ + 1)}\Big(\Big[(t_1 - t_2)^{+} + \left|t_1^{+} - t_2^{+}\right|\Big] \\ &\quad + \left|t_1^{+-1} - t_2^{+-1}\right|\Big).\end{aligned} \tag{12}$$

From (11) and (12), $\|\mathtt{O}(w,z)(t_1) - \mathtt{O}(w,z)(t_2)\|_{\mathtt{W}\times\mathtt{Z}} \to 0$ as $t_2 \to t_1$. Thus, by using the Arzela-Ascoli theorem one can conclude that the operator $\mathtt{O} : \mathtt{W}\times\mathtt{Z} \to \mathtt{W}\times\mathtt{Z}$ is completely continuous.

Finally, it will be verified that the set

$$\Psi = \Big\{ (w,z) \in \mathtt{W}\times\mathtt{Z}, (w,z) = \mathtt{O}(w,z), 0 \leq \leq 1\Big\}$$

is bounded. Let $(w,z) \in \Psi$. Then, for each $t \in [0,1]$, we can write

$$w(t) = \mathtt{O}_1(w,z)(t) \quad \text{and} \quad z(t) = \mathtt{O}_2(w,z)(t).$$

Then, we have

$$|w(t)| \quad \leq \quad \Pi_1|\mathfrak{N}_1(t)|,$$

and

$$|z(t)| \quad \leq \quad \Pi_2|\mathfrak{N}_2(t)|.$$

From (H_3), we obtain

$$|w(t)| \leq \frac{2\Pi_1}{\Gamma(+ + 1)}\left(\lambda_0 + \lambda_1|w(t)| + \lambda_2|z(t)|\right),$$

and

$$|z(t)| \leq \frac{2\Pi_2}{\Gamma(+ + 1)}\left(\gamma_0 + \gamma_1|w(t)| + \gamma_2|z(t)|\right).$$

Hence, we have

$$\|w\| \leq \sum_{i=1}^{k} \frac{2\Pi_1}{\Gamma(+ + 1)}\left(\lambda_i + \gamma_i\|w\| + \omega_i\|z\|\right),$$

and

$$\|z\| \leq \sum_{i=1}^{k} \frac{2\Pi_2}{\Gamma(+ + 1)}\left(\lambda_i' + \gamma_i'\|w\| + \omega_i'\|z\|\right),$$

which imply that

$$\begin{aligned}&\|w\| + \|z\| \\ &\leq \sum_{i=1}^{k} \frac{2\Pi_1}{\Gamma(+ + 1)}\lambda_i + \sum_{i=1}^{k} \frac{2\Pi_2}{\Gamma(+ + 1)}\lambda_i' \\ &+ \left(\sum_{i=1}^{k} \frac{2\Pi_1}{\Gamma(+ + 1)}\gamma_i + \sum_{i=1}^{k} \frac{2\Pi_2}{\Gamma(+ + 1)}\gamma_i'\right)\|w\| \\ &+ \left(\sum_{i=1}^{k} \frac{2\Pi_1}{\Gamma(+ + 1)}\omega_i + \sum_{i=1}^{k} \frac{2\Pi_2}{\Gamma(+ + 1)}\omega_i'\right)\|z\|.\end{aligned}$$

Consequently,

$$\begin{aligned}\|(w,z)\|_{\mathtt{W}\times\mathtt{Z}} \leq \frac{1}{G}\Big[&\sum_{i=1}^{k} \frac{2\Pi_1}{\Gamma(+ + 1)}\lambda_i \\ &+ \sum_{i=1}^{k} \frac{2\Pi_2}{\Gamma(+ + 1)}\lambda_i'\Big],\end{aligned}$$

for all $t \in [0,1]$, where $G = \min\{\mathfrak{d}_1, \mathfrak{d}_2\}$, in which

$$\mathfrak{d}_1 = 1 - \left(\sum_{i=1}^{k} \frac{2\Pi_1}{\Gamma(+ + 1)}\gamma_i + \sum_{i=1}^{k} \frac{2\Pi_2}{\Gamma(+ + 1)}\gamma_i'\right),$$

and

$$\mathfrak{d}_2 = 1 - \left(\sum_{i=1}^{k} \frac{2\Pi_1}{\Gamma(+ + 1)}\omega_i + \sum_{i=1}^{k} \frac{2\Pi_2}{\Gamma(+ + 1)}\omega_i'\right).$$

This shows that the set Ψ is bounded. Hence all the conditions of Lemma 6 are satisfied and consequently the operator $\mathtt{O}$ has at least one fixed point, which corresponds to a solution of the system (1). This completes the proof. □

In the next result, we establish the existence of uniqueness solutions to the fractional hybrid system (1) by using Banach's fixed point theorem.

Theorem 2. *Assume that $(H_j)_{j=1,2}$ hold and that*

$$\begin{aligned}&\sum_{i=1}^{k} \frac{\pi_i}{\Gamma(+ + 1)} < \frac{1}{4\Pi_1}, i = 1,2,\cdots,k, \\ &\sum_{i=1}^{k} \frac{\vartheta_i}{\Gamma(+ + 1)} < \frac{1}{4\Pi_2}, i = 1,2,\cdots,k.\end{aligned} \tag{13}$$

Then the problem (1) *has a unique solution on* $[0,1]$.

Proof. Define $\sup_{t\in[0,1]}|\varphi_i(t,0,0)| = \Lambda_i < \infty$ and $\sup_{t\in[0,1]}|\phi_i(t,0,0)| = \nabla_i < \infty$, $i = 1,2,...,k$ such that $\max\{\wp_1, \wp_2\} \leq, i = 1,2,...,k$, where

$$\wp_1 = \sum_{i=1}^{k} \frac{\Pi_1 \Lambda_i}{\Gamma(+ + 1)} \left[\frac{1}{4} - \sum_{i=1}^{k} \frac{\Pi_1 \pi_i}{\Gamma(+ + 1)} \right]^{-1},$$

and

$$\wp_2 = \sum_{i=1}^{k} \frac{\Pi_2 \nabla_i}{\Gamma(+ + 1)} \left[\frac{1}{4} - \sum_{i=1}^{k} \frac{\Pi_2 \vartheta_i}{\Gamma(+ + 1)} \right]^{-1}.$$

Firstly, we show that $\mathtt{OB} \subset \mathtt{B}$, where $\mathtt{B} = \left\{ (w, z) \in \mathtt{W} \times \mathtt{Z} : \|(w, z)\|_{\mathtt{W}\times\mathtt{Z}} \leq \right\}$. For all $(w, z) \in \mathtt{B}$ and $t \in [0, 1]$, we have

$$\begin{aligned} &|\varphi_i(t, w(t), z(t))| \\ &\leq |\varphi_i(t, w(t), z(t)) - \varphi_i(t, 0, 0)| + |\varphi_i(t, 0, 0)| \\ &\leq \pi_i (|w(t)| + |z(t)|) + \Lambda_i \leq \pi_i (\|w\| + \|z\|) + \Lambda_i \\ &\leq \pi_i \|(w, z)\| + \Lambda_i \leq \pi_i + \Lambda_i, \ i = 1, 2, ..., k. \end{aligned}$$

Similarly, we have

$$\begin{aligned} &|\phi_i(t, w(t), z(t))| \\ &\leq |\phi_i(t, w(t), z(t)) - \phi_i(t, 0, 0)| + |\phi_i(t, 0, 0)| \\ &\leq \vartheta_i (|w(t)| + |z(t)|) + \nabla_i \leq \vartheta_i (\|w\| + \|z\|) + \nabla_i \\ &\leq \vartheta_i \|(w, z)\| + \nabla_i \leq \vartheta_i + \nabla_i, \ i = 1, 2, ..., k, \end{aligned}$$

Using (3), we can write

$$\begin{aligned} |\mathtt{O}_1(w, z)(t)| &\leq \Pi_1 \sup_{t\in[0,1]} \left\{ \mathfrak{N}_1(t) \right\} \\ &\leq \frac{\sum_{i=1}^{k} 2\Pi_1 \pi_i}{\Gamma(+ + 1)} + \frac{\sum_{i=1}^{k} 2\Pi_1 \nabla_i}{\Gamma(+ + 1)}, \end{aligned}$$

which implies that

$$\begin{aligned} &\|\mathtt{O}_1(w, z)\| \\ &\quad\leq \sum_{i=1}^{k} \frac{\Pi_1 \pi_i}{\Gamma(+ + 1)} + \sum_{i=1}^{k} \frac{\Pi_1 \Lambda_i}{\Gamma(+ + 1)} \\ &\quad\leq \frac{}{4}. \end{aligned}$$

Also, by (3), we have

$$\begin{aligned} &\|\mathtt{O}_2(w, z)\| \\ &\quad\leq \sum_{i=1}^{k} \frac{\Pi_2 \vartheta_i}{\Gamma(+ + 1)} + \sum_{i=1}^{k} \frac{\Pi_2 \nabla_i}{\Gamma(+ + 1)} \\ &\quad\leq \frac{}{4}. \end{aligned}$$

From the definition of $\| \cdot \|_{\mathtt{W}\times\mathtt{Z}}$, we have

$$\begin{aligned} &\|O(w, z)\|_{\mathtt{W}\times\mathtt{Z}} \\ &\leq \sum_{i=1}^{k} \left(\frac{\Pi_1 \pi_i}{\Gamma(+ + 1)} + \frac{\Pi_1 \vartheta_i}{\Gamma(+ + 1)} \right) \\ &\qquad + \sum_{i=1}^{k} \left(\frac{\Pi_2 \Lambda_i}{\Gamma(+ + 1)} + \frac{\Pi_2 \nabla_i}{\Gamma(+ + 1)} \right) \\ &\leq \frac{}{2}, \end{aligned}$$

which implies that $OB \subset B$. Next, for $(w_1, z_1), (w_2, z_2) \in B$ and for each $t \in [0, 1]$, we have

$$\begin{aligned} &\left| \mathtt{O}_1(w_1, z_1)(t) - \mathtt{O}_1(w_2, z_2)(t) \right| \\ &\quad\leq \Pi_1 \sup_{t\in[0,1]} \left\{ \sum_{i=1}^{k} \int_0^t \frac{(t-s)^{+-1}}{\Gamma(+)} \Upsilon(s) ds \right. \\ &\qquad\left. + t^{+-1} \sum_{i=1}^{k} \int_0^1 \frac{(1-s)^{+-1}}{\Gamma(+)} \Upsilon_2(s) ds \right\}. \end{aligned}$$

where

$$\begin{aligned} \Upsilon_2(s) &= |\varphi_i(s, w_1(s), z_1(s)) - \varphi_i(s, w_2(s), z_2(s))|, \\ \Upsilon_2(s) &= |\varphi_i(s, w_1(s), z_1(s)) - \varphi_i(s, w_2(s), z_2(s))|. \end{aligned}$$

From (H_1), we can write

$$\begin{aligned} &\|\mathtt{O}_1(w_1, z_1) - \mathtt{O}_1(w_2, z_2)\| \\ &\quad\leq \sum_{i=1}^{k} \frac{2\Pi_1 \pi_i}{\Gamma(+ + 1)} \|(w_1 - w_2, z_1 - z_2)\|_{\mathtt{W}\times\mathtt{Z}}. \end{aligned}$$

Similarly, we obtain

$$\begin{aligned} &\|\mathtt{O}_2(w_1, z_1) - \mathtt{O}_2(w_2, z_2)\| \\ &\quad\leq \sum_{i=1}^{k} \frac{2\Pi_2 \vartheta_i}{\Gamma(+ + 1)} \|(w_1 - w_2, z_1 - z_2)\|_{\mathtt{W}\times\mathtt{Z}}. \end{aligned}$$

Consequently, we obtain

$$\begin{aligned} &\|\mathtt{O}(w_1, z_1) - \mathtt{O}(w_2, z_2)\|_{\mathtt{W}\times\mathtt{Z}} \\ &= \|\mathtt{O}_1(w_1, z_1) - \mathtt{O}_1(w_2, z_2)\| \\ &\qquad + \|\mathtt{O}_2(w_1, z_1) - \mathtt{O}_2(w_2, z_2)\| \\ &\leq \left[\sum_{i=1}^{k} \left(\frac{2\Pi_1 \pi_i}{\Gamma(+ + 1)} + \frac{2\Pi_2 \vartheta_i}{\Gamma(+ + 1)} \right) \right] \\ &\qquad\qquad \times \left\| (w_1 - w_2, z_1 - z_2) \right\|_{\mathtt{W}\times\mathtt{Z}}. \end{aligned}$$

Thanks to (13), we conclude that $\mathtt{O}$ is a contraction mapping. Hence, by the Banach fixed point theorem, there exists a unique fixed point which is a solution of system (1). This completes the proof. □

4. Stability in Ulam-Hyers-Rassias sense

In the following section, we consider the Ulam's type stability of the fractional hybrid system (1). For $t \in [0,1]$, we give the following inequalities:

$$\begin{cases} \left| {}^{\mathtt{RL}}\mathtt{D}\left[{}^{\mathtt{C}}\mathtt{D}\left[\dfrac{w_1(t)}{\psi_1(t,w_1(t),z_1(t))}\right]\right] - \displaystyle\sum_{i=1}^{k}\varphi_i(t,w_1(t),z_1(t))\right| \leq d_1, \\ \left| {}^{\mathtt{RL}}\mathtt{D}\left[{}^{\mathtt{C}}\mathtt{D}\left[\dfrac{z_1(t)}{\psi_2(t,w_1(t),z_1(t))}\right]\right] - \displaystyle\sum_{i=1}^{k}\phi_i(t,w_1(t),z_1(t))\right| \leq d_2, \end{cases} \tag{14}$$

and

$$\begin{cases} \left| {}^{\mathtt{RL}}\mathtt{D}\left[{}^{\mathtt{C}}\mathtt{D}\left[\dfrac{w_1(t)}{\psi_1(t,w_1(t),z_1(t))}\right]\right] - \displaystyle\sum_{i=1}^{k}\varphi_i(t,w_1(t),z_1(t))\right| \leq d_1 u(t), \\ \left| {}^{\mathtt{RL}}\mathtt{D}\left[{}^{\mathtt{C}}\mathtt{D}\left[\dfrac{z_1(t)}{\psi_2(t,w_1(t),z_1(t))}\right]\right] - \displaystyle\sum_{i=1}^{k}\phi_i(t,w_1(t),z_1(t))\right| \leq d_2 u(t), \end{cases} \tag{15}$$

where $d_j, j=1,2$ are positive reals numbers and $u:[0,1] \to \mathbb{R}^+$, is continuous function.

Definition 4. *[40] System (1) is Ulam-Hyers stable if there exists a real number $\rho_{\varphi_i,\phi_i} = (\rho_{\varphi_i}, \rho_{\phi_i}) > 0, i = 1,2,...,k$ such that for each $d = \max(d_1,d_2) > 0$ and for each solution $(w_1,z_1) \in \mathtt{W} \times \mathtt{Z}$ of the inequality (14) there exists a solution $(w,z) \in \mathtt{W} \times \mathtt{Z}$ of the system (1) with*

$$|(w_1(t) - w(t), z_1(t) - z(t))| \leq \rho_{\varphi_i,\phi_i} d,$$

for $t \in [0,1]$, $i = 1,2,\cdot,k$.

Definition 5. *[40] System (1) is Ulam-Hyers-Rassias stable with respect to $u \in C([0,1],\mathbb{R})$ if there exists a real number $\varsigma_{\varphi_i,\phi_i,u} = (\varsigma_{\varphi_i,u}, \varsigma_{\phi_i,u}) > 0$ such that for each $d = \max(d_1,d_2) > 0$ and for each solution $(w_1,z_1) \in \mathtt{W} \times \mathtt{Z}$ of the inequality (15) there exists a solution $(w,z) \in \mathtt{W} \times \mathtt{Z}$ of the system (1) with*

$$|(w_1(t) - w(t), z_1(t) - z(t))| \leq \varsigma_{\varphi_i,\phi_i,u} d u(t),$$

for $t \in [0,1]$, $i = 1,2,\cdot,k$.

Theorem 3. *Assume that $(H_j)_{j=1,2}$ hold. If*

$$\begin{cases} \displaystyle\sum_{i=1}^{k} \frac{\pi_i}{\Gamma(+ + 1)} < \frac{1}{\Pi_1}, \\ \displaystyle\sum_{i=1}^{k} \frac{\vartheta_i}{\Gamma(+ + 1)} < \frac{1}{\Pi_2}, \end{cases} \tag{16}$$

then the problem (1) is Ulam-Hyers stable.

Proof. Let $(w_1,z_1) \in \mathtt{W} \times \mathtt{Z}$ be a solution of the inequality (14) and let $(w,z) \in \mathtt{W} \times \mathtt{Z}$ be the unique solution of the system

$$\begin{cases} {}^{\mathtt{RL}}\mathtt{D}\left[{}^{\mathtt{C}}\mathtt{D}\left[\dfrac{w(t)}{\psi_1(t,w(t),z(t))}\right]\right] = \displaystyle\sum_{i=1}^{k}\varphi_i(t,w(t),z(t)), \\ {}^{\mathtt{RL}}\mathtt{D}\left[{}^{\mathtt{C}}\mathtt{D}\left[\dfrac{z(t)}{\psi_2(t,w(t),z(t))}\right]\right] = \displaystyle\sum_{i=1}^{k}\phi_i(t,w(t),z(t)), \\ w(0) = w_1(0), w(1) = w_1(1), \\ z(0) = z_1(0), z(1) = z_1(1). \end{cases}$$

By Lemma 5, we have

$$w(t) = \psi_1(t,w(t),z(t)) \left[\sum_{i=1}^{k} \mathtt{I}^{+} g_i^w(t) + \frac{a_1 \Gamma()}{\Gamma(+)} t^{+-1} + a_2\right],$$

and

$$z(t) = \psi_2(t,w(t),z(t)) \left[\sum_{i=1}^{k} \mathtt{I}^{+} h_i^z(t) + \frac{b_1 \Gamma()}{\Gamma(+)} t^{+-1} + b_2\right],$$

such that

$$g_i^w(t) = \varphi_i(t,w(t),z(t)),\ i = 1,2,\cdots,k,$$
$$h_i^z(t) = \phi_i(t,w(t),z(t)),\ i = 1,2,\cdots,k.$$

Integrating (14), we obtain

$$\left| w_1(t) - \psi_1(t,w(t),z(t)) \left[\sum_{i=1}^{k} \mathtt{I}^{+} g_i^w(t) + \frac{a_3 \Gamma()}{\Gamma(+)} t^{+-1} + a_4\right]\right| \leq \frac{d_1 t^{+}}{\Gamma(+ + 1)} \leq \frac{d_1}{\Gamma(+ + 1)},$$

and

$$\left|z_1(t) - \psi_2(t, w(t), z(t))\left[\sum_{i=1}^{k} \mathtt{I}^{+} h_i^z(t) + \frac{b_3\Gamma()}{\Gamma(+)} t^{+-1} + b_4\right]\right| \leq \frac{d_2 t^{+}}{\Gamma(++1)} \leq \frac{d_2}{\Gamma(++1)}.$$

From $(H_j)_{j=1,2}$, we have

$$\begin{aligned} &|w_1(t) - w(t)| \\ &\leq \left|w_1(t) - \psi_1(t, w(t), z(t))\left[\sum_{i=1}^{k} \mathtt{I}^{+} g_i^w(t) + \frac{a_3\Gamma()}{\Gamma(+)} t^{+-1} + a_4\right]\right| \\ &\quad + |\psi_1(t, w(t), z(t))| \sum_{i=1}^{k} \mathtt{I}^{+} |g_i^{w_1}(t) - g_i^w(t)| \\ &\leq \frac{d_1}{\Gamma(++1)} + \sum_{i=1}^{k} \Pi_1 \mathtt{I}^{+} |g_i^{w_1}(t) - g_i^w(t)|, \end{aligned}$$

this implies that

$$\begin{aligned} &|w_1(t) - w(t)| \\ &\leq \frac{d_1}{\Gamma(++1)} + \sum_{i=1}^{k} \frac{\Pi_1 \pi_i}{\Gamma(++1)}\Big[|w_1(t) - w(t)| \\ &\quad + |z_1(t) - z(t)|\Big]. \end{aligned}$$

Similarly, we get

$$\begin{aligned} &|z_1(t) - z(t)| \\ &\leq \frac{d_2}{\Gamma(++1)} + \sum_{i=1}^{k} \frac{\Pi_2 \vartheta_i}{\Gamma(++1)}\Big[|w_1(t) - w(t)| \\ &\quad + |z_1(t) - z(t)|\Big]. \end{aligned}$$

Thus,

$$|(w_1(t), z_1(t)) - (w(t), z(t))| \leq \frac{\frac{1}{\Gamma(++1)} + \frac{1}{\Gamma(++1)}}{\min\{\mathfrak{x}_1, \mathfrak{x}_2\}} d := \rho_{\varphi_i,\phi_i} d,$$

where

$$\mathfrak{x}_1 = \frac{1}{\Pi_1} - \sum_{i=1}^{k} \frac{\pi_i}{\Gamma(++1)},$$

$$\mathfrak{x}_2 = \frac{1}{\Pi_2} - \sum_{i=1}^{k} \frac{\vartheta_i}{\Gamma(++1)}.$$

Hence the system (1) is Ulam-Hyers stable. □

Theorem 4. *Assume that $(H_j)_{j=1,2}$ and (16) hold. Suppose there exist $\upsilon_{1u} > 0, \upsilon_{2u} > 0$ such that*

$$\mathtt{I}^{+} u(t) \leq \upsilon_{1u} u(t), \mathtt{I}^{+} u(t) \leq \upsilon_{2u} u(t), t \in [0,1], \tag{17}$$

where $u \in C([0,1], \mathbb{R}_+)$ is nondecreasing. Then the system (1) is Ulam-Hyers-Rassias stable.

Proof. Let $(w_1, z_1) \in \mathtt{W} \times \mathtt{Z}$ is a solution of the inequality (15) and let us assume that $(w, z) \in \mathtt{W} \times \mathtt{Z}$ is a solution of system (1). Thus, we have

$$\begin{aligned} w(t) &= \psi_1(t, w(t), z(t))\left[\sum_{i=1}^{k} \mathtt{I}^{+} g_i^w(t) + \frac{a_1\Gamma()}{\Gamma(+)} t^{+-1} + a_2\right], \\ z(t) &= \psi_2(t, w(t), z(t))\left[\sum_{i=1}^{k} \mathtt{I}^{+} h_i^z(t) + \frac{b_1\Gamma()}{\Gamma(+)} t^{+-1} + b_2\right], \end{aligned}$$

From inequality (15), we have

$$\left|w_1(t) - \psi_1(t, w(t), z(t))\left[\sum_{i=1}^{k} \mathtt{I}^{+} g_i^w(t) + \frac{a_3\Gamma()}{\Gamma(+)} t^{+-1} + a_4\right]\right| \leq d_1 \mathtt{I}^{+} u(t),$$

and

$$\left|z_1(t) - \psi_2(t, w(t), z(t))\left[\sum_{i=1}^{k} \mathtt{I}^{+} h_i^z(t) + \frac{b_3\Gamma()}{\Gamma(+)} t^{+-1} + b_4\right]\right| \leq d_2 \mathtt{I}^{+} u(t).$$

Now, using $(H_j)_{j=1,2}$ and (17), we get

$$\begin{aligned} &|w_1(t) - w(t)| \\ &\leq d_1 \upsilon_{1u} u(t) + \sum_{i=1}^{k} \frac{\Pi_1 \pi_i}{\Gamma(++1)}(|w_1(t) - w(t)| \\ &\quad + |z_1(t) - z(t)|), \end{aligned}$$

and

$$\begin{aligned} &|z_1(t) - z(t)| \\ &\leq d_2 \upsilon_{2u} u(t) + \sum_{i=1}^{k} \frac{\Pi_2 \vartheta_i}{\Gamma(++1)}(|w_1(t) - w(t)| \\ &\quad + |z_1(t) - z(t)|). \end{aligned}$$

Consequently,

$$\begin{aligned}|(w_1(t), z_1(t)) - (w(t), z(t))| &\leq \frac{\upsilon_{1u} + \upsilon_{2u}}{\min\{\Bbbk_1, \Bbbk_2\}} du(t) \\ &:= \varsigma_{\varphi_i,\phi_i,u} du(t),\end{aligned}$$

where

$$\Bbbk_1 = 1 - \sum_{i=1}^{k} \frac{\Pi_1 \pi_i}{\Gamma(+ + 1)},$$

and

$$\Bbbk_2 = 1 - \sum_{i=1}^{k} \frac{\Pi_2 \vartheta_i}{\Gamma(+ + 1)}.$$

Hence the system (1) is stable in Ulam-Hyers-Rassias sense. □

5. Application

To illustrate our main results, we treat the following example.

Example 1. *Consider the following fractional hybrid system:*

$$\begin{cases} {}^{\mathtt{RL}}\mathtt{D}^{\frac{4}{5}}\left[{}^{\mathtt{C}}\mathtt{D}^{\frac{2}{3}}\left[\dfrac{w(t)}{\frac{\sin w(t)+1}{15}+1+\frac{1}{13}e^{-t^2}\cos z(t)}\right]\right] \\ = \dfrac{\cos(2\pi w(t))}{60\pi} + \dfrac{|z(t)|}{30(1+|z(t)|)} + \arctan\left(t^2+2t+1\right) \\ + \dfrac{|w(t)|}{32(e^t+3\sqrt{\pi})(1+|w(t)|)} + \dfrac{\sin^2 z(t)}{16(5t^2+2(1+3\sqrt{\pi}))} \\ + \dfrac{\ln(1+t)}{3}, \\ {}^{\mathtt{RL}}\mathtt{D}^{\frac{5}{6}}\left[{}^{\mathtt{C}}\mathtt{D}^{\frac{3}{4}}\left[\dfrac{z(t)}{\frac{3}{7}t\cos w(t)+\dfrac{1}{7+z(t)}}\right]\right] \\ = \dfrac{\cos(w(t)+z(t))}{19(\ln(1+t)+2\sqrt{\pi})} + \dfrac{\left(1+2e^{1+t}\right)}{2} \\ + \dfrac{|w(t)|}{3(\pi t+3)^2(1+|w(t)|)} + \dfrac{\tan^{-1} z(t)}{27} + \sinh\left(1+13e^t\right), \\ w(0)=w(1)=0,\ z(0)=z(1)=0, \end{cases} \tag{18}$$

and the following inequalities

$$\begin{cases} {}^{\mathtt{RL}}\mathtt{D}^{\frac{4}{5}}\left[{}^{\mathtt{C}}\mathtt{D}^{\frac{2}{3}}\left[\dfrac{w(t)}{\psi_1(t,w(t),z(t))}\right]\right] \\ \qquad - \displaystyle\sum_{i=1}^{2}\varphi_i(t,w(t),z(t)) \leq d_1, \\ {}^{\mathtt{RL}}\mathtt{D}^{\frac{5}{6}}\left[{}^{\mathtt{C}}\mathtt{D}^{\frac{3}{4}}\left[\dfrac{z(t)}{\psi_2(t,w(t),z(t))}\right]\right] \\ \qquad - \displaystyle\sum_{i=1}^{2}\phi_i(t,w(t),z(t)) \leq d_2, \end{cases}$$

and

$$\begin{cases} {}^{\mathtt{RL}}\mathtt{D}^{\frac{4}{5}}\left[{}^{\mathtt{C}}\mathtt{D}^{\frac{2}{3}}\left[\dfrac{w(t)}{\psi_1(t,w(t),z(t))}\right]\right] \\ \qquad - \displaystyle\sum_{i=1}^{2}\varphi_i(t,w(t),z(t)) \leq d_1 u(t), \\ {}^{\mathtt{RL}}\mathtt{D}^{\frac{5}{6}}\left[{}^{\mathtt{C}}\mathtt{D}^{\frac{3}{4}}\left[\dfrac{z(t)}{\psi_2(t,w(t),z(t))}\right]\right] \\ \qquad - \displaystyle\sum_{i=1}^{2}\phi_i(t,w(t),z(t)) \leq d_2 u(t), \end{cases}$$

where

$$\begin{aligned}\varphi_1(t,w,z) &= \frac{\cos(2\pi w)}{60\pi} + \frac{|z|}{30(1+|z|)} \\ &\quad + \arctan\left(t^2+2t+1\right), \\ \varphi_2(t,w,z) &= \frac{|w|}{32(e^t+3\sqrt{\pi})(1+|w|)} + \frac{\ln(1+t)}{3} \\ &\quad + \frac{\sin^2 z}{16(5t^2+2(1+3\sqrt{\pi}))}, \\ \phi_1(t,w,z) &= \frac{\cos(w+z)}{19(\ln(1+t)+2\sqrt{\pi})} + \frac{\left(1+2e^{1+t}\right)}{2}, \\ \phi_2(t,w,z) &= \frac{|w|}{3(\pi t+3)^2(1+|w|)} + \frac{\tan^{-1} z}{27} \\ &\quad + \sinh\left(1+13e^t\right),\end{aligned}$$

and

$$\begin{aligned}\psi_1(t,w,z) &= \frac{1}{5}(\sin w+1) + 1 + \frac{1}{13}e^{-t^2}\cos z, \\ \psi_2(t,w,z) &= \frac{2}{7}t\cos w + \frac{1}{7+z}.\end{aligned}$$

For $(w_i, z_i) \in \mathbb{R}^2, i = 1, 2$ *and* $t \in [0,1]$, *we have*

$$\begin{aligned}&|\varphi_1(t,w_1,z_1) - \varphi_1(t,w_2,z_2)| \\ &\leq \frac{1}{30}(|w_1-w_2| + |z_1-z_2|), \\ &|\varphi_2(t,w_1,z_1) - \varphi_2(t,w_2,z_2)| \\ &\leq \frac{1}{32(1+3\sqrt{\pi})}(|w_1-w_2| + |z_1-z_2|), \\ &|\phi_2(t,w_1,z_1) - \phi_2(t,w_2,z_2)| \\ &\leq \frac{1}{38\sqrt{\pi}}(|w_1-w_2| + |z_1-z_2|), \\ &|\phi_1(t,w_1,z_1) - \phi_2(t,w_2,z_2)| \\ &\leq \frac{1}{27}(|w_1-w_2| + |z_1-z_2|),\end{aligned}$$

and

$$|\psi_1(t,w,z)| \leq \frac{27}{65}, \quad |\psi_2(t,w,z)| \leq \frac{3}{7}.$$

So, we take $\pi_1 = \frac{1}{30}, \pi_2 = \frac{1}{32}$, $\vartheta_1 = \frac{1}{32(1+3\sqrt{\pi})}$, $\vartheta_2 = \frac{1}{38\sqrt{\pi}}$, $\Pi_1 = \frac{27}{65}$ *and* $\Pi_2 = \frac{3}{7}$.

Hence, we obtain

$$\sum_{i=1}^{2}\frac{\pi_i}{\Gamma(++1)}=4.972\,2\times10^{-2}<\frac{1}{4\Pi_1}=0.103\,85,$$

and

$$\sum_{i=1}^{2}\frac{\vartheta_i}{\Gamma(++1)}=1.401\,9\times10^{-2}<\frac{1}{4\Pi_2}=0.107\,14.$$

By Theorem 1, we conclude that the system (18) has a unique solution. And from Theorem 3 we deduce that (18) is Ulam-Hyers stable with

$$|(w_2(t),z_2(t))-(w_1(t),z_1(t))|\leq 0.365\,68d,$$

for $t\in[0,1]$, $d>0$. *Let* $u(t)=t^{\frac{\sqrt{5}}{2}}$, *then*

$$\mathrm{I}^{\frac{4}{5}+\frac{2}{3}}u_1(t)=\mathrm{I}^{\frac{4}{5}+\frac{2}{3}}t^{\frac{\sqrt{5}}{2}}\leq\frac{\Gamma\left(\frac{\sqrt{5}+2}{2}\right)}{\Gamma\left(\frac{\sqrt{5}}{2}+\frac{37}{15}\right)}t^{\frac{\sqrt{5}}{2}}=\upsilon_{1u}u(t),$$

and

$$\mathrm{I}^{\frac{5}{6}+\frac{3}{4}}u_2(t)=\mathrm{I}^{\frac{5}{6}+\frac{3}{4}}t^{\frac{\sqrt{5}}{2}}\leq\frac{\Gamma\left(\frac{\sqrt{5}+2}{2}\right)}{\Gamma\left(\frac{\sqrt{5}}{2}+\frac{31}{12}\right)}t^{\frac{\sqrt{5}}{2}}=\upsilon_{2u}u(t).$$

Thus, the condition (17) of Theorem 4 is satisfied with $u(t)=t^{\frac{\sqrt{5}}{2}}$ *and* $\upsilon_{1u}=0.289\,01$, $\upsilon_{2u}=0.252\,74$. *Hence from Theorem 4, the system (18) is Ulam-Hyers-Rassias stable with*

$$|(w_1(t),z_1(t))-(w(t),z(t))|\leq 0.948\,04dt^{\frac{\sqrt{5}}{2}},$$

for $t\in[0,1]$, $d>0$.

Remark 1. *One can easily figure out that problem* (18) *is not commented by any of the relevant existing results in the literature.*

Acknowledgments

M. Houas is thankful to Khemis Miliana University, J. Alzabut is thankful to Prince Sultan University and OSTİM Technical University, and M. Khuddush is thankful to Dr. Lankapalli Bullayya College of Engineering for their endless support during the achievement of this paper.

References

[1] Gaul, L., Klein, P. & Kemple, S. (1991). Damping description involving fractional operators. *Mechanical Systems and Signal Processing*, 5, 81-88.

[2] Glockle, W. G., Nonnenmacher, T. F. (1995). A fractional calculus approach to self-semilar protein dynamics. *Biophysical Journal*, 68(1), 46-53.

[3] Metzler, R., Schick, W., Kilian, H. G., & Nonnenmacher, T. F. (1995). Relaxation in filled polymers: a fractional calculus approach. *The Journal of Chemical Physics*, 103, 7180-7186.

[4] Scher, H., Montroll, E. W. (1975). Anomalous transit-time dispersion in amorphous solids. *Physical Review B*, 12, 2455-2477.

[5] Anbalagan, P., Ramachandran, R., Alzabut, J., Hincal, E. & Niezabitowski, M. (2022). Improved results on finite-time passivity and synchronization problem for fractional-order memristor-based competitive neural networks: interval matrix approach. *Fractal and Fractional*, 6(1), 1-36.

[6] Diethelm, K., Ford, N. J. (2002). Analysis of fractional differential equations. *Journal of Mathematical Analysis and Applications,* 265, 229-248.

[7] Joseph, D., Raja, R., Alzabut, J., Niezabitowski, M., Selvam, A. G. M. & Bagdasar, O. O. (2021). An LMI approach based mathematical model to control Aedes Aegypti mosquitoes population via biological control. *Mathematical Problems in Engineering*, 2021, Article ID 5565949, 1-18. https://doi.org/10.1155/2021/556599

[8] Khuddush, M., Prasad, K. R. (2023). Existence, uniqueness and stability analysis of a tempered fractional order thermistor boundary value problems. *Journal of Analysis,* 31, 85-107. https://doi.org/10.1007/s41478-022-00438-6

[9] Khuddush, M., Prasad, K. R. & Leela. D. (2022). Existence of solutions to the ∞-point Fractional BVP posed on half-line via a family of measure of noncompactness in the H$\acute{}$older Space $\mathbb{C}^{\ell,}(\mathbb{R}^+)$. *Filomat*, 36(10), 3527-3543. https://doi.org/10.2298/FIL2210527K

[10] Khuddush, M., Prasad, K. R. & Veeraiah, P. (2022). Infinitely many positive solutions for an iterative system of fractional BVPs with multistrip Riemann–Stieltjes integral boundary conditions. *Afrika Matematika*, 33, 91. https://doi.org/10.1007/s13370-022-01026-4

[11] Khuddush, M., Kathun, S. (2023). Infinitely many positive solutions and Ulam–Hyers stability of fractional order two-point boundary value problems. *Journal of Analysis.* https://doi.org/10.1007/s41478-023-00549-8

[12] Kilbas, A. A., Marzan, S. A. (2005). Nonlinear differential equation with the Caputo fraction derivative in the space of continuously differentiable functions. *Differential Equations*, 41, 84-89.

[13] Podlubny, L. (1999). *Fractional differential equations*, Academic Press, New York.

[14] Pratap, A., Raja, R., Cao, C., Alzabut, J. & Huang, C. (2020). Finite-time synchronization criterion of graph theory perspective fractional order coupled discontinuous neural networks. *Advances in Difference Equations* 2020, 97. https://doi.org/10.1186/s13662-020-02551-x

[15] Seemab, S., Feckan, M., Alzabut, J. & Abbas, S. (2021). On the existence and Ulam-Hyers stability of a new class of partial (ϕ,χ)-fractional differential equations with impulses. *Filomat*, 35(6), 1977-1991.

[16] Shah, K., Abdeljawad1, T., Abdalla, B. & Abualrub, M. (2022). Utilizing fixed point approach to investigate piecewise equations with nonsingular type derivative. *AIMS Mathematics*, 7(8), 14614–14630.

[17] Shah, K., Arfan, M., Ullah, A., Al-Mdallal, Q., Ansari, K. J. & Abdeljawad, T. (2022).

Computational study on the dynamics of fractional order differential equations with applications. *Chaos, Solitons & Fractals,*, 157, 111955. https://doi.org/10.1016/j.chaos.2022.111955

[18] Victor, D. W. J., Khuddush, M. (2022). Existence of solutions for n-dimensional fractional order BVP with ∞–point boundary conditions via the concept of measure of noncompactness. *Advanced Studies: Euro-Tbilisi Mathematical Journal*, 15(1), 19–37. https://doi.org/10.32513/asetmj/19322008202

[19] Dhage, B. C. (2004). A nonlinear alternative in Banach algebras with applications to functional differential equations. *Nonlinear Functional Analysis and Applications*, 8, 563-575.

[20] Dhage, B. C. (2005). On a fixed point theorem in Banach algebras with applications. *Applied Mathematics Letters*, 18(3), 273-280.

[21] Dhage, B. C., Jadhav, N. (2013). Basic results in the theory of hybrid differential equations with linear perturbations of second type. *Tamkang Journal of Mathematics*, 44(2), 171-186.

[22] Ali, A., Shah, K. & Khan, R. A. (2017). Existence of solution to a coupled system of hybrid fractional differential equations, *Bulletin of Mathematical Analysis and Applications*, 9(1), 9-18.

[23] Alzabut, J., Selvam, A. G. M., Vignesh, D. & Gholami, Y. (2021). Solvability and stability of nonlinear hybrid Δ-difference equations of fractional-order. *International Journal of Nonlinear Sciences and Numerical Simulation*, 2021. https://doi.org/10.1515/ijnsns-2021-0005

[24] Baleanu, D., Etemad, S., Pourrazi, S. & Rezapour, S. (2019). On the new fractional hybrid boundary value problems with three-point integral hybrid conditions. *Advances in Difference Equations*, 473, 1-21.

[25] Buvaneswari, K., Karthikeyan, P. & Baleanu, D. (2020). On a system of fractional coupled hybrid Hadamard differential equations with terminal conditions. *Advances in Difference Equations*, 419, 1-12.

[26] Herzallah, M. A. E., Baleanu, D. (2014). On fractional order hybrid differential equations. *Abstract and Applied Analysis*, 2014, 1-8.

[27] Houas, M. (2021). Existence and stability results for hybrid fractional $q-$ differential pantograph equations. *Asia Mathematika*, 5(2), 20-35.

[28] Houas, M. (2018). Solvability of a system of fractional hybrid differential equations. *Communications in Optimization Theory*, Article ID 12, 1-9. https://doi.org/10.23952/cot.2018.12

[29] Nazir, G., Shah, K., Abdeljawad, T., Khalil, H. & and Khan, R. A. (2020). A prior estimate method to investigate sequential hybrid fractional differential equations. *Fractals*, 28(8), 1-12.

[30] Baitiche, Z., Guerbati, K., Benchohra, M. & Henderson, J. (2020). Boundary value problems for hybrid caputo sequential fractional differential equations. *Communications on Applied Nonlinear Analysis*, 4, 1-16.

[31] Jamil, M., Khan, R. A. & Shah, K. (2019). Existence theory to a class of boundary value problems of hybrid fractional sequential integro-differential equations. *Boundary Value Problems*, 2019: 77, 1-12.

[32] Khan, H., Alshehri, H. M. & Khan, Z. A. (2021). A fractional-order sequential hybrid system with an application to a biological system. *Complexity*, 2021, Article ID 2018307, 1-9.

[33] Khan, R. A., Gul, S., Jarad, F. & Khan, H. (2021). Existence results for a general class of sequential hybrid fractional differential equations. *Advances in Difference Equations*, 2021, 284, 1-14.

[34] Prasad, K. R., Khuddush, M. & Leela, D. (2021). Existence of solutions for $n-$ dimensional fractional order hybrid BVPs with integral boundary conditions by an application of $n-$fixed point theorem. *The Journal of Analysis*, 29(3), 963-985.

[35] Dhage, B. C., Lakshmikantham, V. (2010). Basic results on hybrid differential equations. *Nonlinear Analysis: Hybrid Systems*, 4(3), 414-424.

[36] Zhao, Y, Sun, S., Hana, Z. & Li, Q. (2011). Theory of fractional hybrid differential equations. *Computers & Mathematics with Applications*. 62(3), 1312-1324.

[37] Ahmad, B., Ntouyas, S. K. & Alsaedi, A. (2014). Existence results for a system of coupled hybrid fractional differential equations. *The Scientific World Journal*, 2014. Article ID 426438, 1-7.

[38] Kilbas, A. A., Srivastava, H. M. & Trujillo, J. J. (2006). *Theory and applications of fractional differential equations*. North-Holland Mathematics Studies, 204, Elsevier Science B. V., Amsterdam.

[39] Granas, A., Dugundji, J. (2003). *Fixed Point Theory*. Springer, New York, NY, USA.

[40] Ahmad, B., Ntouyas, S. K. (2015). Existence results for a coupled system of Caputo type sequential fractional differential equations with nonlocal integral boundary conditions. *Applied Mathematics and Computation*, 266, 615-622.

Mohamed Houas *is working as an assistant professor at Universite Djilali BOUNAAMA Khemis Miliana, Algeria and his research interest are fractional differential equations and fractional integral inequalities.*

https://orcid.org/0000-0001-6256-0511

Jehad Alzabut *is working as a professor at Prince Sultan University, Saudi Arabia and his research interest are fractional differential equations, and dynamic equations on time scales.*

https://orcid.org/0000-0002-5262-1138

Mahammad Khuddush *is working as an assistant professor at Dr. Lankapalli Bullayya College of Engineering, India and his research interest are fractional differential equations, dynamic equations on time scales, fixed point theory, neural networks, global existence and blow-up solutions of PDE.*

https://orcid.org/0000-0002-1236-8334

An International Journal of Optimization and Control: Theories & Applications (http://www.ijocta.org)

An International Journal of Optimization and Control: Theories & Applications
ISSN:2146-0957 eISSN:2146-5703
Vol.13, No.2, pp.236-243 (2023)
http://doi.org/10.11121/ijocta.2023.1326

RESEARCH ARTICLE

Regional enlarged controllability of a fractional derivative of an output linear system

Rachid Larhrissi, Mustapha Benoudi*

MACS Laboratory, Faculty of Sciences, Moulay Ismail University, Meknes 50000, Morocco
r.larhrissi@umi.ac.ma, mustaphabenoudi@gmail.com

ARTICLE INFO

Article History:
Received 3 October 2022
Accepted 20 June 2023
Available 29 July 2023

Keywords:
Regional controllability
Fractional derivatives
Lagrangian method
Optimal control

AMS Classification 2010:
35F35; 26A33; 93B05

ABSTRACT

This new research aims to extend the topic of the enlarged controllability of a fractional output linear system. Thus, we characterize the optimal control by two methods, ensuring that the Riemann-Liouville fractional derivative of the final state of the considered system lies between two given functions on a subregion of the evolution domain. Firstly, we transform the considered problem into the saddle point using the Lagrangian multiplier approach. Then, in the second one, we provide the technique of the subdifferential, which allows us to present the cost-explicit formula of the minimum energy control. Moreover, we construct an algorithm of Uzawa type to illustrate the theoretical results obtained through numerical simulations.

1. Introduction

The concept of fractional calculus has attracted increasing attention from many researchers, and it was introduced in the 19th century by Riemann, Liouville, and Letnikov. Their objective was to extend classic differentiation and integration using non-integer orders, they have been used in mechanics since the 1930s and later in electrochemistry in the 1960s (see [1]). In addition, the integer derivative of a function φ at a point x_0 remains a local property. However, the fractional-order differentiation of a function φ at x_0 depends on all values of φ, including those that are not in the neighborhood of x_0.

The regional controllability is a crucial and modern topic in advancing control theory and engineering. It is a qualitative property of controlled systems and has an exceptional property in control theory. The last notion is the basis of a mathematical description of a dynamical system, which is also related to the realization theory of quadratic optimality in linear time-invariant controlled systems.

The problem of regional controllability involves determining whether it is possible to find a control that can bring the state of a system from its initial state to the desired state exclusively within a subregion ω at a finite moment. The concept of regional controllability for distributed systems was introduced in the 1990s by Professors El Jai and Zerrik (see [2–4]), in which it was possible to study the idea only on a subregion ω of the domain Ω.

This topic has admitted many applications and has led to crucial results such as the possibility of reaching a state of the system only on an internal subregion ω of Ω or on a subregion of the boundary $\partial\Omega$ of Ω (see [5], [6]). Also, the problem of driving a system to a state between two known functions is well detailed in [7]. Furthermore, in [8], they have investigated and developed the problem of the regional controllability of the gradient state. This problem involves directing the state gradient of the considered system towards a specified function that is only defined in the domain subset $\omega \subset \Omega$. Furthermore, authors

*Corresponding Author

have examined a problem of regional gradient controllability, which is emphasized by concentrating on a control that would realize a given final gradient on ω with minimum energy (see [9]). Finally, in [10], the authors have proved the fractional controllability of linear hyperbolic systems by using an extension of HUM.

As the optimal linear filter and estimator, the Kalman Filter design for linear infinite-dimensional systems has been widely employed for state estimation and prediction in the realm of lumped parameter systems (see [11]). Besides that, fractional derivatives have been applied to the modelling of combustion processes, offering unique insights into the dynamics and features of these systems. They allow us to characterize processes that involve under- or superdiffusion, where the diffusion rate does not follow the classical diffusion equations. Our problematic is about studying the regional controllability of the fractional state of the considered system. In particular, if $\omega = \Omega$ and $\alpha = 0$, we obtain global enlarged controllability over the evolution domain. On the other hand, we achieve enlarged regional controllability of the system's state gradient with $\alpha = 1$ in all parts of ω within Ω. Hence, we show that the obtained control allows us to generalize the latter cases using the concept of the fractional derivative of order $\alpha \in [0,\ 1]$. In order to solve this problem, we employ the approaches of subdifferential and Lagrangian to determine the optimal control that steers the fractional derivative of an output of the considered system between two known functions on subregion ω in the interior of Ω as shown in the following figure: (e.g. see Figure 1).

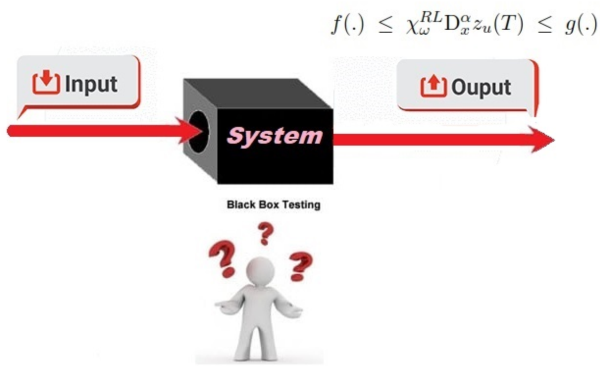

Figure 1. The goal of this research.

The structure of this research is as follows. Section 2 is devoted to recalling some definitions and the statement of the considered problem. In Section 3, we use two procedures, one based on subdifferential tools and the other on the Lagrangian approach, which allows us to determine the explicit formula of optimal control. Finally, the theoretical results achieved are illustrated through numerical simulations by applying an algorithm to the one-dimensional diffusion equation.

2. Problem statement

Let Ω be an open bounded subset of $\mathbb{R}^n$ with a boundary $\partial\Omega$. For $T > 0$ we denote $Q = \Omega \times]0, T[$.

Let's consider the linear system with internal control described by:

$$\begin{cases} \dfrac{\partial z}{\partial t}(x,t) = Az(x,t) + Bu(t) & Q \\ z(\eta, t) = 0 & \partial\Omega \times]0,T[\\ z(x,0) = z_0(x) & \Omega \end{cases} \tag{1}$$

where A generates a C_0-semigroup S(t), $t \geq 0$ in $H_0^1(\Omega)$ and B $\in \mathcal{L}(\mathbb{R}^p, H_0^1(\Omega))$, u $\in \mathbb{U} = L^2(0,T;\mathbb{R}^p)$ and $z_0 \in H_0^1(\Omega)$.

• The problem (1) admits a unique solution $z_u(.)$ such that $z_u(T) \in H_0^1(\Omega)$ and given by the variation of constants formula (see [12], page 106)

$$z_u(t) = S(t)z_0 + \int_0^t S(t-r)Bu(r)dr.$$

• The operator of controllability L_T is defined by:

$$\begin{aligned} L_T : \mathbb{U} &\rightarrow H_0^1(\Omega) \\ u &\mapsto \int_0^T S(T-t)Bu(t)dt \end{aligned}$$

and its adjoint $L_T^* z = B^* S^*(T - .)z$.

• Let ${}^{RL}\mathrm{D}_x^\alpha : H_0^1(\Omega) \rightarrow L^2(\Omega)$ the fractional Riemann-Liouville operator of order α and $({}^{RL}\mathrm{D}_x^\alpha)^*$ its adjoint (see [13]).

• Consider ω as a subregion of Ω. Let $\chi_\omega : L^2(\Omega) \rightarrow L^2(\omega)$ be the restriction operator to ω. The adjoint operator of χ_ω is denoted by χ_ω^* and is given by

$$(\chi_\omega^* z)(x) = \begin{cases} z(x), & x \in \omega, \\ 0, & \text{otherwise.} \end{cases}$$

Definition 1. *(see [1] and [14]) Let $\Re(\alpha) > 0$ and $\psi : [a,b) \rightarrow \mathbb{R}$ be continuous and integrable. For $x > a$, we call*

$$\mathrm{I}_a^\alpha \psi(x) = \frac{1}{\Gamma(\alpha)} \int_a^x (x-t)^{\alpha-1}\psi(t)dt. \tag{2}$$

the Riemann-Liouville fractional integral of ψ of order α

Definition 2. *(see [1] and [14]) Let α such that $0 \leq \alpha < 1$.*

The fractional derivative of Riemann-Liouville of order α of a function ψ is given by:

$$\begin{aligned} {}^{RL}\mathrm{D}_x^\alpha \psi(x) &= \frac{d}{dx}\mathrm{I}_a^{1-\alpha}\psi(x) \\ &= \frac{1}{\Gamma(1-\alpha)}\frac{d}{dx}\int_a^x (x-t)^{-\alpha}\psi(t)dt. \end{aligned} \tag{3}$$

• Let $f,\ g \in L^2(\omega)$ with $f(.) \leq g(.)$ a.e in ω. In all the following we set:

$$[f(.),\ g(.)] = \left\{ \begin{array}{l} \chi_\omega^{RL}\mathrm{D}_x^\alpha z \in L^2(\omega)\ / \\ f(.) \leq\ \chi_\omega^{RL}\mathrm{D}_x^\alpha z \leq g(.)\ a.e.\ on\ \omega \end{array} \right\}$$

Definition 3. *(General definition of old one [8]) System (1) is said to be $[f(.),\ g(.)]$-controllable on ω, if there exists $u \in \mathbb{U}$ such that*

$$f(.) \leq \chi_\omega^{RL}\mathrm{D}_x^\alpha z_u(T) \leq g(.) \quad a.e\ on\ \omega.$$

Definition 4. *(General definition of old one [8]) We say that the actuator $(D,\ h)$ is $[f(.),\ g(.)]$-strategic on ω, if the excited system is $[f(.),\ g(.)]$-controllable on ω.*

3. Minimization problem

In this section, we exploit two methods to find a control with minimum energy that allows driving the system (1) from z_0 to the fractional output between $f(.)$ and $g(.)$ on ω. Later, let's consider the following minimization problem:

$$\left\{ \begin{array}{l} \min \frac{1}{2}\|u\|^2 \\ u \in \mathcal{U}_{ad} \end{array} \right. \tag{4}$$

where the set of admissible controls is given by

$$\mathcal{U}_{ad} = \left\{ \begin{array}{l} u \in \mathbb{U}\ / \\ f(.) \leq\ {}^{RL}\mathrm{D}_x^\alpha z_u(T) \leq g(.)\ a.e.\ on\ \omega \end{array} \right\}.$$

Proposition 1. *Problem (4) has a unique solution if the system (1) is $[f(.),\ g(.)]$-controllable on ω.*

Proof. By hypothesis, system (1) is $[f(.),\ g(.)]$-controllable on ω, then $\mathcal{U}_{ad} \neq \emptyset$. Moreover, $u \to \frac{1}{2}\|u\|^2$ is strictly convex and lower semi-continuous in $\mathbb{U}$. As result, it suffices to verify that $\mathcal{U}_{ad}$ is a closed convex set of $\mathbb{U}$.
We can deduce the convexity of $\mathcal{U}_{ad}$ from the linearity of the map $u \to \chi_\omega^{RL}\mathrm{D}_x^\alpha z_u(T)$.
Now, we show that $\mathcal{U}_{ad}$ is closed. Let $(u_n)_n$ in $\mathcal{U}_{ad}$ such that $u_n \to u$ strongly in $\mathbb{U}$. Since that $\chi_\omega^{RL}\mathrm{D}_x^\alpha L_T$ is continuous, then $\chi_\omega^{RL}\mathrm{D}_x^\alpha L_T u_n \to \chi_\omega^{RL}\mathrm{D}_x^\alpha L_T u$ strongly in $L^2(\omega)$, we know that $\chi_\omega^{RL}\mathrm{D}_x^\alpha z_{u_n} \in [f(.),\ g(.)]$ which is closed, then $\chi_\omega^{RL}\mathrm{D}_x^\alpha z_u \in [f(.),\ g(.)]$. We deduce that $u \in \mathcal{U}_{ad}$.
Consequently, $\mathcal{U}_{ad}$ is closed.
Therefore, problem (4) admits a unique solution. □

We will provide two methods to characterize the optimal control solution of (4) in the later subsections.

3.1. First method: Subdifferential method

In this subsection, we provide an expression that characterizes the solution to the problem (4) using the subdifferential approach.
Problem (4) is equivalent to solve the following problem without fractional constraints:

$$\left\{ \begin{array}{l} min\left(\frac{1}{2}\|u\|^2 +\ \Psi_{\mathcal{U}_{ad}}(u)\right) \\ u \in \mathbb{U} \end{array} \right. \tag{5}$$

where, for a nonempty subset F of $\mathbb{U}$, we have

$$\Psi_F(u) = \left\{ \begin{array}{ll} 0\ if & u \in F \\ +\infty & otherwise, \end{array} \right. \tag{6}$$

the indicator function of F.

• Let

$$\Sigma(\mathbb{U}) = \left\{ \begin{array}{l} \sigma : \mathbb{U} \to\,]-\infty,\ +\infty],\ convex\ proper \\ and\ lower\ semi-continuous\ on\ \mathbb{U} \end{array} \right\}.$$

• Let $\sigma \in \Sigma(\mathbb{U})$, $\mathrm{dom}(\sigma) = \{u \in \mathbb{U}\ /\ \sigma(u) < \infty\}$ and σ^* is the polar function of σ defined by:

$$\sigma^*(v^*) = \sup_{u \in dom(\sigma)} \{\langle v^*,\ u\rangle - \sigma(u)\} \quad \forall v^* \in \mathbb{U}.$$

Definition 5. *(see [15]) The set of subgradients of σ at $u_0 \in \mathbb{U}$ is called the subdifferential of σ at u_0. We denote it as follows:*

$$\partial\sigma(u_0) = \left\{ \begin{array}{l} v^* \in \mathbb{U}\ / \\ \sigma(u) \geq \sigma(u_0) + \langle v^*,\ u - u_0\rangle\ \forall\ u \in \mathbb{U} \end{array} \right\}.$$

The following result characterizes the solution to the problem (5):

Proposition 2. *Assume that system (1) is $[f(.),\ g(.)]$-controllable on ω, then $u^\star$ is the solution of Equation (5) if and only if*

$$u^\star \in \mathcal{U}_{ad} \quad and \quad \Psi^*_{\mathcal{U}_{ad}}(-u^\star) = -\|u^\star\|^2. \tag{7}$$

Proof. By the properties of the subdifferential, we deduce that $u^\star$ is a solution of (5) if and only if $0 \in \partial(\sigma + \Psi_{\mathcal{U}_{ad}})(u^\star)$.

Therefore, $\sigma(u) = \frac{1}{2}\|u\|^2 \in \Sigma(\mathbb{U})$, and $\mathcal{U}_{ad}$ is closed, convex not empty, then $\Psi_{\mathcal{U}_{ad}} \in \Sigma(\mathbb{U})$. In addition, system (1) is $[f(.),\ g(.)]$-controllable on ω and $dom(\sigma) \cap dom(\Psi_{\mathcal{U}_{ad}}) \neq \emptyset$. However, σ is continuous, where

$$\partial\left(\sigma + \Psi_{\mathcal{U}_{ad}}\right)(u^\star) = \partial\sigma(u^\star) + \partial\Psi_{\mathcal{U}_{ad}}(u^\star).$$

Consequently, $u^\star$ is the solution of Equation (5) if and only if $0 \in \partial\sigma(u^\star) + \partial\Psi_{\mathcal{U}_{ad}}(u^\star)$.

On the other hand, we know that σ is Freshet-differentiable, then $\partial\sigma(u^\star) = \{\nabla\sigma(u^\star)\} = \{u^\star\}$. We conclude that $u^\star$ is the solution of (5) if and only if $-u^\star \in \partial\Psi_{\mathcal{U}_{ad}}(u^\star)$, one has

$$\begin{aligned}
&\Psi_{\mathcal{U}_{ad}}(u) \geq \Psi_{\mathcal{U}_{ad}}(u^\star) + \langle u^\star,\ u - (-u^\star)\rangle \\
&\quad \Leftrightarrow 0 \geq \Psi_{\mathcal{U}_{ad}}(u^\star) + \langle u^\star,\ u - (-u^\star)\rangle - \Psi_{\mathcal{U}_{ad}}(u) \\
&\quad\quad 0 = \Psi_{\mathcal{U}_{ad}}(u^\star) + \|u^\star\|^2 + \sup_{u\in\mathcal{U}_{ad}} \{\langle u^\star,\ u\rangle \\
&\quad\quad\quad - \Psi_{\mathcal{U}_{ad}}(u)\}.
\end{aligned}$$

Then, $u^\star \in \mathcal{U}_{ad}$ and $\Psi_{\mathcal{U}_{ad}}(u^\star) + \Psi^*_{\mathcal{U}_{ad}}(-u^\star) = -\|u^\star\|^2$. We know that $u^\star \in \mathcal{U}_{ad}$, so $\Psi_{\mathcal{U}_{ad}}(u^\star) = 0$. Finally, we obtain that $u^\star \in \mathcal{U}_{ad}$ and $\Psi^*_{\mathcal{U}_{ad}}(-u^\star) = -\|u^\star\|^2$. □

We put $\alpha(.) = f(.) - \chi_\omega^{RL}\mathrm{D}_x^\alpha S(T)z_0$ and $\beta(.) = g(.) - \chi_\omega^{RL}\mathrm{D}_x^\alpha S(T)z_0$, then

$$\mathcal{U}_{ad} = \left\{u \in \mathbb{U} \ /\ \chi_\omega^{RL}\mathrm{D}_x^\alpha L_T u \in [\alpha(.),\ \beta(.)]\right\}.$$

As a result, we get the following:

Proposition 3. *$u^\star$ is the solution of Equation (5) if and only if*

$$\min\left\{\begin{array}{l} \left\langle(\chi_\omega^{RL}\mathrm{D}_x^\alpha L_T)^\dagger\alpha(.),\ u^\star\right\rangle, \\ \left\langle(\chi_\omega^{RL}\mathrm{D}_x^\alpha L_T)^\dagger\beta(.),\ u^\star\right\rangle \end{array}\right\} = \|u^\star\|^2, \tag{8}$$

where the pseudo-inverse operator of $\chi_\omega^{RL}\mathrm{D}_x^\alpha L_T$ is given by (see [16]):

$$(\chi_\omega^{RL}\mathrm{D}_x^\alpha L_T)^\dagger = (\chi_\omega^{RL}\mathrm{D}_x^\alpha L_T)^* \left((\chi_\omega^{RL}\mathrm{D}_x^\alpha L_T)(\chi_\omega^{RL}\mathrm{D}_x^\alpha L_T)^*\right)^{-1}.$$

Proof. We have

$$\mathcal{U}_{ad} = (\chi_\omega^{RL}\mathrm{D}_x^\alpha L_T)^\dagger\left([\alpha(.),\ \beta(.)]\right).$$

Applying the proposition 2, we get $u^\star$ which is the solution of (5) if and only if $u^\star \in \mathcal{U}_{ad}$ and $\Psi^*_{\mathcal{U}_{ad}}(-u^\star) = -\|u^\star\|^2$.

In addition, for all $u^\star \in \mathbb{U}$, we have

$$\begin{aligned}
\Psi^*_{\mathcal{U}_{ad}}(-u^\star) &= \sup_{v\in\mathbb{U}}\left\{\langle -u^\star,\ v\rangle - \Psi_{\mathcal{U}_{ad}}(v)\right\}, \\
&= \sup_{v\in\mathcal{U}_{ad}}\langle -u^\star,\ v\rangle = -\inf_{v\in\mathcal{U}_{ad}}\langle u^\star,\ v\rangle, \\
&= -\inf_{v\in(\chi_\omega^{RL}\mathrm{D}_x^\alpha L_T)^\dagger([\alpha(.),\ \beta(.)])}\langle u^\star,\ v\rangle \\
&= -\inf_{z\in[\alpha(.),\ \beta(.)]}\left\langle u^\star,\ (\chi_\omega^{RL}\mathrm{D}_x^\alpha L_T)^\dagger z\right\rangle \\
&= -\inf_{\lambda\in[0,1]}\left\langle\left((\chi_\omega^{RL}\mathrm{D}_x^\alpha L_T)^\dagger\right)^* u^\star, \lambda\alpha(.) + (1-\lambda)\beta(.)\right\rangle.
\end{aligned}$$

The mapping

$$L : [0,\ 1] \ \to\ \mathbb{R}$$

$$L(\lambda) = \left\langle\left((\chi_\omega^{RL}\mathrm{D}_x^\alpha L_T)^\dagger\right)^* u^\star,\ \lambda\alpha(.) + (1-\lambda)\beta(.)\right\rangle,$$

is convex and continuous, using the Krein-Milman Theorem (see [17], page 362), we obtain

$$\Psi^*_{\mathcal{U}_{ad}}(-u^\star) = -\inf_{\lambda\in\{0,1\}}\left\langle\left((\chi_\omega^{RL}\mathrm{D}_x^\alpha L_T)^\dagger\right)^* u^\star, \lambda\alpha(.) + (1-\lambda)\beta(.)\right\rangle,$$

from (7), we conclude that

$$\begin{aligned}
&\Psi^*_{\mathcal{U}_{ad}}(-u^\star) = \\
&= -\min\left\{\begin{array}{l} \left\langle u^\star,\ (\chi_\omega^{RL}\mathrm{D}_x^\alpha L_T)^\dagger\alpha(.)\right\rangle, \\ \left\langle u^\star,\ (\chi_\omega^{RL}\mathrm{D}_x^\alpha L_T)^\dagger\beta(.)\right\rangle \end{array}\right\} \\
&= -\|u^\star\|^2.
\end{aligned}$$

□

3.2. Second method: Lagrangian multiplier method

Problem (4) is equivalent to solve the coming problem:

$$\left\{\begin{array}{l} \min\dfrac{1}{2}\|u\|^2 \\ (u,\ y) \in \mathcal{V} \end{array}\right. \tag{9}$$

where

$$\mathcal{V} = \left\{\begin{array}{l} (u,\ y) \in \mathbb{U}\times[f(.),\ g(.)] \ / \\ \chi_\omega^{RL}\mathrm{D}_x^\alpha z_u(T) - y = 0 \end{array}\right\}.$$

We define the assistant variable $y \in [f(.),\ g(.)]$ related to u by equation $\chi_\omega^{RL}\mathrm{D}_x^\alpha z_u(T) - y = 0$. We transform problem (9) into a saddle point problem using the Lagrange multiplier.

Definition 6. *(see [8]) We call the Lagrangian associated with problem (9) the function $\mathcal{L}$ defined by: $\forall\ (u,\ y,\ \mu) \in \mathbb{U}\times[f(.),\ g(.)]\times L^2(\omega)$,*

$$\mathcal{L}(u,\ y,\ \mu) = \frac{1}{2}\|u\|^2 + \langle\mu,\ \chi_\omega^{RL}\mathrm{D}_x^\alpha z_u(T) - y\rangle_{L^2(\omega)}.$$

Definition 7. *(see [8]) We say that $(u^\star,\ y^\star,\ \mu^\star)$ is a saddle point of $\mathcal{L}$ if*

$$\max_{\mu\in L^2(\omega)}\mathcal{L}(u^\star,\ y^\star,\ \mu) = \mathcal{L}(u^\star,\ y^\star,\ \mu^\star) = \min_{u\in\mathbb{U},\ y\in[f(.),\ g(.)]}\mathcal{L}(u,\ y,\ \mu^\star).$$

Suppose that system (1) is excited by a zone actuator $(D,\ h)$. Then, we consider the problem (4) and can characterize its solution by the following result:

Proposition 4. *If the actuator $(D,\ h)$ is $[f(.),\ g(.)]$-strategic on ω, then the solution of (4) is characterized by*

$$u^\star = -(\chi_\omega^{RL}\mathrm{D}_x^\alpha L_T)^*\mu^\star \tag{10}$$

whither $\mu^\star$ verifies

$$\left\{\begin{array}{l} G_{\alpha,\omega}\mu^\star + y^\star = 0 \\ y^\star = \mathcal{P}_{[f(.),\ g(.)]}(r\mu^\star + y^\star) \end{array}\right. \tag{11}$$

where $\mathcal{P}_{[f(.),\ g(.)]} : L^2(\Omega) \to [f(.),\ g(.)]$ *designates the projection operator,* $G_{\alpha,\omega} = \left(\chi_\omega^{RL}\mathrm{D}_x^\alpha L_T\right)\left(\chi_\omega^{RL}\mathrm{D}_x^\alpha L_T\right)^*$ *and* $r > 0$.

Proof. Suppose that the actuator $(D,\ h)$ is $[f(.),\ g(.)]$-strategic on ω, then $\mathcal{U}_{ad} \neq \emptyset$ and (4) has a unique solution.

It's clear that $\mathbb{U} \times [f(.),\ g(.)]$ is nonempty and closed convex. Moreover, we know that the function $\mu \to \mathcal{L}(u,\ y,\ \mu)$ is differentiable, concave, and upper semi-continuous. Likewise the function $(u,\ y) \to \mathcal{L}(u,\ y,\ \mu)$ is differentiable, convex and lower semi-continuous.

We deduce that there exists $\mu_0 \in L^2(\omega)$ and $(u_0,\ y_0) \in \mathbb{U} \times [f(.),\ g(.)]$ such that

$$\lim_{\|(u,\ y)\| \to +\infty} \mathcal{L}(u,\ y,\ \mu_0) = +\infty, \tag{12}$$

and

$$\lim_{\|\mu\| \to +\infty} \mathcal{L}(u_0,\ y_0,\ \mu) = -\infty. \tag{13}$$

As a result, $\mathcal{L}$ possesses a saddle point.
In the following, assume that $(u^\star,\ y^\star,\ \mu^\star)$ is a saddle point of $\mathcal{L}$ and prove that $u^\star$ is a solution of (4).
Now, for all $(u,\ y,\ \mu) \in \mathbb{U} \times [f(.),\ g(.)] \times L^2(\omega)$, we have

$$\mathcal{L}(u^\star,\ y^\star,\ \mu) \ \leq\ \mathcal{L}(u^\star,\ y^\star,\ \mu^\star) \ \leq\ \mathcal{L}(u,\ y,\ \mu^\star).$$

The inequality one gives

$$\langle \mu,\ \chi_\omega^{RL}\mathrm{D}_x^\alpha z_{u^\star}(T) - y^\star \rangle \leq \langle \mu^\star,\ \chi_\omega^{RL}\mathrm{D}_x^\alpha z_{u^\star}(T) - y^\star \rangle, \quad \forall\ \mu \in L^2(\omega),$$

means that $\chi_\omega^{RL}\mathrm{D}_x^\alpha z_{u^\star}(T) = y^\star$. Consequently, $\chi_\omega^{RL}\mathrm{D}_x^\alpha z_{u^\star}(T) \in [f(.),\ g(.)]$.
Using the second inequality, we obtain

$$\begin{aligned}\frac{1}{2}\|u^\star\|^2 + \langle \mu^\star,\ \chi_\omega^{RL}\mathrm{D}_x^\alpha z_{u^\star}(T) - y^\star \rangle \\ \leq \frac{1}{2}\|u\|^2 + \langle \mu^\star,\ \chi_\omega^{RL}\mathrm{D}_x^\alpha z_u(T) - y \rangle, \\ \forall (u,\ y) \in \mathbb{U} \times [f(.),\ g(.)]\,.\end{aligned}$$

Since $\chi_\omega^{RL}\mathrm{D}_x^\alpha z_{u^\star}(T) = y^\star$, we will have

$$\begin{aligned}\frac{1}{2}\|u^\star\|^2 \ \leq\ \frac{1}{2}\|u\|^2 + \langle \mu^\star,\ \chi_\omega^{RL}\mathrm{D}_x^\alpha z_u(T) - y \rangle, \\ \forall\ (u,\ y) \in \mathbb{U} \times [f(.),\ g(.)]\,.\end{aligned}$$

For $\chi_\omega^{RL}\mathrm{D}_x^\alpha z_u(T) = y$, we get $\frac{1}{2}\|u^\star\|^2 \ \leq\ \frac{1}{2}\|u\|^2$.
Therefore, $u^\star$ is of minimum energy.
On the other hand, if $(u^\star,\ y^\star,\ \mu^\star)$ is a saddle point of $\mathcal{L}$, then the following assumptions are satisfied:

$$\langle u^\star,\ u - u^\star \rangle + \langle \mu^\star,\ \chi_\omega^{RL}\mathrm{D}_x^\alpha L_T(u - u^\star) \rangle = 0, \quad \forall u \in \mathbb{U} \tag{14}$$

$$-\langle \mu^\star,\ y - y^\star \rangle \geq 0, \quad \forall y \in [f(.),\ g(.)] \tag{15}$$

$$\langle \mu - \mu^\star,\ \chi_\omega^{RL}\mathrm{D}_x^\alpha z_{u^\star}(T) - y^\star \rangle = 0, \quad \forall \mu \in L^2(\omega). \tag{16}$$

From the equation (14) gives (10).
Then, using (16), we get $\chi_\omega^{RL}\mathrm{D}_x^\alpha L_T(u^\star) = y^\star$.
Hence, with (10,) we deduce (11).
Applying inequality (15), we get

$$\langle (r\mu^\star + y^\star) - y^\star,\ y - y^\star \rangle \ \leq\ 0, \quad \forall y \in [f(.),\ g(.)]$$

and $r > 0$, that is equivalent to

$$y^\star = \mathcal{P}_{[f(.),\ g(.)]}(r\mu^\star + y^\star).$$

□

Corollary 1. *If system (1) is* $[f(.),\ g(.)]$*-controllable on* ω*, then* $(y^\star,\ \mu^\star)$ *is a unique solution of system (11), where* $r > 0$ *is suitably chosen.*

Proof. Assume that system (1) is $[f(.),\ g(.)]$-controllable, implies that $(\chi_\omega^{RL}\mathrm{D}_x^\alpha L_T)^*$ and $G_{\alpha,\omega}$ are one to one. In addition, if $(u^\star,\ y^\star,\ \mu^\star)$ is a saddle point of $\mathcal{L}$, we deduce then system (11) is equivalent to

$$\begin{cases} \mu^\star = -G_{\alpha,\omega}^{-1} y^\star \\ y^\star = \mathcal{P}_{[f(.),\ g(.)]}(-rG_{\alpha,\omega}^{-1} y^\star + y^\star). \end{cases} \tag{17}$$

Therefore, $y^\star$ is a fixed point of

$$\begin{aligned} N_r \ :\ [f(.),\ g(.)] &\to [f(.),\ g(.)] \\ x &\mapsto \mathcal{P}_{[f(.),\ g(.)]}(-rG_{\alpha,\omega}^{-1} x + x), \end{aligned}$$

since that the operator $G_{\alpha,\omega}^{-1}$ is coercive, which means

$$\exists\ k \geq 0 \quad such \quad that \quad \langle G_{\alpha,\omega}^{-1} x,\ x \rangle \geq k\|x\|^2.$$

Hence,

$$\begin{aligned} &\|N_r(x) - N_r(y)\|^2 \\ &= \|\mathcal{P}_{[f(.),\ g(.)]}(-rG_{\alpha,\omega}^{-1} x + x) \\ &\quad - \mathcal{P}_{[f(.),\ g(.)]}(-rG_{\alpha,\omega}^{-1} y + y)\|^2 \\ &= \ \|(-rG_{\alpha,\omega}^{-1} x + x) - (-rG_{\alpha,\omega}^{-1} y + y)\|^2 \\ &= \ \|(-rG_{\alpha,\omega}^{-1}(x - y)) + (x - y)\|^2 \\ &= |\ \left\langle -rG_{\alpha,\omega}^{-1}(x - y),\ -rG_{\alpha,\omega}^{-1}(x - y) \right\rangle \\ &\quad - 2r\left\langle G_{\alpha,\omega}^{-1}(x - y),\ x - y \right\rangle + \langle x - y,\ x - y \rangle\ | \\ &\leq\ (1 + r^2\|G_{\alpha,\omega}^{-1}\|^2 - 2rk)\|x - y\|^2, \\ &\forall x,\ y \in [f(.),\ g(.)]\,. \end{aligned}$$

If we chose $r < \dfrac{2k}{\|G_{\alpha,\omega}^{-1}\|^2}$, we conclude that N_r is a contraction, which implies that $y^\star$ and $\mu^\star$ are unique. □

4. Applications and simulations

In this section, we solve the equations (10) and (11) numerically and propose an Uzawa-type algorithm to evaluate the effectiveness of the Lagrangian method (see [18], page 3).

4.1. Algorithm

step 1: Initial data: Ω, zone of action D, subregion ω, precision threshold ε is sufficiently small and a fractional order α.
step 2: Initiate two functions $(y_0,\ \mu_1) \in [f(.),\ g(.)] \times L^2(\omega)$.
step 3: $(y_{n-1},\ \mu_n)$ is known, we determine u_n and y_n by the equations

$$u_n(t) = -\sum_{k=1}^{\infty} e^{\lambda_k(T-t)} \left(\int_D \varphi_k(x)dx\right) \times \left(\int_\Omega \chi_\omega^{RL}\mathrm{D}_x^\alpha \varphi_k(x)\mu_n(x)dx\right), \tag{18}$$

$$y_n(x) = \begin{cases} f(x) & if\ r\mu_n(x) + y_{n-1}(x) \leq f(x) \\ r\mu_n(x) + y_{n-1}(x) & if\ f(x) \leq r\mu_n(x) + y_{n-1}(x) \leq g(x) \\ g(x) & if\ r\mu_n(x) + y_{n-1}(x) \geq g(x). \end{cases} \tag{19}$$

step 4: While $\|y_n - y_{n-1}\|_{L^2(\omega)} > \varepsilon$,

$$\mu_{n+1}(x) = \mu_n(x) + \sum_{k=1}^{\infty}\left(\int_D \varphi_k(x)dx\right) \chi_\omega^{RL}\mathrm{D}_x^\alpha\varphi_k(x) \times \int_0^T e^{\lambda_k(T-t)}u_n(t)dt - y_n(x), \tag{20}$$

and return to step 3.
Where $(\varphi_n)_{n\in\mathbb{N}}$ is a complete basis of eigenfunctions of A in $H^1(\Omega)$ associated with the eigenvalues λ_n.

4.2. Simulations

This part aims to test the effectiveness of the Lagrangian approach through numerical simulations.
Example 1:
Let $\Omega =]0,\ 1[$ and consider the ensuing system:

$$\begin{cases} \dfrac{\partial z}{\partial t}(t,x) = \dfrac{\partial^4 z}{\partial x^4}(t,x) + \mathcal{X}_D u(t), & \Omega \times]0,\ T[, \\ z(0,x) = 0, & x \in \Omega, \\ z(t,0) = z(t,1) = 0, & t \in]0,\ T[, \\ \dfrac{\partial^2 z}{\partial x^2}(t,0) = \dfrac{\partial^2 z}{\partial x^2}(t,1) = 0, & t \in]0,\ T[, \end{cases} \tag{21}$$

taking T $= 2$ and the actuator is located at D.
Let $f(x) = \dfrac{1}{2}x^2(1-x)$ and $g(x) = 4x^2(1-x^3)$.
The operator $Az = \dfrac{\partial^4 z}{\partial x^4}$ admits a complete set of eigenfunctions

$$\varphi_n(x) = \sqrt{2}\sin(n\pi x)$$

and the associated eigenvalues $\lambda_n = -n^4\pi^4$. Applying the above Algorithm, the simulations give the following results.

4.3. First case: $\omega =]0.3,\ 0.9[$

▷ Zone of action $D =]0.4,\ 0.8[$.

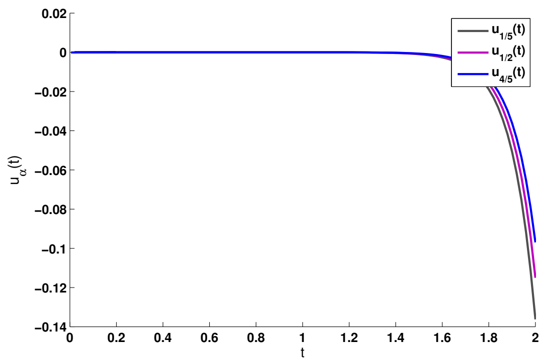

Figure 2. Control Function.

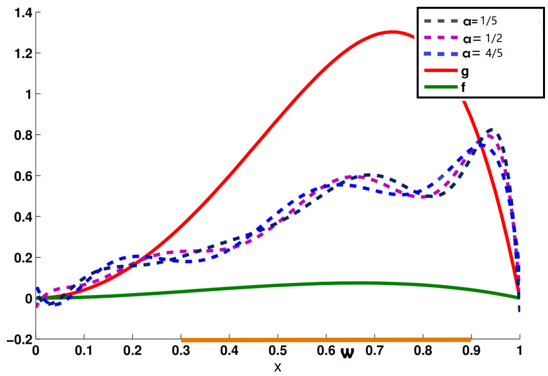

Figure 3. Final state between $[f(.),\ g(.)]$

Figure 2 displays the evolution of the control function over $[0,\ T = 2]$. Figure 3 shows that the fractional final state with different values of α is between $f(.)$ and $g(.)$ on ω. Therefore, the $[f(.),\ g(.)]$-controllability on ω is obtained with transfer cost $\|u^\star_{\frac{1}{5}}\|^2 = 0.258$, $\|u^\star_{\frac{1}{2}}\|^2 = 0.164$ and $\|u^\star_{\frac{4}{5}}\|^2 = 0.0912$.

Example 2:
Let $\Omega =]0,\ 1[$ and consider the following system:

$$\begin{cases} \dfrac{\partial z}{\partial t}(t,x) = \dfrac{\partial^2 z}{\partial x^2}(t,x) + \mathcal{X}_D u(t), & \Omega \times]0,\ T[, \\ z(0,x) = 0, & x \in \Omega, \\ z(t,0) = z(t,1) = 0, & t \in]0,\ T[, \end{cases} \tag{22}$$

taking T $= 2$ and the actuator is located at D.
Let $f(x) = \dfrac{1}{2}x^2(1-x^2)$ and $g(x) = 4x(1-x)$.

The operator $Az = \dfrac{\partial^2 z}{\partial x^2}$ admits a complete set of eigenfunctions

$$\varphi_n(x) = \sqrt{2}\sin(n\pi x)$$

and the associated eigenvalues $\lambda_n = -n^2\pi^2$. The simulations provide the following outcomes after applying the aforesaid Algorithm.

4.4. Second case: $\omega =]0.25,\ 0.6[$

$\triangleright$ Zone of action $D =]0.1,\ 0.4[$

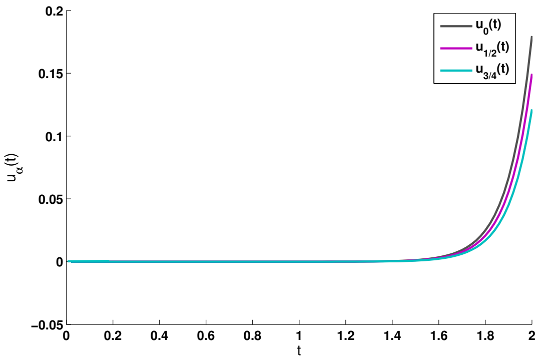

Figure 4. Control function

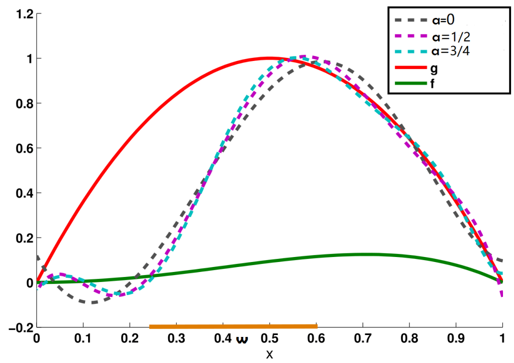

Figure 5. Final state between $[f(.),\ g(.)]$

Figure 4 displays the evolution of the control function over $[0,\ T = 2]$. Figure 5 shows that the fractional final state for various values of α is between $f(.)$ and $g(.)$ on ω. Therefore, the $[f(.),\ g(.)]$-controllability on ω is obtained with transfer cost $\|u_0^\star\|^2 = 0.0054$, $\|u_{\frac{1}{2}}^\star\|^2 = 0.0183$ and $\|u_{\frac{3}{4}}^\star\|^2 = 0.0038$.

Remark 1.

1) *The simulation results show the effectiveness of the proposed control approach in achieving the desired goal of maintaining the fractional state between two given functions over the subregion. Overall, Figures 2 and 4 provide a clear visual representation of the simulation results of the proposed control approach. The different plots in Figures 3 and 5 depict the behavior of the system's fractional state with varying values of the fractional order and constraint.*
2) *The relationship study between the monotonicity of the cost function and the order of the fractional derivative α is not obvious. However, the question still remains open.*

5. Conclusion

We studied the concept of regional controllability, which realizes a situation in which the fractional output of the system lies on between two known functions in a subregion of the evolution domain. Hence, we used two methods to characterize the optimal control. Additionally, we explored the numerical simulations to check the implementation of the theoretical part with different values of α and subregion ω.

Acknowledgments

The authors approve to express their gratitude to reviewers and editors for their thorough reading and helpful recommendations for improving the manuscript.

References

[1] Oldham, K., & Spanier, J. (1974). *The Fractional Calculus Theory and Applications of Differentiation and Integration to Arbitrary Order*. Elsevier.

[2] El Jai A., & El Yacoubi, S. (1993). On the number of actuators in parabolic system. *International Journal of Applied Mathematics and Computer Science*, 3(4), 673–686.

[3] Zerrik, E. (1994). Controlabilité et observabilité regionales d'une classe de systemes distribues. *PhD thesis Perpignan.*

[4] El Jai, A., Simon, C., & Zerrik, E., Pritchard, J. (1995). Regional controllability of distributed parameter systems. *International Journal of Control*, 62(6), 1351–1365.

[5] Zerrik, E., Boutoulout, A., & El Jai A. (2002). Actuators and regional boundary controllability of parabolic systems. *International Journal of Systems Science*, 31(1), 73–82.

[6] Zerrik, E., Boutoulout, A., & Bourray, H. (2001). Boundary strategic actuators. *Sensors and Actuators A: Physical*, 94(3), 197–203.

[7] Zerrik, E., & Ghafrani, F. (2002). Minimum energy control subject to output constraints: numerical approach. *IEE Proceedings-Control Theory and Applications*, 149(1), 105–110.

[8] Zerrik, E., & Ghafrani, F. (2003). Regional gradient-constrained control problem. Approaches and simulations. *Journal of dynamical and control systems*, 9(4), 585–599.

[9] Zerrik, E., Boutoulout, A., & Kamal, A. (1996). Regional gradient controllability of parabolic systems. *International Journal of Applied Mathematics and Computer Science*, 9(4), 767–787.

[10] Benoudi, M., & Larhrissi, R. (2023). Fractional controllability of linear hyperbolic systems. *International Journal of Dynamics and Control*, 11(3), 1375-1385.

[11] Xie, J., & Dubljevic, S. (2019). Discrete-time Kalman filter design for linear infinite-dimensional systems. *Processes*, 7(7), 451.

[12] Pazy, A. (1983). *Semi-Groups of Linear Operators and Applications to Partial Differential Equations*. Springer Verlag, New York.

[13] Podlubny, I., & Chen, Q. (2007). Adjoint fractional differential expressions and operators. *International Design Engineering Technical Conferences and Computers and Information in Engineering Conference*, 4806, 1385–1390.

[14] Miller, S., & Ross, B. (1993). *An Introduction to the Fractional Calculus and Fractional Differential Equations*. Wiley.

[15] Ioffe, A. D. (2012). On the theory of sub differentials. *Advances in Nonlinear Analysis*, 1, 47-120.

[16] Labrousse, J-Ph., M'bekhta, M. (1992). Les opérateurs points de continuité pour la conorme et l'inverse de Moore-Penrose. *Houston Journal of Mathematics*, 18(1), 7-23.

[17] Yosida, K. (1980). *Functional Analysis*. Springer Verlag, Berlin-Heidelberg, New York.

[18] Fortin, M., & Glowinski, R. (2000). *Augmented Lagrangian Methods: Applications to the Numerical Solution of Boundary Value Problems*. Elsevier, North-Holland-Amsterdam, New York, Oxford.

Rachid Larhrissi *is a professor at the University of Moulay Ismail of Meknes, Morocco. He got his doctorate in Control Theory (2003) at the Faculty of Sciences in Meknes. He wrote many papers in the area of systems analysis and control.*

https://orcid.org/0000-0001-5664-3660

Mustapha Benoudi *is a doctorate researcher in Applied Mathematics at Moulay Ismail University, Meknes, Morocco. His research field is the analysis and control of infinite dimensional systems and fractional calculus.*

https://orcid.org/0000-0002-5647-434X

An International Journal of Optimization and Control: Theories & Applications
ISSN:2146-0957 eISSN:2146-5703
Vol.13, No.2, pp.244-258 (2023)
http://doi.org/10.11121/ijocta.2023.1366

RESEARCH ARTICLE

The effect of fractional order mathematical modelling for examination of academic achievement in schools with stochastic behaviors

Pelin Yaprakdal Uzun,[a] Kıvanç Uzun,[b] Ilknur Koca[c] *

[a] *Department of Mathematics, Institute of Science, Burdur Mehmet Akif Ersoy University, Burdur, Turkey*
[b] *Career Development Practice and Research Center, Burdur Mehmet Akif Ersoy University, Burdur, Turkey*
[c] *Department of Accounting and Financial Management, Seydikemer High School of Applied Sciences, Mugla Sıtkı Kocman University, Mugla, Turkey*
pelinyaprakdal@gmail.com, kuzun@mehmetakif.edu.tr, ilknurkoca@mu.edu.tr

ARTICLE INFO

Article History:
Received 1 February 2023
Accepted 21 March 2023
Available 29 July 2023

Keywords:
Academic achievement
Fractional differential equation
Crossover behaviour
Numerical simulation

AMS Classification 2010:
26A33; 34A34; 35B44; 65M06

ABSTRACT

Academic achievement is very important, as it enables students to be well-equipped for professional and social life and shapes their future. In the case of a possible academic failure, students generally face many cognitive, social, psychological, and behavioral problems. This problem experienced by the students has been addressed with the mathematical model in this study. This mathematical model will be handled with the help of the fractional operator, and the existence, uniqueness, and positivity of the solutions to the model equation system will be examined. In addition, local and global stability analyses of the equilibrium points of the model are planned. Numerical simulations are performed with different values of fractional orders and densities of randomness. This study is very important in terms of its original and multidisciplinary approach to a subject in the field of social sciences.

1. Introduction

Academic achievement is an almost compulsory process that occurs as a result of social progress. Because the professions that emerge as a result of the division of labor require very broad and comprehensive knowledge, as well as technical expertise and new perspectives, It has become a necessity for individuals who want to have a job and a profession to enroll in long and comprehensive education programs and succeed in teaching processes in order to acquire knowledge and skills related to that profession. The concept of success is expressed as reaching the desired result, reaching the intended goal, and achieving the desired [1]. Academic achievement, on the other hand, is defined as the skills or the expression of learned knowledge that are developed in the lessons taught at school and determined by grades appreciated by teachers, test scores, or both [2]. In addition to the grades deemed appropriate by the teachers, the recently developed standard achievement tests are also preferred as a criterion for measuring academic achievement [3]. Some criteria are taken into account when determining whether a student is academically accomplished. Some of these criteria are the general goals and desired behaviors determined for the education level of the student, the overall success of the student's class or group, all the topics that need to be learned, norms of achievement developed at the country or local level, opinions of teachers and relevant experts, the student's own level of ability, the student's level of success at entry to the education program, the student's socioeconomic level, and current conditions and opportunities [4]. Another important academic achievement criterion is grade point average (GPA). According to York, Gibson, and

*Corresponding Author

Rankin, GPA is one of the best indicators to reflect the academic achievement of students [5]. The GPA is a summary of all the effort put forth by the student in a given time period. GPA is not based on a single course but can be defined as the numerical expression of the achievements obtained from different courses in which various tasks are given. From this point of view, while determining the main actors of this research, the grade point averages of the students were taken into account. The students were handled in three different groups: those with achievement above GPA, those with average achievement, and those with below average achievement. With the help of the mathematical model developed within the scope of this research, it is aimed to determine the main factors that play a role in determining the academic achievement levels of students, to what extent they are effective, and to determine their relations with each other, to determine the level of academic failure in schools, and to obtain important findings about how to prevent failure. The tendency of students toward academic achievement is not only related to the individual characteristics of students but also to the fact that many factors such as family and social-cultural environment play a role. Studies have shown that students who achieve academically owe their success primarily to themselves, while family and school are shown as auxiliary factors [6]. In this context, it can be said that all three factors are important in studies aimed at increasing academic achievement. In the meta-analysis study conducted by Sarer, self-efficacy perception, student motivation, and self-esteem came to the fore as factors related to academic achievement with students [7]. Self-efficacy refers to an individual's personal judgment of his or her ability to perform in any field [8]. An individual's self-efficacy belief affects whether he or she can successfully perform a given job [9]. In this context, it can be said that a positive self-efficacy belief motivates the individual to be successful, encourages the unknown and difficult tasks to be overcome, and encourages them to make an effort [10]. Studies have shown that there is a highly significant relationship between students' self-efficacy and academic achievement [11], they revealed that self-efficacy and motivation are important predictors of academic achievement [12]. As students succeed in the academic field, their self-efficacy will increase, and they will be more motivated for academic achievement [13]. Another individual characteristic that affects the academic achievement of students is motivation. Academic achievement motivation can be defined as doing an action skillfully, accomplishing it perfectly, overcoming obstacles, doing better than others, resisting failure, and striving to accomplish a task [14]. In this context, it can be said that high motivation for academic achievement will lead to high academic achievement. The social cognitive approach emphasizes that motivation can change with the influence of the social environment. From this point of view, success motivation is not a fixed feature for the student; it can be said that it varies in relation to class, school, social environment, family, and the context of the subject. The last factor related to academic achievement is self-esteem. Rosenberg conceptualized self-esteem as a positive or negative attitude towards the self, which is derived from the sum of self-evaluation across different domains [15]. When the literature is examined, it is understood that there is a positive relationship between self-esteem and academic achievement [16]. In this context, it can be said that positive self-esteem will increase students' academic achievement. Another important factor affecting the academic achievement of students is family. In his meta-analysis study, Sarer determined the family-related factors affecting the academic achievement of students as parents' attitudes and behaviors, participation in education, the educational status of parents, and the socioeconomic level of the family [7]. The child is born into a family environment. It should not be overlooked that this environment has a significant impact on the child's social adaptation and personality development, as well as on academic achievement [17]. The family is the first institution where the child starts school. The child forms his/her perspective on education for the first time here [18]. If a home is a place where the child's basic needs are met and he lives in peace and security, this positive atmosphere will contribute to the child's self-confidence in school [19]. In addition to a healthy and orderly family environment, the parents' interest in and inclinations toward the academic field will positively affect the child's interest in academic activities and his or her desire to achieve success. The education level of the parents is another factor that shapes the academic achievement of the child. It is known that as the education level of the parents increases, the attitudes of the parents change positively [20], which enables parents to act more consciously about their children's educational lives. In addition, the socioeconomic level of the family is shown as one of the most important factors affecting the child's ability, interests, and attitude toward education, and thus his success and harmony at school [21]. Studies have shown that as the socioeconomic status of the family increases, students' success [22] and their motivation may increase [23]. The last important factor that affects the academic achievement of students is school. In his meta-analysis study, Sarer found some school-related factors that are determinants of academic achievement: school culture, teacher behavior, and the leadership of the school principal [7]. Students spend most of their daily lives at school. For this reason, it is inevitable that the structure of the school and the attitudes of teachers will have significant effects on students' behavior and academic achievement [17]. The existence of a positive school climate not only facilitates students' academic achievement and learning but also contributes to their healthy social and emotional development [24]. The dominant culture in a school has an impact on the behavior of everyone working in that school and on students. A collaborative or positive school culture causes students to be more committed to the school's goals, and as a result, academic achievement rises. Otherwise, academic achievement is expected to be low [25]. On the other hand, it was found that the supportive behaviors of the teachers increased the success of the students. It is known that children who perceive the school environment as safe and supportive have higher school success [26]. In addition to the observations and inspections he makes, the decisions he makes, and the high expectations he creates for teaching, the school principal can significantly affect the academic achievement of the students with his leadership behaviors, such as providing the necessary resources for quality education, evaluating and developing teachers, and leading the formation of a learning-centered school climate [27]. It can be seen that all these variables, which are effective on the academic achievement of the students, interact with each other and determine which group the student will be in in terms of academic achievement. Because of the interaction between the variables, academic achievement in this study was handled with the mathematical model developed through the metapopulation model. Mathematical models can be helpful in explaining a system, examining the effects of different components, and predicting behavior. Mathematical models can be used in the social sciences (economics, psychology, sociology, political science, etc.) as well as the natural sciences (physics, biology, earth science, meteorology, etc.) and engineering disciplines (computer science, artificial intelligence, etc.) [28–33]. In the literature review, it was understood that a comprehensive mathematical model for academic achievement, which is an extremely important concept for social sciences and students, has not yet been developed and that the limited number of studies [34] are still at the initial level. Based on this deficiency in the literature, our study aimed to develop a realistic mathematical model for academic achievement. The idea seems efficient if we model problems with crossover behaviors. Because of this, in this paper, we aim to modify a metapopulation model with the concept of stochastic situations.

2. Preliminaries

In this section, we give some important definitions of non-integer fractional derivatives and their useful properties [35–37].

Definition 1. *The Gamma function* $\Gamma(x)$ *is defined by the integral expression given as*

$$\Gamma(x) = \int_0^\infty e^{-t} t^{x-1} dt, \tag{1}$$

which converges in the right half of the complex plane $Re(x) > 0$.

Definition 2. *Riemann-Liouville definition of fractional order differ-integral:*

$${}_aD_t^{\upsilon} f(t) = \frac{1}{\Gamma(n-\upsilon)} \frac{d^n}{dt^n} \int_a^t (t-\tau)^{n-\upsilon-1} f(\tau)\, d\tau, \tag{2}$$

where

$$n-1 < \upsilon \leqslant n, n \in \mathbb{N} \tag{3}$$

and $\upsilon \in \mathbb{R}$ *(*$\mathbb{R}$ *is the set of real numbers) is a fractional order of the differ-integral of the function* $f(t)$.

Definition 3. *Caputo's definition of fractional order differ-integral:*

$${}_a^CD_t^{\upsilon} f(t) = \frac{1}{\Gamma(\upsilon-n)} \int_a^t \frac{f^n(\tau)}{(t-\tau)^{\upsilon+1-n}} d\tau, \tag{4}$$

where $n-1 < \upsilon \leqslant n, n \in \mathbb{N}$, $\upsilon \in \mathbb{R}$ *is a fractional order of the differ-integral of the function* $f(t)$.

Definition 4. *Let* f *be continuous not necessary differentiable in* $[t_1, T]$. *Thus, the piecewise Riemann-Liouville derivative is presented as*

$${}_0^{PRL}D_t^{\upsilon} f(t) = \begin{cases} f'(t), & \text{if } 0 \le t \le t_1 \\ {}_{t_1}^{RL}D_t^{\upsilon} f(t), & \text{if } t_1 \le t \le T \end{cases}, \tag{5}$$

where ${}_0^{PRL}D_t^{\upsilon}$ *presents classical derivative on* $0 \le t \le t_1$ *and Riemann-Liouville fractional derivative on* $t_1 \le t \le T$.

Definition 5. *Let f be continuous and $\upsilon > 0$ then a piecewise integral of f is given as*

$$
{}^{PPL}J_t^{\upsilon} f(t) = \begin{cases} \int\limits_0^{t_1} f(\tau)d\tau, & \text{if } 0 \le t \le t_1 \\ \frac{1}{\Gamma(\upsilon)} \int\limits_{t_1}^{t} (t-\tau)^{\upsilon-1} f(\tau)d\tau, & \text{if } t_1 \le t \le T \end{cases} \tag{6}
$$

where ${}^{PPL}J_t^{\upsilon} f(t)$ presents classical integral on $0 \le t \le t_1$ and the integral with power-law kernel on $t_1 \le t \le T$.

3. Model derivation

In this paper, we considered and studied an academic achievement model with given standard incidence with takes the following form [34]:

$$
\begin{aligned}
\frac{dP}{dt} &= \mu - \beta PK - \mu P + \alpha I, \\
\frac{dK}{dt} &= \beta PK - \mu K - \delta(1-\gamma) K, \\
\frac{dI}{dt} &= \delta(1-\gamma) K - (\mu + \alpha) I,
\end{aligned} \tag{7}
$$

where P, K, I denotes the numbers of students with above average achievement (aac) at any time t, students with average achievement (ac), students with below-average achievement (bac) and $N = P + K + I$ is the number of total population of individuals.

$$
P(t_0) = P_0, \; K(t_0) = K_0 \text{ and } I(t_0) = I_0. \tag{8}
$$

The parameter β denotes the rate of students exposed to negative teacher attitudes; μ denotes rate of students with academic motivation; γ is rate of students with high self-efficacy, δ denotes the rate of students with low self-esteem and α denotes the rate of students with positive family attitudes. The parameters involved in the system (7) are all positive constans.

Fractional calculus, which means fractional derivatives and fractional integrals is of increasing interest among researchers. It is known that fractional operators describe the system behavior more accurately and efficiently than integer-order derivatives. Because of the great advantage of memory properties, let us modify the above system by replacing the integer-order time derivative by the Caputo fractional derivative below:

$$
\begin{aligned}
{}_0^C D_t^{\alpha} P(t) &= \mu - \beta PK - \mu P + \alpha I, \\
{}_0^C D_t^{\alpha} K(t) &= \beta PK - \mu K - \delta(1-\gamma) K, \\
{}_0^C D_t^{\alpha} I(t) &= \delta(1-\gamma) K - (\mu + \alpha) I,
\end{aligned} \tag{9}
$$

with the initial conditions

$$
P(t_0) = P_0, K(t_0) = K_0 \text{ and } I(t_0) = I_0. \tag{10}
$$

3.1. Positiveness and boundness of solutions

In this section, to show the positivity of the solutions of system for $\forall t \geqslant 0$, we define the norm

$$
\|f\|_{\infty} = \sup_{t \in [0,T]} |f(t)|. \tag{11}
$$

Let us write the system and start with the second equation

$$
\begin{aligned}
\frac{dP(t)}{dt} &= \mu - \beta P(t) K(t) - \mu P(t) + \alpha I(t), \forall t \geqslant 0, \\
&\ge -(\beta K(t) + \mu) P(t), \forall t \geqslant 0, \\
&\ge -\left(\beta \sup_{t \in [0,T]} |K(t)| + \mu\right) P(t), \forall t \geqslant 0, \\
&\ge -(\beta \|K\|_{\infty} + \mu) P(t), \forall t \geqslant 0.
\end{aligned} \tag{12}
$$

Then this provides that

$$
P(t) \ge P_0 e^{-(\beta\|K\|_{\infty} + \mu)t}, \forall t \geqslant 0. \tag{13}
$$

Secondly for the function $I(t)$, we obtain

$$
\begin{aligned}
\frac{dI(t)}{dt} &= \delta(1-\gamma) K(t) - (\mu + \alpha) I(t), \forall t \geqslant 0, \\
&\ge -(\mu + \alpha) I(t), \forall t \geqslant 0.
\end{aligned} \tag{14}
$$

So this provides that

$$
I(t) \ge I_0 e^{-(\mu+\alpha)t}, \forall t \geqslant 0. \tag{15}
$$

Finally we assume that $P(t) K(t)$ are nonnegative then for the function $K(t)$, we obtain

$$
\begin{aligned}
\frac{dK(t)}{dt} &= \beta P(t) K(t) - \mu K(t) - \delta(1-\gamma) K(t), \forall t \geqslant 0, \\
&\ge -(\mu + \delta(1-\gamma)) K(t), \forall t \geqslant 0.
\end{aligned}
$$

This provides that

$$
K(t) \ge K_0 e^{-(\mu + \delta(1-\gamma))t}, \forall t \geqslant 0. \tag{16}
$$

Now let us check for the following total population size is given by

$$\begin{aligned} N'(t) &= P'(t) + K'(t) + I'(t) \\ &= \mu - \beta P(t) K(t) - \mu P(t) + \alpha I(t) \\ &+ \beta P(t) K(t) - \mu K(t) - \delta(1-\gamma) K(t) \\ &+ \delta(1-\gamma) K(t) - (\mu+\alpha) I(t) \\ &= \mu - \mu(P(t) + K(t) + I(t)) \\ &= \mu - \mu N(t) \end{aligned} \tag{17}$$

Integrating over $[0, t]$ then we get,

$$N(t) = 1 - e^{-\mu t} + N(0) e^{-\mu t}, \tag{18}$$
$$\lim_{t\to\infty} N(t) = 1.$$

So the model has the following feasible region

$$\Gamma = \left\{ P(t), K(t), I(t) \in R_+^3 : N(t) \le 1 \right\}. \tag{19}$$

3.2. Equilibrium points of system

In this subsection, we find equilibrium points by solving the equations obtained by equating time derivatives in the system to zero.

$$\begin{aligned} P'(t) &= \mu - \beta P(t) K(t) - \mu P(t) + \alpha I(t) = 0, \\ K'(t) &= \beta P(t) K(t) - \mu K(t) - \delta(1-\gamma) K(t) = 0, \\ I'(t) &= \delta(1-\gamma) K(t) - (\mu+\alpha) I(t) = 0. \end{aligned}$$

Then we write

$$\begin{aligned} \mu - \beta P^* K^* - \mu P^* + \alpha I^* &= 0, \\ \beta P^* K^* - \mu K^* - \delta(1-\gamma) K^* &= 0, \\ \delta(1-\gamma) K^* - (\mu+\alpha) I^* &= 0. \end{aligned} \tag{20}$$

From the last equality, we get

$$\delta(1-\gamma) K^* = (\mu+\alpha) I^*, \tag{21}$$
$$K^* = \frac{(\mu+\alpha)}{\delta(1-\gamma)} I^*$$

and from the second equality we get

$$\beta P^* K^* = \mu K^* + \delta(1-\gamma) K^*, \tag{22}$$
$$P^* = \frac{\mu + \delta(1-\gamma)}{\beta}.$$

If we put them in the first equation we will get following

$$\begin{aligned} \mu - (\beta K^* + \mu) P^* + \alpha I^* &= 0, \\ \mu - \left(\beta \frac{(\mu+\alpha)}{\delta(1-\gamma)} I^* + \mu\right) \left(\frac{\mu + \delta(1-\gamma)}{\beta}\right) + \alpha I^* &= 0, \\ \mu - \left\{ (\mu+\alpha) I^* \left(\frac{\mu}{\delta(1-\gamma)} + 1\right) + \frac{\mu^2 + \delta\mu(1-\gamma)}{\beta} \right\} + \alpha I^* &= 0, \end{aligned}$$

from the last equality

$$I^* = \frac{\mu - \frac{\mu^2 + \delta\mu(1-\gamma)}{\beta}}{(\mu+\alpha)\left(\frac{\mu}{\delta(1-\gamma)} + 1\right) - \alpha}. \tag{23}$$

So we have success equilibrium point $E^* = (P^*, K^*, I^*)$ given as:

$$E^* = \left(\frac{\mu + \delta(1-\gamma)}{\beta}, \frac{(\mu+\alpha)}{\delta(1-\gamma)} I^*, \frac{\mu - \frac{\mu^2 + \delta\mu(1-\gamma)}{\beta}}{(\mu+\alpha)\left(\frac{\mu}{\delta(1-\gamma)} + 1\right) - \alpha} \right), \tag{24}$$

and success free equilibrium point $E^0 = \left(P^0, K^0, I^0\right) = (1, 0, 0)$ given as

$$\begin{aligned} \mu - \beta P^* K^* - \mu P^* + \alpha I^* &= 0, \\ \beta P^* K^* - \mu K^* - \delta(1-\gamma) K^* &= 0, \\ \delta(1-\gamma) K^* - (\mu+\alpha) I^* &= 0, \end{aligned} \tag{25}$$

$$\begin{aligned} K^* = 0 \ &and \ I^* = 0, \\ \mu - \mu P^* &= 0, \\ \mu &= \mu P^*, \\ P^* &= 1. \end{aligned} \tag{26}$$

3.3. Reproductive number for model

Here we will discuss the reproductive number of the academic achievement model by considering the next generation matrix method. Remembering the system;

$$\begin{aligned} \frac{dP(t)}{dt} &= \mu - \beta P(t) K(t) - \mu P(t) + \alpha I(t), \\ \frac{dK(t)}{dt} &= \beta P(t) K(t) - \mu K(t) - \delta(1-\gamma) K(t), \\ \frac{dI(t)}{dt} &= \delta(1-\gamma) K(t) - (\mu+\alpha) I(t), \end{aligned} \tag{27}$$

and divide the system into two parts.

We call f with the nonlinear part of system and V is called with linear part of system as below:

$$\begin{bmatrix} P' \\ K' \\ I' \end{bmatrix} = f - V. \tag{28}$$

So we have the following matrices

$$f = \begin{bmatrix} -\beta P(t) K(t) \\ \beta P(t) K(t) \\ 0 \end{bmatrix}, V = \begin{bmatrix} -\mu + \mu P(t) - \alpha I(t) \\ \mu K(t) + \delta(1-\gamma) K(t) \\ -\delta(1-\gamma) K(t) + (\mu+\alpha) I(t) \end{bmatrix}, \tag{29}$$

From the above matrices, we will obtain F and V which are partial derivatives of f and V.

$$F = \begin{bmatrix} -\beta K & -\beta P & 0 \\ \beta K & \beta P & 0 \\ 0 & 0 & 0 \end{bmatrix}, V = \begin{bmatrix} \mu & 0 & -\alpha \\ 0 & \mu + \delta (1-\gamma) & 0 \\ 0 & -\delta (1-\gamma) & \mu + \alpha \end{bmatrix} \tag{30}$$

and

$$V^{-1} = \begin{bmatrix} \frac{1}{\mu} & \frac{\alpha\delta(1-\gamma)}{\mu^3+\mu^2\alpha+\mu^2\delta(1-\gamma)+\mu\alpha\delta(1-\gamma)} & \frac{\alpha}{\mu^2+\mu\alpha} \\ 0 & \frac{1}{\mu+\delta(1-\gamma)} & 0 \\ 0 & \frac{\delta(1-\gamma)}{\mu^2+\mu\alpha+\mu\delta(1-\gamma)+\alpha\delta(1-\gamma)} & \frac{1}{\mu+\alpha} \end{bmatrix}, \tag{31}$$

$$F(E_0) = \begin{bmatrix} 0 & -\beta & 0 \\ 0 & \beta & 0 \\ 0 & 0 & 0 \end{bmatrix}, \tag{32}$$

$$FV^{-1}(E_0) = \begin{bmatrix} 0 & \frac{-\beta}{\mu+\delta(1-\gamma)} & 0 \\ 0 & \frac{\beta}{\mu+\delta(1-\gamma)} & 0 \\ 0 & 0 & 0 \end{bmatrix}, \tag{33}$$

$$R_0 = \max\{\lambda_i\}_{i=1,2,3} \tag{34}$$

where λ_i are obtained from

$$\left|FV^{-1} - \lambda I\right| = 0. \tag{35}$$

So we have the following reproductive number which is important for us while deciding the analysis

$$R_0 = \frac{\beta}{\mu + \delta(1-\gamma)}. \tag{36}$$

3.4. Strength number

The concept of strength number (A_0) has been suggested and will be used in this section [38]. The component F_A is obtained with deriving the nonlinear part of the model classes. In our model there are two nonlinear classes given by

$$\frac{dP(t)}{dt} = \mu - \beta P(t) K(t) - \mu P(t) + \alpha I(t), \tag{37}$$
$$\frac{dK(t)}{dt} = \beta P(t) K(t) - \mu K(t) - \delta(1-\gamma) K(t).$$

Again here we use nonlinear parts for $\frac{dP(t)}{dt}$ and $\frac{dK(t)}{dt}$ classes

$$\frac{dP(t)}{dt} = -\beta P(t) K(t), \tag{38}$$
$$\frac{dK(t)}{dt} = \beta P(t) K(t).$$

Then

$$\frac{\partial}{\partial P} = -\beta K(t), \tag{39}$$
$$\frac{\partial}{\partial K} = -\beta P(t),$$

and

$$\frac{\partial^2}{\partial P^2} = 0, \tag{40}$$
$$\frac{\partial^2}{\partial K^2} = 0.$$

In this case, we can have the following

$$F_A = \begin{bmatrix} 0 \\ 0 \end{bmatrix}. \tag{41}$$

Then

$$\det(F_A V^{-1} - \lambda I) = 0, \tag{42}$$

leads to

$$A_0 = 0. \tag{43}$$

$A_0 = 0$ means there is no strength. Also, there are more conclusions when strength is zero. Students will get motivation for having good marks and expecting a good future, therefore, the number of incompetent students.

4. Stability analysis of equilibrium points

In this section, a detailed analysis of equilibrium points is presented. To do this we search for local and global stability.

4.1. Local stability analysis

There exist two equilibrium points of the model that are found by solving the equations obtained by equating time derivatives in the system to zero.Then we have $E^0 = (1,0,0)$ and $E^* = (P^*, K^*, I^*)$.

Theorem 1. *The academic achievement free equilibrium point E^0 of system is locally asymptotically stable if and only if $R_0 < 1$.*

Proof. Let us consider the right sides of equations by solving functions $F_i : 1 \leq i \leq 3$.

$$F_1(t, P(t)) = \mu - \beta P(t) K(t) - \mu P(t) + \alpha I(t),$$
$$F_2(t, K(t)) = \beta P(t) K(t) - \mu K(t) - \delta(1-\gamma) K(t),$$
$$F_3(t, I(t)) = \delta(1-\gamma) K(t) - (\mu + \alpha) I(t). \tag{44}$$

The Jacobian matrix of the system is given by

$$J=\begin{bmatrix} \frac{\partial F_1}{\partial P} & \frac{\partial F_1}{\partial K} & \frac{\partial F_1}{\partial I} \\ \frac{\partial F_2}{\partial P} & \frac{\partial F_2}{\partial K} & \frac{\partial F_2}{\partial I} \\ \frac{\partial F_2}{\partial P} & \frac{\partial F_3}{\partial K} & \frac{\partial F_3}{\partial I} \end{bmatrix} \tag{45}$$
$$=\begin{bmatrix} -\beta K-\mu & -\beta P & \alpha \\ \beta K & \beta P-\mu-\delta(1-\gamma) & 0 \\ 0 & \delta(1-\gamma) & -(\mu+\alpha) \end{bmatrix}$$

at $E^0=(1,0,0)$,

$$J=\begin{bmatrix} -\mu & -\beta & \alpha \\ \beta K & \beta-\mu-\delta(1-\gamma) & 0 \\ 0 & \delta(1-\gamma) & -(\mu+\alpha) \end{bmatrix}. \tag{46}$$

If we solve the associated characteristic equation we will get the following eigenvalues;

The academic achievement free equilibrium point is asymptotically stable if all of the eigenvalues λ_1,λ_2,λ_3 of $J(E^0)$ satisfy the condition

$$|\arg\lambda_i|>\frac{\upsilon\pi}{2}, i=1,2,3. \tag{47}$$

These eigenvalues can be determined by solving the characteristic equation $\det(J(E^0)-\lambda I)=0$ which leads to the following equation;

$$\det(J(E^0)-\lambda I)$$
$$=\begin{vmatrix} -\mu-\lambda & -\beta & \alpha \\ \beta K & \beta-\mu-\delta(1-\gamma)-\lambda & 0 \\ 0 & \delta(1-\gamma) & -(\mu+\alpha)-\lambda \end{vmatrix}, \tag{48}$$
$$=(-\mu-\lambda)(\beta-\mu-\delta(1-\gamma)-\lambda)(-(\mu+\alpha)-\lambda)$$

$$\lambda_1=\mu,\ \lambda_2=\beta-\mu-\delta(1-\gamma) \text{ and } \lambda_3=-(\mu+\alpha). \tag{49}$$

Here λ_1,λ_3 are negative. For λ_2 following must be satisfied;

$$\lambda_2=\beta-\mu-\delta(1-\gamma)<0, \tag{50}$$
$$\beta<\mu+\delta(1-\gamma),$$
$$R_0=\frac{\beta}{\mu+\delta(1-\gamma)}<1.$$

So the proof is completed. □

Theorem 2. *The academic achievement equilibrium point $E^*=(P^*,K^*,I^*)$ of system is locally asymptotic stable if and only if $R_0>1$.*

Proof. The Jacobian matrix $J(P^*,K^*,I^*)$ for the system given in (7) is.

$$J=\begin{bmatrix} -\beta K^*-\mu & -\beta P^* & \alpha \\ \beta K^* & \beta P^*-\mu-\delta(1-\gamma) & 0 \\ 0 & \delta(1-\gamma) & -(\mu+\alpha) \end{bmatrix}. \tag{51}$$

We now discuss the asymptotics stability of the $E^*=(P^*,K^*,I^*)$ equilibrium the system given before:

$$P^*=\frac{\mu+\delta(1-\gamma)}{\beta}, \tag{52}$$
$$K^*=\frac{(\mu+\alpha)}{\delta(1-\gamma)}I^*,$$
$$I^*=\frac{\mu-\frac{\mu^2+\delta\mu(1-\gamma)}{\beta}}{(\mu+\alpha)\left(\frac{\mu}{\delta(1-\gamma)}+1\right)-\alpha}.$$

The characteristic equation of the system is obtained via the determination of

$$L(\lambda)=\det(J-\lambda I)=0. \tag{53}$$

The characteristic roots are obtained by solving the following equation

$$L(\lambda)=\lambda^3+a_1\lambda^2+a_2\lambda+a_3=0. \tag{54}$$

where

$$a_1=\beta K^*+\mu-\beta P^*+\mu\delta(1-\gamma),$$
$$a_2=(\mu+\alpha)(\beta K^*+\mu-\beta P^*+\mu\delta(1-\gamma))$$
$$+\beta K^*\mu\delta(1-\gamma)-\mu\beta P^*+\mu^2\delta(1-\gamma),$$
$$a_3=(\mu+\alpha)\left(\beta K^*\mu\delta(1-\gamma)-\mu\beta P^*+\mu^2\delta(1-\gamma)\right)$$
$$-\alpha\beta K^*\delta(1-\gamma).$$

For $a_1,a_2,a_3>0$ and $a_1a_2-a_3>0$, so by Routh-Hurwitz Criterion, all characteristics roots have negative real parts [39]. Therefore academic achievement equilibrium point is asymptotic stable. □

4.2. Global stability of equilibrium point

In this section, we present the global stability of (PKI) model named by the academic achievement model. Let us consider the model again;

$$P'(t)=\mu-\beta P(t)K(t)-\mu P(t)+\alpha I(t)=0,$$
$$K'(t)=\beta P(t)K(t)-\mu K(t)-\delta(1-\gamma)K(t)=0,$$
$$I'(t)=\delta(1-\gamma)K(t)-(\mu+\alpha)I(t)=0. \tag{55}$$

Theorem 3. *If $R_0\geq 1$, the point $C^*(P^*,K^*,I^*)$ is global asymptotically stable.*

Proof. Here we show the proof of the theorem by using the Lyapunov function. We start with defining the Lyapunov function associated the system as below:

$$L(C^*(P^*,K^*,I^*))=\left(P-P^*+P^*\log\frac{P^*}{P}\right)$$
$$+\left(K-K^*+K^*\log\frac{K^*}{K}\right)+\left(I-I^*+I^*\log\frac{I^*}{I}\right).$$

By the derivative of the Lyapunov function with respect to t, we get

$$\begin{aligned} L'(t) &= \left(\frac{P-P^*}{P}\right)P' + \left(\frac{K-K^*}{K}\right)K' + \left(\frac{I-I^*}{I}\right)I', \\ &= \left(1-\frac{P^*}{P}\right)(\mu-\beta PK-\mu P+\alpha I) \\ &+ \left(1-\frac{K^*}{K}\right)(\beta PK-\mu K-\delta(1-\gamma)K) \\ &+ \left(1-\frac{I^*}{I}\right)(\delta(1-\gamma)K-(\mu+\alpha)I) \\ &= 0. \end{aligned} \tag{56}$$

Then we write;

$$\begin{aligned} L'(t) &= \mu-\beta PK-\mu P+\alpha I-\frac{P^*}{P}\mu+\beta P^*K+\mu P^*-\frac{P^*}{P}\alpha I \\ &+\beta PK-\mu K-\delta(1-\gamma)K-\beta PK^*+\mu K^*+\delta(1-\gamma)K^* \\ &+\delta(1-\gamma)K-(\mu+\alpha)I-\frac{I^*}{I}\delta(1-\gamma)K+(\mu+\alpha)I^*. \end{aligned}$$

Let us write above also two part (positive and negative terms) below;

$$L'(t) = \phi_1 - \phi_2, \tag{57}$$

where

$$\begin{aligned} \phi_1 &= \mu+\alpha I+\beta P^*K+\mu P^*, \\ &+\beta PK+\mu K^*+\delta(1-\gamma)K^*, \\ &+\delta(1-\gamma)K+(\mu+\alpha)I^*, \end{aligned} \tag{58}$$

and

$$\begin{aligned} \phi_2 &= \beta PK+\mu P+\frac{P^*}{P}\mu+\frac{P^*}{P}\alpha I, \\ &+\mu K+\delta(1-\gamma)K+\beta PK^*, \\ &+(\mu+\alpha)I+\frac{I^*}{I}\delta(1-\gamma)K. \end{aligned} \tag{59}$$

Therefore if

$$\begin{aligned} &\phi_1-\phi_2>0 \text{ then } L'(t)>0, \\ &\phi_1-\phi_2=0 \text{ then } L'(t)=0, \\ &\phi_1-\phi_2<0 \text{ then } L'(t)<0. \end{aligned} \tag{60}$$

□

5. Existence and uniqueness

In this section, we present a detailed analysis of the existence and uniqueness of the system of equations. To achieve this, the following theorem is to be verified [38].

Theorem 4. *Assume that there exists positive constants $\kappa_i, \overline{\kappa}_i$ such that*

(i) $\forall i \in \{1,2,3\}$,

$$\left|F_i(x_i,t)-F_i(x_i',t)\right|^2 \le \kappa_i\left|x_i-x_i'\right|^2. \tag{61}$$

(ii) $\forall(x,t)\in R^3\times[0,T]$,

$$|F_i(x_i,t)|^2 \le \overline{\kappa}_i\left(1+|x_i|^2\right). \tag{62}$$

We now recall our model,

$$\begin{aligned} \frac{dP(t)}{dt} &= \mu-\beta P(t)K(t)-\mu P(t)+\alpha I(t) = F_1(t,P), \\ \frac{dK(t)}{dt} &= \beta P(t)K(t)-\mu K(t)-\delta(1-\gamma)K(t) = F_2(t,K), \\ \frac{dI(t)}{dt} &= \delta(1-\gamma)K(t)-(\mu+\alpha)I(t) = F_3(t,I). \end{aligned}$$

We start with the function $F_1(t,P(t))$. Then we will show that

$$|F_1(P,t)-F_1(P_1,t)|^2 \le \kappa_1|P-P_1|^2. \tag{63}$$

Then, we write

$$\begin{aligned} |F_1(P,t)-F_1(P_1,t)|^2 &= |\mu-\beta PK-\mu P+\alpha I \\ &-\mu+\beta P_1K+\mu P_1-\alpha I|^2, \\ &= |P(-\beta K-\mu)-P_1(-\beta K-\mu)|^2, \\ &= |-\beta K-\mu|^2|P-P_1|^2, \\ &\le \left\{2\beta^2|K|^2+2\mu^2\right\}|P-P_1|^2, \\ &\le \left\{2\beta^2\sup_{t\in[0,T]}|K(t)|^2+2\mu^2\right\}|P-P_1|^2, \\ &\le \left\{2\beta^2\|K\|_\infty^2+2\mu^2\right\}|P-P_1|^2, \\ &\le \kappa_1|P-P_1|^2 \end{aligned}$$

where $\kappa_1 = \left\{2\beta^2\|K\|_\infty^2+2\mu^2\right\}$.

Now we continue the function $F_2(t,P(t))$. Then we get

$$\begin{aligned} |F_2(K,t)-F_2(K_1,t)|^2 &= \left|\begin{array}{c} \beta PK-\mu K-\delta(1-\gamma)K \\ -\beta PK_1+\mu K_1+\delta(1-\gamma)K_1 \end{array}\right|^2, \\ &\le \left\{2\beta^2|P|^2+2(\mu+\delta(1-\gamma))^2\right\} \\ &\quad\times|(K-K_1)|^2, \\ &\le \left\{2\beta^2\sup_{t\in[0,T]}|P(t)|^2+2(\mu+\delta(1-\gamma))^2\right\} \\ &\quad\times|(K-K_1)|^2, \\ &\le \left\{2\beta^2\|P\|_\infty^2+2(\mu+\delta(1-\gamma))^2\right\} \\ &\quad\times|(K-K_1)|^2, \\ &\le \kappa_2|(K-K_1)|^2 \end{aligned}$$

where

$$\kappa_2 = \left\{2\beta^2\|P\|_\infty^2+2(\mu+\delta(1-\gamma))^2\right\}. \tag{64}$$

Similary we get,

$$\begin{aligned}&|F_3(I,t)-F_3(I_1,t)|^2\\&=|\delta(1-\gamma)K-(\mu+\alpha)I-\delta(1-\gamma)K+(\mu+\alpha)I_1|^2,\\&=|-(\mu+\alpha)I+(\mu+\alpha)I_1|^2,\\&=|-(\mu+\alpha)|^2|(I-I_1)|^2,\\&\le 2(\mu^2+\alpha^2)|(I-I_1)|^2,\\&\le\kappa_3|(I-I_1)|^2\end{aligned}$$

where

$$\kappa_3=2(\mu^2+\alpha^2). \tag{65}$$

We verified the first condition for all functions. We now verify the second condition for our model.

$$\begin{aligned}|F_1(P,t)|^2&=|\mu-\beta PK-\mu P+\alpha I|^2,\\&\le 2\mu^2+2(\beta K+\mu)^2|P|^2+2\alpha^2|I|^2,\\&\le 2\mu^2+4\left(\beta^2|K|^2+\mu^2\right)|P|^2+2\alpha^2|I|^2,\\&\le 2\mu^2+4\left(\beta^2\sup_{t\in[0,T]}|K(t)|^2+\mu^2\right)|P|^2\\&+2\alpha^2\sup_{t\in[0,T]}|I(t)|^2,\\&\le\left(2\mu^2+2\alpha^2\|I\|_\infty^2\right)\left(1+\frac{2\left(\beta^2\|K\|_\infty^2+\mu^2\right)}{\mu^2+\alpha^2\|I\|_\infty^2}|P|^2\right),\\&\le\overline{\kappa}_1\left(1+|P|^2\right)\end{aligned}$$

under the condition

$$\frac{2\left(\beta^2\|K\|_\infty^2+\mu^2\right)}{\mu^2+\alpha^2\|I\|_\infty^2}<1, \tag{66}$$

and

$$\begin{aligned}|F_2(K,t)|^2&=|\beta PK-\mu K-\delta(1-\gamma)K|^2,\\&\le 3\left(\beta^2|P|^2+\mu^2+\delta^2(1-\gamma)^2\right)\left(1+|K|^2\right),\\&\le 3\left(\beta^2\sup_{t\in[0,T]}|P(t)|^2+\mu^2+\delta^2(1-\gamma)^2\right)\left(1+|K|^2\right),\\&\le 3\left\{\beta^2\|P\|_\infty^2+\mu^2+\delta^2(1-\gamma)^2\right\}\left(1+|K|^2\right),\\&\le\overline{\kappa}_2\left(1+|K|^2\right).\end{aligned}$$

Finally, we get

$$\begin{aligned}|F_3(I,t)|^2&=|\delta(1-\gamma)K-(\mu+\alpha)I|^2,\\&\le 2\delta^2(1-\gamma)^2|K|^2+2(\mu+\alpha)^2|I|^2,\\&\le 2\delta^2(1-\gamma)^2\sup_{t\in[0,T]}|K(t)|^2+2(\mu+\alpha)^2|I|^2,\\&\le 2\delta^2(1-\gamma)^2\|K\|_\infty^2\left(1+\frac{(\mu+\alpha)^2}{\delta^2(1-\gamma)^2\|K\|_\infty^2}|I|^2\right),\\&\le\overline{\kappa}_3\left(1+|I|^2\right)\end{aligned}$$

under the condition

$$\frac{(\mu+\alpha)^2}{\delta^2(1-\gamma)^2\|K\|_\infty^2}<1. \tag{67}$$

Therefore, if the condition on linear growth holds such that

$$\max\left\{\begin{array}{c}\frac{2\left(\beta^2\|K\|_\infty^2+\mu^2\right)}{\mu^2+\alpha^2\|I\|_\infty^2}\\\frac{(\mu+\alpha)^2}{\delta^2(1-\gamma)^2\|K\|_\infty^2}\end{array}\right\}<1, \tag{68}$$

the system of equations has a unique system of solutions. Therefore, if the condition on linear growth holds, the system has a unique solution.

6. Stochastic version of model

Stochastic modeling shows many interesting outcomes that account for certain levels of randomness. Also, stochastic models give different results for a set of values. Recently, many mathematicians have developed several stochastic mathematical models with the aim to show results more variability. So in this section, we convert the deterministic academic achievement model to the following system:

$$\begin{aligned}&dP(t)=[\mu-\beta P(t)K(t)-\mu P(t)+\alpha I(t)]\,dt+\sigma_1P(t)dB_1(t),\\&dK(t)=[\beta P(t)K(t)-\mu K(t)-\delta(1-\gamma)K(t)]\,dt+\sigma_2K(t)dB_2(t),\\&dI(t)=[\delta(1-\gamma)K(t)-(\mu+\alpha)I(t)]\,dt+\sigma_3I(t)dB_3(t),\\&P(0)=P_0,\ K(0)=K_0,\ \text{and } I(0)=I_0.\end{aligned}$$

We can present a numerical solution of the model by converting the stochastic model into an integral system below with different kernels, such as power, exponential and Mittag-Leffler.

6.1. Numerical Simulation for the stochastic-deterministic model of academic achievement

In this section, we give a numerical simulation of the system of fractional stochastic differential equations. The notion of piecewise that was recently suggested is perhaps the future of modeling processes with crossover in patterns. So we have made use of the model with the piecewise differential operators and the numerical scheme where the Lagrange polynomial interpolation is used [40]. While modeling with the piecewise idea, the first part is classical, the second part is fractional, and the last part is stochastic [36]. The numerical simulation is performed for different values of fractional orders. So the stochastic-deterministic model is given as

$$\left\{\begin{array}{l}\frac{dP(t)}{dt}=\mu-\beta P(t)K(t)-\mu P(t)+\alpha I(t),\\\frac{dK(t)}{dt}=\beta P(t)K(t)-\mu K(t)-\delta(1-\gamma)K(t),\quad\text{if } 0\le t\le W_1\\\frac{dI(t)}{dt}=\delta(1-\gamma)K(t)-(\mu+\alpha)I(t),\end{array}\right. \tag{69}$$

$$\begin{cases} {}^{C}_{w_1}D_t^{\upsilon}P(t) = \mu - \beta P(t)K(t) - \mu P(t) + \alpha I(t), \\ {}^{C}_{w_1}D_t^{\upsilon}K(t) = \beta P(t)K(t) - \mu K(t) - \delta(1-\gamma)K(t), \\ {}^{C}_{w_1}D_t^{\upsilon}I(t) = \delta(1-\gamma)K(t) - (\mu+\alpha)I(t), \end{cases} \tag{70}$$

$$\text{if } W_1 \le t \le W_2$$
$$0 < \upsilon \le 1.$$

$$\begin{cases} dP(t) = [\mu - \beta P(t)K(t) - \mu P(t) + \alpha I(t)]\,dt + \sigma_1 P(t)dB_1(t), \\ dK(t) = [\beta P(t)K(t) - \mu K(t) - \delta(1-\gamma)K(t)]\,dt + \sigma_2 K(t)dB_2(t), \\ dI(t) = [\delta(1-\gamma)K(t) - (\mu+\alpha)I(t)]\,dt + \sigma_3 I(t)dB_3(t), \end{cases} \tag{71}$$

if $W_2 \le t \le W$. For simplicity, we consider right side of the system as

$$\begin{cases} \dot{P} = F_1(P,K,I), \\ \dot{E} = F_2(P,K,I), \\ \dot{I} = F_3(P,K,I). \end{cases} \tag{72}$$

Using the numerical scheme presented in this paper with piecewise derivative, the numerical solution of the stochastic-deterministic model is given as follows:

$$\begin{aligned} P_i^{n_1} &= P_i(0) + \sum_{k_1=0}^{n_1}\left\{\frac{3\Delta t}{2}F_1(t_{k_1},P(t_{k_1})) - F_1(t_{k_1-1},P(t_{k_1-1}))\frac{\Delta t}{2}\right\}, \quad 0 \le t \le W_1 \\ P_i^{n_2} &= P_i(W_1) + \frac{(\Delta t)^{\upsilon}}{\Gamma(\upsilon+2)}\sum_{k_2=n_1}^{n_2} F_1(t_{k_2},P(t_{k_2}))\times \begin{bmatrix} (n_2-k_2+1)^{\upsilon}(n_2-k_2+2+\upsilon) \\ -(n_2-k_2)^{\upsilon}(n_2-k_2+2+2\upsilon) \end{bmatrix} \quad W_1 \le t \le W_2 \\ &- \frac{(\Delta t)^{\upsilon}}{\Gamma(\upsilon+2)}\sum_{k_2=n_1}^{n_2} F_1(t_{k_2-1},P(t_{k_2-1}))\times \begin{bmatrix} (n_2-k_2+1)^{\upsilon+1} \\ -(n_2-k_2)^{\upsilon}(n_2-k_2+1+\upsilon) \end{bmatrix}, \\ P_i^{n_3} &= P_i(W_2) + \sum_{k_3=n_2}^{n_3}\left\{\begin{array}{c} \frac{3\Delta t}{2}F_1(t_{k_3},P(t_{k_3})) \\ -F_1(t_{k_3-1},P(t_{k_3-1}))\frac{\Delta t}{2} \end{array}\right\} \quad W_2 \le t \le W \\ &+ \sum_{k_3=n_2}^{n_3}\left\{\frac{\sigma}{2}\left(P(t_{k_3+1}) + P(t_{k_3})\right)\left(B(t_{k_3+1}) - B(t_{k_3})\right)\right\}, \end{aligned} \tag{73}$$

$$\begin{aligned} K_i^{n_1} &= K_i(0) + \sum_{k_1=0}^{n_1}\left\{\frac{3\Delta t}{2}F_2(t_{k_1},K(t_{k_1})) - F_2(t_{k_1-1},K(t_{k_1-1}))\frac{\Delta t}{2}\right\}, \quad 0 \le t \le W_1 \\ K_i^{n_2} &= K_i(W_1) + \frac{(\Delta t)^{\upsilon}}{\Gamma(\upsilon+2)}\sum_{k_2=n_1}^{n_2} F_2(t_{k_2},K(t_{k_2}))\times \begin{bmatrix} (n_2-k_2+1)^{\upsilon}(n_2-k_2+2+\upsilon) \\ -(n_2-k_2)^{\upsilon}(n_2-k_2+2+2\upsilon) \end{bmatrix}, \quad W_1 \le t \le W_2 \\ &- \frac{(\Delta t)^{\upsilon}}{\Gamma(\upsilon+2)}\sum_{k_2=n_1}^{n_2} F_2(t_{k_2-1},K(t_{k_2-1}))\times \begin{bmatrix} (n_2-k_2+1)^{\upsilon+1} \\ -(n_2-k_2)^{\upsilon}(n_2-k_2+1+\upsilon) \end{bmatrix} \\ K_i^{n_3} &= K_i(W_2) + \sum_{k_3=n_2}^{n_3}\left\{\begin{array}{c} \frac{3\Delta t}{2}F_2(t_{k_3},K(t_{k_3})) \\ -F_2(t_{k_3-1},K(t_{k_3-1}))\frac{\Delta t}{2} \end{array}\right\} \\ &W_2 \le t \le W. \\ &+ \sum_{k_3=n_2}^{n_3}\left\{\frac{\sigma}{2}\left(K(t_{k_3+1}) + K(t_{k_3})\right)\left(B(t_{k_3+1}) - B(t_{k_3})\right)\right\} \end{aligned} \tag{74}$$

$$\begin{aligned} I_i^{n_1} &= I_i(0) + \sum_{k_1=0}^{n_1}\left\{\frac{3\Delta t}{2}F_3(t_{k_1},I(t_{k_1})) - F_3(t_{k_1-1},I(t_{k_1-1}))\frac{\Delta t}{2}\right\}, \\ &0 \le t \le W_1, \\ I_i^{n_2} &= I_i(W_1) + \frac{(\Delta t)^{\upsilon}}{\Gamma(\upsilon+2)}\sum_{k_2=n_1}^{n_2} \cup_3(t_{k_2},I(t_{k_2}))\times \begin{bmatrix} (n_2-k_2+1)^{\upsilon}(n_2-k_2+2+\upsilon) \\ -(n_2-k_2)^{\upsilon}(n_2-k_2+2+2\upsilon) \end{bmatrix}, \quad W_1 \le t \le W_2 \\ &- \frac{(\Delta t)^{\upsilon}}{\Gamma(\upsilon+2)}\sum_{k_2=n_1}^{n_2} F_3(t_{k_2-1},I(t_{k_2-1}))\times \begin{bmatrix} (n_2-k_2+1)^{\upsilon+1} \\ -(n_2-k_2)^{\upsilon}(n_2-k_2+1+\upsilon) \end{bmatrix}, \\ I_i^{n_3} &= I_i(W_2) + \sum_{k_3=n_2}^{n_3}\left\{\begin{array}{c} \frac{3\Delta t}{2}F_3(t_{k_3},I(t_{k_3})) \\ -F_3(t_{k_3-1},I(t_{k_3-1}))\frac{\Delta t}{2} \end{array}\right\} \\ &W_2 \le t \le W. \\ &+ \sum_{k_3=n_2}^{n_3}\left\{\frac{\sigma}{2}\left(I(t_{k_3+1}) + I(t_{k_3})\right)\left(B(t_{k_3+1}) - B(t_{k_3})\right)\right\}. \end{aligned} \tag{75}$$

6.2. Numerical simulations

In this section, we show the numerical simulations for the considered stochastic model with piecewise derivative. Also, for the numerical simulations of the system, we consider the values of the parameters as follows:

$$\begin{gathered} \beta = 0.001, \mu = 0.002, \\ \gamma = 0.021, \delta = 0.029, \alpha = 0.047. \end{gathered} \tag{76}$$

In the model, the densities of randomness values for Figure 1-6 are given as

$$\sigma_1 = 0.19, \ \sigma_2 = 0.3, \ \sigma_3 = 0.4.$$

Figure 1-3 is given with fractional order $\upsilon = 1$ and Figure 4-6 is given with fractional order $\upsilon = 0.6$.

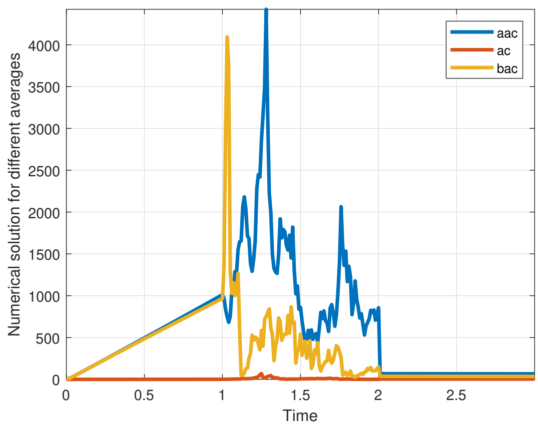

Figure 1. Numerical simulations of the system with initial conditions are given as $P(1) = 10$, $K(1) = 0$, $I(1) = 10$.

In Figure 1, It is also assumed that there are no students (ac) with average academic achievement in the school. When the simulation in Figure 1, drawn with this assumption, is examined, it is seen that when the number of students (aac) with academic achievement above the school's grade point average increases, the number of students (bac) with academic achievement below the average decreases. In this context, it has been understood that there is an inverse proportion between the number of students (aac) who are above the school's academic grade point average and the number of students (bac) who are below it. According to Figure 1, it can be said that there is an interaction between the number of students divided into groups according to their academic grade averages, there are transitions between the groups in the process, and the resulting process develops in the direction expected by the researchers.

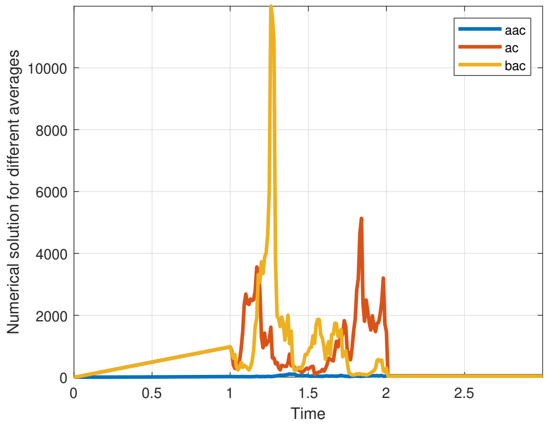

Figure 2. Numerical simulations of the system with initial conditions are given as $P(1) = 10$, $K(1) = 10$, $I(1) = 0$.

In Figure 2, it is assumed that there are no students (bac) with below average academic achievement in the school. When the simulation in Figure 2, which is drawn with this assumption, is examined, it is seen that the number of students (ac) with average academic achievement decreased along with the increase in the number of students (aac) with achievement above the school's academic grade average. In this context, it has been understood that there is an inverse proportion between the number of students (aac) who are above the school's academic grade point average and the number of students (ac) who have an average level of academic achievement. According to Figure 2, it can be said that there is an interaction between the number of students divided into groups according to their academic grade averages, there are transitions between the groups in the process, and the resulting process develops in the direction expected by the researchers.

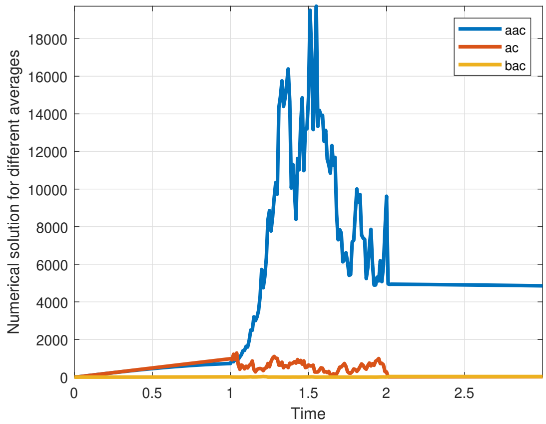

Figure 3. Numerical simulations of the system with initial conditions are given as $P(1) = 10$, $K(1) = 0$, $I(1) = 10$.

In Figure 3, It is also assumed that there are no students (ac) with average academic achievement in the school. When the simulation in Figure 3, drawn with this assumption, is examined, it is seen that when the number of students (bac) with achievement below the school's academic grade average increases, the number of students (aac) with academic achievement above the average decreases. In this context, it has been understood that there is an inverse proportion between the number of students (bac) who are below the school's academic grade point average and the number of students (aac) who are above it. According to Figure 3, it can be said that there is an interaction between the number of students divided into groups according to their academic grade averages, there are transitions between the groups in the process, and the resulting process develops in the direction expected by the researchers.

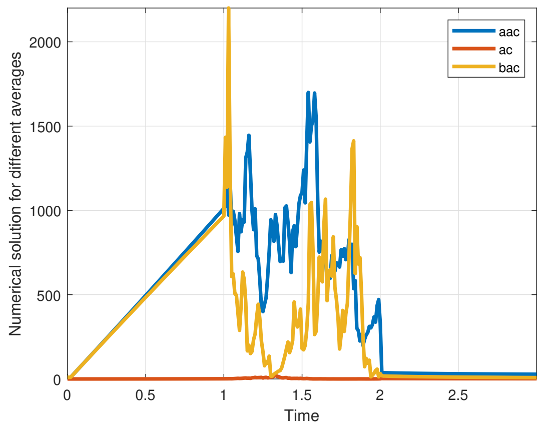

Figure 4. Numerical simulations of the system with initial conditions are given as $P(1) = 0$, $K(1) = 10$, $I(1) = 10$.

In Figure 4, it is assumed that there are no students (aac) with above average academic achievement in the school. When the simulation in Figure 4, drawn with this assumption, is examined, it is seen that when the number of students (ac) with average academic achievement increases, the number of students (bac) with below average academic achievement decreases. In this context, it has been understood that there is an inverse proportion between the number of students (ac) with average academic achievement and the number of students (bac) who are below the academic grade point average. According to Figure 4, it can be said that there is an interaction between the number of students divided into groups according to their academic grade averages, there are transitions between the groups in the process, and the resulting process develops in the direction expected by the researchers.

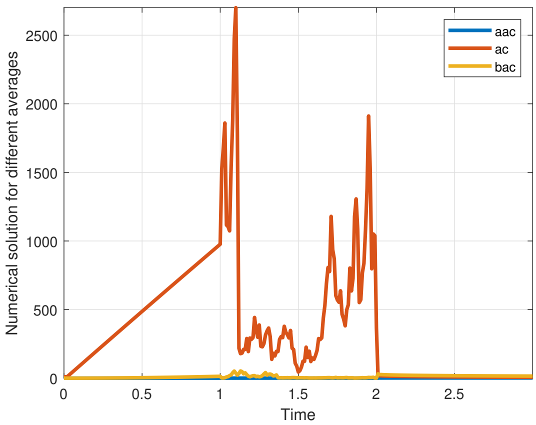

Figure 5. Numerical simulations of the system with initial conditions are given as $P(1) = 10$, $K(1) = 10$, $I(1) = 0$.

In Figure 5, it is assumed that there are no students (bac with below average academic achievement in the school. When the simulation in Figure 5, drawn with this assumption, is examined, it is seen that when the number of students (ac) with average academic achievement increases, the number of students (aac) with achievement above the academic grade point average decreases. In this context, it has been understood that there is an inverse proportion between the number of students (ac) who have an average academic achievement level at school and the number of students (aac) who are above their academic grade point average. According to Figure 5, it can be said that there is an interaction between the number of students divided into groups according to their academic grade averages, there are transitions between the groups in the process, and the resulting process develops in the direction expected by the researchers.

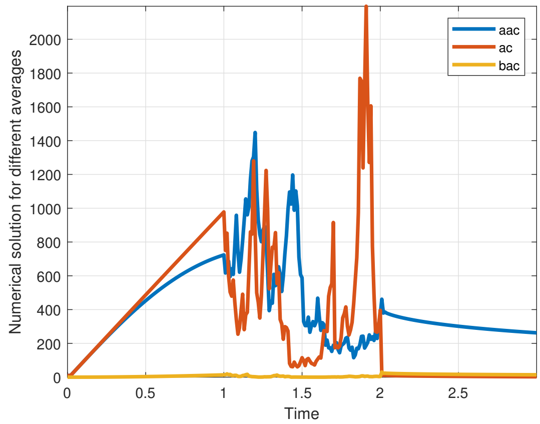

Figure 6. Numerical simulations of the system with initial conditions are given as $P(1) = 10$, $K(1) = 10$, $I(1) = 10$.

In Figure 6, It is assumed that the number of students in the groups separated according to their academic grade averages are equal to each other within the school. When the simulation in Figure 6, drawn with this assumption is examined, it is seen that there is an interaction between the number of students divided into groups according to their academic grade averages, there are transitions between the groups in the process, and over time, the students (ac) pile up into the group with average academic achievement

7. Discussion, conclusion and recommendations

Academic achievement is very important, as it enables students to be well-equipped for professional and social life and shapes their future. In the event of any academic failure, students generally face many emotional, cognitive, and behavioral problems. In this study, it was tried to calculate the academic achievement levels of the students throughout the school with the help of the mathematical model developed through the metapopulation model in order to find solutions to the possible problems that students may experience due to their academic failures. In the model developed for this purpose, academic achievement was determined by taking the GPA into account.

The students were considered three different actor groups: above-average, average, and below-average students. Individual characteristics, family, and school variables were taken into consideration as factors affecting these actors. By following this path, it was possible to calculate the academic achievement levels of the schools, in particular for the students. The developed mathematical model will make significant contributions to the determination of the effect levels of the variables that can support and harm students' academic achievement. After the relevant variables are processed, schools with low academic achievement will be able to learn from the variables which variables they need to carry out preventive and protective studies. Preventive and protective studies can be planned for the academic achievement level of the students. In these study plans, studies can be added on individual reasons (self-efficacy, self-esteem, motivation, etc.), family-related reasons (attitudes and behaviors of parents, their participation in education, education level of parents, socioeconomic level of the family, etc.), and school-related reasons (school culture, teacher behavior, school principal's leadership, etc.) included in the mathematical model developed. Although all of these variables interact with each other, they are also determinants of the probability of students being included in the academic failure risk group. In this context, it can be said that in order to minimize the problem of academic failure in schools, all these variables should be considered together and improved within the framework of a common understanding (the school and parents are in communication).

For example, both the structural characteristics of the family and the attitude of the family towards the lessons have an important place in affecting the student's motivation towards any subject or course. Therefore, the family should constantly support their child and try to keep her/his motivation high in order to be successful at school [41]. In order for parents with low educational levels, professional status, and family income levels to acquire academic predispositions; seminars, conferences, etc. informative meetings. A strong school culture causes students to be more attached to their goals and school, and as a result, academic achievement increases. School principals should be aware that they are directly influential in the creation of a strong organizational culture and the development of student success, and they should transform their institutions into learning organizations by demonstrating effective leadership behaviors. Teachers can help create a positive attitude towards lessons by taking into account the interests and needs of students, organizing various learning activities, exemplifying the application areas of the lessons in current and professional life, and emphasizing the role of lessons in the development of critical thinking and reasoning skills [7]. In addition, school counselors should organize awareness-raising seminars and plan individual and group counseling services in order to increase students' self-efficacy, self-esteem and motivation levels.

In this study, using a multidisciplinary method, academic achievement, which is a very important issue for the field of social sciences (psychology and educational sciences), is handled through a mathematical model. The fact that a subject in the field of social sciences is handled with a mathematical model apart from the computerized statistical programs (SPSS, Amos, Lisrel, Nvivo, etc.), which are frequently used in the literature, makes this study very unique in terms of method. Starting with a similar approach, the number of multidisciplinary studies can be increased by developing mathematical models about other concepts and phenomena (peer bullying, school burnout, etc.) that are important for the field of social sciences. In addition, when the literature is examined, it is striking that there are almost no studies that develop mathematical models in students. Low academic achievements will negatively affect students' chances to become successful, happy, and socially integrated individuals in their future lives. In addition, considering the potential importance of students for the society they live in, it is clear that new studies should be planned to overcome this deficiency. Of course, as with any study, this one also has some limitations. In this study, students who were above average, average, and below average (according to GPA) were taken as the actors of academic achievement. Individual, family, and school-related variables that affect these actors are emphasized. In the models to be developed later, new characters can be added among the actors of academic achievement by reducing the GPA score intervals. In addition, the variables affecting the actors include learning speed, intelligence, gender, interest, personality traits, readiness, etc. The mathematical model can be enriched by addition. It should not be forgotten! Every study that will be carried out related to academic achievement will add a different value to the literature and prepare the basis for the formation of new ideas.

Acknowledgments

The authors express their gratitude to the anonymous reviewers and the editor for their insightful comments and suggestions.

References

[1] Nartgün, Ş., & Çakır, M. (2014). Examining the high school students' academic achievement in terms of academic motivation and academic procrastination. *Journal of Research in Education and Teaching*, 3(3), 379-391.

[2] Carter, V., & Good, E. (1973). *Dictionary of education.* (4th ed.) New York: McGraw Hill Book Company.

[3] Kenç, M. F., & Oktay, B. (2002). The relationship between academic self-concept and academic success. *Education and Science*, 27(124), 71-79.

[4] Özgüven, İ. E. (2014). *Psychological tests* [Psikolojik testler] (12th ed.). Ankara: Nobel Akademik Yayıncılık.

[5] York, T. T., Gibson, C., & Rankin, S. (2015). Defining and measuring academic success. *Practical Assessment, Research, and Evaluation*, 20(1), 1-20.

[6] Kasatura, İ. (1991). *From school success to life success* [Okul başarısından hayat başarısına]. İstanbul: Altın Kitaplar Yayınevi.

[7] Sarıer, Y. (2016). The factors that affects students' academic achievement in Turkey: A meta-analysis study. *Hacettepe University Journal of Education*, 31(3), 609-627.

[8] Bandura, A. (1997). *Self-efficacy: The exercise of control.* New York: W. H. Freeman and Company.

[9] Bong, M. (1995). *Epistemological beliefs and generalizability of self-efficacy: Implications for instructional design* (Unpublished doctoral dissertation). University of Southern California, California.

[10] Uzun, K., & Karataş, Z. (2020). Predictors of academic self efficacy: Intolerance of uncertainty, positive beliefs about worry and academic locus of control. *International Education Studies*, 13(6), 104-116.

[11] Komarraju, M., & Nadler, D. (2013). Self-efficacy and academic achievement: Why do implicit beliefs, goals, and effort regulation matter?, *Learning and Individual Differences*, 25, 67-72.

[12] Alivernini, F., & Lucidi, F. (2011). Relationship between social context, self-efficacy, motivation, academic achievement, and intention to drop out of high school: A longitudinal study. *The Journal of Educational Research*, 104(4), 241-252.

[13] Bandura, A. (1982). Self-efficacy mechanism in human agency. *American Psychologist, 37*(2), 122-147.

[14] Akandere, M., Özyalvaç, N. T., & Duman, S. (2010). The attitudes of the students in secondary education to physical education lesson and the investigation of their success motivations: Konya anatolian high school sample. *The Journal of Selcuk University Social Sciences Institute*, (24), 1-10.

[15] Rosenberg, M. (1965). *Society and the adolescent self-image.* New Jersey: Princeton University Press.

[16] Sharma, P., & Sharma, M. (2021). Relationship between self-esteem and academic achievement of secondary school students. *Elementary Education Online*, 20(1), 3208-3212.

[17] Deveci, T. (2021). *The effects of family structure on the individual's motivation for academic success, academic permission and the level of happiness: Erzincan center and Tercan district example* (Unpublished master's thesis). Sivas Cumhuriyet University, Graduate School of Social Sciences, Sivas.

[18] Şentürk, M. (2019).*Analysis of the effect of family factor on academic achievement of primary school students* (Unpublished master's thesis). Çanakkale Onsekiz Mart University, Graduate School of Educational Sciences, Çanakkale.

[19] Glasser, W. (2012). *Schools without fail.* New York: HarperCollins Publishers.

[20] Tezel-Şahin, F., & Özyürek, A. (2008). Examining of the effects to child raising attitudes of demographic characteristics of parents that have 5-6 years children group. *The Journal of Turkish Educational Sciences*, 6(3), 395-414.

[21] Sirin, S. R. (2005). Socioeconomic status and academic achievement: A meta-analytic review of research. *Review of Educational Research*, 75(3), 417-453.

[22] Akyol, G., Sungur, S., & Tekkaya, C. (2010). The contribution of cognitive and metacognitive strategy use to students' science achievement. *Educational Research and Evaluation*, 16(1), 1-21.

[23] Koutsoulis, M. K., & Campbell, J. R. (2001). Family processes affect students' motivation, and science and math achievement in Cypriot high schools. *Structural Equation Modeling: A Multidisciplinary Journal*, 8(1), 108-127.

[24] Preble, B., & Gordon, R. (2011). *Transforming school climate and learning-beyond bullying and compliance.* California, USA: Corwin A Sage Company.

[25] Demirtaş, Z. (2010). The relationship between school culture and student achievement. *Education and Science, 35*(158), 3-13.

[26] Kızıldağ, S. (2009). *Loneliness, submissive acts and social support as the determiners of academic success* (Unpublished master's thesis). Hacettepe University, Graduate School of Social Sciences, Ankara.

[27] Şişman, M. (2018). *Teaching leadership* [Öğretim liderliği] (6th ed.). Ankara: Pegem Akademi Yayıncılık.

[28] Wikipedia (2022). *Mathematical model.* Access address (01.08.2022): https://en.wikipedia.org/wiki/Mathematical_model

[29] Sheergojri, A. R., Iqbal, P., Agarwal, P., & Ozdemir, N. (2022). Uncertainty-based Gompertz growth model for tumor population and its numerical analysis. *An International Journal of Optimization and Control: Theories & Applications (IJOCTA)*, 12(2), 137-150.

[30] Benson, D. A., Wheatcraft, S. W., & Meerschaert, M. M. (2000). Application of a fractional advection-dispersion equation. *Water Resources Research*, 36(6), 1403-1412.

[31] Koca, İ. (2019). Modeling the heat flow equation with fractional-fractal differentiation. *Chaos, Solitons & Fractals*, 128, 83-91.

[32] Evirgen F. (2023). Transmission of Nipah virus dynamics under Caputo fractional derivative, Journal of Computational and Applied. Mathematics, 418, Article 114654.

[33] Uçar E., Özdemir N., Altun E. (2023) Qualitative analysis and numerical simulations of new model describing cancer, Journal of Computational and Applied. Mathematics, 422, Article 114899.

[34] Yusuf, A., Qureshi, S., Mustapha, U. T., Musa, S. S., & Sulaiman, T. A. (2022). Fractional modeling for improving scholastic performance of students with optimal control. *International Journal of Applied and Computational Mathematics*, 8(1), 1-20.

[35] Ross, B. (1975). A brief history and exposition of the fundamental theory of fractional calculus. *Fractional Calculus and its Applications*, 57, 1-36.

[36] Atangana, A., & İgret-Araz, S. (2021). New concept in calculus: Piecewise differential and integral operators. *Chaos, Solitons & Fractals*, 145, 110638.

[37] Podlubny, I. (1998). *Fractional differential equations: An introduction to fractional derivatives, fractional differential equations, to methods of their solution and some of their applications.* Academic Press: Cambridge, MA, USA.

[38] Atangana, A. (2021). Mathematical model of survival of fractional calculus, critics and their impact: How singular is our world? *Advances in Difference Equations*, 2021, 403.

[39] Debnath, L. (2004). A brief historical introduction to fractional calculus. *International Journal of Mathematical Education in Science and Technology*, 35(4), 487-501.

[40] Toufik, M., Atangana, A. (2017). New numerical approximation of fractional derivative with non-local and non-singular kernel: application to chaotic models. *The European Physical Journal Plus*, 132(10), 444.

[41] Dinç, A. R. (2017). *Relationship between the students who educated at a boarding highschool both daytime and boarding education and percieved parents support level* (Unpublished master's thesis). Hasan Kalyoncu University, Graduate School of Social Sciences, Gaziantep.

Pelin Yaprakdal Uzun *received her undergraduate degree in mathematics from Gazi University in 2016 and her master's degree in mathematics from Burdur Mehmet Akif Ersoy University in 2019. She is currently studying for her doctorate at Burdur Mehmet Akif Ersoy University. She has been working as a mathematics teacher in various schools since 2016. Her main field of study is fractional calculus.*

https://orcid.org/0000-0002-3261-2509

Kıvanç Uzun *received his undergraduate degree in 2014 and his master's degree in 2016 from the Guidance and Psychological Counseling program of Burdur Mehmet Akif Ersoy University. He is currently continuing his doctoral studies at the same university. Between 2014-2020, he worked as a school psychological counselor in various schools affiliated to the Ministry of National Education. He has been working as a lecturer at Burdur Mehmet Akif Ersoy University since 2020. Its main field of study is preventive and intervention services to support the psychological health of adolescents.*

https://orcid.org/0000-0002-6816-1789

Ilknur Koca *received the B.Sc. and M.Sc. degrees in 2007 and 2009 from the Department of Mathematics from Ankara University, Turkey respectively. She received her Ph.D. degree from the same university in 2013. She is working as an Associate Professor at the Department of Accounting and Financial Management, Seydikemer High School of Applied Sciences, Mugla Sıtkı Kocman University, Mugla, Turkey. Her research interests are methods and applications of partial and ordinary differential equations, fractional differential equations, and iterative methods.*

https://orcid.org/0000-0003-4393-1588

An International Journal of Optimization and Control: Theories & Applications
ISSN:2146-0957 eISSN:2146-5703
Vol.13, No.2, pp.259-268 (2023)
http://doi.org/10.11121/ijocta.2023.1327

RESEARCH ARTICLE

Some stability results on non-linear singular differential systems with random impulsive moments

Arumugam Vinodkumar[a*], Sivakumar Harinie[a], Michal Fečkan [b,c] Jehad Alzabut [d,e]

[a] *Department of Mathematics, Amrita School of Physical Sciences, Coimbatore-641 112, Amrita Vishwa Vidyapeetham, India*
[b] *Department of Mathematical Analysis and Numerical Mathematics, Faculty of Mathematics, Physics and Informatics, Comenius University in Bratislava, Mlynská dolina, 842 48, Bratislava, Slovakia*
[c] *Mathematical Institute, Slovak Academy of Sciences, Štefánikova 49, 814 73 Bratislava, Slovakia*
[d] *Department of Mathematics and General Sciences, Prince Sultan University, 11586 Riyadh, Saudi Arabia*
[e] *Department of Industrial Engineering, OSTİM Technical University, Ankara 06374, Turkey*
a_vinodkumar@cb.amrita.edu, hariniesiva960@gmail.com, Michal.Fecka@fmph.uniba.sk, jalzabut@psu.edu.sa

ARTICLE INFO

Article History:
Received 4 October 2022
Accepted 31 May 2023
Available 29 July 2023

Keywords:
Random impulses
Lyapunov function
Exponential stability
Singular differential systems

AMS Classification 2010:
34A37; 34B16; 37B25

ABSTRACT

This paper studies the exponential stability for random impulsive non-linear singular differential systems. We established some new sufficient conditions for the proposed singular differential system by using the Lyapunov function method with random impulsive time points. Further, to validate the theoretical results' effectiveness, we finally gave two numerical examples that study with graphical illustration and an additional example involving matrices with complex entries, proving the results to be true in that case as well.

1. Introduction

Singular systems are widely connected to various applications such as power systems, electrical networks, and robotics. However, it has some exceptional features like regular and impulse free that do not exist in normal state-space systems. These exceptional characteristics may cause some challenges upon studying the singular systems. Further, because of the singularity matrix E, it is not easy to formulate easy-to-check conditions for analysis and synthesis problems. Due to the above justifications, the study of singular systems has been scrutinized more attention over the past decades [1]. The past two decades have spotted an important development on the theory of singular differential systems (SDSs), and many basic and most significant concepts have been favorably examined including stability analysis, stabilization, guaranteed cost control, filtering, observer design, sliding mode control and so on [2, 3]. The main target is to show the latest developments in the analysis and synthesis of SDSs. Since the system is chronicled by algebraic and differential equations, the SDSs may disclose instability behavior and thus poor performance may be raised on the basis of presence of time delay. Hence the investigation of stability character of SDSs becomes compulsory. By applying various methods and ideas, several authors have studied the SDS. In [4], the author studied the delay-dependent stability criteria by using Writinger-based inequality. The delay-dependent robust stability norms for two classes of SDSs with norm-bounded uncertainties are discussed in [5].

*Corresponding Author

In [6] the exponential stability problems of singular impulsive switched systems was investigated. Impulsive stabilization problem for a class of linear singular systems with time-delays can be seen in [7]. The problem of exponential stability analysis for a class of singular systems with interval time-varying discrete and distributed delays is discussed in [8]. The stability problem of singular systems with time-varying delay by first transforming it into a neutral system with time-varying delay and constructing an appropriate Lyapunov-Krasovskii functional, is studied in [9]. In [10] the control problem of switched singular systems was investigated aiming to compress their inconsistent state jumps when switch occurs between two different singular subsystems. In [11] we can see a definition of a transform that reformulates the system with delays into a singular linear system of differential equations whose coefficients are non-square constant matrices where the number of their columns is greater than the number of their rows. Further, in engineering applications, the complexity increases mean accuracy will not be described by linear singular systems. To overcome this type of problem, we need generalized nonlinear singular systems to solve the problem. Very few authors have studied the nonlinear singular system models [6, 12–15] and the references therein. Moreover, The problem of sliding mode control with torpidity of a class of uncertain nonlinear SDSs had been discussed in [16]. Many other valuable results are obtained for stability and stabilization for SDSs, see [7, 17–26] and the references therein.

Stability is a condition in which a slight disturbance in a system does not generate too disrupting effect on that system. The dynamics of SDS are by a mixture of differential- algebraic equations, so the study of $\mathcal{E}$-exponential stability ($\mathcal{E}$-ES) was first introduced by [12]. In [3, 6], the authors analyzed the connection between the exponential stability (ES) and the $\mathcal{E}$-ES for linear and non-linear singular impulsive differential systems and they claimed that the $\mathcal{E}$-ES is nearly equal to its ES. Hence it is essential to speak about the exponential stability of random impulsive nonlinear SDSs. On the other hand, impulsive systems stand up when dynamics generate discontinuous trajectories. Discontinuities arise when movements of states occur over a small interlude that simulates a point-mass measure. There are several works contributed to study the impulses at fixed point (see the monograph [27, 28] and [29–35]). The significant concepts of impulsive control have been disputed with a wide field of uses in analysis and control of complex systems in [36]. Some stability criteria for impulsive differential systems had been discussed in [37]. Global ES for impulsive system with infinite distributed delay based on flexible impulse frequency are discussed in [38]. In [39], impulse control is used to study nonlinear systems with partial unmeasurable states. Very few research have been carried for random impulsive systems. When the reactions of the impulse drawn at random time points, the results follow as a stochastic process. Random impulses are different from fixed-time impulse effects. Recently in [40], the authors studied the exponential stability based on fixed and random time effect of the impulses while they proved the robust mean square stability for random impulsive control systems in [41]. Then, by considering the impulse moments at random time points in [42], the authors proved the stability results for differential systems. Moreover and to the best of authors' knowledge, we like to point out that there is no paper about the investigation of the ES on the random impulsive SDSs. For further information the reader can refer to [43–48].

Inspired by the above discussion, in this paper, we generalized the $\mathcal{E}$-ES result for p^{th} moment and also proved the equivalence to ES for a nonlinear singular system. Further, we address new sufficient conditions to develop the exponential stability criteria ($\mathcal{E}$-ES and ES) for random impulsive nonlinear SDSs. The waiting time between two consecutive impulses is considered to follow an exponential distribution when the effects of the impulses taken at random time points. By employing the effect of impulses and Lyapunov-function approach, we achieve the desired performance. The rest of this paper follows through some definitions and lemmas in Section 2. In Section 3, we prove the $\mathcal{E}$-ES and ES results for random impulsive SDSs by using the Lyapunov-function approach. In Section 4, three numerical examples are discussed, the last of which involves the usage of matrices with complex entries and finally in Section 5 a conclusion is given.

Notations: Let $\Re$ indicate the set of all real numbers, $\Re_+$ the set of all positive real numbers and Z_+ the set of all positive integers. Let $\Re^n$ be the Euclidean space provided with norm $\|\cdot\|$, and $(\Omega, \mathcal{F}, \mathcal{P})$ be a probability space. We use $\mathcal{PC}([t_0, T], \Re^n)$, to indicate the set of all piecewise right continual real-valued random variables $\varphi : [t_0, T] \to \Re^n$, with the norm is described by $E\|\varphi\|^p = \sup_{\theta\in[t_0,T]} E\|\varphi(\theta)\|^p$. Furthermore, A^T represents the transpose of A where the maximum and minimum eigenvalues of the matrix indicated by $\lambda_{max}(\cdot)$, and $\lambda_{min}(\cdot)$. Then $E[\cdot]$, indicates the expectation operator with respect to the given probability $\mathcal{P}$.

2. Model description and essential preliminaries

Let $\{\chi_m^{'}\}_{m=0}^{\infty}$ be the non-decreasing sequence of random variables and $\{\tau_m^{'}\}_{m=1}^{\infty}$ is a sequence of an independent exponentially distributed random variable with parameter γ defined on sample space Ω. Note that $\chi_0^{'} = t_0$, where $t_0 \geq 0$ is a fixed point and $\chi_m^{'} = \chi_{m-1}^{'} + \tau_m^{'}$ for $m = 1, 2, \cdots$, where $\tau_m^{'}$ define the delay (waiting) time between two consecutive impulses where $\sum_{m=1}^{\infty} \tau_m^{'} = \infty$ with probability 1.
Consider, the random impulsive non-linear SDSs:

$$\begin{cases} \mathcal{E}\dot{x}(t) = Ax(t) + f(x(t), t), \chi_m^{'} < t < \chi_{m+1}^{'}, \\ x(\chi_m^{'+}) = C_m(\tau_m^{'})x(\chi_m^{'-}), m \in Z_+ \\ x_{t_0} = x_0, \end{cases} \tag{1}$$

where $t \geq t_0$, $x(t) \in \Re^n, A \in \Re^{n\times n}$ is system matrix, $C_m(\tau_m^{'})$ is the jump altitude and the matrix $\mathcal{E} \in \Re^{n\times n}$ is singular with rank $\mathcal{E} = k \leq n$. $f(x(t), t) : \Re^n \times \Re^+ \to \Re^{n\times n}$ are piecewise continual vector-valued functions assuring the existence and uniqueness of solutions for systems (1) with $f(0, t) \equiv 0$ and satisfies the Lipschitz condition for all $(x, t), (x^*, t) \in \Re^n \times \Re^+$

$$\|f(x(t), t) - f(x^*(t), t)\| \leq \|F(x(t) - x^*(t))\|, \tag{2}$$

where F is a constant matrix with an appropriate dimension. Consequently, from (2), we have

$$\|f(x(t), t)\| \leq \|Fx(t)\|. \tag{3}$$

Remark 1. *Let $\{\chi_m\}_{m=0}^{\infty}$ be non-decreasing sequence of points, where χ_m are values of the correlated random variables $\chi_m^{'}, \forall\ m = 1, 2, \cdots$, and $\{\tau_m\}_{m=1}^{\infty}$ be a sequence of points, where τ_m are arbitrary values of the random variable $\tau_m^{'}, \forall\ m = 1, 2, \cdots$. For satisfaction, we define $\chi_0 = t_0$ and $\chi_m = \chi_{m-1} + \tau_m$, $\forall\ m = 1, 2, \cdots$, where τ_m represents the value of the delay (waiting) time. Then system (1) becomes*

$$\begin{cases} \mathcal{E}\dot{x}(t) = Ax(t) + f(x(t), t), t \neq \chi_m, t \geq t_0, \\ x(\chi_m^+) = C_m(\tau_m)x(\chi_m^-), m \in Z_+ \\ x_{t_0} = x_0. \end{cases} \tag{4}$$

The solutions of the system (4) are controlled not only by the initial condition but also by the moments of impulses χ_m, $m = 1, 2, \cdots$. That is, the result depends on the selected arbitrary values τ_m of the random variable $\tau_m^{'}, \forall\ m = 1, 2, \cdots$. We will assume $x(\chi_m) = \lim_{t\to\chi_m - 0} x(t)$.
Moreover, the set of all solutions of system (4), is known as a sample path solution of system (1). Thus, the sample path solution produces a stochastic process. We can assure that it is a solution of the system (1).

Lemma 1. *[41, 42], When there will be exactly m impulses until the time $t, t \geq t_0$, and the waiting time between two consecutive impulses follow an exponential distribution with parameter γ, then the probability*

$$\mathcal{P}(I_{[\chi_m^{'}, \chi_{m+1}^{'})}(t)) = \frac{\gamma^m (t - t_0)^m}{m!} e^{-\gamma(t-t_0)},$$

where the events

$$I_{[\chi_m^{'}, \chi_{m+1}^{'})}(t) = \{\omega \in \Omega : \chi_m^{'}(\omega) < t < \chi_{m+1}^{'}(\omega)\},$$

$m = 1, 2, \cdots$.

Remark 2. *[41, 42], Let $x(t)$ be the solution of the random impulsive differential equations then the expected value of $x(t)$ satisfies*

$$E[\|x(t)\|^p] = \sum_{m=0}^{\infty} E[\|x(t)\|^p | I_{[\chi_m^{'}, \chi_{m+1}^{'})}(t)] \mathcal{P}(I_{[\chi_m^{'}, \chi_{m+1}^{'})}(t)),$$

where $\chi_m^{'}$ is the impulse moments.

Definition 1. *[6], The pair $(\mathcal{E}, A)$ is called regular if $det(s\mathcal{E} - A)$ is not identical zero. The pair $(\mathcal{E}, A)$ is called impulse free if $deg(det(s\mathcal{E} - A)) = rank(\mathcal{E})$.*

Definition 2. *[6, 12], System (1) is said to have a Lyapunov-like property if there exists a matrix P such that $\mathcal{E}^T P = P^T \mathcal{E} \geq 0$ and $[Ax(t) + f(x(t), t)]^T Px + x^T P[Ax(t) + f(x(t), t)] < 0$.*

Remark 3. *[6, 12] For a nonlinear system, it is sufficient that the solution exists and is unique on $[0, \infty)$, if there exists a matrix P satisfying definition 2.*

From [6, 36], we have that the pair $(\mathcal{E}, A)$ is regular and impulse free, then we have that there exists matrices $\mathcal{G}_1 \in \Re^{r\times n}, \mathcal{G}_2 \in \Re^{(n-r)\times n}, \mathcal{Q}_1 \in \Re^{n\times r}, \mathcal{Q}_2 \in \Re^{n\times(n-r)}$, such that $\mathcal{G} = col(\mathcal{G}_1, \mathcal{G}_2)$ and $\mathcal{Q} = row(\mathcal{Q}_1, \mathcal{Q}_2) \in \Re^{n\times n}$ are two non-singular matrices and the following standard decomposition holds

$$\mathcal{G}\mathcal{E}\mathcal{Q} = diag\{I_r, 0\}, \mathcal{G}A\mathcal{Q} = diag\{A_1, I_{n-r}\}$$

where $r = Rank(\mathcal{E}), A_1 \in \Re^{r\times r}$. Non-singularity of $\mathcal{G}$ implies that $\mathcal{G}_2$ is full-row and then $\mathcal{G}_2(\mathcal{G}_2)^T$ is positive definite. Without loss of generality, we always assume that $\|\mathcal{G}_2\| \leq 1$.

Lemma 2. *[6], Let $\mathcal{V} \in \Re^{n\times n}$ be a positive-definite matrix, then*

$$\lambda_{min}(\mathcal{V})x^T x \leq x^T \mathcal{V} x \leq \lambda_{max}(\mathcal{V})x^T x, \quad \forall\, x \in \Re^n.$$

Lemma 3. *[49] For any constant $\epsilon > 0$, and vectors $x, y \in \Re^n$, then we have*

$$x^T y + y^T x \leq \epsilon^{-1} x^T x + \epsilon y^T y, holds.$$

Definition 3. *System (1) is said to be p^{th} moment $\mathcal{E}$-ES, if there exist two positive numbers $\lambda > 0, M > 0$ such that, the solution x of system (1) satisfies*

$$E\,\|\mathcal{E}x(t)\|^p \leq ME[\|\mathcal{E}x_0\|^p]e^{-\lambda(t-t_0)}, \quad t \geq t_0.$$

Definition 4. *System (1) is said to be p^{th} moment ES, if there exist two positive numbers $\lambda > 0, M > 0$ such that, the solution x of the system (1), satisfies*

$$E\,\|x(t)\|^p \leq ME[\|\mathcal{E}x_0\|^p]e^{-\lambda(t-t_0)}, \quad t \geq t_0.$$

If $p = 2$, then it is mean square exponential stable.

3. Main results

Theorem 1. *Let $\tau' = \max_{m\in Z_+}\left\{\chi'_m - \chi'_{m-1}\right\} < \infty$. Assume that system (1) satisfies a Lyapunov-like property and there exists an invertible matrix P, and positive constants $\kappa > 0$, $\omega_m > 0$, such that $E[\omega_m] \leq \kappa$, $\zeta < 0$ be a negative real number, $\epsilon > 0$, exponential distribution parameter γ and the following conditions hold,*

$$\begin{gathered} (A^T P + P^T A) + \lambda_{max}(\tfrac{1}{\epsilon}F^T F + \epsilon P^T P)I \\ < \zeta \mathcal{E}^T P, \\ \Gamma = (C_m(\tau_m)^T \mathcal{E}^T P C_m(\tau_m) - \omega_m \mathcal{E}^T P) \\ \leq 0 \\ \zeta + \gamma(\kappa - 1) < 0. \end{gathered} \tag{5}$$

Then, the trivial solution of system (1) is p^{th} moment $\mathcal{E}$-ES.

Proof. Let x be the sample path solution of systems (4). For convenience we take $V(x(t)) = V(t, x(t))$, and consider the Lyapunov function

$$V(x(t)) = x^T(t)\mathcal{E}^T P x(t). \tag{6}$$

Taking the derivative of $V(x(t))$ along the solution of system (4) at the continuous interval $[\chi_{m-1}, \chi_m), m \in Z_+$, then we have

$$\begin{aligned} &\dot{V}(x(t)) \\ &= \dot{x}^T(t)\mathcal{E}^T P x(t) + x^T(t)P^T \mathcal{E}\dot{x}(t), \qquad (7) \\ &= x^T(t)(A^T P + P^T A)x(t) + 2f^T(x(t), t)Px(t). \end{aligned}$$

From condition (5), we have

$$\begin{aligned} &\dot{V}(x(t)) \\ &= x^T(t)(A^T P + P^T A)x(t) + 2f^T(x(t), t)Px(t), \\ &= x^T(t)(A^T P + P^T A)x(t) + 2f^T(x(t), t)Px(t), \\ &\leq x^T(t)(A^T P + P^T A)x(t) \\ &\quad + x^T(t)(\frac{1}{\epsilon}F^T F + \epsilon P^T P)Ix(t) \\ &\leq x^T(t)\zeta \mathcal{E}^T P x(t) \\ &\leq \zeta V(x(t)). \end{aligned}$$

Hence we have,

$$\dot{V}(x(t)) - \zeta V(x(t)) \leq 0, \tag{8}$$

or

$$\dot{V}(x(t)) \leq \zeta V(x(t)),\ t \in [\chi_{m-1}, \chi_m), m \in Z_+. \tag{9}$$

Note that for any $m \in Z_+$, at instant $t = \chi_m$, we have

$$\begin{aligned} &V(\chi_m{}^+) - \omega_m V(\chi_m{}^-) \\ &= x^T(\chi_m{}^+)\mathcal{E}^T P x(\chi_m{}^+) - \omega_m x^T(\chi_m{}^-)\mathcal{E}^T P x(\chi_m{}^-) \\ &= [C_m(\tau_m)x(\chi_m{}^-)]^T \mathcal{E}^T P [C_m(\tau_m)x(\chi_m{}^-)] \\ &\quad -\omega_m [x(\chi_m{}^-)]^T \mathcal{E}^T P [x(\chi_m{}^-)] \qquad (10) \\ &= [x^T(\chi_m)C_m(\tau_m)^T]\mathcal{E}^T P [C_m(\tau_m)x(\chi_m)] \\ &\quad -\omega_m [x^T(\chi_m)]\mathcal{E}^T P [x(\chi_m)] \\ &= x^T(\chi_m)(C_m(\tau_m)^T \mathcal{E}^T P C_m(\tau_m) - \omega_m \mathcal{E}^T P)x(\chi_m) \\ &= x^T(\chi_m)\Gamma x(\chi_m) \\ &\leq 0. \end{aligned}$$

Therefore, from (4) and by using simple induction, from (9) and (10), we have

$$V(x(t)) \leq V(x_0(t))\prod_{i=1}^{m}\omega_i e^{\zeta(t-t_0)}, \forall m \in Z_+. \tag{11}$$

By the Lyapunov-like property, there exists a positive definite symmetric matrix L such that $\mathcal{E}^T P = \mathcal{E}^T L \mathcal{E}$. Then, we have

$$\begin{aligned} &\lambda_{min}(L)\,\|\mathcal{E}x(t)\|^p \\ &\qquad \leq V(x(t)) \\ &\qquad \leq V(x_0(t))\prod_{i=1}^{m}\omega_i e^{\zeta(t-t_0)}. \end{aligned} \tag{12}$$

Hence, we obtain

$$\begin{aligned} \|\mathcal{E}x(t)\|^p &\leq \frac{\lambda_{max}(L)}{\lambda_{min}(L)}\,\|\mathcal{E}x(t_0)\|^p \prod_{i=1}^{m}\omega_i e^{\zeta(t-t_0)}, \\ &\leq \frac{\lambda_{max}(L)}{\lambda_{min}(L)}\,\|\mathcal{E}x_0\|^p \prod_{i=1}^{m}\omega_i e^{\zeta(t-t_0)}, \end{aligned}$$

where $t \in [\chi_{m-1}, \chi_m), m \in Z_+$. This equation generates a stochastic process and it is defined by

$$\|\mathcal{E}x(t)\|^p \leq M\|\mathcal{E}x_0\|^p \prod_{i=1}^{m}\omega_i e^{\zeta(t-t_0)}, \chi'_{m-1} < t < \chi'_m,$$

where $M = \frac{\lambda_{max}(L)}{\lambda_{min}(L)}$. Taking expectation, by using Lemma 1, and remark 2, we get

$$
\begin{aligned}
&E\left[\|\mathcal{E}x(t)\|^p\right] \\
&= \sum_{m=0}^{\infty} E[\|\mathcal{E}x(t)\|^p | I_{[\chi_m',\chi_{m+1}')}(t)] \\
&\quad \mathcal{P}(I_{[\chi_{m-1}',\chi_m')}(t)), \\
&\le ME[\|\mathcal{E}x_0\|^p] \sum_{m=0}^{\infty}\prod_{i=1}^{m} E\left[\omega_i\right] e^{\zeta(t-t_0)} \\
&\quad \mathcal{P}(I_{[\chi_{m-1}',\chi_m')}(t)) \\
&= ME[\|\mathcal{E}x_0\|^p] \sum_{m=0}^{\infty}\prod_{i=1}^{m} E\left[\omega_i\right] e^{\zeta(t-t_0)} \\
&\quad \frac{\gamma^m(t-t_0)^m}{m!} e^{-\gamma(t-t_0)}, \\
&= ME[\|\mathcal{E}x_0\|^p] e^{\zeta(t-t_0)} \sum_{m=0}^{\infty} \frac{[\gamma\kappa]^m (t-t_0)^m}{m!} \\
&\quad e^{-\gamma(t-t_0)},
\end{aligned}
$$

Hence,

$$E\left[\|\mathcal{E}x(t)\|^p\right] \le ME[\|\mathcal{E}x_0\|^p] e^{[\zeta+\gamma(\kappa-1)](t-t_0)}, \quad (13)$$

where $\zeta + \gamma(\kappa - 1)$ is the convergent rate. This implies that the trivial solution of (1) is $\mathcal{E}$-exponentially stable. □

Corollary 1. *For system* (1)*, its p^{th} moment $\mathcal{E}$-exponentially stability is equivalent to its p^{th} moment exponential stability and its satisfies $1 - 2^{p-1}E\|F\mathcal{Q}_2\|^p > 0$.*

Proof. The pair $(\mathcal{E}, A)$ is regular and impulse free, we introduce the coordinate transformation

$$x(t) = \mathcal{Q}\ col(x_1, x_2). \quad (14)$$

It follows that system (1) is equivalent to

$$
\begin{aligned}
\dot{x_1} &= A_1 x_1 + \mathcal{G}_1 f(x(t), t), && (15)\\
&\quad \chi_m' < t < \chi_{m+1}', t \ge t_0, \\
0 &= x_2 + \mathcal{G}_2 f(x(t), t), && (16)\\
&\quad \chi_m' < t < \chi_{m+1}', t \ge t_0 \\
x(\chi_m'^{+}) &= C_m x(\chi_m'^{-}), m \in Z_+ && (17)\\
x_{t_0} &= x_0,
\end{aligned}
$$

where $x_1 \in \Re^r, x_2 \in \Re^{n-r}$ and $\mathcal{G} = col(\mathcal{G}_1, \mathcal{G}_2), \mathcal{G}_1 \in \Re^{r\times n}, \mathcal{G}_2 \in \Re^{(n-r)\times n}$, $\mathcal{Q} = row(\mathcal{Q}_1, \mathcal{Q}_2) \in \Re^{n\times n}$, $\mathcal{Q}_1 \in \Re^{n\times r}$, $\mathcal{Q}_2 \in \Re^{n\times(n-r)}$. Hence,

$$
\begin{aligned}
\mathcal{G}\mathcal{E}x(t) &= \mathcal{G}\mathcal{E}\mathcal{Q}\ col(x_1, x_2) \\
&= diag(I_r, 0) col(x_1, x_2) \\
&= col(x_1, 0) && (18)
\end{aligned}
$$

From (13) and (18), we have

$$
\begin{aligned}
E\|x_1\|^p &= E\|\mathcal{G}\mathcal{E}x\|^p \\
&\le \|\mathcal{G}\|^p E\|\mathcal{E}x\|^p \\
&\le \|\mathcal{G}\|^p ME[\|\mathcal{E}x_0\|^p] e^{[\zeta+\gamma(\kappa-1)](t-t_0)}. && (19)
\end{aligned}
$$

Here we understood that the solution of the system (1) is p^{th} moment globally exponentially stable.

Now, It is necessary to prove that that x_2 is also exponentially stable. It follows from equation (3) and (17) that

$$
\begin{aligned}
\|x_2\| &\le \|\mathcal{G}_2\| \|f(x(t), t)\| \le \|f(x(t), t)\| \\
&\le \|Fx(t)\| = \|F\mathcal{Q}_1\ x_1 + F\mathcal{Q}_2\ x_2\| \\
&\le \|F\mathcal{Q}_1\ x_1\| + \|F\mathcal{Q}_2\ x_2\| \\
&\le \|F\mathcal{Q}_1\| \|x_1\| + \|F\mathcal{Q}_2\| \|x_2\|.
\end{aligned}
$$

Thus, taking expectation and the p^{th} moment on both sides, we get

$$(1 - 2^{p-1}E\|F\mathcal{Q}_2\|) E\|x_2\|^p \le 2^{p-1}E\|F\mathcal{Q}_1\| E\|x_1\|^p,$$

where $\mathcal{Q}$ is non singular matrix can be suitably taken to satisfy $1 - 2^{p-1}E\|F\mathcal{Q}_2\|^p > 0$. Therefore from (19),

$$
\begin{aligned}
E\|x_2\|^p &\le \frac{2^{p-1}E\|F\mathcal{Q}_1\|^p}{1 - 2^{p-1}E\|F\mathcal{Q}_2\|^p} E\|x_1\|^p \\
&\le \frac{2^{p-1}E\|F\mathcal{Q}_1\|^p}{1 - 2^{p-1}E\|F\mathcal{Q}_2\|^p} \|\mathcal{G}\|^p ME[\|\mathcal{E}x_0\|^p] \\
&\quad e^{[\zeta+\gamma(\kappa-1)](t-t_0)}.
\end{aligned}
$$

From (19) and the above equation, we conclude that the trivial solution of (1) is p^{th} moment exponentially stable. The proof is completed. □

When $f(x(t), t) = 0$, then the system (1) becomes a linear SDSs with random impulses. In this case, the following corollary can be easily obtained.

Corollary 2. *Let $\tau' = \max_{m\in Z_+} \left\{\chi_m' - \chi_{m-1}'\right\} < \infty$. Assume that system* (1) *with $f(x(t), t) = 0$ satisfies a Lyapunov-like property and there exists an invertible matrix P, and there exists positive constant $\kappa > 0$, $\omega_m > 0$, such that $E[\omega_m] \le \kappa$, $\zeta < 0$, exponential distribution parameter γ and the following conditions hold,*

$$
\begin{aligned}
&(A^T P + P^T A) < \zeta \mathcal{E}^T P, && (20)\\
&\Gamma = (C_m(\tau_m)^T \mathcal{E}^T P C_m(\tau_m) - \omega_m \mathcal{E}^T P) \le 0 \\
&\zeta + \gamma(\kappa - 1) < 0.
\end{aligned}
$$

Then, the trivial solution of system (1) *is p^{th} moment $\mathcal{E}$-ES.*

The proof is similar to the proof of Theorem 1 and hence it is omitted.

When $\mathcal{E} = I_n$, then the system (1) becomes a nonlinear state-space system with random impulses.

In this case, the following corollary can be easily obtained.

Corollary 3. *Let* $\tau' = \max_{m \in Z_+} \left\{ \chi'_m - \chi'_{m-1} \right\} < \infty$. *Assume that system* (1) *with* $\mathcal{E} = I_n$ *satisfies a Lyapunov-like property and there exists a positive definite matrix* P, *and there exists positive constant* $\kappa > 0$, $\omega_m > 0$, *such that* $E[\omega_m] \leq \kappa$, $\zeta < 0$, $\epsilon > 0$, *exponential distribution parameter* γ *and the following conditions hold,*

$$
\begin{aligned}
&(A^T P + P^T A) + \lambda_{max}(\frac{1}{\epsilon} F^T F + \epsilon P^T P) I < \zeta P, \\
&\Gamma = (C_m(\tau_m))^T P C_m(\tau_m) - \omega_m P) \leq 0 \qquad (21) \\
&\zeta + \gamma(\kappa - 1) < 0.
\end{aligned}
$$

Then, the trivial solution of system (1) *is* p^{th} *moment ES.*

The proof is similar to the proof of Theorem 1 and hence it is omitted.

Remark 4. *From the condition* (5) *and* $\mathcal{E}^T P = P^T \mathcal{E} \geq 0$, *different matrices* P *can be chosen based on the matrices* $\mathcal{E}$, A *and* F.

Remark 5. *We carried out the following four conditions from the convergent rate* $\zeta + \gamma(\kappa - 1)$, *in Theorem 1,*

(i) *If* $\zeta < 0$ *in the inequality* $\dot{V}(x(t)) \leq \zeta V(x(t))$, *then the singular system* (1) *is stable. In this case, the impulsive strength* $\kappa \in (0, 1)$ *and the arrival rate of impulses do not necessarily satisfy any condition.*

(ii) *If* $\zeta < 0$ *in the inequality* $\dot{V}(x(t)) \leq \zeta V(x(t))$, *then the singular system* (1) *is stable. In this case, the system does not have an arrival rate of impulses when the impulsive strength* $\kappa = 1$.

(iii) *If* $\zeta < 0$ *in the inequality* $\dot{V}(x(t)) \leq \zeta V(x(t))$, *then the singular system* (1) *is stable. In this case, the arrival rate of impulses must be satisfied with this condition* $\gamma < \frac{-\zeta}{\kappa - 1}$, *where the impulsive strength* $\kappa > 1$.

4. Applications

In this section, numerical examples are discussed to support the proposed results. We illustrate the results by graphs to support the results.

Example 1. *Consider system* (1) *where*

$$
\mathcal{E} = \begin{bmatrix} 1 & 0 & 0 \\ 0 & 1 & 0 \\ 0 & 0 & 0 \end{bmatrix}, A = \begin{bmatrix} -0.3 & 0.1 & 0.1 \\ -1 & -3 & 1 \\ -0.6 & -1.5 & -2.5 \end{bmatrix},
$$

$$
x_0 = \begin{bmatrix} -0.1 \\ 0.1 \\ 0.2 \end{bmatrix}, f(x(t), t) = \begin{bmatrix} \frac{1}{10\sqrt{3}} \tanh x_1(t) \\ \frac{1}{10\sqrt{3}} \tanh x_2(t) \\ \frac{1}{10\sqrt{3}} \tanh x_3(t) , \end{bmatrix},
$$

$$
C_m(\tau_m) = \begin{bmatrix} 0.5 & 0 & 0 \\ 0 & 0.5 & 0 \\ 0 & 0 & 0.5 \end{bmatrix}.
$$

It is easy to verify that $\mathcal{E}^T P = P^T \mathcal{E} \geq 0$ *with* $P = I_3$ *and* $f(x(t), t)$ *satisfies the Lipschitz condition with* $F = \frac{1}{10\sqrt{3}} I$.

Here, $\zeta = -3$, $\epsilon = 0.05$ *with impulse arrival rate* $\gamma = 25, \kappa = 0.5$ *and* $\tau' = \max_{m \in Z_+} \left\{ \xi'_m - \xi'_{m-1} \right\} = 0.026$, *then the conditions* (5) *in Theorem 1 are satisfied. Hence system* (1) *is* $\mathcal{E}$*-ES. Figure 1 illustrates the graphical behaviour of the solution. When there are no impulses, then the above system is unstable.*

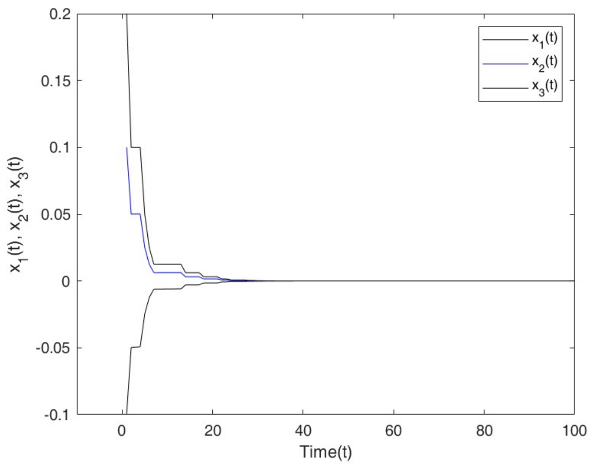

Figure 1. $\mathcal{E}$- Exponential stability.

Example 2. *Consider system* (1) *where*

$$
\begin{aligned}
\mathcal{E} &= \begin{bmatrix} 4 & 0 \\ 2 & 0 \end{bmatrix}, A = \begin{bmatrix} -2 & 1 \\ 1 & -2 \end{bmatrix}, \\
C_m(\tau_m) &= \begin{bmatrix} -0.7 & 0 \\ 0 & -0.5 \end{bmatrix}, x_0 = \begin{bmatrix} -0.1 \\ 0.1 \end{bmatrix}, \\
f(x(t), t) &= \begin{bmatrix} \frac{\sin x_1(t)}{4\sqrt{3}} \\ \frac{\sin x_2(t)}{4\sqrt{3}} \end{bmatrix}.
\end{aligned}
$$

It is easy to verify that $\mathcal{E}^T P = P^T \mathcal{E} \geq 0$ *with* $P = \begin{bmatrix} 1 & -0.5 \\ 0 & 1 \end{bmatrix}$ *and* $f(x(t), t)$ *satisfies the Lipschitz conditions with* $F = \frac{1}{4\sqrt{3}} I$.

Choose $p = 2$, $\mathcal{G} = \begin{bmatrix} 0.2 & 0.1 \\ -0.4 & 0.8 \end{bmatrix}$,
$\mathcal{Q} = \begin{bmatrix} 1 & 0 \\ 0.8 & -0.5 \end{bmatrix}$, *such that* $\mathcal{G}\mathcal{E}\mathcal{Q} = \begin{bmatrix} 1 & 0 \\ 0 & 0 \end{bmatrix}$, *and*
$\mathcal{G}A\mathcal{Q} = \begin{bmatrix} -0.3 & 0 \\ 0 & 1 \end{bmatrix}$.

Hence, it is easy to verify that $\|\mathcal{G}_2\| \leq 1$ *and* $1 - E\|F\mathcal{Q}_2\|^2 > 0$.

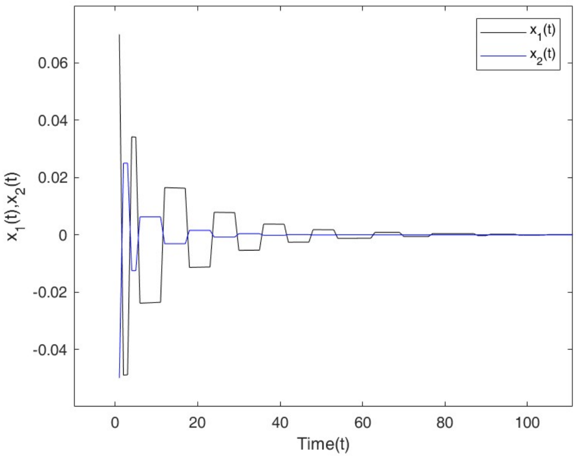

Figure 2. Exponential stability.

Then the singular system (1) *becomes*

$$\begin{aligned} \dot{x}_1(t) &= -0.3x_1(t) + 0.0404\frac{\sin x_1(t)}{4\sqrt{3}} \\ &\quad -0.0072\frac{\sin x_2(t)}{4\sqrt{3}}, \\ &\quad \chi_m^{'} < t < \chi_{m+1}^{'}, t \geq t_0, \end{aligned}$$

and

$$\begin{aligned} 0 &= x_2(t) + 0.0346\frac{\sin x_1(t)}{4\sqrt{3}} - 0.0577\frac{\sin x_2(t)}{4\sqrt{3}}, \\ &\quad \chi_m^{'} < t < \chi_{m+1}^{'}, t \geq t_0, \\ x(\chi_m^+) &= C_m(\tau_m)x(\chi_m^-), m \in Z_+. \end{aligned}$$

Choose $\zeta = -2$, $\gamma = 4$, *and* $\epsilon = 0.05$ *such that* $(A^TP + P^TA) + \lambda_{max}(\frac{1}{\epsilon}F^TF + \epsilon P^TP) - \zeta\mathcal{E}^TP < 0$. *Further, take* $\kappa = 1.5$ *and* $\tau^{'} = \max_{m\in Z_+}\left\{\xi_m^{'} - \xi_{m-1}^{'}\right\} = 0.026$, *then conditions* (5) *in Theorem* 1 *are satisfied. Hence system* (1) *is mean square ES. Figure 2 demonstrates the graphical behaviour of the solution. When there are no impulses, then the above system is unstable.*

Example 3. *Consider system* (1) *where*

$$\mathcal{E} = \begin{bmatrix} 1+i & 0 & 0 \\ 0 & 1+i & 0 \\ 0 & 0 & 0 \end{bmatrix}, x_0 = \begin{bmatrix} -0.5+0.1i \\ -0.4+0.2i \\ 0.2+i \end{bmatrix},$$

$$A = \begin{bmatrix} -0.5+i & 0.2-0.3i & 0.1+0.3i \\ 0.2+0.5i & -1-0.5i & -0.1-i \\ -1.2+i & -0.4-0.3i & -0.2-0.5i \end{bmatrix},$$

$$f(x(t),t) = \begin{bmatrix} \frac{1}{2}(|x_1(t)+1| - |x_1(t)-1|) \\ \frac{1}{2}(|x_2(t)+1| - |x_2(t)-1|) \\ \frac{1}{2}(|x_3(t)+1| - |x_3(t)-1|) \end{bmatrix},$$

$$C_m(\tau_m) = \begin{bmatrix} 0.25+0.1i & 0 & 0 \\ 0 & 0.25+0.1i & 0 \\ 0 & 0 & 0.25+0.1i \end{bmatrix}.$$

It is easy to verify that $\mathcal{E}^TP = P^T\mathcal{E} \geq 0$ *with* $P = I_3$ *and* $f(x(t),t)$ *satisfies the Lipschitz condition with* $F = \frac{1}{2}I$.

Here, $\zeta = -5$, $\epsilon = 0.01$ *with impulse arrival rate* $\gamma = 10, \kappa = 0.7$ *and* $\tau^{'} = \max_{m\in Z_+}\left\{\xi_m^{'} - \xi_{m-1}^{'}\right\} = 0.005$, *then the conditions* (5) *in Theorem* 1 *are satisfied. Hence system* (1) *is* $\mathcal{E}$*-ES.*

Remark 6. *In the above example, we have proved that the results hold true even when the matrices involved have complex entries. However, the function* f *involved is still a real valued function.*

5. Conclusion

In this paper, we consider the exponential stability of random impulsive nonlinear singular differential system. It is worth mentioning that the system under consideration involves random impulses which may cause some technical difficulties comparing with systems with fixed impulses. Less restrictive conditions are established for the $\mathcal{E}$-ES and ES of the system. To support the theoretical findings, we give two numerical examples along with their graphical representations. We illustrate that the obtained results are consistent with the main theorem. We have additionally proved the truth of the results in case of matrices involving complex entries as well, while the function involved still remains real-valued. Proving the results true for complex valued functions could be considered to be a future problem. Moreover, as done in [11], we can consider analyzing a system with delay by reformulating it into a singular linear system of differential equations, as a future work. We believe that the results of this paper are of great significant for relevant community and can be used for instance to investigate switched singular time delay systems.

Acknowledgments

M. Fečkan would like to thank the Slovak Research and Development Agency under the contract No. APVV-18-0308, and the Slovak Grant Agency VEGA No. 1/0084/23 and No. 2/0127/20 for supporting and funding this work. J. Alzabut expresses his sincere thanks to Prince Sultan University and OSTIM Technical University for supporting this research.

References

[1] Xu, S., & Lam, J. (2006). *Robust control and filtering of singular systems* (Vol. 332, pp. xii+-234). Springer, Berlin.

[2] Dai, L. (Ed.). (1989). *Singular control systems.* Springer, Berlin Heidelberg.

[3] Guan, Z. H., Yao, J., & Hill, D. J. (2005). Robust H/sub/spl infin//control of singular impulsive systems with uncertain perturbations. *IEEE Transactions on Circuits and Systems II: Express Briefs*, 52(6), 293-298.

[4] Liu, G. (2017). New results on stability analysis of singular time-delay systems. *International Journal of Systems Science*, 48(7), 1395-1403.

[5] Zhu, S., Zhang, C., Cheng, Z., & Feng, J. (2007). Delay-dependent robust stability criteria for two classes of uncertain singular time-delay systems. *IEEE Transactions on Automatic Control*, 52(5), 880-885.

[6] Feng, G., & Cao, J. (2015). Stability analysis of impulsive switched singular systems. *IET Control Theory & Applications*, 9(6), 863-870.

[7] Chen, W. H., Zheng, W. X., & Lu, X. (2017). Impulsive stabilization of a class of singular systems with time-delays. *Automatica*, 83, 28-36.

[8] Van Hien, L., Vu, L. H., & Phat, V. N. (2015). Improved delay-dependent exponential stability of singular systems with mixed interval time-varying delays. *IET Control Theory & Applications*, 9(9), 1364-1372.

[9] Zhi, Y. L., He, Y., Shen, J., & Wu, M. (2018). New stability criteria of singular systems with time-varying delay via free-matrix-based integral inequality. *International Journal of Systems Science*, 49(5), 1032-1039.

[10] Shi, S., Zhang, Q., Yuan, Z., & Liu, W. (2011). Hybrid impulsive control for switched singular systems. *IET Control Theory & Applications*, 5(1), 103-111.

[11] Dassios, I. (2022). On the relations between a singular system of differential equations and a system with delays. *Mathematical Modelling and Numerical Simulation with Applications*, 2(4), 221-227.

[12] Dolezal, V. (1986). Generalized solutions of semistate equations and stability. Circuits, *Systems and Signal Processing*, 5, 391-403.

[13] Zheng, G., Boutat, D., & Wang, H. (2017). A nonlinear Luenberger-like observer for nonlinear singular systems. *Automatica*, 86, 11-17.

[14] Jin, Z., & Wang, Z. (2021). Input-to-state stability of the nonlinear singular systems via small-gain theorem. *Applied Mathematics and Computation*, 402, 126171.

[15] Boutat, D., & Zheng, G. (2021). *Observer design for nonlinear dynamical systems.* Springer International Publishing.

[16] Jiang, B., Gao, C., & Xie, J. (2015). Passivity based sliding mode control of uncertain singular Markovian jump systems with time-varying delay and nonlinear perturbations. *Applied Mathematics and Computation*, 271, 187-200.

[17] Debeljkovic, D. L. (2004). Singular control systems. *Dynamics of Continuous Discrete and Impulsive Systems Series A*, 11, 691-706.

[18] Han, Y., Kao, Y., Gao, C., & Jiang, B. (2017). Robust sliding mode control for uncertain discrete singular systems with time-varying delays. *International Journal of Systems Science*, 48(4), 818-827.

[19] Zhai, D., Zhang, Q. L., & Li, J. H. (2014). Fault detection for singular multiple time-delay systems with application to electrical circuit. *Journal of the Franklin Institute*, 351(12), 5411-5436.

[20] Liu, P. L. (2013). Improved delay-dependent robust exponential stabilization criteria for uncertain time-varying delay singular systems. *International Journal of Innovative Computing, Information and Control*, 9(1), 165-178.

[21] Xiong, W., Zhang, D., & Cao, J. (2017). Impulsive synchronisation of singular hybrid coupled networks with time-varying nonlinear perturbation. *International Journal of Systems Science*, 48(2), 417-424.

[22] Guan, Z. H., Chan, C. W., Leung, A. Y., & Chen, G. (2001). Robust stabilization of singular-impulsive-delayed systems with nonlinear perturbations. *IEEE Transactions on Circuits and Systems I: Fundamental Theory and Applications*, 48(8), 1011-1019.

[23] Xu, J., & Sun, J. (2010). Finite-time stability of linear time-varying singular impulsive systems [Brief Paper]. *IET Control Theory & Applications*, 10(4), 2239-2244.

[24] Liu, Q., Tian, S., & Gu, P. (2018). Iterative learning control for a class of singular impulsive systems. *International Journal of Systems Science*, 49(7), 1383-1390.

[25] Zhan, T., Ma, S., & Chen, H. (2019). Impulsive stabilization of nonlinear singular switched systems with all unstable-mode subsystems. *Applied Mathematics and Computation*, 344, 57-67.

[26] Yang, X., Li, X., & Cao, J. (2018). Robust finite-time stability of singular nonlinear systems with interval time-varying delay. *Journal of the Franklin Institute*, 355(3), 1241-1258.

[27] Lakshmikantham, V., & Simeonov, P. S. (1989). *Theory of impulsive differential equations* (Vol. 6). World Scientific.

[28] Yang, T. (2001). *Impulsive control theory* (Vol. 272). Springer Science & Business Media.

[29] Shah, S. O., Zada, A., & Hamza, A. E. (2019). Stability analysis of the first order non-linear impulsive time varying delay dynamic system on time scales. *Qualitative Theory of Dynamical Systems*, 18, 825-840.

[30] Zada, A., Alam, L., Kumam, P., Kumam, W., Ali, G., & Alzabut, J. (2020). Controllability of impulsive non–linear delay dynamic systems on time scale. *IEEE Access*, 8, 93830-93839.

[31] Xu, J., Pervaiz, B., Zada, A., & Shah, S. O. (2021). Stability analysis of causal integral evolution impulsive systems on time scales. *Acta Mathematica Scientia*, 41(3), 781-800.

[32] Vinodkumar, A., Prakash, M., & Joo, Y. H. (2019). Impulsive observer-based output control for PMSG-based wind energy conversion system. *IET Control Theory & Applications*, 13(13), 2056-2064.

[33] Stamov, G. T., Alzabut, J. O., Atanasov, P., & Stamov, A. G. (2011). Almost periodic solutions for an impulsive delay model of price fluctuations in commodity markets. *Nonlinear Analysis: Real World Applications*, 12(6), 3170-3176.

[34] Saker, S. H., & Alzabut, J. O. (2009). On the impulsive delay hematopoiesis model with periodic coefficients. *The Rocky Mountain Journal of Mathematics*, 1657-1688.

[35] Zada, A., Alzabut, J., Waheed, H., & Popa, I. L. (2020). Ulam–Hyers stability of impulsive integrodifferential equations with Riemann–Liouville boundary conditions. *Advances in Difference Equations*, 2020(1), 1-50.

[36] Li, Z., Soh, Y., & Wen, C. (2005). *Switched and impulsive systems: Analysis, design and applications* (Vol. 313). Springer Science & Business Media.

[37] Liu, X. (1994). Stability results for impulsive differential systems with applications to population growth models. *Dynamics and stability of systems*, 9(2), 163-174.

[38] Zhao, Y., Li, X., & Cao, J. (2020). Global exponential stability for impulsive systems with infinite distributed delay based on flexible impulse frequency. *Applied Mathematics and Computation*, 386, 125467.

[39] Li, M., Chen, H., & Li, X. (2021). Exponential stability of nonlinear systems involving partial unmeasurable states via impulsive control. *Chaos, Solitons & Fractals*, 142, 110505.

[40] Li, X., Vinodkumar, A., & Senthilkumar, T. (2019). Exponential stability results on random and fixed time impulsive differential systems with infinite delay. *Mathematics*, 7(9), 843.

[41] Vinodkumar, A., Senthilkumar, T., & Li, X. (2018). Robust exponential stability results for uncertain infinite delay differential systems with random impulsive moments. *Advances in Difference Equations*, 2018(1), 1-12.

[42] Agarwal, R., Hristova, S., & O'Regan, D. (2013). Exponential stability for differential equations with random impulses at random times. *Advances in Difference Equations*, 2013, 1-12.

[43] Vidyasagar, M. (2002). *Nonlinear systems analysis*. Society for Industrial and Applied Mathematics.

[44] Mao, X. (1994). *Exponential Stability of Stochastic Differential Equations*. Marcel Dekker.

[45] Vinodkumar, A., Senthilkumar, T., Hariharan, S., & Alzabut, J. (2021). Exponential stabilization of fixed and random time impulsive delay differential system with applications. *Mathematical Biosciences and Engineering*, 18(3), 2384-2400.

[46] Waheed, H., Zada, A., & Xu, J. (2021). Well-posedness and Hyers-Ulam results for a class of impulsive fractional evolution equations. *Mathematical Methods in the Applied Sciences*, 44(1), 749-771.

[47] Zada, A., Pervaiz, B., Shah, S. O., & Xu, J. (2020). Stability analysis of first-order impulsive nonautonomous system on timescales. *Mathematical Methods in the Applied Sciences*, 43(8), 5097-5113.

[48] Vinodkumart, A., Loganathan, C., & Vijay, S. (2020). Approximate Controllability Results for Integro-Quasilinear Evolution Equations Via Trajectory Reachable Sets. *Acta Mathematica Scientia*, 40(2), 412-424.

[49] Khargonekar, P. P., Petersen, I. R., & Zhou, K. (1990). Robust stabilization of uncertain linear systems: quadratic stabilizability and H/sup infinity/control theory. *IEEE Transactions on Automatic Control*, 35(3), 356-361.

Arumugam Vinodkumar *works as an Associate Professor in the Department of Mathematics, School of Physical Sciences, Amrita Vishwa Vidyapeetham, Coimbatore Campus. He completed his Ph.D. in Random impulsive Differential Systems and Stochastic Differential Systems. Now he is working on qualitative behaviors of the differential systems. He serves as a reviewer for some prestigious journals and societies.*
`https://orcid.org/0000-0002-5314-8768`

Sivakumar Harinie *is currently working as an Amazon and Key Accounts Analyst at Hatley Little Blue House Inc, Montreal, Canada. She completed her Master's Degree, MSc in Mathematics, at the School of Physical Sciences, Amrita Vishwa Vidyapeetham, Coimbatore Campus. Additionally, she has completed a Master's Program in Data Analyst and Data Scientist at Simplilearn, Bangalore.*
`https://orcid.org/0009-0003-3172-3869`

Michal Fečkan *has been a Professor of Mathematics at the Department of Mathematical Analysis and Numerical Mathematics in the Faculty of Mathematics, Physics, and Informatics at Comenius University in Bratislava, Slovakia, since 2003. He received his Master's degree from Comenius University in Bratislava in 1985 and his Ph.D. from the Mathematical Institute of the Slovak Academy of Sciences in Bratislava,*

Slovakia, in 1993. He is interested in nonlinear functional analysis, bifurcation theory, dynamical systems, and fractional calculus with applications to mechanics, vibrations, and economics. He is a Highly Cited Researcher in Mathematics.
https://orcid.org/0000-0002-7385-6737

Jehad Alzabut *is a professor of Applied Mathematics. He received his Ph.D. degree from Middle East Technical University, Turkey. His area of interest is qualitative properties of delay, difference, fractional, and impulsive differential equations. He has particular interest in mathematical models describing biological and medical phenomena. He serves the role of an editor and a reviewer for some prestigious journals and societies.*
https://orcid.org/0000-0002-5262-1138

An International Journal of Optimization and Control: Theories & Applications (http://www.ijocta.org)

An International Journal of Optimization and Control: Theories & Applications
ISSN:2146-0957 eISSN:2146-5703
Vol.13, No.2, pp.269-276 (2023)
http://doi.org/10.11121/ijocta.2023.1371

RESEARCH ARTICLE

The solvability of the optimal control problem for a nonlinear Schrödinger equation

Nigar Yildirim Aksoy,[a*] Ercan Celik,[b] Muhammed Emin Dadas[a]

[a]*Department of Mathematics, Faculty of Arts and Sciences, Kafkas University, Kars, Turkey*
[b]*Department of Applied Mathematics and Informatics, Kyrgyz-Turkish Manas University, Bishkek, Kyrgyzstan*
nyaksoy55@hotmail.com, ercan.celik@manas.edu.kg, emin_dad@hotmail.com

ARTICLE INFO

Article History:
Received 15 February 2023
Accepted 30 March 2023
Available 29 July 2023

Keywords:
Optimal control problem
Schrödinger equation
Frechet differentiability
Optimality conditions

AMS Classification 2010:
49J20; 35J10; 49K20

ABSTRACT

In this paper, we analyze the solvability of the optimal control problem for a nonlinear Schrödinger equation. A Lions-type functional is considered as the objective functional. First, it is shown that the optimal control problem has at least one solution. Later, the Frechet differentiability of the objective functional is proved and a formula is obtained for its gradient. Finally, a necessary optimality condition is derived.

1. Introduction

The nonlinear Schrödinger equation (NLSE) describes the behavior of wave packets in weakly nonlinear media. It is an adaptable model to many disciplines in applied sciences such as dynamical systems, materials science, nonlinear optics, fluid dynamics, astrophysics, particle physics, and nonlinear transmission networks. NLSE represents the evolution of optical waves in a nonlinear fiber, various biological systems, and the price of options in economics [1].

In the present paper, we consider a specific case of the following Schrödinger equation

$$\varepsilon\frac{\partial u}{\partial \tau} + R_2(\varsigma,\tau,u)\frac{\partial^2 u}{\partial \varsigma^2} + R_1(\varsigma,\tau,u)\frac{\partial u}{\partial \varsigma} + R_0(\varsigma,\tau,u)u = 0, \qquad (1)$$

where $\varepsilon = const.$, $u(\varsigma,\tau)$ is the wave's complex amplitude. The coefficients $R_j(\varsigma,\tau,u)$ for $j = 0,1,2$ describe the variation of the medium. If the functions R_j depend on $u(\varsigma,\tau)$, it shows that the medium has the nonlinear properties [2]. Linear and nonlinear Schrödinger equations are obtained from equation (1) with respect to the characteristics of the coefficients $R_j(\varsigma,\tau,u)$ for $j = 0,1,2$ and $\varepsilon = i$.

Optimal control problems (OCPs) arise in many branches of science. They have numerous applications in optics, medical imaging, geophysics, system identification, communication theory, astronomy, medicine [3–11].

As it is known, in the OCPs, there is an objective functional, a controlled system, and a set of admissible controls. The objective functionals can be diversely chosen with regard to our purpose such as final, boundary or Lions-type functional [12]. In the studies [13–22], the objective functional is considered as a final functional and the controlled system is generally stated by the Schrödinger equation. In [23–27], the OCPs with Lions functional has been studied and the controlled system is stated by linear or nonlinear Schrödinger equations. Also, in [28–30], the

*Corresponding Author

OCPs for systems whose state is expressed by the Schrödinger equation with the boundary functional has been studied.

In this paper, we consider an OCP with Lions functional for NLSE derived from (1). It is proved that the OCP has a unique solution and the objective functional is Frechet differentiable. Also, by proving the continuity of the gradient of the objective functional, a necessary optimality condition is obtained.

Differently from the previous studies, in this paper, we analyze the solution of the OCP for NLSE derived from (1) for $R_2 = R_2(\varsigma,\tau)$, $R_1 = R_1(\varsigma,\tau)$, $R_0(\varsigma,\tau,u) = R_0(\varsigma,\tau,u)$ with different coefficients which are in the larger space than previous works.

2. The statement of optimal control problem

The OCP is the problem of finding the minimum of the objective functional

$$J_\alpha(p) = ||u_1 - u_2||^2_{L_2(\Omega)} + \alpha||p - w||^2_{L_2(I)} \quad (2)$$

subject to

$$i\frac{\partial u_1}{\partial \tau} + a_0\frac{\partial^2 u_1}{\partial \varsigma^2} + ia_1(\varsigma)\frac{\partial u_1}{\partial \varsigma} - a_2(\varsigma)u_1 + p(\varsigma)u_1 + ia_3|u_1|^2u_1 = f_1, \quad (3)$$

$$\left.\begin{array}{c} u_1(\varsigma,0) = \vartheta_1(\varsigma),\ \varsigma \in I, \\ u_1(0,\tau) = u_1(l,\tau) = 0, \tau \in (0,T) \end{array}\right\} \quad (4)$$

and

$$i\frac{\partial u_2}{\partial \tau} + a_0\frac{\partial^2 u_2}{\partial \varsigma^2} + ia_1(\varsigma)\frac{\partial u_2}{\partial \varsigma} - a_2(\varsigma)u_2 + p(\varsigma)u_2 + ia_3|u_2|^2u_2 = f_2, \quad (5)$$

$$\left.\begin{array}{c} u_2(\varsigma,0) = \vartheta_2(\varsigma),\ \varsigma \in I, \\ \frac{\partial u_2}{\partial \varsigma}(0,\tau) = \frac{\partial u_2}{\partial \varsigma}(l,\tau) = 0, \tau \in (0,T) \end{array}\right\} \quad (6)$$

on admissible controls set

$$P \equiv \{p \in L_2(I):\ |p(\varsigma)| \le b_0 \ for\ almost\ all\ \varsigma \in I\},$$

where $\varsigma \in I = (0,l)$, $\tau \in Q = [0,T]$, $i = \sqrt{-1}$. Let $\Omega = I \times (0,T)$, $\Omega_\tau = I \times (0,\tau)$, $\widetilde{\Omega}_\tau = I \times (\tau,T)$ and $a_0, a_3, b_0 > 0$ are given real numbers, $a_1(\varsigma)$, $a_2(\varsigma)$, ϑ_1, ϑ_2, f_1, f_2 are functions which satisfy the conditions, respectively

$$\left.\begin{array}{c} |a_1(\varsigma)| \le \mu_1,\ \left|\frac{da_1(\varsigma)}{d\varsigma}\right| \le \mu_2 \ for\ almost\ all\ \varsigma \in I, \\ a_1(0) = a_1(l) = 0,\ \ \mu_1,\mu_2 = const. > 0, \end{array}\right\} \quad (7)$$

$$0 < \mu_3 \le a_2(\varsigma) \le \mu_4 \ for\ almost\ all\ \varsigma \in I, \quad \mu_3,\mu_4 = const. > 0, \quad (8)$$

$$\left.\begin{array}{c} \vartheta_1 \in \mathring{W}^2_2(I),\ \vartheta_2 \in W^2_2(I),\ \frac{\partial \vartheta_2(0)}{\partial \varsigma} = \frac{\partial \vartheta_2(l)}{\partial \varsigma} = 0, \\ f_r \in W^{0,1}_2(\Omega) \text{ for } r = 1,2, \end{array}\right\} \quad (9)$$

where $W^m_s(I), W^{m,n}_s(\Omega), \mathring{W}^m_s(I)$ for $m \ge 0$, $s \ge 1$ are Sobolev spaces. These Sobolev spaces are in detail explained in [31]. Also, $\alpha \ge 0$ is a Tikhonov regularization parameter [32] and $w \in L_2(I)$ is a given element.

Since the solutions of (3)-(4) and (5)-(6) evidently depend on p, we denote $u_r = u_r(\varsigma,\tau) \equiv u_r(\varsigma,\tau;p)$ for $r = 1,2$.We are interested in solutions of problems (3)-(4) and (5)-(6) in the following sense:

Definition 1. *A function $u_1 \in U_1 \equiv C^0(Q,\mathring{W}^2_2(I)) \cap C^1(Q,L_2(I))$ is said to be a solution of problem (3)-(4), if it holds (3) for almost all $\varsigma \in I$ and any $\tau \in Q$, (4) for almost all $\varsigma \in I$ and for almost all $\tau \in (0,T)$, respectively.*

Definition 2. *A function $u_2 \in U_2 \equiv C^0(Q,W^2_2(I)) \cap C^1(Q,L_2(I))$ is said to be a solution of problem (5)-(6), if it holds (5) for almost all $\varsigma \in I$ and any $\tau \in Q$, (6) for almost all $\varsigma \in I$ and for almost all $\tau \in (0,T)$, respectively.*

In the definitions above, for any nonnegative integer k, $C^k(Q,B)$ is the Banach space of all $B-$valued, k times continuously differentiable functions on Q with the norm

$$||u||_{C^k(Q,B)} = \sum_{m=0}^{k} \max_{0\le t\le T} ||\frac{d^m u(t)}{dt^m}||_B$$

for $u \in C^k(Q,B)$.

By the methodology in [33], we can readily prove the theorem below:

Theorem 1. *Assume that a_1, a_2, ϑ_r, f_r for $r = 1,2$ satisfy the conditions (7), (8) and (9), respectively. Then, problems (3)-(4) and (5)-(6) for each $p \in P$ have unique solutions $u_1 \in U_1$, $u_2 \in U_2$, respectively, and the functions u_1, u_2 satisfy the estimates*

$$||u_1(.,\tau)||^2_{\mathring{W}^2_2(I)} + \left\|\frac{\partial u_1}{\partial \tau}\right\|^2_{L_2(I)} \le c_1\left(||\vartheta_1||^2_{\mathring{W}^2_2(I)} + ||f_1||^2_{W^{0,1}_2(\Omega)} + ||\vartheta_1||^6_{\mathring{W}^1_2(I)}\right), \quad (10)$$

$$||u_2(.,\tau)||^2_{W_2^2(I)} + \left\|\frac{\partial u_2}{\partial \tau}\right\|^2_{L_2(I)} \leq \tag{11}$$
$$c_2\left(||\vartheta_2||^2_{W_2^2(I)} + ||f_2||^2_{W_2^{0,1}(\Omega)} + ||\vartheta_2||^6_{W_2^1(I)}\right),$$

for any $\tau \in Q$*, where the constants* c_1, $c_2 > 0$ *are independent from* $\vartheta_1, f_1, \vartheta_2, f_2$ *and* τ.

For simplicity, let's rewrite problems (3)-(4) and (5)-(6) in the form

$$i\frac{\partial u_r}{\partial \tau} + a_0\frac{\partial^2 u_r}{\partial \varsigma^2} + ia_1(\varsigma)\frac{\partial u_r}{\partial \varsigma} -$$
$$a_2(\varsigma)u_r + p(\varsigma)u_r + ia_3\left|u_r\right|^2 u_r = f_r \tag{12}$$
$$for\ r = 1,2,$$

$$u_r(\varsigma,0) = \vartheta_r(\varsigma), \varsigma \in I\ for\ r = 1,2, \tag{13}$$

$$\left.\begin{array}{l} u_1(0,\tau) = u_1(l,\tau) = 0,\ \tau \in (0,T)\,, \\ \frac{\partial u_2(0,\tau)}{\partial \varsigma} = \frac{\partial u_2(l,\tau)}{\partial \varsigma} = 0,\ \tau \in (0,T)\,. \end{array}\right\} \tag{14}$$

Thus, the OCP is to minimize the objective functional (2) on P under conditions (12)-(14).

3. The solvability of optimal control problem

In this section, we show that the OCP has a unique solution on a dense subset of $L_2(I)$ and it has at least one solution on $L_2(I)$.

Lemma 1. *The functional* $J_0(p) = ||u_1 - u_2||^2_{L_2(\Omega)}$ *is continuous on* P.

Proof. Suppose $u_r = u_r(\varsigma,\tau;p)$ and $u_{r\delta} = u_r(\varsigma,\tau;p+\delta p)$ for $r =$ 1,2 are solutions of problem (12)-(14) corresponding to $p \in P$, $p+\delta p \in P$, respectively, where $\delta p \in L_\infty(I)$ is an increment of any $p \in P$. Then, for $r = 1,2$, the functions $\delta u_r \equiv u_r(\varsigma,\tau;p+\delta p) - u_r(\varsigma,\tau;p)$ hold the boundary value problem

$$i\frac{\partial \delta u_r}{\partial \tau} + a_0\frac{\partial^2 \delta u_r}{\partial \varsigma^2} + ia_1(\varsigma)\frac{\partial \delta u_r}{\partial \varsigma} -$$
$$a_2(\varsigma)\delta u_r + (p(\varsigma) + \delta p(\varsigma))\delta u_r +$$
$$ia_3\left[\left(\left|u_{r\delta}\right|^2 + \left|u_r\right|^2\right)\delta u_r\right] + \tag{15}$$
$$ia_3 u_{r\delta}u_r\left(\delta\overline{u}_r\right) = -\delta p(\varsigma)u_r,$$

$$\delta u_r(\varsigma,0) = 0,\ \varsigma \in I,\ r = 1,2, \tag{16}$$

$$\left.\begin{array}{l} \delta u_1(0,\tau) = \delta u_1(l,\tau) = 0, \tau \in (0,T) \\ \frac{\partial \delta u_2(0,\tau)}{\partial \varsigma} = \frac{\partial \delta u_2(l,\tau)}{\partial \varsigma} = 0,\ \tau \in (0,T)\,. \end{array}\right\} \tag{17}$$

Now we multiply both sides of equation (15) by $\delta\overline{u}_r$ for $r =$ 1,2, and integrate over Ω_τ. If we subtract their complex conjugates from equalities obtained with the help of integration by parts and use condition (16), we get

$$\left\|\delta u_r(.,\tau)\right\|^2_{L_2(I)} + \int\limits_{\Omega_\tau} \frac{\partial}{\partial \varsigma}\left(a_1(\varsigma)\left|\delta u_r\right|^2\right)d\varsigma dt +$$
$$2a_3\int\limits_{\Omega_\tau}\left|\delta u_r\right|^2\left(\left|u_{r\delta}\right|^2 + \left|u_r\right|^2\right)d\varsigma dt +$$
$$2a_3\int\limits_{\Omega_\tau} Re\left(u_{r\delta}u_r(\delta\overline{u}_r)^2\right)d\varsigma dt = \tag{18}$$
$$-2\int\limits_{\Omega_\tau} Im\left(\delta p u_r \delta\overline{u}_r\right)d\varsigma dt +$$
$$\int\limits_{\Omega_\tau}\frac{\partial a_1(\varsigma)}{\partial \varsigma}\left|\delta u_r\right|^2 d\varsigma dt.$$

Using conditions (7), (17) and Young's inequality in (18),we obtain

$$\left\|\delta u_r(.,\tau)\right\|^2_{L_2(I)} +$$
$$a_3\int\limits_{\Omega_\tau}\left|\delta u_r\right|^2\left(\left|u_{r\delta}\right|^2 + \left|u_r\right|^2\right)d\varsigma dt \leq \tag{19}$$
$$(1+\mu_2)\int\limits_{\Omega_\tau}\left|\delta u_r\right|^2 d\varsigma dt + \int\limits_{\Omega_\tau}\left|\delta p\right|^2\left|u_r\right|^2 d\varsigma dt.$$

Since $a_3 > 0$ and $\int\limits_{\Omega_\tau}\left|\delta p\right|^2\left|u_r\right|^2 d\varsigma dt \leq \left\|\delta p\right\|^2_{L_\infty(I)}\left(\int\limits_0^T\left\|u_r(.,t)\right\|^2_{L_2(I)}dt\right)$, from (19) by virtue of estimates (10) and (11) we get

$$\left\|\delta u_r(.,\tau)\right\|^2_{L_2(I)} +$$
$$a_3\int\limits_{\Omega_\tau}\left|\delta u_r\right|^2\left(\left|u_{r\delta}\right|^2 + \left|u_r\right|^2\right)d\varsigma dt \leq \tag{20}$$
$$c_3\left\|\delta p\right\|^2_{L_\infty(I)},\ r = 1,2$$

for any $\tau \in Q$, where the positive constant c_3 does not depend on δp and τ.

Using formula (2) for $\alpha = 0$, we obtain

$$\delta J_0(p) = J_0(p+\delta p) - J_0(p) =$$
$$2\int\limits_{\Omega} Re\left[\left(u_1 - u_2\right)\left(\delta\overline{u}_1 - \delta\overline{u}_2\right)\right]dxdt +$$
$$\left\|\delta u_1\right\|^2_{L_2(\Omega)} + \left\|\delta u_2\right\|^2_{L_2(\Omega)} - \tag{21}$$
$$2\int\limits_{\Omega} Re\left(\delta u_1\delta\overline{u}_2\right)dxdt$$

which implies that

$$\begin{aligned}|\delta J_0(p)| &\leq 2\|u_1\|_{L_2(\Omega)}\|\delta u_1\|_{L_2(\Omega)} + \\ &2\|u_1\|_{L_2(\Omega)}\|\delta u_2\|_{L_2(\Omega)} + \\ &2\|u_2\|_{L_2(\Omega)}\|\delta u_1\|_{L_2(\Omega)} + \\ &2\|u_2\|_{L_2(\Omega)}\|\delta u_2\|_{L_2(\Omega)} + \\ &2\|\delta u_1\|^2_{L_2(\Omega)} + 2\|\delta u_2\|^2_{L_2(\Omega)}.\end{aligned}$$

If we use estimates (10), (11), (20) in the inequality above, we get the inequality

$$|J_0(p+\delta p) - J_0(p)| \leq c_4\left(\|\delta p\|_{L_\infty(I)} + \|\delta p\|^2_{L_\infty(I)}\right)$$

for any $p \in P$, where c_4 is a positive constant independent from δp. Thus, we obtain that $|\delta J_0(p)| \to 0$ as $\|\delta p\|_{L_\infty(I)} \to 0$ for *any* $p \in P$, which concludes the proof. □

Theorem 2. *Let Theorem 1 be satisfied and $w \in L_2(I)$. Then, there exists a dense subset $V \subset L_2(I)$ such that OCP has a unique solution for any $w \in V$ and $\alpha > 0$.*

Proof. From Lemma 1, $J_0(p)$ is a lower semicontinuous functional. Also, it is clear that $J_0(p)$ is lower bounded. As known, $L_2(I)$ is a uniformly convex Banach space. Furthermore, P is a closed, bounded subset of $L_2(I)$. Therefore, based on Theorem 4 in [34] we can say that the OCP has a unique solution on a dense subset $V \subset L_2(I)$. This completes the proof. □

Theorem 3. *Let $w \in L_2(I)$ be a given function and $\alpha \geq 0$. Also, assume that Theorem 1 is satisfied. Then, the OCP has at least one solution.*

Proof. The proof of Theorem 3 is carried out as in [22]. □

4. The gradient of functional and a necessary optimality condition

In this section, we introduce the adjoint problem to investigate the differentiability of the objective functional and get a formula for its gradient. Finally, a necessary optimality condition for the OCP is derived.

By using Lagrange multiplier functions, we obtain the adjoint problem as follows:

$$\begin{aligned}&i\frac{\partial \eta_r}{\partial \tau} + a_0\frac{\partial^2 \eta_r}{\partial \varsigma^2} + i\frac{\partial}{\partial \varsigma}\left(a_1(\varsigma)\eta_r\right) - \\ &a_2(\varsigma)\eta_r + p(\varsigma)\eta_r - 2ia_3|u_r|^2\eta_r + \\ &ia_3u_r^2\overline{\eta}_r = 2(-1)^r\left(u_1 - u_2\right) \;\; for\ r = 1, 2,\end{aligned} \tag{22}$$

$$\eta_r(\varsigma, T) = 0 \;\; for\ r = 1, 2,\ \varsigma \in I, \tag{23}$$

$$\left.\begin{aligned}&\eta_1(0,\tau) = \eta_1(l,\tau) = 0, \tau \in (0,T),\\ &\frac{\partial \eta_2}{\partial \varsigma}(0,\tau) = \frac{\partial \eta_2}{\partial \varsigma}(l,\tau) = 0,\ \tau \in (0,T),\end{aligned}\right\} \tag{24}$$

where the functions $u_r = u_r(\varsigma,\tau)$ are solutions of problem (12)-(14) for any $p \in P$. It can be seen that the adjoint problem (22)-(24) includes the two boundary value problems. One of them is a Dirichlet problem with respect to η_1 and the other is a Neumann problem with respect to η_2. If we use transform $t = T - \tau$ to the adjoint problem, we come to the conclusion that the adjoint problem is in the form of problem (12)-(14). As a solution of (22)-(24), we consider two functions $\eta_1(\varsigma,\tau) \in U_1$, $\eta_2(\varsigma,\tau) \in U_2$ satisfying equation (22) *for almost all* $\varsigma \in I$ and *any* $\tau \in Q$, the condition (23) *for almost all* $\varsigma \in I$ and the conditions (24) *for almost all* $\tau \in (0,T)$, respectively. Hence, we can state the validity of the following theorem for the solution of the adjoint problem (22)-(24):

Theorem 4. *Let the assumptions of Theorem 1 be fulfilled. Then adjoint problem (22)-(24) has a unique solution $\eta_1 \in U_1$, $\eta_2 \in U_2$ for any $p \in P$ and the following estimates hold*

$$\begin{aligned}&||\eta_1(.,\tau)||^2_{\overset{\circ}{W}{}^2_2(I)} + \left\|\frac{\partial \eta_1}{\partial \tau}\right\|^2_{L_2(I)} \leq \\ &c_5\|u_1 - u_2\|_{W_2^{0,1}(\Omega)},\end{aligned} \tag{25}$$

$$\begin{aligned}&||\eta_2(.,\tau)||^2_{W^2_2(I)} + \left\|\frac{\partial \eta_2}{\partial \tau}\right\|^2_{L_2(I)} \leq \\ &c_6\|u_1 - u_2\|_{W_2^{0,1}(\Omega)}\end{aligned} \tag{26}$$

for any $\tau \in Q$, where the positive constants c_5, c_6 do not depend on τ.

This theorem can be easily proved by the Galerkin's method similarly to the proof of Theorem 1.

Now, let's get the enhancement $\delta J_\alpha(p) = J_\alpha(p+\delta p) - J_\alpha(p)$ of $J_\alpha(p)$ for any $p \in P$, where $\delta p \in L_\infty(I)$ is an increment given to any $p \in P$ such that $p + \delta p \in P$. If we use formula (2), we achieve

$$\begin{aligned}\delta J_\alpha(p) &= \int_\Omega \delta p(\varsigma)Re(u_1\overline{\eta}_1)d\varsigma d\tau + \\ &\int_\Omega \delta p(\varsigma)Re(u_2\overline{\eta}_2)d\varsigma d\tau + \\ &2\alpha\int_0^l (p - w)\,\delta p d\varsigma + R,\end{aligned} \tag{27}$$

where

$$R = \int_\Omega \delta p(\varsigma) Re(\delta u_1 \overline{\eta}_1) d\varsigma d\tau + \int_\Omega \delta p(\varsigma) Re(\delta u_2 \overline{\eta}_2(\varsigma,\tau)) d\varsigma d\tau + \|\delta u_1\|^2_{L_2(\Omega)} + \|\delta u_2\|^2_{L_2(\Omega)} - a_3 \int_\Omega (|u_{1\delta}|^2 - |u_1|^2) Im(\delta u_1 \bar{\eta}_1) d\varsigma d\tau - a_3 \int_\Omega (|u_{2\delta}|^2 - |u_2|^2) Im(\delta u_2 \bar{\eta}_2) d\varsigma d\tau - a_3 \int_\Omega |\delta u_1|^2 Im\,(u_1 \bar{\eta}_1)\, d\varsigma d\tau - a_3 \int_\Omega |\delta u_2|^2 Im\,(u_2 \bar{\eta}_2)\, d\varsigma d\tau + \alpha \|\delta p\|^2_{L_2(I)}$$

and $\delta u_r \equiv u_r(\varsigma,\tau;p+\delta p) - u_r(\varsigma,\tau;p)$ for $r = 1,2$ hold problem (15) for any $p \in P$. By Young's inequality for the term R, we get

$$|R| \le \frac{5}{2}\|\delta u_1\|^2_{L_2(\Omega)} + \frac{5}{2}\|\delta u_2\|^2_{L_2(\Omega)} + \alpha \|\delta p\|^2_{L_2(I)} + \frac{T}{2}\left(\max_{0\le\tau\le T} \|\eta_1(.,\tau)\|^2_{L_\infty(I)}\right)\|\delta p\|^2_{L_2(I)} + \frac{T}{2}\left(\max_{0\le\tau\le T} \|\eta_2(.,\tau)\|^2_{L_\infty(I)}\right)\|\delta p\|^2_{L_2(I)} + a_3 \int_\Omega \left(|u_{1\delta}|^2 + |u_1|^2\right)|\delta u_1|^2 d\varsigma d\tau + a_3 \int_\Omega \left(|u_{2\delta}|^2 + |u_2|^2\right)|\delta u_2|^2 d\varsigma d\tau + a_3 \int_0^T \|\eta_1(.,\tau)\|^2_{L_\infty(I)} \|\delta u_1(.,\tau)\|^2_{L_2(I)} d\tau + a_3 \int_0^T \|\eta_2(.,\tau)\|^2_{L_\infty(I)} \|\delta u_2(.,\tau)\|^2_{L_2(I)} d\tau + \frac{1}{2}a_3 \int_0^T \|u_1(.,\tau)\|^2_{L_\infty(I)} \|\delta u_1(.,\tau)\|^2_{L_2(0,l)} d\tau + \frac{1}{2}a_3 \int_0^T \|u_2(.,\tau)\|^2_{L_\infty(I)} \|\delta u_2(.,\tau)\|^2_{L_2(I)} d\tau.$$

In the inequality above, if we use estimates (10), (11), (20), (25), (26) and the well known inequality in [31]

$$\|u(.,\tau)\|^2_{L_\infty(I)} \le \beta_2 \left\|\frac{\partial u(.,\tau)}{\partial\varsigma}\right\|_{L_2(I)} \|u(.,\tau)\|_{L_2(I)}, \quad \beta_2 = const. > 0 \tag{28}$$

for any $\tau \in Q$, we achive

$$|R| \le c_7 \|\delta p\|^2_{L_2(I)} \le c_8 \|\delta p\|^2_{L_\infty(I)}$$

which shows that $R = o\left(||\delta p||_{L_\infty(I)}\right)$, that is, $\lim\limits_{||\delta p||_{L_\infty(I)}\to 0} \frac{R}{||\delta p||_{L_\infty(I)}} = 0$, where the constants $c_7, c_8 > 0$ are independent from δp and τ. So, from (27), we can write

$$\delta J_\alpha(p) = \int_0^l \left(\int_0^T Re(u_1\overline{\eta}_1 + u_2\overline{\eta}_2) d\tau\right)\delta p(\varsigma) d\varsigma + \int_0^l 2\alpha\,(p - w)\,\delta p(\varsigma) d\varsigma + o\left(||\delta p||_{L_\infty(I)}\right)$$

which implies that

$$J'_\alpha(p) = \int_0^T Re(u_1\overline{\eta}_1 + u_2\overline{\eta}_2) d\tau + 2\alpha\,(p - w)\,. \tag{29}$$

Consequently, the differentiability of $J_\alpha(p)$ in the meaning of Frechet is shown and the next theorem is proved:

Theorem 5. *Let $w \in L_2(I)$ be a given function. Assume that the conditions of Theorem 4 are satisfied. Then, $J_\alpha(p)$ is a differentiable functional on P and moreover, its gradient is given by formula (29).*

Lemma 2. *The functional $J'_\alpha(p)$ is continuous on P.*

Proof. Let's prove that $|J'_\alpha(p+\delta p) - J'_\alpha(p)| \longrightarrow 0$ as $\|\delta p\|_{L_\infty(I)} \longrightarrow 0$ on the set P. Using formula (29), we get

$$J'_\alpha(p+\delta p)-J'_\alpha(p)= \int_0^T Re\left(u_{1\delta}\delta\overline{\eta}_1+u_{2\delta}\delta\overline{\eta}_2\right)d\tau+ \int_0^T Re\left(\delta u_1\overline{\eta}_1+\delta u_2\overline{\eta}_2\right)d\tau+2\alpha\delta p(\varsigma), \tag{30}$$

where the functions $\delta\eta_r=\delta\eta_r(\varsigma,\tau)\equiv\eta_r(\varsigma,\tau;p+\delta p)-\eta_r(\varsigma,\tau;p)$ for $r=1,2$ satisfy the problem

$$\begin{gathered} i\frac{\partial\delta\eta_r}{\partial\tau}+a_0\frac{\partial^2\delta\eta_r}{\partial\varsigma^2}+i\frac{\partial\left(a_1(\varsigma)\delta\eta_r\right)}{\partial\varsigma}- a_2(\varsigma)\delta\eta_r+(p(\varsigma)+\delta p(\varsigma))\delta\eta_r=-\delta p\eta_r- \\ ia_3\left(2|u_{r\delta}|^2\eta_{r\delta}-u_{r\delta}^2\overline{\eta}_{r\delta}\right)+ ia_3\left(2|u_r|^2\eta_r-u_r^2\overline{\eta}_r\right)+2(-1)^r\left(\delta u_1-\delta u_2\right), \\ \delta\eta_r(\varsigma,T)=0,\ \varsigma\in I,\ r=1,2, \end{gathered}$$

$$\begin{aligned} \delta\eta_1(0,\tau) &= \delta\eta_1(l,\tau)=0,\ \tau\in(0,T) \\ \frac{\partial\delta\eta_2}{\partial\varsigma}(0,\tau) &= \frac{\partial\delta\eta_2}{\partial\varsigma}(l,\tau)=0,\ \tau\in(0,T). \end{aligned}$$

For this problem, as similar to obtain of inequality (20), we get the estimate

$$\|\delta\eta_r(.,\tau)\|^2_{L_2(I)}+ a_3\int_{\widetilde{\Omega}_\tau}|u_{r\delta}|^2|\delta\eta_r|^2d\varsigma d\tau\le c_9\|\delta p\|^2_{L_\infty(I)} \tag{31}$$

for any $\tau\in Q$ and $r=1,2$. From (30), we get

$$\left|J'_\alpha(p+\delta p)-J'_\alpha(p)\right|\le \int_0^T|u_{1\delta}|\,|\delta\eta_1|\,d\tau+\int_0^T|u_{2\delta}|\,|\delta\eta_2|\,d\tau+ \int_0^T|\delta u_1|\,|\eta_1|\,d\tau+\int_0^T|\delta u_2|\,|\eta_2|\,d\tau+ 2\alpha\,|\delta p(\varsigma)|$$

which is equivalent to

$$\left\|J'_\alpha(p+\delta p)-J'_\alpha(p)\right\|^2_{L_2(I)}\le 5T\|u_{1\delta}\|^2_{L_\infty(\Omega)}\int_0^T\|\delta\eta_1\|^2_{L_2(I)}d\tau+ 5T\|u_{2\delta}\|^2_{L_\infty(\Omega)}\int_0^T\|\delta\eta_2\|^2_{L_2(I)}d\tau+ 5T\|\eta_1\|^2_{L_\infty(\Omega)}\int_0^T\|\delta u_1\|^2_{L_2(I)}d\tau+ 5T\|\eta_2\|^2_{L_\infty(\Omega)}\int_0^T\|\delta u_2\|^2_{L_2(I)}d\tau+ 20\alpha^2\|\delta p\|^2_{L_2(I)}.$$

In inequality above, using estimates (10), (11), (20), (25), (26), (31) and inequality (28) we get

$$\left\|J'_\alpha(p+\delta p)-J'_\alpha(p)\right\|^2_{L_2(I)}\le c_{10}\|\delta p\|^2_{L_\infty(I)}\ \text{ for any } p\in P$$

which implies that

$$\left|J'_\alpha(p+\delta p)-J'_\alpha(p)\right|\longrightarrow 0 \text{ as } \|\delta p\|_{L_\infty(I)}\longrightarrow 0,$$

where the constants $c_9,c_{10}>0$ are independent from δp and τ. Thus, the proof is completed. □

Theorem 6. *Presume that the Theorem 5 and Lemma 2 hold and let $p^*=p^*(\varsigma)$ be a solution of the OCP. Then, the inequality*

$$\int_0^l\left(\int_0^T Re(u_1^*\overline{\eta}_1^*+u_2^*\overline{\eta}_2^*)d\tau\right)(p-p^*)\,d\varsigma+ \int_0^l\left(2\alpha\left(p^*-w\right)\right)(p-p^*)\,d\varsigma\le 0$$

is valid for any $p\in P$, where the functions u_r^* and η_r^*, $r=1,2$ are solutions of (12)-(14) and the adjoint problem corresponding to $p^*\in P$, respectively.

Proof. It is clear that the functional $J_\alpha(p)$ is the sum of the functionals $J_0(p)$ and $\alpha\|p-w\|^2_{L_2(I)}$. Since $\alpha\|p-w\|^2_{L_2(I)}$ is a continuous functional on P, from Lemma 1, we deduce that the functional $J_\alpha(p)$ is continuous on the set P. Also if we take into account Lemma 2, we say that $J_\alpha(p)$ is a continuous differentiable functional on the convex set P. Thus, by virtue of known theorem in [35], if the functional $J_\alpha(p)$ has a minimum value at $p^* \in P$, then

$$\left(J'_\alpha(p^*), p - p^*\right)_{L_2(I)} \geq 0 \text{ for any } p \in P$$

which concludes the proof. $\square$

5. Conclusions

In this study, we examined an optimal control problem for a system whose state is expressed by the nonlinear Schrödinger equation. We regard Lions functional as the objective functional. As it is seen from the definition of P, the admissible controls set contains the measurable bounded functions from $L_2(I)$. We have shown the existence and uniqueness of the solution to the optimal control problem. By means of an adjoint problem, we demonstrated that the objective functional is differentiable in the sense of Frechet. Finally, by proving that the objective functional is a continuously differentiable functional on the set of admissible controls, we derived a necessary optimality condition for the optimal control problem.

As a future direction, we will consider the optimal control problem, in which the set of admissible controls will be chosen from the wider class of functions.

References

[1] Liu, Wu-M., & Kengne, E. (2019). *Schrödinger Equations in Nonlinear Systems,* Springer Nature Singapore Pte. Ltd., Singapore.

[2] Zhuravlev, V. M. (1996). Models of nonlinear wave processes that allow for soliton solutions. *Journal of Experimental and Theoretical Physics,* 83 (6), 1235-1245.

[3] Elhia, M., Balatif, O., Boujalla, L., & Rachik, M. (2021). Optimal control problem for a tuberculosis model with multiple infectious compartments and time delays. *An International Journal of Optimization and Control: Theories & Applications,* 11 (1), 75-91.

[4] Gisser, M., & Sanchez, D. A. (1980). Competition versus optimal control in groundwater pumping. *Water Resources Research*, 16 (4), 638-642.

[5] Imer, O. C., Yüksel, S., & Başar, T. (2006). Optimal control of LTI systems over unreliable communication links. *Automatica,* 42, 1429 – 1439.

[6] Moussouni, N., & Aliane, M. (2021). Optimal control of COVID-19. *An International Journal of Optimization and Control: Theories & Applications,* 11 (1), 114-122.

[7] Trelat, E. (2012). Optimal Control and Applications to Aerospace: Some Results and Challenges. *Journal of Optimization Theory and Applications,* 154 (2012), 713–758.

[8] Van-Reeth, E., Ratiney, H., Lapert, M., Glaser, S. J., & Sugny, D. (2017). Optimal control theory for applications in Magnetic Resonance Imaging, *Pacific Journal of Mathematics for Industry,* 9(9), 1-10.

[9] Hamdache, A., Saadi, S., & Elmouki, I. (2016). Free terminal time optimal control problem for the treatment of HIV infection. *An International Journal of Optimization and Control: Theories & Applications,* 6(1), 33-51.

[10] Ulus, A. Y. (2018). On discrete time infinite horizon optimal growth problem. *An International Journal of Optimization and Control: Theory and Applications,* 8(1), 102-116.

[11] Vorontsov, M. A., & Shmalgauzen, V. I. (1985). *The Principles of Adaptive Optics,* Izdatel'stvo Nauka, Moscow (in Russian).

[12] Lions, J.-L. (1971). *Optimal Control of Systems Described by Partial Differential Equations.* Berlin; New York, Springer-Verlag.

[13] Baudouin, L., & Salomon, J. (2008). Constructive solution of a bilinear optimal control problem for a Schrödinger equation. *Systems and Control Letters,* 57(6), 453-464.

[14] Butkovskiy, A. G., & Samoilenko, Yu.I. (1990). *Control of Quantum-Mechanical Processes and Systems. Mathematics and its Applications* (56). Kluwer Academic Publishers Group, Dordrecht.

[15] Guliyev, H. F., & Gasimov, Y. S. (2014). Optimal control method for solving the Cauchy-Neumann problem for the Poisson equation. *Journal of Mathematical Physics, Analysis, Geometry,* 10(4), 412-421.

[16] Hao, D. N. (1986). Optimal control of quantum systems. *Automat Remote Control,* 47(2), 162–168.

[17] Iskenderov, A. D. (2005). Identification problem for the time dependent Schrödinger type equation. *Proceedings of the Lankaran State University,* Natural Sciences Series, 31-53.

[18] Iskenderov, A. D., & Yagubov, G. Y. (2007). Optimal control problem with unbounded potential for multidimensional, nonlinear and nonstationary Schrödinger equation. *Proceedings of the Lankaran State University,* Natural Sciences Series, 3-56.

[19] Iskenderov, A. D., Yagubov, G. Ya., & Musayeva, M. A. (2012). *The Identification of Quantum Mechanics Potentials.* Çaşıoğlu, Baku.

[20] Keller, D. (2013). Optimal conrol of a linear stochastic Schrödinger equation. *Discrete Continuous Dynamical Systems Supplement,* 437-446.

[21] Yagubov, G. Ya., & Musayeva, M. A. (1997). On the identification problem for nonlinear Schrödinger equation, *Differ. Equ.* 33 (12), 1695-1702.

[22] Yildirim Aksoy, N., Aksoy, E., & Kocak, Y. (2016). An optimal control problem with final

observation for systems governed by nonlinear Schrödinger equation. *Filomat,* 30(3), 649-665.

[23] Iskenderov, A. D. (1984). On variational formulations of multidimensional inverse problems of mathematical physics. *Doklady Akademii Nauk USSR,* 274(3), 531-533.

[24] Iskenderov, A. D., Yagubov, G. Ya., Ibragimov, N. S., & Aksoy, N.Y. (2014). Variation formulation of the inverse problem of determining the complex-coefficient of equation of quasioptics. *Eurasian Journal of Mathematical and Computer Applications,* 2(2), 102-121.

[25] Kücük, G. D., Yagub, G., & Celik, E. (2019). On the existence and uniqueness of the solution of an optimal control problem for Schrödinger equation. *Discrete Continuous Dynamical Systems Series-S,* 12(3), 503-512.

[26] Mahmudov, N. M. (2010). On an optimal control problem for the Schrödinger equation with the real coefficient. *Izv. VUZOV,* 11, 31-40.

[27] Salmanov, V. (2020). Existence and uniqueness of the solution to the optimal control problem with integral criterion over the entire domain for a nonlinear Schrödinger equation with a special gradient term. *Control and Cybernetics*, 49(3), 277-290.

[28] Yagub, G., Ibrahimov, N.S., Musayeva, M.A., & Zengin, M. (2019). Optimal control problem with the boundary functional for a Schrödinger equation with a special gradient term, 34th International Conference Problems of Decision Making under Uncertainties (PDMU); September 23-27; Lviv, Ukraine, pp. 116-117.

[29] Yildirim Aksoy, N., Celik, E., & Zengin, M. (2022). On optimal control of a charged particle in a varying electromagnetic field, *Waves in Random and Complex Media.*

[30] Zengin, M., Ibrahimov, N. S., & Yagub, G. (2021). Existence and uniqueness of the solution of the optimal control problem with boundary functional for nonlinear stationary quasi-optical equation with a special gradient term. *Sci Proc Lankaran State Univ., Math Nat Sci Ser 1.*, 27-42.

[31] Ladyzhenskaya, O. A., Solonnikov, V. A., & Ural'ceva, N. N. (1968). *Linear and Quasilinear Equations of Parabolic Type.* Amer. Math. Soc. (English Trans.), Providence, RI.

[32] Tikhonov, A. N., & Arsenin, V. Y. (1977). *Solutions of Ill-Posed Problems,* V.H. Winston&Sons, Washington DC.

[33] Yagub, G., Ibrahimov, N. S., & Zengin, M. (2018). The solvability of the initial-boundary value problems for a nonlinear Schrödinger equation with a special gradient term, *Journal of Mathematical Physics, Analysis, Geometry,* 14 (2), 214-232.

[34] Goebel, M. (1979). On existence of optimal control, *Mathematische Nachrichten*, 93(1), 67-73.

[35] Vasilyev, F. P. (1981). *Methods of Solving for Extremal Problems,* Nauka, Moskow (in Russian).

Nigar Yildirim Aksoy *received her Ph.D. degree from the Department of Mathematics, Atatürk University in 2009. She is an Associate Professor in the Department of Mathematics, Kafkas University. Her research interests include optimal control theory, variational Methods, and numerical methods.*
https://orcid.org/0000-0001-6767-3363

Ercan Celik *received his Ph.D. degree from the Department of Mathematics, Atatürk University in 2002. He is a Professor in the Department of Applied Mathematics and Informatics, Kyrgyz-Turkish Manas University. His research interests include applied mathematics, numerical analysis, fractional calculus, optimal control, and differential algebraic equations.*
https://orcid.org/0000-0001-5971-7653

Muhammed Emin Dadas *received his M.Sc. degree from the Department of Mathematics, Kafkas University in 2019. His research interests include optimal control theory and numerical methods.*
https://orcid.org/0000-0001-8099-5383

ISSN: 2146-0957, eISSN: 2146-5703, http://www.ijocta.org

INSTRUCTIONS FOR AUTHORS

Aims and Scope

An International Journal of Optimization and Control: Theories & Applications (IJOCTA) is a scientific, peer-reviewed, open-access journal that publishes original research papers and review articles of high scientific value in all areas of applied mathematics, optimization and control. It aims to focus on multi/inter-disciplinary research into the development and analysis of new methods for the numerical solution of real-world applications in engineering and applied sciences. The basic fields of this journal cover mathematical modeling, computational methodologies and (meta)heuristic algorithms in optimization, control theory and their applications. Note that new methodologies for solving recent optimization problems in operations research must conduct a comprehensive computational study and/or case study to show their applicability and practical relevance.

Journal Topics

The topics covered in the journal are (not limited to):

Applied Mathematics, Financial Mathematics, Control Theory, Optimal Control, Fractional Calculus and Applications, Modeling of Bio-systems for Optimization and Control, Linear Programming, Nonlinear Programming, Stochastic Programming, Parametric Programming, Conic Programming, Discrete Programming, Dynamic Programming, Nonlinear Dynamics, Stochastic Differential Equations, Optimization with Artificial Intelligence, Operational Research in Life and Human Sciences, Heuristic and Metaheuristic Algorithms in Optimization, Applications Related to Optimization in Engineering.

Submission of Manuscripts

New Submissions

Solicited and contributed manuscripts should be submitted to IJOCTA via the journal's online submission system. You need to make registration prior to submitting a new manuscript (please click here to register and do not forget to define yourself as an "Author" in doing so). You may then click on the "New Submission" link on your User Home.

IMPORTANT: If you already have an account, please click here to login. It is likely that you will have created an account if you have reviewed or authored for the journal in the past.

On the submission page, enter data and answer questions as prompted. Click on the “Next” button on each screen to save your work and advance to the next screen. The names and contact details of at least four internationally recognized experts who can review your manuscript should be entered in the "Comments for the Editor" box.

You will be prompted to upload your files: Click on the “Browse” button and locate the file on your computer. Select the description of the file in the drop down next to the Browse button. When you have selected all files you wish to upload, click the “Upload” button. Review your submission before sending to the Editors. Click the “Submit” button when you are done reviewing. Authors are responsible for verifying all files have uploaded correctly.

You may stop a submission at any phase and save it to submit later. Acknowledgment of receipt of the manuscript by IJOCTA Online Submission System will be sent to the corresponding author, including an assigned manuscript number that should be included in all subsequent correspondence. You can also log-on to submission web page of IJOCTA any time to check the status of your manuscript. You will receive an e-mail once a decision has been made on your manuscript.

Each manuscript must be accompanied by a statement that it has not been published elsewhere and that it has not been submitted simultaneously for publication elsewhere.

Manuscripts can be prepared using LaTeX (.tex) or MSWord (.docx). However, manuscripts with heavy mathematical content will only be accepted as LaTeX files.

Preferred first submission format (for reviewing purpose only) is Portable Document File (.pdf). Please find below the templates for first submission.

Click here to download Word template for first submission (.docx)

Click here to download LaTeX template for first submission (.tex)

Revised Manuscripts

Revised manuscripts should be submitted via IJOCTA online system to ensure that they are linked to the original submission. It is also necessary to attach a separate file in which a point-by-point explanation is given to the specific points/questions raised by the referees and the corresponding changes made in the revised version.

To upload your revised manuscript, please go to your author page and click on the related manuscript title. Navigate to the "Review" link on the top left and scroll down the page. Click on the "Choose File" button under the "Editor Decision" title, choose the revised article (in pdf format) that you want to submit, and click on the "Upload" button to upload the author version. Repeat the same steps to upload the "Responses to Reviewers/Editor" file and make sure that you click the "Upload" button again.

To avoid any delay in making the article available freely online, the authors also need to upload the source files (Word or LaTex) when submitting revised manuscripts. Files can be compressed if necessary. The two-column final submission templates are as follows:

Click here to download Word template for final submission (.docx)

Click here to download LaTeX template for final submission (.tex)

Authors are responsible for obtaining permission to reproduce copyrighted material from other sources and are required to sign an agreement for the transfer of copyright to IJOCTA.

Article Processing Charges

There are **no charges** for submission and/or publication.

English Editing

Papers must be in English. Both British and American spelling is acceptable, provided usage is consistent within the manuscript. Manuscripts that are written in English that is ambiguous or incomprehensible, in the opinion of the Editor, will be returned to the authors with a request to resubmit once the language issues have been improved. This policy does not imply that all papers must be written in "perfect" English, whatever that may mean. Rather, the criteria require that the intended meaning of the authors must be clearly understandable, i.e., not obscured by language problems, by referees who have agreed to review the paper.

Presentation of Papers

Manuscript style

Use a standard font of the **11-point type: Times New Roman** is preferred. It is necessary to single line space your manuscript. Normally manuscripts are expected not to exceed 25 single-spaced pages including text, tables, figures and bibliography. All illustrations, figures, and tables are placed within the text at the appropriate points, rather than at the end.

During the submission process you must enter: (1) the full title, (2) names and affiliations of all authors and (3) the full address, including email, telephone and fax of the author who is to check the proofs. Supply a brief **biography** of each author at the end of the manuscript after references.

- Include the name(s) of any **sponsor(s)** of the research contained in the paper, along with **grant number(s).**
- Enter an **abstract** of no more than 250 words for all articles.

Keywords

Authors should prepare no more than 5 keywords for their manuscript.

Maximum five **AMS Classification number** (http://www.ams.org/mathscinet/msc/msc2010.html) of the study should be specified after keywords.

Writing Abstract

An abstract is a concise summary of the whole paper, not just the conclusions. The abstract should be no more than 250 words and convey the following:

1. An introduction to the work. This should be accessible by scientists in any field and express the necessity of the experiments executed.
2. Some scientific detail regarding the background to the problem.
3. A summary of the main result.
4. The implications of the result.
5. A broader perspective of the results, once again understandable across scientific disciplines.

It is crucial that the abstract conveys the importance of the work and be understandable without reference to the rest of the manuscript to a multidisciplinary audience. Abstracts should not contain any citation to other published works.

Reference Style

Reference citations in the text should be identified by numbers in square brackets "[ ]". All references must be complete and accurate. Please ensure that every reference cited in the text is also present in the reference list (and vice versa). Online citations should include date of access. References should be listed in the following style:

Journal article

Author, A.A., & Author, B. (Year). Title of article. Title of Journal, Vol(Issue), pages.

Castles, F.G., Curtin, J.C., & Vowles, J. (2006). Public policy in Australia and New Zealand: The new global context. Australian Journal of Political Science, 41(2), 131–143.

Book

Author, A. (Year). Title of book. Publisher, Place of Publication.

Mercer, P.A., & Smith, G. (1993). Private Viewdata in the UK. 2nd ed. Longman, London.

Chapter

Author, A. (Year). Title of chapter. In: A. Editor and B. Editor, eds. Title of book. Publisher, Place of publication, pages.

Bantz, C.R. (1995). Social dimensions of software development. In: J.A. Anderson, ed. Annual review of software management and development. CA: Sage, Newbury Park, 502–510.

Internet document

Author, A. (Year). Title of document [online]. Source. Available from: URL [Accessed (date)].

Holland, M. (2004). Guide to citing Internet sources [online]. Poole, Bournemouth University. Available from: http://www.bournemouth.ac.uk/library/using/guide_to_citing_internet_sourc.html [Accessed 4 November 2004].

Newspaper article

Author, A. (or Title of Newspaper) (Year). Title of article. Title of Newspaper, day Month, page, column.

Independent (1992). Picking up the bills. Independent, 4 June, p. 28a.

Thesis

Author, A. (Year). Title of thesis. Type of thesis (degree). Name of University.

Agutter, A.J. (1995). The linguistic significance of current British slang. PhD Thesis. Edinburgh University.

Illustrations

Illustrations submitted (line drawings, halftones, photos, photomicrographs, etc.) should be clean originals or digital files. Digital files are recommended for highest quality reproduction and should follow these guidelines:

- 300 dpi or higher
- Sized to fit on journal page
- TIFF or JPEG format only
- Embedded in text files and submitted as separate files (if required)

Tables and Figures

Tables and figures (illustrations) should be embedded in the text at the appropriate points, rather than at the end. A short descriptive title should appear above each table with a clear legend and any footnotes suitably identified below.

Proofs

Page proofs are sent to the designated author using IJOCTA EProof system. They must be carefully checked and returned within 48 hours of receipt.

Offprints/Reprints

Each corresponding author of an article will receive a PDF file of the article via email. This file is for personal use only and may not be copied and disseminated in any form without prior written permission from IJOCTA.

Submission Preparation Checklist

As part of the submission process, authors are required to check off their submission's compliance with all of the following items, and submissions may be returned to authors that do not adhere to these guidelines.

1. The submission has not been previously published, nor is it before another journal for consideration (or an explanation has been provided in Comments for the Editor).
2. The paper is in PDF format and prepared using the IJOCTA's two-column template.
3. All references cited in the manuscript have been listed in the References list (and vice-versa) following the referencing style of the journal.
4. There is no copyright material used in the manuscript (or all necessary permissions have been granted).
5. Details of all authors have been provided correctly.
6. ORCID profile numbers of "all" authors are mandatory, and they are provided at the end of the manuscript as in the template (visit https://orcid.org for more details on ORCID).
7. The text adheres to the stylistic and bibliographic requirements outlined in the Author Guidelines.
8. Maximum five AMS Classification number (http://www.ams.org/mathscinet/msc/msc2010.html) of the study have been provided after keywords.
9. The names and email addresses of at least FOUR (4) possible reviewers have been indicated in "Comments for the Editor" box in "Paper Submission Step 1-Start". Please note that at least two of the recommendations should be from different countries. Avoid suggesting reviewers you have a conflict of interest.

Peer Review Process

All contributions, prepared according to the author guidelines and submitted via IJOCTA online submission system are evaluated according to the criteria of originality and quality of their scientific content. The corresponding author will receive a confirmation e-mail with a reference number assigned to the paper, which he/she is asked to quote in all subsequent correspondence.

All manuscripts are first checked by the Technical Editor using plagiarism detection software (iThenticate) to verify originality and ensure the quality of the written work. If the result is not satisfactory (i.e. exceeding the limit of 30% of overlapping), the submission is rejected and the author is notified.

After the plagiarism check, the manuscripts are evaluated by the Editor-in-Chief and can be rejected without reviewing if considered not of sufficient interest or novelty, too preliminary or out of the scope of the journal. If the manuscript is considered suitable for further evaluation, it is first sent to the Area Editor. Based on his/her opinion the paper is then sent to at least two independent reviewers. Each reviewer is allowed up to four weeks to return his/her feedback but this duration may be extended based on his/her availability. IJOCTA has instituted a blind peer review process where the reviewers' identities are not known to authors. When the reviews are received, the Area Editor gives a decision and lets the author know it together with the reviewer comments and any supplementary files.

Should the reviews be positive, the authors are expected to submit the revised version usually within two months the editor decision is sent (this period can be extended when the authors contact to the editor and let him/her know that they need extra time for resubmission). If a revised paper is not resubmitted within the deadline, it is considered as a new submission after all the changes requested by reviewers have been made. Authors are required to submit a new cover letter, a response to reviewers letter and the revised manuscript (which ideally shows the revisions made in a different color or highlighted). If a change in authorship (addition or removal of author) has occurred during the revision, authors are requested to clarify the reason for change, and all authors (including the removed/added ones) need to submit a written consent for the change. The revised version is evaluated by the Area editor and/or reviewers and the Editor-in-Chief brings a decision about final acceptance based on their suggestions. If necessary, further revision can be asked for to fulfil all the requirements of the reviewers.

When a manuscript is accepted for publication, an acceptance letter is sent to the corresponding author and the authors are asked to submit the source file of the manuscript conforming to the IJOCTA two-column final submission template. After that stage, changes of authors of the manuscript are not possible. The manuscript is sent to the Copyeditor and a linguistic, metrological and technical revision is made, at which stage the authors are asked to make the final corrections in no more than a week. The layout editor prepares the galleys and the authors receive the galley proof for final check before printing. The authors are expected to correct only typographical errors on the proofs and return the proofs within 48 hours. After the final check by the layout editor and the proofreader, the manuscript is assigned a DOI number, made publicly available and listed in the forthcoming journal issue. After printing the issue, the corresponding metadata and files published in this issue are sent to the databases for indexing.

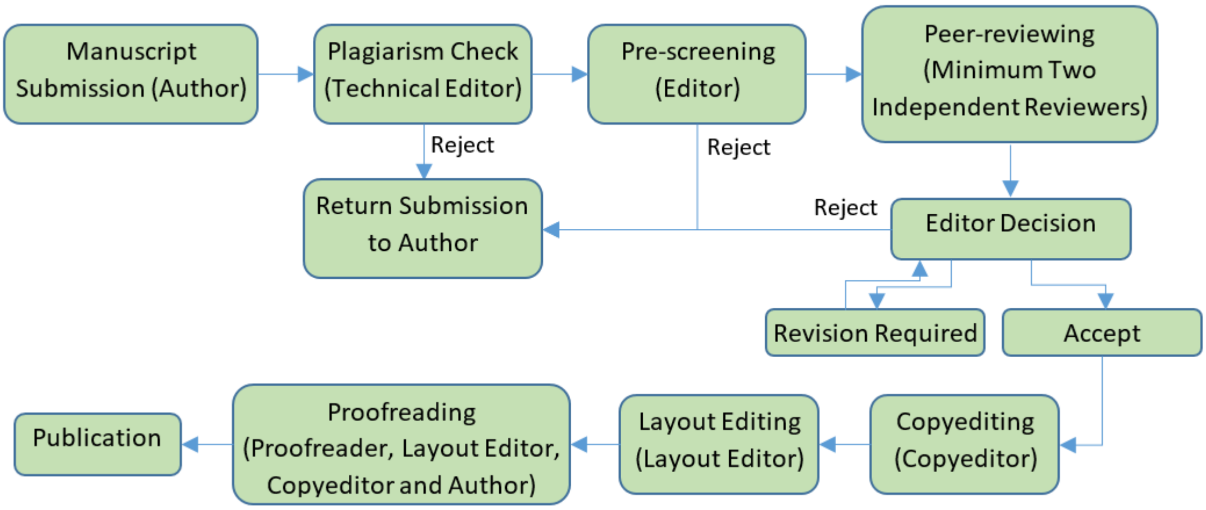

Publication Ethics and Malpractice Statement

IJOCTA is committed to ensuring ethics in publication and quality of articles. Conforming to standards of expected ethical behavior is therefore necessary for all parties (the author, the editor(s), the peer reviewer) involved in the act of publishing.

International Standards for Editors

The editors of the IJOCTA are responsible for deciding which of the articles submitted to the journal should be published considering their intellectual content without regard to race, gender, sexual orientation, religious belief, ethnic origin, citizenship, or political philosophy of the authors. The editors may be guided by the policies of the journal's editorial board and constrained by such legal requirements as shall then be in force regarding libel, copyright infringement and plagiarism. The editors may confer with other editors or reviewers in making this decision. As guardians and stewards of the research record, editors should encourage authors to strive for, and adhere themselves to, the highest standards of publication ethics. Furthermore, editors are in a unique position to indirectly foster responsible conduct of research through their policies and processes.

To achieve the maximum effect within the research community, ideally all editors should adhere to universal standards and good practices.

- Editors are accountable and should take responsibility for everything they publish.
- Editors should make fair and unbiased decisions independent from commercial consideration and ensure a fair and appropriate peer review process.
- Editors should adopt editorial policies that encourage maximum transparency and complete, honest reporting.
- Editors should guard the integrity of the published record by issuing corrections and retractions when needed and pursuing suspected or alleged research and publication misconduct.
- Editors should pursue reviewer and editorial misconduct.
- Editors should critically assess the ethical conduct of studies in humans and animals.
- Peer reviewers and authors should be told what is expected of them.
- Editors should have appropriate policies in place for handling editorial conflicts of interest.

Reference:

Kleinert S & Wager E (2011). Responsible research publication: international standards for editors. A position statement developed at the 2nd World Conference on Research Integrity, Singapore, July 22-24, 2010. Chapter 51 in: Mayer T & Steneck N (eds) Promoting Research Integrity in a Global Environment. Imperial College Press / World Scientific Publishing, Singapore (pp 317-28). (ISBN 978-981-4340-97-7) [Link].

International Standards for Authors

Publication is the final stage of research and therefore a responsibility for all researchers. Scholarly publications are expected to provide a detailed and permanent record of research. Because publications form the basis for both new research and the application of findings, they can affect not only the research community but also, indirectly, society at large. Researchers therefore have a responsibility to ensure that their publications are honest, clear, accurate, complete and balanced, and should avoid misleading, selective or ambiguous reporting. Journal editors also have responsibilities for ensuring the integrity of the research literature and these are set out in companion guidelines.

- The research being reported should have been conducted in an ethical and responsible manner and should comply with all relevant legislation.
- Researchers should present their results clearly, honestly, and without fabrication, falsification or inappropriate data manipulation.
- Researchers should strive to describe their methods clearly and unambiguously so that their findings can be confirmed by others.
- Researchers should adhere to publication requirements that submitted work is original, is not plagiarised, and has not been published elsewhere.
- Authors should take collective responsibility for submitted and published work.
- The authorship of research publications should accurately reflect individuals' contributions to the work and its reporting.
- Funding sources and relevant conflicts of interest should be disclosed.
- When an author discovers a significant error or inaccuracy in his/her own published work, it is the author's obligation to promptly notify the journal's Editor-in-Chief and cooperate with them to either retract the paper or to publish an appropriate erratum.

Reference:

Wager E & Kleinert S (2011) Responsible research publication: international standards for authors. A position statement developed at the 2nd World Conference on Research Integrity, Singapore, July 22-24, 2010. Chapter 50 in: Mayer T & Steneck N (eds) Promoting Research Integrity in a Global Environment.

Imperial College Press / World Scientific Publishing, Singapore (pp 309-16). (ISBN 978-981-4340-97-7) [Link].

Basic principles to which peer reviewers should adhere

Peer review in all its forms plays an important role in ensuring the integrity of the scholarly record. The process depends to a large extent on trust and requires that everyone involved behaves responsibly and ethically. Peer reviewers play a central and critical part in the peer-review process as the peer review assists the Editors in making editorial decisions and, through the editorial communication with the author, may also assist the author in improving the manuscript.

Peer reviewers should:

- respect the confidentiality of peer review and not reveal any details of a manuscript or its review, during or after the peer-review process, beyond those that are released by the journal;
- not use information obtained during the peer-review process for their own or any other person's or organization's advantage, or to disadvantage or discredit others;
- only agree to review manuscripts for which they have the subject expertise required to carry out a proper assessment and which they can assess within a reasonable time-frame;
- declare all potential conflicting interests, seeking advice from the journal if they are unsure whether something constitutes a relevant conflict;
- not allow their reviews to be influenced by the origins of a manuscript, by the nationality, religion, political beliefs, gender or other characteristics of the authors, or by commercial considerations;
- be objective and constructive in their reviews, refraining from being hostile or inflammatory and from making libellous or derogatory personal comments;
- acknowledge that peer review is largely a reciprocal endeavour and undertake to carry out their fair share of reviewing, in a timely manner;
- provide personal and professional information that is accurate and a true representation of their expertise when creating or updating journal accounts.

Reference:

Homes I (2013). COPE Ethical Guidelines for Peer Reviewers, March 2013, v1 [Link].

An International Journal of Optimization and Control: Theories & Applications

Volume: 13 Number: 2
July 2023

CONTENTS

ISSN 2146-0957

www.ijocta.org
editor@ijocta.org